The Role of Alveolar Macrophages in COVID-19 Pathology

Amy Napier

Sir William Dunn School of Pathology

Lincoln College

University of Oxford

A thesis submitted for the degree of Doctor of Philosophy

Hilary Term 2026

Acknowledgements

I would like to express my gratitude to the Dunn School of Pathology for funding my DPhil. It has been a privilege to undertake my PhD in such an inspiring place with its 100-year legacy of important scientific discoveries.

My sincere thanks go to my supervisors, Prof Miles Carroll, Prof William James and Dr Sally Cowley. I feel incredibly fortunate to have been guided by passionate and principled scientists, whose mentorship has shaped me into the scientist I am today. Thank you for being a constant source of wisdom, support and encouragement throughout my PhD.

I am also grateful to Dr Jack Tan for his valuable input into my project and for generously providing so many antibodies and reagents. Thank you to Dr Peter Wing for his help with smFISH and microscopy. I would also like to thank Dr Robert Hedley and Vasiliki Tsioligka, who always go above and beyond to help with flow cytometry.

A big thank you to the lovely post-docs in the Cowley lab; Ishan, Madeeha, Anna, Anne and Andy, for all your support and friendship over the years. I am also very grateful to the members of the Carroll lab for embracing me into the group. I took so much inspiration from lab meetings and our interesting chats, particularly with Cillian, about all things virology, vaccines and immunology.

Thank you to my wonderful friends, Veronika and Michelle, for sharing this strange and incredible Oxford journey with me from the very beginning, and Daniel, for the long beach walks that somehow always put everything into perspective.

Finally, thank you to Alfie, Rachel, Mum and Dad, for everything. Mum and Dad, you've always been my inspiration to become a scientist, and I would not be where I am today without you.

Declaration

All experimental work and analysis were conducted by myself, with the following exceptions.

- SARS-CoV-2 antibodies and proteins used in this project were designed, expressed and purified by Dr Jack Tan and Diana Melnyk. RBD-Fc was designed by Prof William James and expressed by Dr Madeeha Afzal.

- smFISH protocol development, microscopy and analysis were by Dr Peter Wing.

- Reverse genetic SARS-CoV-2 viruses were made by Dr Madeeha Afzal.

- IFNAR-/- and TREM2 -/- iPSC lines were generated by the Cowley/James lab.

I confirm that the generative artificial intelligence tool ChatGPT (version 5.3), provided by OpenAI, was used solely to assist with language refinement, including improving clarity, grammar, and style. No AI-generated content was used to develop substantive arguments, analysis, or original research findings. The use of AI has been carried out in accordance with the guidance issued by the Medical Sciences Division, in accordance with the University of Oxford's AI Use in Summative Assessment policy.

Abstract

Tissue-resident alveolar macrophages (AMs) are among the first immune cells to encounter SARS-CoV-2 and initiate a protective immune response. However, in severe COVID-19, macrophage responses become hyperinflammatory and dysregulated. While SARS-CoV-2 entry into macrophages is well-documented, the route of entry, their capacity to support viral replication, and their direct contribution to disease pathology remain unclear.

In this thesis, I used iPSC-derived macrophages as a model of tissue-resident AMs to define the mechanisms and consequences of SARS-CoV-2 interaction with macrophages. I show that macrophages efficiently internalise SARS-CoV-2 via non-specific mechanisms independent of ACE2 or high-affinity spike-binding receptors. Using single-molecule fluorescence in situ hybridisation (smFISH) and qRT-PCR, I demonstrate that macrophages do not support productive viral replication and instead degrade viral RNA.

Notably, I demonstrate that macrophages become permissive to productive infection when an alternative entry route is provided, including transgenic ACE2 expression or specific class 1/4 anti-RBD antibodies. I propose that antibody-mediated infection occurs through a cooperative mechanism involving Fab-dependent stabilisation of spike and Fcγ receptor-mediated virion tethering. In addition, I identify a clinically developed class 1/4 anti-RBD antibody with infection-promoting activity. Under these conditions, viral replication is enhanced by inhibition of interferon signalling.

Functionally, macrophages release inflammatory cytokines in response to internalisation of ancestral SARS-CoV-2 but not Omicron variants. They present viral antigens to $CD4^+$, but not $CD8^+$, T cells, consistent with exogenous antigen processing. Importantly, viral exposure does not impair macrophage viability or key cellular functions. Collectively, these findings suggest that direct infection of alveolar macrophages is unlikely to be a major driver of COVID-19 pathology. Instead, macrophage dysregulation may arise indirectly through inflammatory mediators and epithelial cell damage.

Abbreviations

Abbreviation	Definition
ARDS	acute respiratory distress syndrome
AM(s)	alveolar macrophage(s)
ACE2	angiotensin-converting enzyme 2
ADCC	antibody-dependent cellular cytotoxicity
ADCP	antibody-dependent cellular phagocytosis
ADE	Antibody-dependent enhancement
BSA	bovine serum albumin
BAL	bronchoalveolar lavage
Cav-1	caveolin-1
CME	clathrin-mediated endocytosis
COVID-19	coronavirus disease 2019
DAMP	Damage-associated molecular pattern
DMV(s)	double-membrane vesicle(s)
ERGIC	endoplasmic reticulum-golgi intermediate compartment
ELISA	Enzyme-linked immunosorbent assay
FcγR	Fc gamma receptor
FFA	Focus-forming assay
FFU	Focus-forming unit
Fab	Fragment antigen-binding
Fc	Fragment crystallisable
iPSC(s)	induced pluripotent stem cell(s)
IFNAR	Interferon alpha receptor
IFNγ	Interferon gamma
IFN(s)	interferon(s)
ISG	Interferon-stimulated gene
IL	Interleukin
JAK	Janus kinase
M-CSF	macrophage colony-stimulating factor
MHC	Major histocompatibility complex
mNG	mNeonGreen
MOI	multiplicity of infection
NP	Nucleoprotein
ORF	Open reading frame
PLpro	papain-like protease
PAMP	Pathogen-associated molecular pattern
PRR(s)	pattern recognition receptor(s)
PBMC(s)	peripheral blood mononuclear cell(s)
PS	phosphatidylserine
PSR(s)	phosphatidylserine receptor(s)
PI	Post-infection
ROS	reactive oxygen species

RBD	receptor-binding domain
RBM	Receptor-binding motif
RT-qPCR	reverse transcription quantitative PCR
RdRp	RNA-dependent RNA polymerase
SARS-CoV-2	severe acute respiratory syndrome coronavirus 2
smFISH	Single-molecule fluorescence in situ hybridisation
sgRNA(s)	subgenomic RNA(s)
TLR(s)	Toll-like receptor(s)
TMPRSS2	transmembrane serine protease 2
WT	wild-type

Table of Contents

Chapter 1: Introduction

1.1 SARS-CoV-2 and COVID-19

SARS-CoV-2: Virology and emergence

Severe acute respiratory syndrome coronavirus 2 (SARS-CoV-2) is a betacoronavirus that emerged in 2019 and is the causative agent of coronavirus disease 2019 (COVID-19). SARS-CoV-2 is primarily transmitted via respiratory droplets and infects cells of the respiratory epithelium. Phylogenetic analyses suggest that SARS-CoV-2 is of zoonotic origin, most closely related to bat coronaviruses, with the first recognised human outbreak occurring in late 2019 and leading to a global pandemic[1]. SARS-CoV-2 belongs to the Coronaviridae family, which includes other human and zoonotic coronaviruses such as hCoV-OC43, Middle East respiratory syndrome coronavirus (MERS-CoV), and severe acute respiratory syndrome coronavirus (SARS-CoV).

SARS-CoV-2: Genome organisation and structural proteins

SARS-CoV-2 is an enveloped, positive-sense single-stranded RNA virus. Approximately two-thirds of its ~30kb genome encodes two large replicase open reading frames (ORFs), ORF1a and ORF1b. These ORFs are translated by a ribosomal frameshift mechanism into polyproteins which are subsequently cleaved by the virally encoded papain-like protease (PLpro, nsp3) and main protease (Mpro, nsp5) to generate sixteen non-structural proteins (nsps 1-16). Together, these proteins form the viral replication-transcription complex (RTC), which is responsible for viral RNA synthesis, proofreading, RNA capping, and modulation of host-cell response[2].

The remaining one-third of the genome encodes structural proteins: spike (S), envelope (E), membrane (M), and nucleocapsid (N) and several accessory proteins (Figure 1.1A, B). The spike glycoprotein forms homotrimers that are embedded in the viral membrane and mediate binding to the host receptor, angiotensin-converting enzyme 2 (ACE2)[3]. The membrane protein is the most abundant structural component of the virion and serves as a central organiser of virion assembly through interactions with the other structural proteins. The envelope protein is a small transmembrane viroporin that contributes to virion assembly, budding, and pathogenesis. The nucleocapsid protein binds and packages the viral RNA genome into a ribonucleoprotein complex and also participates in regulation of viral replication and host-cell responses[4].

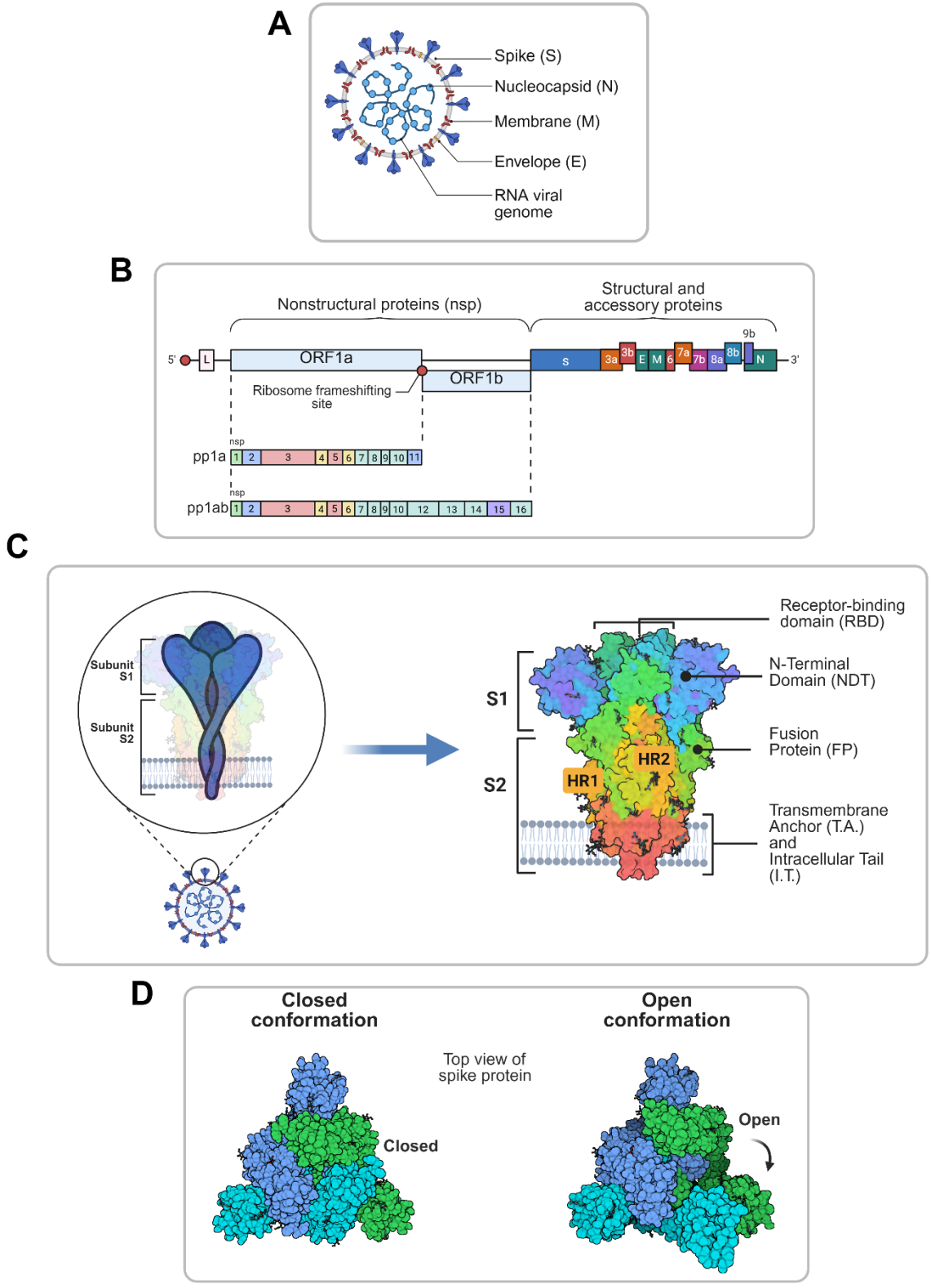

Figure 1.1 SARS-CoV-2 Structure **(A)** Schematic depicting the SARS-CoV-2 virion. **(B)** Schematic outlining the SARS-CoV-2 genome structure. **(C)** SARS-CoV-2 spike protein crystal structure (PDB ID: 6VXX-PDB). **(D)** SARS-CoV-2 spike crystal structures in the open (PDB: 6VYB) and closed (PBD: 6VXX) conformations. Figures were adapted from Biorender templates.

Structure and function of SARS-CoV-2 spike protein.

The spike protein is a heavily glycosylated, type I transmembrane protein (Figure 1.1C) [5]. The spike protein consists of two subunits: S1 and S2. The S1 subunit is comprised of the N-terminal domain (NTD) and receptor binding domain (RBD). The S2 subunit is comprised of the fusion peptide, the heptapeptide repeat sequence (HR1), HR2, transmembrane domain (TM) and cytoplasmic domain. Together, the S1 and S2 subunits non-covalently associate to form a bulbous head and stalk, with the three RBDs of the trimer forming the apex of the head. The S1 subunit mediates binding to ACE2 whilst the S2 subunit anchors the S protein to membrane and mediates fusion. Between the S1 and S2 regions is a polybasic cleavage site, which is cleaved by host cell proteases to facilitate membrane fusion [3]. In the post-fusion state, the S1 subunit disengages from S2.

The three RBDs of the SARS-CoV-2 spike protein trimer can adopt either an "up" or "down" conformation (Figure 1.1D)[6]. When all three RBDs are in the down position, the spike is in a closed conformation, in which the ACE2-binding site is largely occluded. In contrast, the spike is considered open when at least one RBD adopts the up conformation, rendering the receptor-binding motif accessible for ACE2 engagement. Adoption of the open conformation is therefore a critical step for ACE2 binding and subsequent viral entry.

ACE2-mediated entry and viral fusion mechanisms

ACE2 is a type I transmembrane carboxypeptidase that forms part of the renin–angiotensin–aldosterone system. It functions to convert angiotensin I and angiotensin II into angiotensin-(1-9) and angiotensin-(1-7), respectively[7]. ACE2 expression is a key determinant of SARS-CoV-2 cellular tropism, and viral variants have emerged with mutations in the spike protein that enhance binding affinity to ACE2[8]. ACE2 is highly expressed in ciliated epithelial cells of the nasal mucosa, the bronchial epithelium, and type II alveolar cells of the lung, with lower levels of expression reported in other tissues[9].

Entry of SARS-CoV-2 into susceptible cells occurs through a multi-step process. Infection is initiated by binding of the spike receptor-binding domain (RBD) to ACE2. Following receptor engagement, the spike protein must be proteolytically cleaved by host proteases to enable membrane fusion (Figure 1.2A). Transmembrane serine protease 2 (TMPRSS2), expressed at the cell surface, is a major mediator of spike activation and facilitates plasma membrane fusion (early entry pathway)[3]. Alternatively, virus–receptor complexes can be internalised via endocytosis and trafficked to endosomal compartments, where cleavage is mediated by

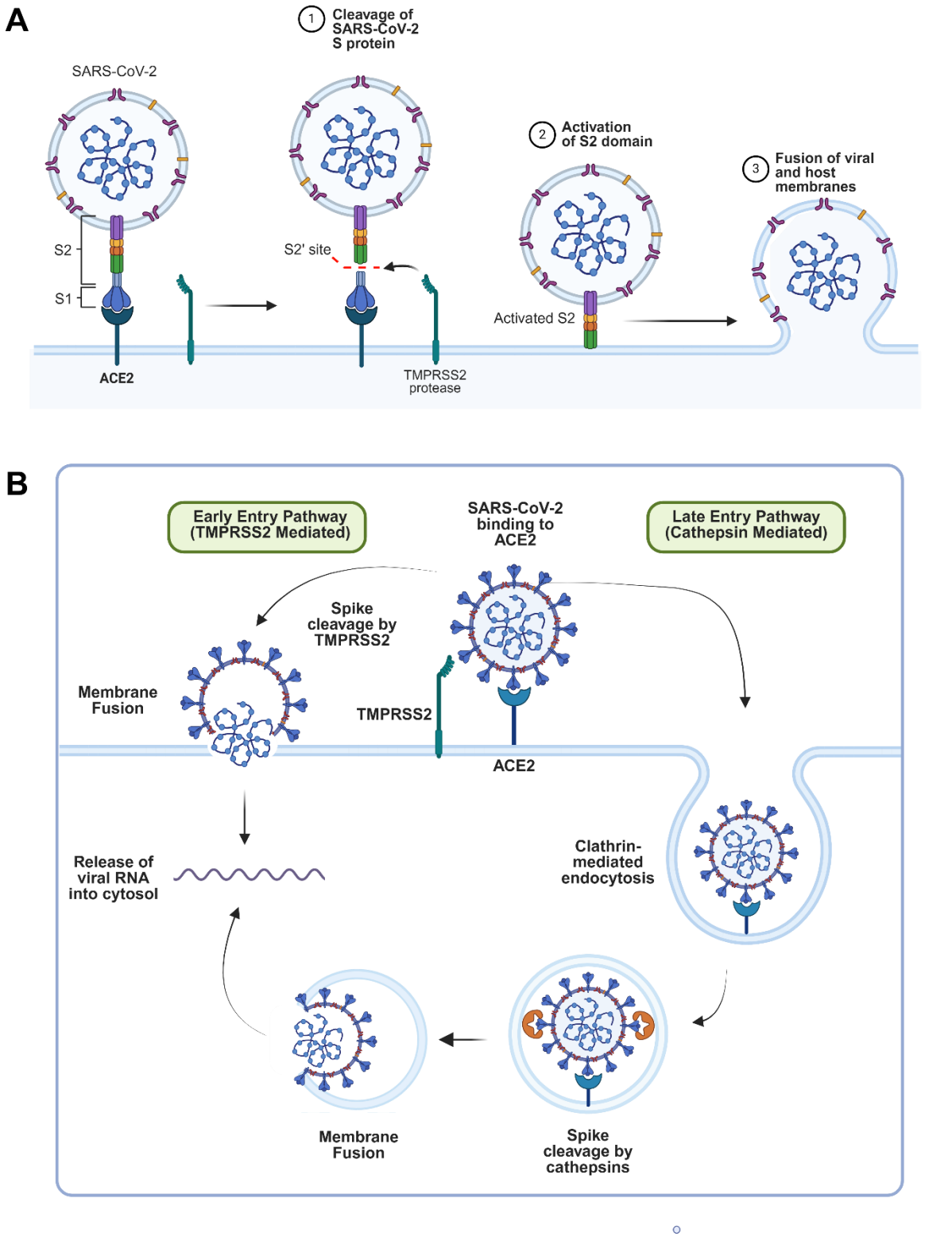

Figure 1.2 ACE2-mediated entry and fusion. (A) Schematic depicting cleavage of the SARS-CoV-2 spike by host proteases and subsequent membrane fusion. **(B)** Schematic outlining the SARS-CoV-2 early (TMPRSS2) and late (cathepsin) entry pathways. Figures were adapted from Biorender templates.

cathepsins, such as cathepsin L or B (endosomal entry pathway) (Figure 1.2B). Although SARS-CoV-2 preferentially utilises TMPRSS2-mediated entry, the endosomal pathway can be used when surface protease expression is limited. Proteolytic activation of spike triggers conformational changes that expose the fusion peptide, allowing insertion into the host membrane, membrane fusion, and release of the viral genome into the cytosol to initiate replication[5].

SARS-CoV-2: Replication cycle

The positive-sense SARS-CoV-2 genomic RNA is translated by host cell machinery to produce polyproteins pp1a and pp1ab (Figure 1.3)[10]. These polyproteins are cleaved by virally encoded proteases, including the main protease (Mpro, nsp5) and papain-like protease (PLpro, part of nsp3), into non-structural proteins (nsps) 1-16. The nsps remodel endoplasmic reticulum membranes to form double-membrane vesicles (DMVs), which serve as the primary sites of viral replication[11]. Within these structures, the replication-transcription complex (RTC), including the RNA-dependent RNA polymerase (RdRp), synthesises full-length negative-sense RNA intermediates. These negative strands act as templates for the production of new genomic RNA.

In addition, a nested set of subgenomic RNAs (sgRNAs) is generated through discontinuous transcription[12]. These sgRNAs are translated to produce structural and accessory proteins. The nucleocapsid (N) protein associates with genomic RNA to form ribonucleoprotein complexes, which are assembled into virions within the endoplasmic reticulum-golgi intermediate compartment (ERGIC)[10]. Newly formed virions are subsequently trafficked through the secretory pathway and released from the cell via exocytosis.

Clinical spectrum and immunopathogenesis of COVID-19

COVID-19 exhibits a broad spectrum of clinical outcomes, ranging from asymptomatic infection to severe respiratory failure[13]. The majority of patients experience mild to moderate symptoms, including cough, fever, and fatigue. However, a subset of individuals develop severe disease characterised by acute respiratory distress syndrome (ARDS), systemic inflammation, and, in some cases, multi-organ dysfunction.

Severe disease is not solely attributable to direct viral cytopathic effects but is strongly associated with dysregulated host immune responses[14]. In particular, excessive activation of innate immune pathways, including monocyte-derived macrophage responses, has been implicated in disease pathogenesis[15]. Severe COVID-19 is associated with elevated levels of pro-inflammatory cytokines and chemokines, including IL-6, TNF-α, and IL-1β, sometimes described

as a “cytokine storm”, although the magnitude and composition of this response vary between patients [16,17]. In addition to hyperinflammation, impaired or delayed type I interferon responses have been linked to severe disease, suggesting a failure of early antiviral control followed by excessive inflammatory activation[18]. In this stage of disease, treatment strategies often include immunomodulatory therapies such as corticosteroids, which dampen excessive inflammation and improve clinical outcomes[19].

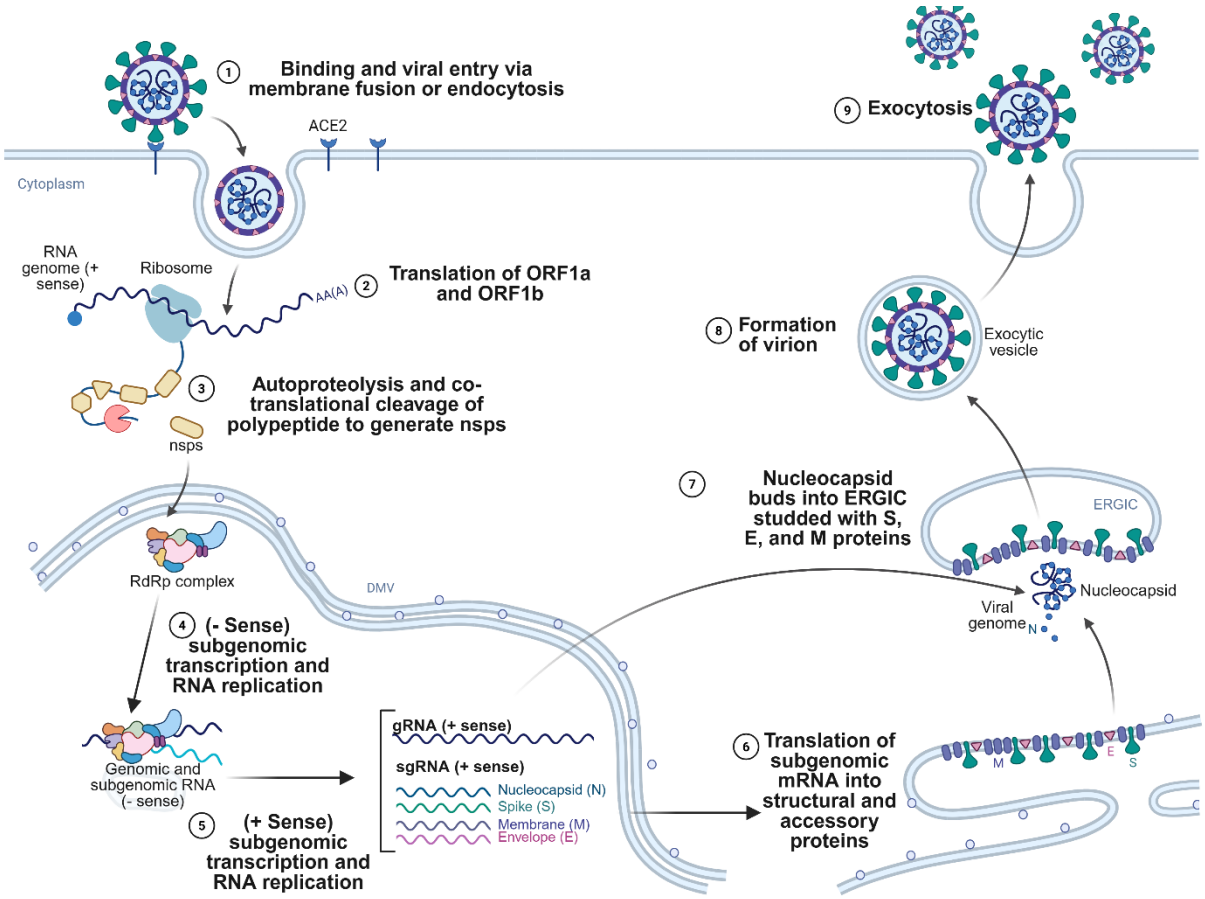

Figure 1.3 SARS-CoV-2 replication cycle. Figure was adapted from Biorender template.

1.2 Immune response to SARS-CoV-2

Cellular immune response to SARS-CoV-2

The nature and severity of COVID-19 are strongly influenced by the host immune response, which determines the extent of viral spread within the respiratory tract and the degree of tissue damage. The ability to mount an effective immune response varies between individuals and is influenced by factors including age, sex, and underlying comorbidities[20].

Infection is initiated when inhaled virions infect permissive epithelial cells within the upper respiratory tract. Epithelial cells represent a critical first line of defence and act as primary sensors of infection. Viral RNA is detected by pattern recognition receptors (PRRs), including endosomal Toll-like receptors (TLR3 and TLR7) and cytoplasmic sensors such as melanoma differentiation-associated protein 5 (MDA5) and retinoic acid–inducible gene I (RIG-I)[21–23]. In addition, TLR2 and TLR4 have been reported to recognise viral proteins such as spike and envelope proteins[24–26]. Activation of these receptors triggers signalling cascades that result in the production of type I interferons (IFNs), which act in both autocrine and paracrine manners to induce antiviral responses. An early and robust interferon response is critical for limiting viral replication and spread, whereas delayed or impaired signalling has been associated with severe disease[18].

Infected epithelial cells also produce pro-inflammatory cytokines, such as IL-1 and IL-6, and chemokines that recruit immune cells to the site of infection[16]. Recruited cells, including monocytes, macrophages, and dendritic cells, further sense viral components through PRRs and amplify the inflammatory response through the production of cytokines such as IL-6 and TNF[15]. This is followed by activation of the adaptive immune response, in which dendritic cells prime T cells and B cells, leading to cytotoxic clearance of infected cells and the production of virus-specific antibodies. In individuals with mild to moderate disease, these responses are typically well coordinated, resulting in viral clearance and restoration of tissue homeostasis, a process supported by regulatory T cells and tissue-resident macrophages.

Antibody responses to SARS-CoV-2

The spike protein is the primary target of the antibody response to SARS-CoV-2[27]. Antibodies can be broadly classified as neutralising or non-neutralising, with neutralising antibodies preventing viral entry into host cells.

Neutralising antibodies have been identified in COVID-19 patients that target multiple regions of the spike protein, including the NTD and RBD within the S1 subunit, as well as the stem helix and fusion peptide within the S2 subunit[28]. Antibodies targeting the RBD dominate the neutralising antibody response[27] and can be further classified according to their binding epitopes, as discussed in Chapter 4. The mechanisms of neutralisation are diverse: some antibodies directly block ACE2 binding, while others inhibit conformational changes in the spike protein, restrict access to the S2' cleavage site, or prevent dissociation of the S1 subunit, thereby inhibiting membrane fusion[29].

A substantial proportion, over 80%, of the anti-spike antibody response consists of non-neutralising antibodies[30]. These antibodies mediate antiviral effects through Fc-dependent effector functions. Antibodies can act as opsonins, binding to viral particles and promoting their uptake and clearance by phagocytes, such as macrophages and neutrophils, through antibody-dependent cellular phagocytosis (ADCP). Antibodies can also activate the complement cascade through binding of C1q to the Fc region, facilitating opsonisation or, in some cases, direct lysis of pathogens. In addition, antibodies that recognise viral antigens on infected cells can promote their elimination via antibody-dependent cellular cytotoxicity (ADCC)[31]. In some contexts, however, Fc-mediated functions may also influence viral entry and infection outcomes.

Fc-mediated effector functions are mediated through interactions between the antibody Fc region and Fc receptors expressed on immune cells. IgG antibodies exist as multiple subclasses that differ in their affinity for Fc receptors and their capacity to mediate effector functions[32]. These differences are discussed in more detail in Chapter 4.

1.3 Macrophage Biology

Macrophage polarisation

Macrophage polarisation refers to the process by which macrophages alter their phenotype and functional responses in response to environmental stimuli. The classical M1–M2 framework describes two extremes of macrophage activation and is widely used to categorise macrophage functional states (Figure 1.4A)[33]. However, this binary model represents an oversimplification, as macrophage activation exists along a continuum of phenotypes influenced by tissue environment and signalling context[34].

Classically activated (M1) macrophages are induced by stimuli such as interferon-γ (IFN-γ) and microbial products including lipopolysaccharide (LPS). These cells exhibit strong antimicrobial

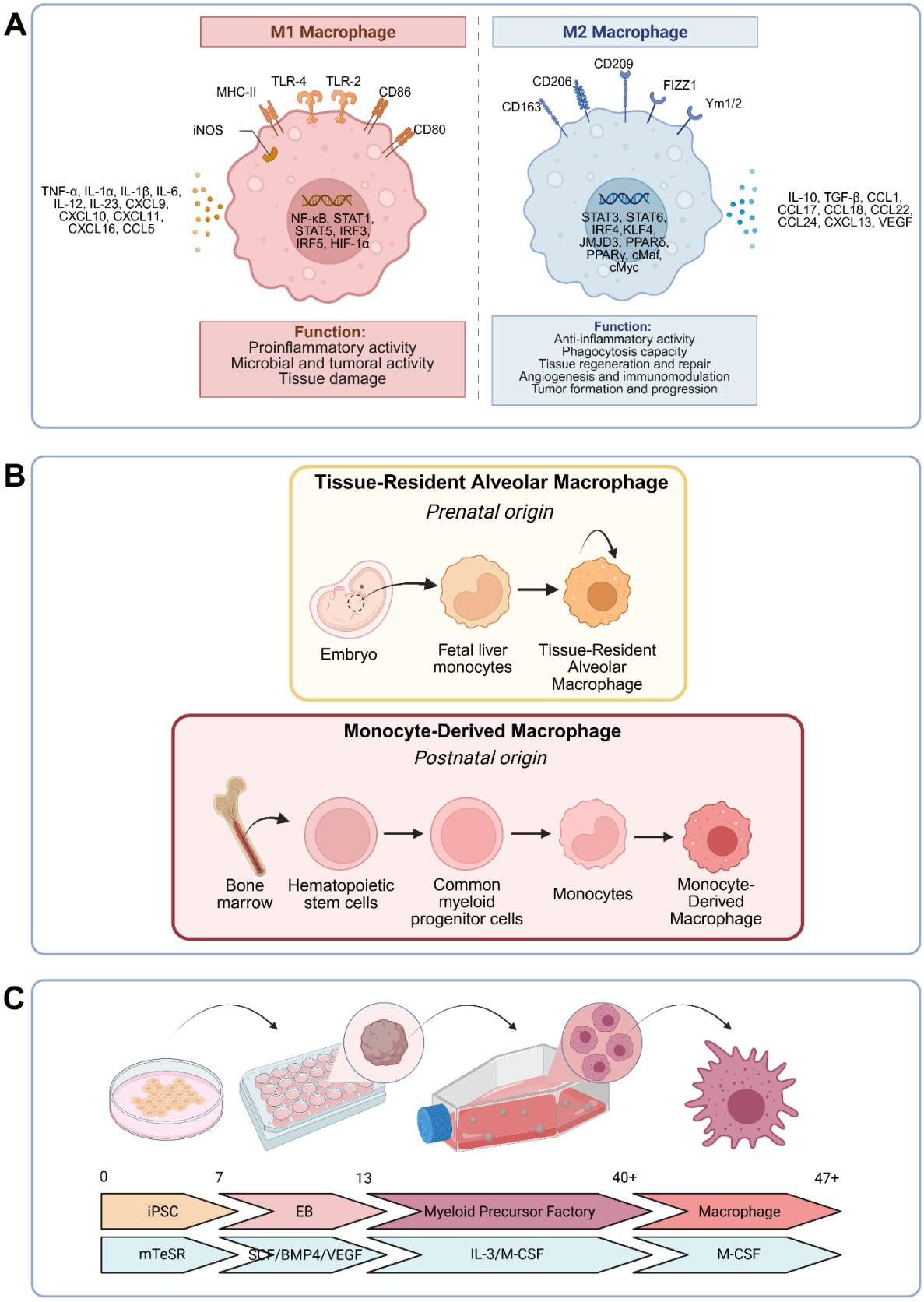

Figure 1.4 Macrophage ontogeny and phenotype. (A) Schematic depicting the M1-M2 framework of macrophage polarisation. (B) Ontogeny of tissue-resident and monocyte-derived macrophages. (C) Method for differentiation of iPSCs to tissue-resident macrophages (Van Wilgenburg et al. 2013). Figure adapted from Washer et al. 2020. Figures adapted from Biorender templates.

activity and produce pro-inflammatory mediators, including reactive oxygen species (ROS) and cytokines such as IL-6, TNF-α, and IL-1β. Alternatively activated (M2) macrophages are typically induced by cytokines such as IL-4 and IL-13. These cells are associated with tissue repair, resolution of inflammation, and enhanced phagocytic capacity, and produce anti-inflammatory mediators including IL-10 and transforming growth factor-β (TGF-β).

Tissue-resident and monocyte-derived macrophages in the lung

Macrophages are the most abundant immune cell in the lung and can be broadly divided into two major subsets: alveolar macrophages (AMs) and monocyte-derived macrophages, which differ in their origin, maintenance, and function (Figure 1.4B)[35].

Alveolar macrophages are tissue-resident immune cells located within the airspace lumen of the pulmonary alveoli. These cells originate from embryonic progenitors, primarily from the yolk sac and foetal liver, and populate the lung shortly after birth [36]. AMs are self-renewing and largely independent of bone marrow input under steady-state conditions, relying on local signals such as GM-CSF and TGF-β for their development and maintenance[37]. The lungs are continuously exposed to inhaled particles and microorganisms[38], and AMs serve as the primary immune cells responsible for maintaining homeostasis in this environment. In the steady state, AMs exhibit a predominantly anti-inflammatory "M2-like" phenotype, characterised by efficient phagocytosis of inhaled particles and apoptotic cells, while limiting excessive inflammatory responses that could damage the delicate alveolar structure[36].

Upon infection or tissue injury, AMs can rapidly shift towards a more pro-inflammatory phenotype, increasing phagocytic activity, reactive oxygen species production, and secretion of cytokines and chemokines to recruit additional immune cells. While this response is essential for pathogen clearance, excessive or prolonged activation can contribute to lung injury and fibrosis. AMs also play a role in antigen presentation and modulation of adaptive immune responses within the lung. Thus, AMs can be considered functionally plastic cells that maintain tissue homeostasis under basal conditions while acting as key sentinels during infection.

In contrast, monocyte-derived macrophages arise from circulating bone marrow-derived monocytes that are recruited to tissues during inflammation. These cells differentiate in situ and are typically associated with inflammatory responses. Compared with AMs, monocyte-derived macrophages have limited self-renewal capacity and are more transient, often undergoing apoptosis or exiting the tissue following resolution of inflammation. They are generally characterised by a more pro-inflammatory phenotype, producing high levels of cytokines and

contributing to pathogen clearance, but can also drive tissue damage if dysregulated. Although often described as "M1-like", their phenotype is highly context-dependent and can evolve during the course of inflammation[34].

Both alveolar and monocyte-derived macrophages have been implicated in the immune response to SARS-CoV-2 infection[15]. However, their distinct functional properties may influence susceptibility to viral infection and functional responses to the virus.

In vitro models for the study of human macrophages

As discussed, monocyte-derived macrophages and tissue-resident alveolar macrophages are distinct cell populations arising from different developmental origins[35]. The selection of an appropriate in vitro model that reflects the macrophage subset under investigation is therefore critical for drawing biologically relevant conclusions.

Primary AMs are challenging to obtain in sufficient quantities. They can be isolated from bronchoalveolar lavage (BAL) fluid collected via bronchoscopy; however, this is an invasive procedure, and access to healthy donor samples is limited. BAL samples are most commonly obtained from individuals with underlying pulmonary disease, which may alter macrophage phenotype. Furthermore, although BAL-derived cells are predominantly tissue-resident macrophages, the presence of recruited monocyte-derived macrophages cannot be excluded. Animal models can also be used as a source of alveolar macrophages, but these are limited by interspecies differences and reduced translational relevance to human biology.

Macrophages derived from human induced pluripotent stem cells (iPSCs) provide an alternative approach that overcomes many limitations of primary models. The differentiation method developed by the James and Cowley laboratory recapitulates embryonic MYB-independent haematopoiesis, generating macrophages with features of tissue-resident populations (Figure 1.4C)[39]. iPSC-derived macrophages have been shown to closely resemble terminally differentiated tissue-resident macrophages in phenotype and function[40]. In addition, this system enables scalable production of cells and allows genetic manipulation, making it a powerful and reproducible model for mechanistic studies.

In contrast, monocyte-derived macrophages can be more readily obtained from peripheral blood. Peripheral blood mononuclear cells (PBMCs), which are routinely isolated from blood donations, provide a readily accessible source of monocytes that can be differentiated into macrophages using macrophage colony-stimulating factor (M-CSF)[41]. While this model is physiologically relevant for studying monocyte-derived macrophages, it is subject to donor-to-

donor variability and unknown donor genetic backgrounds. Moreover, primary macrophages are difficult to genetically manipulate due to their terminal differentiation status and their propensity to mount inflammatory responses to introduced nucleic acids. Importantly, monocyte-derived macrophages do not accurately model tissue-resident macrophage populations.

Immortalised macrophage cell lines are frequently used as an alternative to primary cells and iPSC-derived models. Commonly used examples include RAW264.7 cells, derived from murine macrophages, and THP-1 cells, a human monocytic cell line that can be differentiated into macrophage-like cells using phorbol 12-myristate 13-acetate (PMA). However, these cell lines originate from transformed or cancerous cells and therefore do not fully recapitulate the physiology of primary macrophages. Indeed, several studies have demonstrated significant differences in phenotype and function between THP-1-derived macrophages and primary monocytes [42–45]. While such models are useful for certain functional assays, their relevance to physiological macrophage biology is limited, particularly in the context of tissue-resident macrophages. These considerations are particularly important when investigating macrophage permissiveness to SARS-CoV-2 infection, where cellular origin and activation state may influence susceptibility.

1.4 Role of alveolar macrophages in COVID-19

The highly plastic nature of AMs enables them to rapidly respond to SARS-CoV-2 infection. AM activation can be driven by inflammatory mediators released from infected epithelial cells, as well as potentially through direct sensing of viral components. Upon activation, AMs exhibit increased phagocytic activity, enhanced production of reactive oxygen species (ROS), and elevated secretion of pro-inflammatory cytokines and chemokines, including IL-1β, CCL2, CCL3, and CCL7, which promote the recruitment of CCR2-expressing monocytes to the lung [46]. AMs are also important producers of type I IFNs, which are critical for early antiviral defence, particularly in the context of SARS-CoV-2-mediated suppression of interferon responses in epithelial cells.

In the context of mild to moderate infection, AMs contribute to effective immune control and resolution of inflammation. Following viral clearance, they promote the restoration of tissue homeostasis through phagocytosis of apoptotic cells, including neutrophils, thereby preventing the release of cytotoxic intracellular contents. AMs also produce anti-inflammatory mediators,

such as IL-10, TGF-β, and prostaglandins, which suppress excessive immune activation, and secrete factors including amphiregulin that support epithelial repair.

Ex vivo AMs from patients with COVID-19 have been reported to contain SARS-CoV-2 viral material. However, whether this reflects direct infection or uptake of virions and infected-cell debris, remains controversial. Immunohistochemical analyses of post-mortem lung tissue have demonstrated the presence of SARS-CoV-2 RNA and protein within AMs [47]. Similarly, scRNA-seq studies of COVID-19 lungs have identified viral RNA within AMs [48,49]. Other analyses of human and macaque BAL samples have reported the detection of dsRNA and viral non-structural proteins within AMs, findings that have been interpreted as evidence of active viral replication[50,51]. However, these markers do not definitively prove productive infection, as they could also be acquired through phagocytosis of infected epithelial cells containing replication intermediates and viral proteins. Consequently, although the presence of SARS-CoV-2-derived material within alveolar macrophages is well established, whether macrophages themselves support viral replication in vivo remains unresolved. This question has been investigated extensively using in vitro systems and is discussed in detail in Chapter 4.

Regardless of their infectious status, accumulating evidence suggests that macrophages may contribute to disease pathogenesis in severe COVID-19[52]. Patients with severe disease exhibit increased numbers of macrophages in the lung, many of which display a highly inflammatory transcriptional profile compared with those in mild disease [50,53,54]. Elevated levels of macrophage-derived cytokines and monocyte chemoattractants have been reported and share features with macrophage activation syndrome [55–58]. These findings suggest that dysregulated macrophage activation contributes to the excessive inflammatory response observed in severe disease. This hyperinflammatory state can lead to hypoxia, respiratory failure, and multi-organ dysfunction[17].

In addition to excessive inflammation, impaired resolution of inflammation has been observed in COVID-19[14], potentially due to dysregulation or depletion of key immune cell populations within the lung [59]. This can contribute to the development of pulmonary fibrosis, a process in which normal tissue repair is disrupted, leading to deposition of extracellular matrix and collagen and impaired gas exchange. Macrophages are important regulators of fibrotic responses, in part through the production of profibrotic mediators such as TGF-β and are therefore likely to contribute to fibrosis observed in severe COVID-19.

1.5 Scope of work

Knowledge Gaps

The first knowledge gap addressed in this thesis is how SARS-CoV-2 is internalised into alveolar macrophages. While there is general agreement that SARS-CoV-2 can enter macrophages, the mechanisms underlying this process remain unclear. It is unknown whether viral entry represents a bona fide infection mediated by ACE2 or alternative receptors, or whether uptake occurs through non-specific pathways such as clathrin- or caveolin-mediated endocytosis or fluid-phase macropinocytosis. Defining the mechanisms of viral entry is critical for understanding the subsequent intracellular fate of the virus. The current literature on this topic is reviewed in Chapter 3.

The second knowledge gap addressed is the fate of SARS-CoV-2 following internalisation into alveolar macrophages. Conflicting reports exist regarding whether macrophages support productive viral replication and the conditions under which this may occur. Clarifying whether SARS-CoV-2 undergoes productive, abortive, or degradative processing within macrophages is essential for understanding their role in infection. The relevant literature is outlined in Chapter 4.

The third knowledge gap concerns how exposure to SARS-CoV-2 affects macrophage viability and function, including phagocytosis, antigen presentation, and cytokine secretion. In severe COVID-19, macrophage responses are characterised by hyperinflammation and dysregulation; however, it remains unclear whether these changes arise from direct viral sensing or manipulation, or from secondary effects of the inflammatory lung environment. This includes signals derived from infected epithelial cells and recruited immune populations. Current evidence relating to macrophage functional responses is reviewed in Chapter 5.

Together, these knowledge gaps highlight the need to define the role of alveolar macrophages in COVID-19. Macrophages may contribute to disease through multiple mechanisms, including direct infection, dysregulated inflammatory responses, or impaired execution of key functions such as pathogen clearance, immune coordination, and resolution of inflammation. Alternatively, macrophage dysfunction may arise as a consequence of the inflammatory lung environment rather than direct viral effects.

Although the role of macrophages in COVID-19 has been extensively studied, the rapid pace of research during the pandemic and the frequent use of non-physiological model systems have resulted in a literature that is, at times, inconsistent and difficult to interpret. This thesis aims to

address these challenges by providing a systematic and mechanistic analysis of SARS-CoV-2 interactions with human macrophages, using a physiologically relevant iPSC-derived model to generate clear insights into their role in disease.

DPhil Aims

My PhD research is set out in three results chapters with a defined focus:

1) What is the mechanism of macrophage internalisation of SARS-CoV-2?
2) Are alveolar macrophages permissive to SARS-CoV-2 productive infection?
3) How does SARS-CoV-2 exposure impact alveolar macrophage functions?

Chapter 2: Materials and Methods

2.1 Viral Propagation and Quantification

Propagation of SARS-CoV-2 Stocks

SARS-CoV-2 work was conducted in a Containment Level 3 (CL3) facility within the Department of Pathology, University of Oxford, in accordance with UK Health and Safety Executive regulations. All work was performed under an approved code of practice, with appropriate risk assessments in line with Advisory Committee on Dangerous Pathogens (ACDP) guidance, and standard operating procedures. SARS-CoV-2 isolates were obtained from multiple sources. The ancestral strain Victoria/01/2020 and Alpha (B.1.1.7) were obtained from Public Health England (Porton Down, UK). Beta (B.1.351) was obtained from the Centre for the AIDS Programme of Research in South Africa (CAPRISA), and Delta (B.1.617.2) from the Laboratory of Clinical and Epidemiological Virology, Rega Institute, KU Leuven (Belgium). Omicron (B.1.1.529) subvariant BA.5 was obtained from the African Health Research Institute, and XBB.1.5 from BEI Resources (USA). Omicron subvariants XBB.1.16, EG.5.1, BA.2.86, and JN.1 were generated as reverse genetics-derived spike chimeric viruses[60].

For viral propagation, Vero E6/TMPRSS2 cells were seeded at 4 x 10^6 cells per T75 flask and infected with viral inoculum at a multiplicity of infection (MOI) of 0.01. The inoculum was incubated with cells for 10 min at room temperature (RT), after which 20 mL of Dulbecco's Modified Eagle Medium (DMEM; high glucose, Sigma, D6429) supplemented with 1% foetal bovine serum (FBS; Sigma, F9665) was added. Flasks were incubated at 37 °C with 5% CO_2 for 24 h. Upon observation of cytopathic effect (CPE), viral supernatants were harvested and clarified by centrifugation at 300 xg for 5 min. Clarified supernatants were concentrated using a 100 kDa molecular weight cut-off Amicon® Ultra centrifugal filter (Millipore, UFC510008) by centrifugation at 4,000 xg for 10 min. Viral stocks were aliquoted and stored at −80 °C.

Focus forming assay (FFA) for viral titration

Viral titres were determined by focus-forming assay (FFA). CCL81 Vero cells (ATCC, CCL-81) cells were seeded in 96-well tissue culture plates and cultured to confluence in DMEM supplemented with 10% FBS at 37 °C for 24 h. Media was removed, and cells were inoculated in triplicate with serial dilutions of virus and incubated at 37 °C for 2 h. Following incubation, cells

were overlaid with 1.5% carboxymethylcellulose (CMC; Alfa Aesar, 11449256) in culture medium and incubated at 37 °C for 20 h. The overlay was then removed, and cells were fixed with 4% paraformaldehyde (PFA; Alfa Aesar, J61899) in PBS for 30 min, followed by three washes with PBS. Cells were permeabilised with 2% Triton X-100 (Sigma-Aldrich, T8787) in PBS for 30 min at 37 °C and washed with wash buffer (0.1% Tween-20 (Sigma-Aldrich, P7949) in PBS). Cells were incubated with primary antibody (anti-nucleoprotein human antibody, FB9B, provided by Dr Jack Tan) diluted 1:1000 in wash buffer for 1 h at RT with gentle rocking. Cells were washed three times with wash buffer and incubated with secondary antibody (goat anti-human IgG–HRP, Sigma-Aldrich, A0170) diluted 1:5000 in wash buffer for 1 h at RT with rocking. Following three washes with PBS, cells were incubated with TrueBlue peroxidase substrate (SeraCare, 5510-0050) for 30 min at RT. The staining solution was removed, and cells were washed with dH_2O for 5 min and air-dried. Focus-forming units (FFU) were quantified using an ELISPOT plate reader (AID Autoimmun Diagnostika GmbH).

Ultrafiltration of SARS-CoV-2 stocks

SARS-CoV-2 stocks were concentrated using an ultrafiltration device with a 100 kDa molecular weight cut-off (MWCO; Merck, UFC910008). Viral supernatant harvested from VET cells was applied to the filter and centrifuged at 4,000 xg for 10 min. The filtrate, containing molecules <100 kDa, was discarded, while material >100 kDa, including SARS-CoV-2 virions, was retained in the filter unit. The retained material was resuspended in DMEM supplemented with 1% FBS, resulting in an approximate 20-fold concentration relative to the original viral supernatant. Recovery of infectious viral titre was confirmed by FFA.

UV-C inactivation of SARS-CoV-2 stocks

SARS-CoV-2 stocks with titres of up to 1×10^7 FFU/mL were irradiated with ultraviolet (UV) light to generate replication-deficient viral particles. Aliquots of viral stock (500 µl per well) were transferred to a 24-well tissue culture plate and positioned 3 cm below the UV light source (Stratalinker, UV crosslinker 1800). Plates were maintained on ice throughout irradiation to prevent overheating. UV-C light (254 nm) was applied to a total dose of 200 mJ/cm^2. Complete inactivation of viral replication was confirmed by FFA.

2.2 Cell Culture

Cell Line Culture

Cell lines (Table 2.1) were cultured in T75 flasks in the appropriate culture medium at 37 °C with 5% CO_2. Cells were passaged every 3-4 days. For passaging, cells were harvested using TrypLE™ Express Enzyme (Gibco, 12604013) for 5 min at 37 °C, then gently resuspended in culture medium at a 1:10 dilution. Cells were counted and seeded into plates or flasks at the appropriate density for each experiment.

Table 2.1: Cell lines

Cell Line	Cell Line Origin	Base Medium	Supplements
MDCK	James Lab	DMEM	10% FBS
MDCK-hACE2	James Lab – Transduced by AN	DMEM	10% FBS Puromycin (Alfa Aeasar, J61278; 1 µg/mL)
CCL81 Vero	ATCC	DMEM	10% FBS
Vero E6 TMPRSS2 (VET)	James Lab	DMEM	10% FBS Geneticin (Gibco, 10131035; 200 µg/mL)
Calu-3	ATCC	Advanced DMEM/F12 (Fisher Scientific, 12-634-028)	10% FBS
HEK293T	ATCC	DMEM	10% FBS

Culture of human induced pluripotent stem cells (iPSCs)

Human induced pluripotent stem cell (iPSC) lines used in this study were derived from dermal fibroblasts of disease-free donors and are described in Table 2.2. The SFC840-03-03, SFC841-03-01, and SFC841-03-01 IFNAR2$^{-/-}$ lines were generated at the James and Lillian Martin Centre for Stem Cell Research, University of Oxford, and have been previously described[61–63]. The KOLF2.1S line was generated by the Cellular Operations Gene Editing team at the Wellcome Sanger Institute. iPSCs were thawed into 10 mL Advanced DMEM/F12 (Gibco, 12634028) and centrifuged at 400 xg for 5 min at 15 °C before resuspension in mTeSR (STEMCELL, 05850) supplemented with 10 µM Y-27632 (ROCK inhibitor; Abcam, ab120129) for the first 24 h post-plating. Cells were plated onto Geltrex™-coated plates (Gibco, A1413302) and cultured at 37 °C with 5% CO_2, with complete medium changes every 24 h. At 80-90% confluence, cells were passaged either as a single-cell suspension using TrypLE™ for 3-5 min at 37 °C, or as small clumps using 0.5 mM EDTA (Invitrogen, 15575-030) in PBS for 2-4 min at 37 °C.

Table 2.2: hiPSC Lines				
Line	**Sex**	**Age**	**Bank**	**Reference**
KOLF2.1S	Male	55-59	HipSci	https://hpscreg.eu/cell-line/WTSIi018-B-1
SFC841-03-01 SFC841-03-01 IFNAR2 -/-	Male	35-39	EBiSC	Dafinca et al 2016[62] Hanrath et al., 2022[63]
SFC840-03-03	Female	65-69	EBiSC	Fernandes et al., 2016[61]
BIONi010-C	Male	15-19	EBiSC	Rasmussen et al., 2014[64]
BIONi010-C-17 (TREM2 KO)	Male	15-19	EBiSC	Hall-Roberts et al., 2020[65]

Differentiation of iPSCs into macrophages

iPSCs were differentiated into macrophages using a previously described protocol[39,40]. Embryoid bodies (EBs) were generated by seeding 4 x 10^6 iPSCs into AggreWell™ 800 plates (STEMCELL Technologies, 34815) in mTeSR medium supplemented with 50 ng/mL BMP4 (PeproTech, PHC9534), 50 ng/mL VEGF (PeproTech, PHC9394), 20 ng/mL SCF (Miltenyi Biotec, 130-096-695), and 10 µM ROCK inhibitor. Cells were incubated for 4 days at 37 °C with daily feeding by 75% medium exchange. After 4 days, EBs were transferred into two T175 flasks containing OxM factory medium (Table 2.3). These differentiation cultures ("factories") were maintained at 37 °C with weekly supplementation of 10 mL fresh medium until macrophage precursors (PreMacs) began to be produced. Thereafter, PreMacs were harvested weekly. Harvested PreMacs were seeded at 3 x 10^5 cells per well in 24-well plates or 10 x 10^4 cells per well in 96-well plates in OxM macrophage medium (Table 2.3) and cultured for 7 days to allow terminal differentiation into macrophages. Media was refreshed on day 4.

Table 2.3: Macrophage Media				
	Component	**End Conc.**	**Supplier**	**Cat Number**
OXM Factory medium	Advanced DMEM/F12	96.3%	Gibco	12634010
	GlutaMAX (100x)	2 mM	Gibco	35050-038
	HEPES 1M pH 7.4	15 mM	Gibco	15630080
	Human recombinant Insulin solution	5 µg/mL	Sigma	I9278-5ML
	Tropolone	15 µM	Sigma	T89702-1G
	IL-3	25 ng/mL	Invitrogen	PHC0033
	M-CSF	50 ng/mL	Invitrogen	PHC9501
OXM Macrophage medium	Advanced DMEM/F12	96.5%	Gibco	12634010
	GlutaMAX (100x)	2 mM	Gibco	35050-038
	Human recombinant Insulin solution	5 µg/mL	Sigma	I9278-5ML
	HEPES 1M pH 7.4	15 mM	Gibco	15630080
	M-CSF	50 ng/mL	Invitrogen	PHC9501

Macrophage polarisation

Polarisation of mature macrophages was by a protocol previously described[40]. For the last 16 h of the 7-day differentiation to terminal macrophages, OxM media medium was supplemented with polarising cytokines: 20 ng/mL IFNγ (Thermo, PHC4031) and 100 ng/mL LPS (Sigma-Aldrich, L8274) for 'M1' phenotype, 50 ng/mL IL-4 (R&D systems, 204-IL) for 'M2' phenotype.

THP-1 cell culture and differentiation

THP-1 cells were cultured in suspension in RPMI (Sigma-Aldrich, R8758) supplemented with 10% FBS and maintained at a density of 8 x 10^5 cells/mL. To induce differentiation into macrophage-like cells, THP-1 monocytes were seeded at 4 x 10^5 cells per well in 24-well plates and treated with phorbol 12-myristate 13-acetate (PMA; Alfa Aesar, J63916.M) at 5 ng/mL for 3 days.

Differentiation of primary human monocyte-derived macrophages

Peripheral blood mononuclear cells (PBMCs) were thawed and resuspended in RPMI supplemented with 10% FBS, then seeded at 1 x 10^8 cells per 10 cm dish. Monocytes were allowed to adhere for 6 h, after which non-adherent cells were removed by washing. Adherent monocytes were differentiated into macrophages by culture in medium supplemented with macrophage colony-stimulating factor (M-CSF) at 50 ng/mL for 5 days.

2.3 Lentivirus Generation and Transduction

Lentivirus production

Lentiviral particles were generated by transfecting 1.1 x 10^7 HEK293T (ATCC, CRL-3216) cells in a T175 flask with 5.5 µg psPAX2* (Addgene, 12260), 4.4 µg pMD2.G (Addgene, 12259), and 9.2 µg transgene-encoding plasmid (Table 2.4) using JetPRIME transfection reagent and buffer (Polyplus, 101000046) in DMEM supplemented with 10% FBS. Cells were incubated for 24 h at 37 °C. psPAX2 was omitted for Vpx lentivirus production. Lentiviral supernatants were harvested at 48 h and 72 h post-transfection, clarified by centrifugation at 3,000 rpm to remove cellular debris, and filtered through a 0.45 µM low protein-binding PES filter (Millipore, SLHV033N). Filtered supernatants were concentrated by ultracentrifugation at 29,000 rpm for 2 h at 4 °C. Lentiviral pellets were resuspended in 1.5% bovine serum albumin (BSA; Sigma-Aldrich, A7906) in PBS and stored as single-use aliquots at −80 °C.

Table 2.4: Transfer Plasmids for Lentivirus Generation		
Transgenic Protein	**Plasmid Name**	**Addgene Code**
ACE2	pWPI-IRES-Puro-Ak-ACE2	154985
Vpx	pSIV-D3psi/delta/env/delta Vif/delta Vpr	132928

Transduction of Cell Lines

For transduction with ACE2 lentivirus, cell lines were seeded in 6-well plates in Advanced DMEM/F12 supplemented with 10% FBS to achieve approximately 70% confluence on the day of transduction. Cells were transduced with ACE2 lentivirus diluted 1:100 in culture medium supplemented with 5 µg/mL polybrene (Sigma Aldrich, TR-1003) and incubated for 24 h.
At day 5 post-transduction, puromycin selection was applied at 2 µg/mL. Transduced cell lines were cryopreserved as single-use vials in the vapour phase of liquid nitrogen. For maintenance, transduced cells were cultured in DMEM/F12 supplemented with 10% FBS and 2 µg/mL puromycin to retain transgene expression.

Transduction of Macrophages

PreMacs were seeded at 1 x 10^6 cells per well in 6-well plates in OxM medium. Lentivirus encoding ACE2 and Vpx was added directly to the culture medium at 10 µL ACE2 lentivirus and 1 µL Vpx lentivirus per 1 x 10^6 cells. Cells were incubated for 24 h to allow transduction, followed by differentiation in OxM medium for 7 days.

2.4 SARS-CoV-2 antibodies and recombinant proteins

Monoclonal antibody and recombinant protein expression and purification

SARS-CoV-2 monoclonal antibodies and recombinant spike proteins, and RBD-Fc fusion protein, were expressed and purified by Diana Melynk and Dr Jack Tan (Tan Lab) and Madeeha Afzal (James/Cowley Lab), respectively. The antibodies and recombinant proteins are listed in table 2.5. ExpiCHO cells (Thermo, A29133) were transfected with the plasmids encoding monoclonal antibody, RBD-Fc fusion protein or spike sequences using ExpiFectamine™ transfection reagent (Mirus bio, Cat#MIR2300) and incubated at 37 °C with 8% CO_2 and shaking at 120 rpm. At 24 h post-transfection, cultures were treated with enhancer according to the manufacturer's instructions and incubated at 32 °C with 5% CO_2. After 5–7 days, cells were harvested by centrifugation and supernatants were collected for downstream purification.

Monoclonal antibodies were purified from the supernatant by affinity chromatography using a HiTrap MabSelect SuRe column (Cytiva, 11003493) according to the manufacturer's instructions. Purified antibodies were analysed by SDS–PAGE to assess purity. Endotoxin was quantified using chromogenic endotoxin quant kit (Pierce, A39552) depleted from recombinant spike proteins using high-capacity endotoxin removal spin columns (Pierce, 88275) according to manufacturer's instructions.

Table 2.5: SARS-CoV-2 antibodies and recombinant proteins

Antibody	Type	Epitope	Reference
FI-1C	Neutralising	RBD - Class 1/2	Huang et al., 2021[66]
FI-3A	Neutralising	RBD - Class 1/2	Huang et al., 2021
C121	Neutralising	RBD- Class 2	Robbiani et al., 2020[27]
FD-11A	Neutralising	RBD - Class 3	Huang et al., 2021
FN-12A	Non-neutralising	RBD - Class 3	Huang et al., 2021
FJ-10B	Non-neutralising	RBD - Class 3	Huang et al., 2021
REGN10987	Neutralising	RBD - Class 3	Hansen et al., 2020[67]
S309	Neutralising	RBD - Class 3	Pinto et al., 2020[68]
FD-5D	Neutralising	RBD - Class 3	Huang et al., 2021
C118	Neutralising	RBD - Class 1/4	Jette et al., 2021[69]
S2X-259	Neutralising	RBD - Class 1/4	Tortoricini et al., 2021[70]
EY-6A	Neutralising	RBD - Class 4	Huang et al., 2021
IY-2A	Neutralising	RBD - Class 4	Huang et al., 2021
FD-7C	Non-neutralising	Spike - S1	Huang et al., 2021
EW-8B	Non-neutralising	Spike - S1	Huang et al., 2021
FJ-1C	Neutralising	Spike - S1	Huang et al., 2021
FD-1E	Neutralising	Spike - S1	Huang et al., 2021
FD 11E	Neutralising	Spike - S1	Huang et al., 2021
FB 9D	Non-neutralising	Spike - S2	Huang et al., 2021
FN-2C	Non-neutralising	Spike - S2	Huang et al., 2021
FB 1E	Neutralising	Spike - S2	Huang et al., 2021
E1 Isotype IgG1	Isotype control		
Flu N IgG1	Isotype control		
SpyCatcher-Fc Fusion	Isotype control		
Fc mutated RBD-Fc			
HexaPro Spike Trimer (Various strains)			

Structure and Modelling

Interacting residues between antibody and SARS-CoV-2 RBD were determined using ChimeraX (version 1.11rc202512130101). The PDB structures of RBD-antibody complexes were EY 6A (6ZER), IY 2A (7YCN), C118 (7RKV) and S2X-259 (7RAL). Intermolecular contacts were defined using the Contacts tool, with interactions identified based on an interatomic distance cut-off of ≤ 3.5 Å between atoms of the RBD and antibody chains. Solvent molecules were excluded from the analysis. Residues were considered interacting if at least one atom satisfied this distance criterion. Contact residues were then overlaid on SARS-CoV-2 ancestral RBD structure (PDB: 6M0J).

2.5 General Macrophage Assays

Cell viability assay

Macrophages were pre-treated with the indicated conditions. CellTiter 96® AQueous One Solution Cell Proliferation Assay reagent (Promega, G3582) was added directly to each well containing 100 µL of culture medium and incubated for 1 h at 37 °C. Absorbance was measured at 490 nm. Background absorbance from reagent-only and medium-only controls was subtracted, and values were expressed as a percentage relative to untreated cells.

Cargo internalisation assays

Transferrin-AF647, 70 kDa dextran-TRITC, and zymosan A-AF488 were used as cargo markers for clathrin-mediated endocytosis, macropinocytosis, and phagocytosis, respectively (Table 2.8). Reagent concentrations and flow cytometry settings (lasers and filters) are detailed in Figure 2.8. Macrophages were incubated with cargo particles at indicated concentrations for 2 h at 37 °C. Zymosan particles were sonicated immediately prior to use. Following incubation, cells were washed with PBS, detached using TrypLE™, and fixed in 4% PFA in PBS for 10 min. Intracellular fluorescence was acquired using a BD LSRFortessa™ X-20 flow cytometer.

Pharmacological inhibition assays

Macrophages were pre-treated with inhibitors (table 2.6) at the indicated concentrations for 1 h at 37 °C. Following pre-treatment, virus or control particles were added in the continued presence of inhibitors and incubated for a further 2 h at 37 °C. Cells were then washed twice with PBS, harvested using TrypLE™, and analysed by flow cytometry.

Table 2.6: Pharmacological Inhibitors		
Inhibitor	**Supplier**	**Cat Number**
Dynasore	Cayman	14062
Chlorpromazine	Cayman	CAY16129-500 mg
EIPA	Cayman	14406-5 mg-CAY
Cytochalasin D	Cayman	CAY11330-1 mg
Wortmannin	Cayman	10010591-1 mg-CAY
IPA-3	Cayman	14759-5 mg-CAY
NSC23766	Cayman	13196-1 mg-CAY
UNC569	Cayman	22966-1 mg-CAY

2.6 SARS-CoV-2 Assays

SARS-CoV-2 Challenges

Cells were incubated with SARS-CoV-2 Victoria/01/2020 (VIC01), unless otherwise stated, at the indicated MOI for 2 h at 37 °C. Following incubation, the inoculum was removed, cells were washed twice with PBS, and fresh culture medium was added. Cells were then incubated at 37 °C until the experimental endpoint.

SARS-CoV-2 binding and internalisation assay (RT-qPCR)

Cells were incubated with SARS-CoV-2 VIC01 at a MOI of 1 for 2 h at either 4 °C or 37 °C. Following incubation, cells were washed and treated with proteinase K (Sigma-Aldrich, P6556) at 1 mg/ml for 30 min at 37 °C to remove surface-bound virions. SARS-CoV-2 ORF1ab and N gene levels were quantified by TaqMan RT-qPCR and normalised to RNase P expression, as described in the RT-qPCR methods section.

Inhibition of SARS-CoV-2 internalisation assay (flow cytometry)

Macrophages were pre-treated with inhibitors at the indicated concentrations or anti-IFNAR2 antibody (Thermo, 213851) at 1µg/mL for 1 h at 37 °C. Following pre-treatment, cells were incubated with SARS-CoV-2 VIC01 in the continued presence of inhibitors or antibody for 2 h at 37 °C. Cells were then washed twice with PBS, harvested using TrypLE™, and analysed by intracellular anti-nucleoprotein staining followed by flow cytometry, as described in the flow cytometry section.

Antibody-mediated SARS-CoV-2 internalisation assays

SARS-CoV-2 VIC01 was pre-incubated with antibodies at 1 µg/mL (table 2.5) or human plasma (Caroll lab donors) at NT50, for 15 min at RT, to allow binding. Virus-antibody mixtures were added to macrophages at MOI 10 and incubated for 2 h at 37 °C to allow uptake. Cells were washed, harvested, and stained for intracellular anti-nucleoprotein flow cytometry, as outlined in the flow cytometry section.

Antibody mediated SARS-CoV-2 productive infection assays

SARS-CoV-2 VIC01 was pre-incubated with antibodies at 1 µg/ml or human plasma at NT_{50} (Table 2.5) for 15 min at RT to allow binding. Virus–antibody mixtures were then added to macrophages at MOI 10 and incubated for 2 h at 37 °C to permit uptake. Cells were subsequently washed, harvested, and stained for intracellular anti-nucleoprotein detection by flow cytometry, as described in the flow cytometry section.

Macrophage/T cell antigen presentation assays

Antigen-specific B and T cell clones were provided by the Dong group (Chinese Academy of Medical Sciences, University of Oxford) and are listed in Table 2.7. KOLF2.1S macrophages were seeded at 1 x 10^5 cells per well and infected with SARS-CoV-2 VIC01 at the indicated MOI for 2 h at 37 °C. Cells were then washed, and medium was replaced with OxM before overnight incubation at 37 °C. The following day, macrophage or B cell positive controls were pulsed with compatible peptides (Table 2.7) at 2 µg/ml for 2 h at 37 °C, followed by washing. Antigen-specific $CD4^+$ or $CD8^+$ T cells were then added to macrophages or B cells at the indicated T:M ratio in RPMI supplemented with 10% FBS. Positive control wells were stimulated with cell stimulation cocktail (eBioscience, 00-4975-93). Brefeldin A (5 µg/ml; Sigma-Aldrich, 420601) and monensin (2 µM; BioLegend, 420701) were added to all conditions to inhibit cytokine secretion and allow intracellular accumulation. Anti-human CD107a-PerCP (BioLegend, 328616) was added at 1 µL per 1 x 10^5 T cells. Cells were incubated for 5 h at 37 °C. At the assay endpoint, T cells were resuspended to detach from macrophages and transferred to U-bottom 96-well plates. Cells were pelleted by centrifugation at 400 × g for 5 min and stained with LIVE/DEAD™ Fixable Orange Dead Cell Stain (Invitrogen, L34983) diluted 1:1000 in PBS for 20 min at RT in the dark. Cells were then washed and stained for surface markers and intracellular cytokines as described in the flow cytometry methods.

Table 2.7 Macrophage/T cell Antigen Presentation Assays					
T cell	**HLA Restriction**	**Antigen Specificity**	**T cell Clone Name**	**Compatible peptide control**	**Compatible B cell clone**
CD8	A11	Nucleoprotein	NP-CD8-1502	Nucleoprotein NP51 peptide	
CD8	A11	Nucleoprotein	NP-CD8-1278	Nucleoprotein NP51 peptide	RTH08 1278 BCL
CD8	01:01	Spike	Spike-CD8-3163	Spike epitope S173 LTD	RTH08 1525 BCL
CD4	01:01	Membrane	M-CD4-1525	Membrane M24 peptide	RTH08 1525 BCL

SARS-CoV-2 conditioned media experiments

VET or Calu-3 cells were infected with SARS-CoV-2 variants at MOI 1 for 1 h. Positive and negative control cells were stimulated with Poly(I:C) (Tocris, 4287) at 1 µg/mL or left untreated, respectively. Cells were then washed and cultured for a further 24 h at 37 °C in culture medium. Conditioned medium from infected or control VET or Calu-3 cells was subsequently transferred to macrophages and incubated for 2 h at 37 °C. Cells were then washed and cultured for an additional 24 h at 37 °C. Cytokine production was quantified by IL-6 ELISA or multiplex MSD assay, as described in the cytokine analysis section.

2.7 Flow Cytometry Analysis

Details of antibodies and reagents, laser and filters, are provided in Table 2.8. Fluorescence was acquired using a BD LSRFortessa™ X-20 (BD Biosciences) and analysed using FlowJo (version 10). Specified antibodies and reagents were biotinylated using a One-Step Antibody Biotinylation Kit (Miltenyi Biotec, 130-093-385).

Surface marker staining

Cells were detached using TrypLE™ and transferred to U-bottom 96-well plates. Cells were pelleted by centrifugation at 400 xg for 5 min and resuspended in 50 µL per well PBS supplemented with human IgG (Sigma-Aldrich, I8640) at 100 µg/mL and Fc receptor blocking reagent (Miltenyi Biotec, 130-059-901) at 10 µL per 1 x 10^6 cells, and incubated for 30 min at RT to block non-specific binding. Primary antibody in PBS was added at 50 µL per well and incubated for 1 h at 4 °C. Cells were washed three times with PBS and resuspended in 50 µL PBS.

Recombinant spike and RBD-Fc binding assays

To assess surface binding of spike/RBD, cells were resuspended in biotinylated HexaPro spike trimer (10 µg/mL) or biotinylated Fc-mutated RBD-Fc (2.5 µg/mL) in PBS, and incubated for 1 h at 4 °C. Cells were washed three times with PBS and incubated with streptavidin-AF647 (1 µg/mL) in PBS. Cells were washed three times with PBS and resuspended in 50 µL PBS.

Intracellular anti-nucleoprotein staining

SARS-CoV-2 containing cells were harvested, pelleted by centrifugation and fixed in 4% PFA in PBS for 10 min at RT. Cells were then pelleted and resuspended in 50 µL perm/wash buffer (BD Biosciences, 554723) supplemented with human IgG at 100 µg/mL and Fc receptor blocking reagent, and incubated for 30 min at RT to simultaneously permeabilise and block. Primary antibody diluted in perm/wash buffer was added at 50 µL per well and incubated for 1 h at 4 °C. Cells were washed twice with perm/wash buffer and once with PBS, then resuspended in 50 µL PBS.

Imaging Flow cytometry

Sample preparation was the same as for traditional flow cytometry. Analysis was performed on the ImageStream® system (Cytek Biosciences) and processed in IDEAS software.

Cell viability and oxidative stress flow cytometry

Macrophages were incubated with CellROX™ Deep Red Reagent for 30 min at 37 °C (Table 2.8). Cells were washed once with PBS, detached using TrypLE™, and pelleted in U-bottom 96-well plates. Cells were then incubated with Zombie UV™ Fixable Viability Dye diluted in PBS for 15 min at RT in the dark. Cells were washed and fixed in 4% PFA in PBS for 10 min, resuspended in PBS, and analysed by flow cytometry.

T cell surface marker and intracellular cytokine staining

Cells were harvested, pelleted, and resuspended in Fixable Orange LIVE/DEAD™ stain in PBS, and incubated for 15 min at RT. Cells were washed and fixed in 4% PFA for 10 min at RT. Cells were then pelleted and resuspended in either anti-human CD4 or anti-human CD8 antibody, and incubated for 20 min at RT. Cells were washed with PBS and pelleted, then resuspended in Cytofix/Cytoperm solution (BD Biosciences, 554722) and incubated for 20 min at RT. Cells were washed with Cytofix/Perm Wash buffer (BD Biosciences, 554723) to permeabilise, pelleted, and

resuspended in an intracellular staining cocktail containing anti-IFN-γ and anti-TNFα antibodies, followed by incubation for 20 min at RT. Cells were washed twice with Cytofix/Perm Wash buffer, once with PBS, and resuspended in 50 µL PBS. Compensation single-colour controls were prepared by adding 1 µL antibody to OneComp beads (Thermo Fisher Scientific, 01-1111-42). LIVE/DEAD™ stain controls were prepared using a 1:1 mixture of live T cells and heat-killed cells (65 °C for 10 min).

Table 2.8 Flow Cytometry Antibodies & Reagents

Antibody	Species	Conjugated	Supplier/Cat	Concentration (µg/mL)	Laser/Filter
ACE2 mAb SN0754	Rabbit	-	Invitrogen, MA5-32307	16	-
ACE2 mAb 2F12A4	Mouse	-	Peprotech, 66699	1 – 0.03	-
ACE2 mAb	Goat	-	Invitrogen, PA5-47488	16	-
Anti-Rb IgG	Goat	AF647	Invitrogen, A21244	1:2000	640-670/30
Anti-Goat IgG	Rabbit	AF633	Invitrogen, A21086	1:2000	640-670/30
Anti-Mouse	Donkey	AF647	Invitrogen, A-31571	1:2000	640-670/30
Fc silent™ Anti-ACE2 [h11B11]	Human	Biotinylated	Absolute Antibody, Ab03703-10.3	0.32	-
Anti-Fluorescein Human IgG1, Fc Silent™ (Isotype control)	Human	Biotinylated	Absolute Antibody, Ab00102-10.3	0.32	-
Streptavidin		AF647	Invitrogen, S32357	1 µg/mL	640-670/30
FB9B (anti-nucleoprotein)	-	AF647	Jack Tan		-
FB 9D (anti-spike)	Human	-	Jack Tan	10	-
EY2A (anti-nucleoprotein)	Human	-	Jack Tan	10	-
Anti-human IgG	Donkey	DyLight 488	Invitrogen, SA510126	1:2000	-
FB9B (anti-nucleoprotein)	Human	AF647	Jack Tan	0.4	640-670/30
Anti-TIM4	Rat	-	Biolegend, 130013	2.5 µg/mL	-
Anti-Caveolin	Mouse	-	BD Biosciences, 610406	0.25 µg/mL	-

70 kDa Dextran		CF®350	Biotium, 80138	50 µg/mL	561-586/15
Zymosan A (S. cerevisiae) BioParticles™		AF488	Invitrogen, Z23373	300 µg/mL	488-530/30
Transferrin		AF647	Biotium, 00085	20 µg/mL	640-670/30
Annexin V		-	BD Pharmingen, 556416	(titrated: 5 – 0.008 µg/mL	-
Anti-TNFα		BV421	BioLegend, 502932	2 µL /100 µL	405-450/50
Anti-IFN-γ		AF488	BioLegend, 502515	2 µL /100 µL	488-530/30
LIVE/DEAD™ Dead Cell Stain		Fixable Orange	Invitrogen, L34983	1:1000	561-610/20
Anti-CD107a		PerCP/Cy5.5		1 µL /100 µL	488-710/50
Anti-CD4		APC	BioLegend, 357408	1.5 µL /100 µL	640-670/30
Anti-CD8		APC	BD Biosciences, 345775	1.5 µL /100 µL	640-670/30
Anti-HLA-ABC	Human	PE	Miltenyi, 130-120-141	1:100	561-586/15
Anti-HLA-DR, DP, DQ	Human	APC	Miltenyi, 130-124-037	1:50	640-670/30
Anti-CD80	Human	APC	Miltenyi, 130-117-831	1:50	640-670/30
Anti-CD86	Mouse	PE	Biolegend, 305405	5 µg/mL	561-586/15
CellROX™ Deep Red Reagent	-	-	Thermo Fisher Scientific, C10491	500 nM	640 - 670/30
Zombie UV™ Fixable Viability Dye	-	-	BioLegend, 423107	1:1000	355 - 515/30

2.8 Microscopy

Single-molecule FISH (smFISH)

smFISH analysis and quantification were performed in collaboration with Dr Peter Wing using an established protocol and analysis pipeline [71]. Cells were infected with Wuhan OF6-mNeonGreen

SARS-CoV-2 at MOI 0.1 for 2 h. Cells were fixed in 4% PFA for 30 min at RT at 4 h, 24 h, and 48 h post-inoculation. Cells were permeabilised in PBS containing 0.1% Triton X-100 for 10 min at RT, followed by washes in PBS and 2× saline-sodium citrate buffer (SSC). Cells were pre-hybridised in pre-warmed wash solution (2× SSC, 10% formamide) twice for 20 min at 37 °C. Hybridisation was performed overnight at 37 °C in hybridisation solution (2× SSC, 10% formamide, 10% dextran sulphate) containing 500 nM smFISH probes targeting the ORF (AF647) and N gene (Cy3). Following hybridisation, cells were washed in pre-warmed wash solution for 20 min at 37 °C and counterstained with DAPI (1 µg/mL). Cells were then washed once in wash solution for 20 min at 37 °C and twice in 2× SSC for 10 min each at RT. Cells were mounted in Vectashield, and confocal images were acquired using an Olympus SoRA microscope. Image quantification was performed by Dr Peter Wing.

2.9 Molecular biology analysis

RNA extraction

RNA was extracted using the RNeasy Plus Micro Kit (QIAGEN, 74034), including on-column DNase treatment using the RNase-Free DNase Set (QIAGEN, 79254), and eluted in 14 µL RNase-free water. RNA concentration was quantified using a NanoDrop spectrophotometer.

cDNA synthesis

RNA was reverse transcribed into complementary DNA (cDNA) using the High-Capacity RNA-to-cDNA™ Kit (Applied Biosystems, 10704217). For each experiment, equal amounts of RNA were used across all samples, with up to 9 µL input RNA per reaction.

RT-qPCR (TaqMan)

cDNA was first diluted to within the range of 10-20 ng/µL in nuclease free water then combined with TaqMan™ Fast Advanced (Thermo, 4444556) and TaqMan assays (Table 2.9). Reactions were carried out in duplicate in a 384-well format in 20 µL reactions. Reactions were run on the QuantStudio 5 Flex Real-Time PCR System (Applied Biosystems) using the FAM/VIC scan mode. Cycling conditions are shown in table 2.10**.** Analysis of gene expression was performed by normalisation of Ct values to the average Ct value of the housekeeper gene, and expressed relative to the non-transduced control sample, as calculated by $2^{-\Delta Ct}$.

Table 2.9: TaqMan Assays for SARS-CoV-2 Genes		
Gene	**TaqMan Assay**	**Probe**
TBP	Hs00427620_m1	VIC_MGB_PL
RNase P	4403326	VIC-TAM
ORF1ab gene	Vi07921935_s1	FAM-MGB
N Gene	Vi07918637_s1	FAM-MGB

Table 2.10: TaqMan qPCR Cycling Conditions			
Cycle step	**Temperature (°C)**	**Time**	**Cycles**
Hold	50	2 min	1
Polymerase activation	95	20 sec	1
Denaturation	95	1 sec	40
Anneal/Extension	60	20 sec	

2.10 ELISAs

SARS-CoV-2 spike ELISA

Flat-bottom 96-well plates were coated with recombinant prefusion-stabilised SARS-CoV-2 spike protein (Lake Pharma, 46328) at 5 µg/mL in PBS for 2 h at 37 °C. Plates were washed three times with wash buffer (PBS supplemented with 0.05% Tween-20) and wells were blocked with casein blocking buffer (Thermo Fisher Scientific, 37528) for 30 min at RT. After washing three times, antibodies were added at 1 µg/mL in PBS and incubated for 1 h at RT. Plates were washed three times, and goat anti-human IgG Fc–HRP conjugate was added at a 1:5000 dilution in blocking buffer and incubated for 30 min at RT. Following three additional washes, tetramethylbenzidine (TMB) substrate (BioFX, Cambridge Bioscience, TMBW-1000-01) was added and incubated in the dark for 10 min. The reaction was stopped using stop solution (BioFX, Cambridge Bioscience, LSTP-1000-01), and absorbance was measured at 450 nm using a plate reader.

Fcγ receptor binding ELISA

Flat-bottom 96-well plates were coated with recombinant prefusion-stabilised SARS-CoV-2 spike protein (5 µg/mL) as described above. Following identical blocking and washing steps to the spike ELISA, antibodies were added at 1 µg/mL and incubated for 1 h at RT. Biotinylated recombinant human Fcγ receptors**;** CD32A (FcγRIIA; 2B Scientific, REC32070), CD32B (FcγRIIB; REC32068), CD16A (FcγRIIIA; REC32069), and CD16B (FcγRIIIB; REC32071)**,** were pre-incubated with HRP-conjugated streptavidin (BioLegend, 405210) at 0.5 µg/mL for 10

min at RT prior to addition to the plates. Receptor–streptavidin complexes were then added to antibody-coated wells and incubated for 1 h at RT.
Plates were washed three times, developed using TMB substrate as described above, and absorbance was measured at 450 nm.

Cytokine ELISA

IL-6 concentrations were quantified using the Human IL-6 DuoSet ELISA Kit (R&D Systems, DY206-05), according to the manufacturer's instructions. Supernatants were applied neat in triplicate.

Cytokine MSD

Multiplex cytokine analysis was performed using the Proinflammatory Panel 1 Human Kit (Meso Scale Discovery (MSD), N05049A-1). This assay enables simultaneous quantification of ten proinflammatory cytokines per well, including IFN-γ, IL-1β, IL-2, IL-4, IL-6, IL-8, IL-10, IL-12p70, IL-13, and TNF-α. Electrochemiluminescence signals were measured using an MSD instrument. Samples were diluted 1:4 and analysed in triplicate.

Chapter 3: Macrophage Internalisation of SARS-CoV-2

3.1 Introduction

How is SARS-CoV-2 internalised into macrophages?

Numerous studies have reported the presence of SARS-CoV-2 RNA and protein within macrophages [72–75]. However, the detection of viral material alone does not distinguish between a viral infection or internalised viral debris. The presence of SARS-CoV-2 associated material within macrophages therefore raises important questions regarding whether macrophages are *bona fide* targets of viral entry and infection, or whether intracellular viral signals primarily reflect their role in phagocytic and endocytic clearance.

To address these questions, in this chapter I describe experiments through which I aimed to determine whether macrophages express the canonical SARS-CoV-2 entry receptor, ACE2, or alternative receptors that could mediate viral entry. Subsequently, the endocytic mechanisms by which SARS-CoV-2 may be internalised into macrophages were examined by assessing the involvement of major cellular uptake pathways, including clathrin-mediated endocytosis, caveolin-mediated endocytosis, and macropinocytosis (Figure 3.1).

Clathrin-mediated endocytosis as a route for viral entry

Clathrin-mediated endocytosis (CME) is the most well-characterised endocytic pathway and the most commonly exploited by viruses. CME is the canonical example of receptor-mediated endocytosis, enabling the highly selective uptake of extracellular components required for many homeostatic processes. This pathway involves the binding of cargo molecules to receptors that contain cytoplasmic endocytic sorting motifs, such as tyrosine-based or dileucine motifs, which are recognised by adaptor protein complexes (adaptins) within clathrin-coated pits. Following the binding of cargo to the receptor, clathrin coated pits invaginate and are rapidly internalised to form clathrin-coated vesicles, with the GTPase dynamin assembling at the vesicle neck to mediate membrane scission. These vesicles are delivered to early endosomes, which act as a sorting compartment. Within early endosomes, receptors and/or ligands may be recycled back to the plasma membrane, trafficked to other intracellular compartments, or, if not retrieved, delivered to lysosomes for degradation.

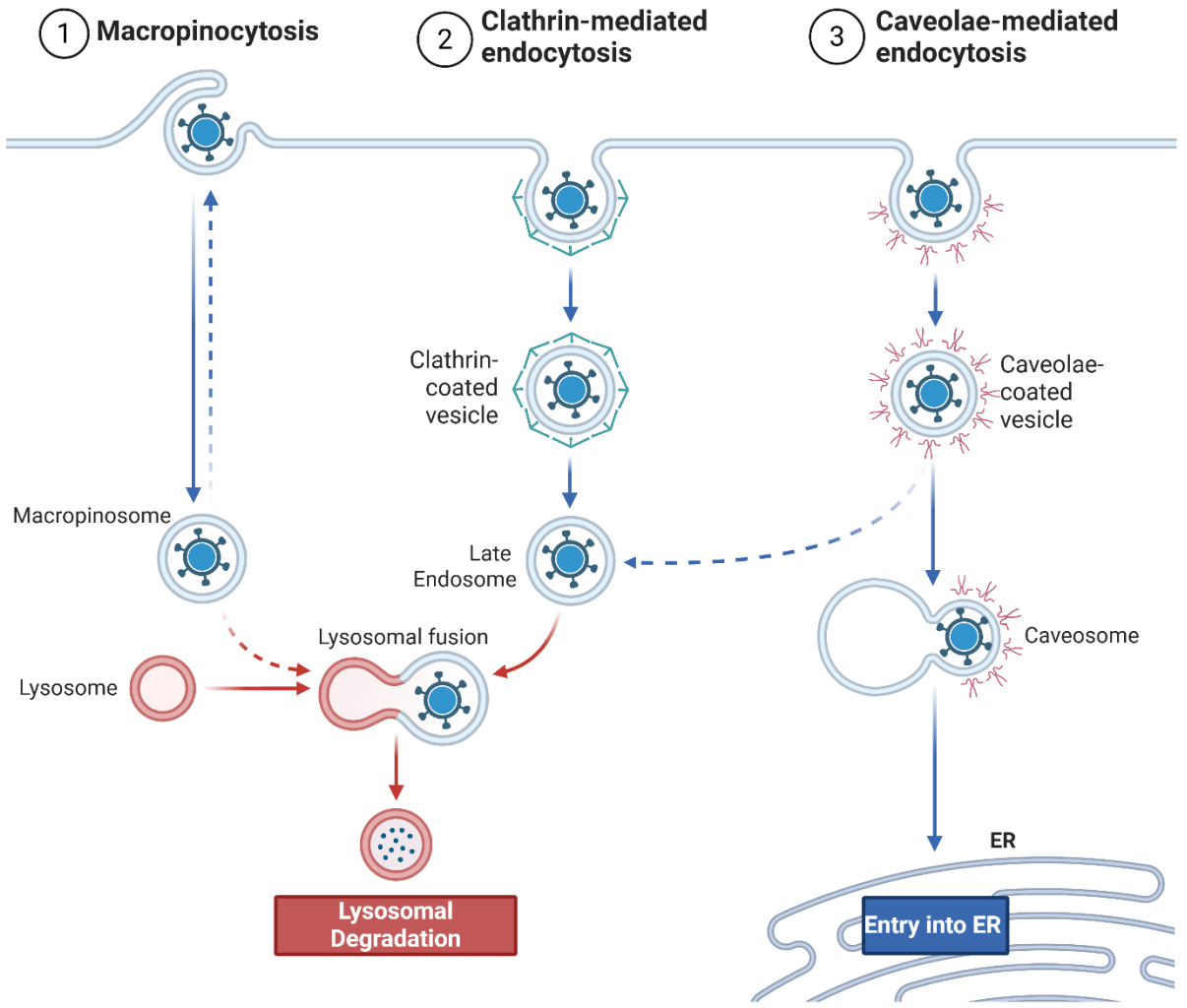

Figure 3.1. Schematic representation of the three principal routes of endocytic viral entry into macrophages. The diagram illustrates viral internalisation via macropinocytosis, clathrin-mediated endocytosis, and caveolin-mediated endocytosis. In macropinocytosis, membrane ruffling drives the non-selective uptake of extracellular fluid and virions into large vesicles termed macropinosomes. In clathrin-mediated endocytosis, viral particles bind to specific cell surface receptors and are internalised within clathrin-coated pits that subsequently form clathrin-coated vesicles. In caveolin-mediated endocytosis, viruses enter through flask-shaped, cholesterol-rich membrane invaginations known as caveolae. Following internalisation, vesicles traffic through the endosomal network, where cargo may be directed towards lysosomal degradation or undergo sorting and transport to the endoplasmic reticulum (ER).

Transferrin is a well-established cargo protein internalised via CME and is used in this thesis as a positive control particle. Transferrin is a soluble iron-binding protein that binds the transferrin receptor at the cell surface and is internalised through clathrin-coated pits. In the acidic environment of the early endosome, transferrin undergoes a conformational change that results in the release of iron while remaining bound to its receptor. The transferrin-receptor complex is subsequently recycled back to the plasma membrane, thereby avoiding lysosomal degradation. CME can be inhibited using drugs such as Dynasore, a dynamin GTPase inhibitor, and chlorpromazine, which disrupts clathrin assembly.

Clathrin-coated pits are typically ~100–150 nm in diameter and therefore tend to favour uptake of relatively small viral particles, although particle size alone does not strictly determine endocytic pathway usage. In susceptible cells lacking surface protease activity, the SARS-CoV-2-ACE2 complex is internalised into clathrin-coated vesicles and trafficked to early endosomes[76]. Many other viruses have been shown to exploit CME through engagement of specific cellular receptors. For example, influenza A virus binds sialic acid-containing receptors, adenoviruses engage the coxsackievirus and adenovirus receptor (CAR), and rhinoviruses bind intercellular adhesion molecule 1 (ICAM-1). In addition, vesicular stomatitis virus and a subset of rhinoviruses exploit members of the low-density lipoprotein receptor (LDLR) family, while New World arenaviruses enter cells via transferrin receptor 1 (TfR1).

Macrophage expression of ACE2

Evidence regarding ACE2 expression in macrophages is conflicting. ACE2 protein expression has been reported on human monocyte-derived macrophages by flow cytometry and on tissue-resident macrophages by immunohistochemical analysis of human lung tissue [77,78]. In addition, ACE2 mRNA has been detected in human monocyte-derived macrophages [79]. Multiple bulk RNA sequencing analyses also report ACE2 expression in macrophages[80,81]. It has also been proposed that monocytes may contain substantial intracellular pools of ACE2 within exosomes, which can be rapidly translocated to the cell surface following TLR4, TLR7, or TLR8 stimulation [82]. In contrast, other transcriptomic analyses of lung tissue have shown that the majority of macrophages lack detectable ACE2 expression [72,75]. Moreover, multiple single-cell RNA sequencing, immunohistochemistry and flow cytometry studies have demonstrated very low or undetectable ACE2 mRNA and protein levels in circulating monocytes and many tissue macrophage populations [83–86]. Taken together, these findings suggest that ACE2 expression in macrophages is not uniform and may be influenced by cellular context. Indeed, ACE2 expression has been reported to be inducible in macrophages following exposure to cytokines, including type I interferons, IL-1β and IL-10, indicating that ACE2 expression may be activation or environment-dependent [73,77,87,88].

In this chapter, I therefore aimed to determine whether iPSC-derived macrophages express ACE2, using flow cytometry, and to validate these findings in monocyte-derived macrophages and THP-1 macrophages. I further investigated whether macrophage polarisation influences ACE2 expression.

Glycan receptors as viral attachment factors and entry receptors

Although clathrin-mediated endocytosis (CME) is often discussed in the context of protein-protein receptor interactions, many viruses exploit this pathway through engagement of glycan-binding receptors[89]. Viral envelope proteins that mediate host–cell interactions are typically glycoproteins, extensively decorated with host-derived glycans. Glycosylation of viral surface proteins serves multiple functions. In addition to promoting correct protein folding and stability, glycans shield underlying protein epitopes from antibody recognition, contributing to immune evasion. Viral glycans can also mediate interactions with host glycan-binding receptors. The carbohydrate moieties displayed on viral glycoproteins act as ligands for host receptors that have evolved to recognise specific glycan patterns rather than protein sequences.

Due to the high density of glycosylation on viral envelope proteins, glycan processing in the Golgi apparatus is often sterically constrained. Consequently, many viral glycoproteins retain a substantial proportion of high-mannose or under-processed N-linked glycans, which are recognised by host lectin receptors. Among the most relevant glycan-binding receptors involved in viral uptake are C-type lectin receptors (CLRs), including DC-SIGN (CD209), L-SIGN (CD209L), the mannose receptor (CD206), langerin (CD207), and, in some contexts, Dectin-1 and Dectin-2.

These glycan receptors facilitate viral infection primarily by capturing virions at the cell surface, thereby increasing the local concentration of virus and promoting encounters with primary entry receptors. In many cases, glycan receptor engagement alone is insufficient to support productive infection, and these receptors function predominantly as attachment or capture factors rather than bona fide entry receptors. However, several CLRs, including DC-SIGN, L-SIGN, and the mannose receptor, internalise via CME. This property allows viruses to exploit glycan receptors as entry cofactors or, in some cases, as primary entry receptors. Less frequently, engagement of lectin receptors can trigger macropinocytosis, particularly when receptor clustering or additional signalling pathways are activated.

For example, HIV-1 requires CD4 and the chemokine co-receptors CCR5 or CXCR4 for membrane fusion and entry; however, interactions between its heavily glycosylated gp120 envelope protein and glycan-binding receptors such as DC-SIGN, the mannose receptor, and galectins facilitate viral capture on macrophages and dendritic cells, thereby enhancing viral dissemination and increasing the likelihood of productive receptor engagement[90]. In contrast, dengue virus utilises DC-SIGN as a primary attachment and entry receptor on dendritic cells, with engagement leading to internalisation predominantly via CME[91]. Ebola virus similarly binds multiple lectins, but instead of CME, lectin engagement contributes to the induction of

macropinocytosis, which facilitates viral uptake; this mechanism is discussed in more detail in later sections.

The SARS-CoV-2 spike protein is also heavily glycosylated [92]. The ancestral SARS-CoV-2 spike contains 22 N-linked glycosylation sites whilst some variants have altered numbers of N-linked glycan sites [93–95]. Numerous studies have demonstrated that the spike glycoprotein can bind to a range of lectins, including DC-SIGN and L-SIGN [96–101]. Alterations in N-linked glycosylation present in different variants may modulate lectin binding [102]. Given the extensive glycosylation of the spike protein, it is unsurprising that SARS-CoV-2 can interact with multiple lectin receptors. A key question, however, is whether these interactions enhance productive viral entry into ACE2-expressing cells. One study demonstrated that the C-type lectin receptors DC-SIGN and L-SIGN, as well as the sialic acid binding immunoglobulin-like lectin 1 (SIGLEC1/CD169), function as attachment receptors by enhancing ACE2-mediated infection in cell lines [103]. Despite this, there is currently no evidence that glycan receptors alone can facilitate ACE2-independent entry of SARS-CoV-2. Studies examining the role of glycan receptors in SARS-CoV-2 infection of macrophages remain limited. Notably, one study identified CD169 as a SARS-CoV-2 attachment and entry factor in macrophages, suggesting that glycan receptors may play a role in binding SARS-CoV-2 to the surface of the membrane [104].

Caveolin-mediated endocytosis as a route for viral entry

Caveolin-mediated endocytosis involves the internalisation of cargo through small, flask-shaped invaginations of the plasma membrane known as caveolae[105]. Caveolae are pre-existing membrane structures enriched in cholesterol, sphingolipids, and caveolin proteins, and are stabilised by cavin proteins. This pathway plays an important role in signal transduction, cholesterol homeostasis, and transcytosis, particularly in endothelial cells. In contrast to clathrin-mediated endocytosis, caveolin-mediated endocytosis relies less on cytoplasmic endocytic sorting motifs and is closely associated with lipid raft microdomains, allowing cargo uptake to be mediated by either protein receptors enriched in caveolae or direct interactions with raft-associated lipids.

Ligand binding within caveolae can activate Src family kinases, leading to phosphorylation of caveolin-1 and subsequent actin remodelling, which promotes vesicle internalisation. As in CME, membrane scission is mediated by the GTPase dynamin, which assembles at the neck of the caveola to release a caveolar vesicle. Consequently, clathrin and caveolar endocytosis can be inhibited by dynamin inhibitors such as Dynasore. Following internalisation, caveolar vesicles

are not directed to lysosomes, but instead are trafficked to early endosomes or Golgi apparatus, depending on cell type and cargo.

A key advantage of caveolin-mediated endocytosis for viruses is the avoidance of lysosomal acidification and degradation, permitting trafficking to neutral intracellular compartments[106]. This pathway is therefore preferentially exploited by non-enveloped viruses, which do not require low pH-triggered membrane fusion for genome delivery. Simian virus 40 is the canonical example of a non-enveloped virus that enters cells via caveolar endocytosis through binding to the GM1 ganglioside and is subsequently trafficked to the endoplasmic reticulum. Echovirus 1 has also been shown to exploit caveolar endocytosis by binding integrins [107]. Although caveolar endocytosis is less commonly the primary entry route for enveloped viruses, it can contribute to viral entry as a supporting or cell-type-dependent mechanism. At present, there is no evidence to support a role for caveolar-mediated endocytosis in SARS-CoV-2 entry, with studies reporting that viral internalisation is not sensitive to caveolar inhibitors [108]. However, these observations have been made in permissive epithelial cell types, and caveolar involvement has not, to our knowledge, been specifically examined in macrophages.

Caveolar endocytosis is dependent on the membrane-associated scaffolding protein caveolin-1 (Cav-1). Evidence for Cav-1 expression in macrophages is conflicting, and consequently the capacity of macrophages to support functional caveolar endocytosis remains debated. Early work reported that macrophages do not express caveolin[109] . Subsequent studies demonstrated low-level Cav-1 expression in macrophage cell lines, including THP-1, J774, and RAW264.7 [110–113]. In contrast, other studies failed to detect Cav-1 in J774 and RAW264.7 macrophages [111,114]. While Cav-1 expression in macrophage cell lines has been controversial, mouse and rat peritoneal macrophages have more consistently been shown to express low levels of Cav-1 by Western blotting [114–116]. Evidence for Cav-1 expression in human macrophages is limited, with reports describing Cav-1 expression in primary human alveolar macrophages and monocyte-derived macrophages [117,118]. However, a previous study from our laboratory did not detect Cav-1 expression in monocyte-derived macrophages [119].

An important consideration when interpreting these studies is that Cav-1 expression has largely been assessed using bulk approaches, such as qPCR and Western blotting, which measure total mRNA or protein levels. Few studies provide direct evidence of Cav-1 localisation at the plasma membrane. As caveolar endocytosis requires the presence of Cav-1 at the cell surface to enable caveolae formation, the detection of Cav-1 protein alone does not necessarily imply functional

caveolar endocytosis. In the absence of surface-localised Cav-1, classical caveolar endocytosis cannot occur.

Taken together, the available evidence suggests that macrophages may express low levels of Cav-1 but lack surface caveolae and, consequently, caveolae-mediated endocytosis. Supporting this interpretation, one study reported minimal overlap between caveolin-1 and caveolin-2 subcellular localisation in primary mouse macrophages, consistent with the absence of caveolae [114]. Despite the apparent lack of surface localisation, Cav-1 has been implicated in macrophage cholesterol homeostasis, lipid transport, and inflammatory signalling [110–112,116,118,120,121].

To date, no studies have examined caveolin-1 expression in iPSC-derived macrophages. In this chapter, I investigated the surface expression of caveolin-1 in iPSC-derived macrophages using flow cytometry.

Macropinocytosis as a route of viral entry

Macropinocytosis is a form of non-selective endocytosis characterised by the uptake of extracellular fluid and solutes into large vesicles known as macropinosomes. Macropinocytosis is driven by actin cytoskeletal remodelling mediated by the Rho family GTPase Rac1 and its downstream effector p21-activated kinase 1 (Pak1), as well as the activity of the Na^+/H^+ exchanger NHE1. These signalling events promote the formation of plasma membrane ruffles that extend outward and subsequently fold back onto the cell surface, enclosing extracellular fluid within macropinosomes typically ranging from approximately 0.5 to several micrometres in diameter.

Dextran is a large, bacterially derived polysaccharide, available in a range of sizes and fluorescent conjugates. High-weight molecular dextran (70kDa or higher) is used as a standard marker cargo for macropinocytosis, because it is too large to fit into smaller clathrin or caveolin coated vesicles. It was used in this study as a positive control particle for macropinocytosis.

Macropinocytosis is exploited as the primary entry pathway for many viruses, predominantly large, enveloped viruses. Ebola virus is the best-studied example of a viral macropinocytic entry[122]. The virus binds to attachment factors, such as C-type lectins, T cell-immunoglobulin and mucin domains, and induces actin remodelling and membrane ruffling. There are several reasons why viruses may have evolved to use macropinocytosis, over other routes of endocytic entry[123]. It is plausible this is because macropinocytosis permits uptake of a larger size of virus, which would be too big for clathrin mediated entry.

Studies have shown that SARS-CoV-2 can use macropinocytosis to facilitate entry into established cell lines [124,125]. However, evidence from physiologically relevant cell types remains limited. To date, only one study has demonstrated that the SARS-CoV-2 spike protein can stimulate macropinocytosis in human and murine macrophages, but this work did not show direct internalisation of intact virions via this pathway [126]. Taken together, the role of macropinocytosis in SARS-CoV-2 infection remains poorly defined. Although SARS-CoV-2 or its spike protein may enhance macropinocytic activity, it is still unclear whether this process contributes to viral uptake or infection in relevant target cell types.

In this chapter, I explored whether non-receptor-mediated SARS-CoV-2 internalisation into macrophages occurs via macropinocytosis. As there is no single assay that can definitively demonstrate use of the macropinocytic pathway, several established criteria were applied [123,127]. Viral internalisation should co-localise with fluid-phase markers such as dextran and be sensitive to inhibitors of actin polymerisation (cytochalasin D), Rho GTPase signalling (NSC23766), the Na^+/H^+ exchanger (EIPA), and kinases involved in macropinocytosis, including PI3K and Pak1 (wortmannin and IPA-3). While Rho GTPases and these kinases are involved in multiple endocytic pathways, inhibition of the Na^+/H^+ exchanger is considered relatively specific for macropinocytosis and is therefore widely used to assess this pathway[128]. Using these criteria, I investigated the role of macropinocytosis in SARS-CoV-2 internalisation into macrophages.

Phosphatidylserine receptors as viral attachment factors and entry receptors

Phosphatidylserine (PS) is a phospholipid present on the inner leaflet of a plasma membrane. During apoptosis, PS is flipped to the external leaflet where it functions as an “eat-me” signal for apoptotic cell clearance. PS is recognised by a range of PS-binding receptors, including the TIM family (TIM-1, TIM-4) and the TAM receptor tyrosine kinases (AXL, TYRO3, and MER), either directly or indirectly via bridging molecules such as Gas6 or Protein S. While whole apoptotic cells and large apoptotic bodies are endocytosed by phagocytosis by professional phagocytes, smaller apoptotic debris is internalised by macropinocytosis.

Many enveloped viruses have PS exposed on their outer membrane, which likely reflects host membrane composition. Exposed PS allows them to hijack PS-apoptotic clearance pathways, by binding to receptors and inducing internalisation by macropinocytosis, a strategy termed apoptotic mimicry[129]. There are many enveloped viruses that exploit phosphatidylserine receptors as a cellular entry route or use to enhance their entry mediated by other receptors[130,131].

Because virions are submicron in size and frequently infect non-professional phagocytes, PS receptor engagement preferentially activates signalling pathways associated with membrane ruffling and actin rearrangement, such as PI3K–Rac1, leading to macropinocytosis rather than classical phagocytosis. This mode of entry is advantageous for viruses, as macropinosomes are less degradative than phagolysosomes and provide an opportunity for endosomal escape. Thus, apoptotic mimicry enables viruses to exploit tolerogenic apoptotic clearance pathways to facilitate internalisation and productive infection. For example, Vaccinia virus has been shown to use macropinocytosis as a route of entry, after initial surface binding to phosphatidylserine receptors. This was demonstrated by the use of Annexin V, a phosphatidylserine binding protein that can block PS-receptor interactions[132]. Flaviviruses have also been shown to use PS-mediated entry through Axl, TIM and TAM receptors[133–135].

SARS-CoV-2 virions have been reported to contain substantial levels of PS in their viral envelope [136]. PS receptors of the TIM and TAM families have been shown to enhance SARS-CoV-2 binding and infection in cells expressing ACE2; however, these receptors do not support productive ACE2-independent viral entry [136]. One study reported that AXL directly binds the SARS-CoV-2 spike protein and mediates ACE2-independent entry in HEK293 cells [137]. However, subsequent studies were unable to replicate these findings and instead demonstrated that AXL enhances infection through interactions with virion-associated PS rather than direct spike binding [136]. In addition, SARS-CoV-2 engagement of ACE2 has been reported to trigger activation of the Ca^{2+}-dependent phospholipid scramblase ANO6, resulting in transient exposure of PS on the outer leaflet of the host cell membrane. This externalised PS promotes membrane fusion between the viral envelope and the host cell, thereby enhancing viral entry and infection [138,139]. Despite these advances, the role of PS and PS receptors in SARS-CoV-2 internalisation by macrophages has not been directly investigated. In this chapter, I therefore examine the roles of the PS receptors AXL, TIM-4 and TREM2 in macrophage internalisation of SARS-CoV-2.

The role of phagocytosis in SARS-CoV-2 infection

Phagocytosis is the principal endocytic pathway employed by macrophages and other professional phagocytes for the uptake of large particles, typically greater than 0.5–1 μm in diameter[140,141]. Viruses smaller than this size range are generally internalised via alternative endocytic routes, as discussed in this chapter. Given the relatively small size of SARS-CoV-2 virions (~80–120 nm), it is unlikely that individual, unopsonised particles would directly trigger phagocytosis. For this reason, phagocytosis is not considered here in this chapter, which focuses exclusively on the uptake of unopsonised SARS-CoV-2 virions.

Phagocytosis is more commonly associated with the uptake of immune complexes or viral aggregates and is a highly regulated process mediated by specific receptors. Efficient phagocytosis often requires opsonisation of the target particle by antibodies or complement components. In the context of a virally infected human lung, viral particles are more likely to be encountered by macrophages as immune complexes containing cellular debris and opsonins, particularly at later stages of infection when antibodies are present. The phagocytosis of antibody-opsonised SARS-CoV-2, and the impact of antibody opsonisation on viral fate within macrophages, is addressed separately in chapter 4.

Chapter hypotheses and aims

The mechanisms by which SARS-CoV-2 interacts with and is internalised into macrophages remain incompletely defined. This chapter therefore examines the internalisation of SARS-CoV-2 into human iPSC-derived macrophages, with the aim of distinguishing receptor-dependent entry mechanisms from non-specific uptake pathways. I hypothesised that SARS-CoV-2 was likely being internalised into the macrophage by clearance mechanisms, which could be receptor-dependent or independent. To address this hypothesis, this chapter aims to answer the following questions:

- Is SARS-CoV-2 internalised into macrophages?
- Is SARS-CoV-2 internalised via ACE2 or other spike-binding receptors through clathrin-mediated endocytosis?
- Does caveolin-dependent endocytosis contribute to SARS-CoV-2 internalisation?
- Is SARS-CoV-2 internalised via classical bulk fluid-phase macropinocytosis?
- Does phosphatidylserine receptors contribute to SARS-CoV-2 internalisation?

3.2 Results

3.2.1 Macrophages internalise SARS-CoV-2

RT-qPCR reveals internalised SARS-CoV-2 RNA in macrophages

To determine whether SARS-CoV-2 virions are internalised into macrophages, iPSC-derived macrophages from two donors (SFC840-03-03 and SFC841-03-01) and Vero/E6-TMPRSS2 (VET) cells, a susceptible control cell line, were inoculated with SARS-CoV-2 at an MOI 1 for 2 h at either at 4 °C or 37 °C. Incubation at 4°C inhibits endocytosis and therefore serves as a control for non-internalised, surface-associated virus detectable by RT-qPCR. Following incubation, cells were washed and treated with proteinase K to remove any surface-bound virions[142]. SARS-CoV-2 ORF1ab and N genes were quantified by RT-qPCR and normalised to RNase P expression. Macrophages showed efficient uptake of SARS-CoV-2, with viral RNA levels approximately two-fold lower than those detected in VET cells (Figure 3.2A). SARS-CoV-2 RNA was readily detectable at 37 °C, and proteinase K treatment had no significant effect on viral RNA levels, while only low levels were detected at 4 °C. Together, these controls indicate that the SARS-CoV-2 RNA detected at 37 °C represents internalised intracellular virus.

smFISH reveals internalised SARS-CoV-2 RNA in macrophages

As further confirmation that SARS-CoV-2 is internalised into macrophages, single-molecule fluorescence in situ hybridization (smFISH) was used to visualise intracellular SARS-CoV-2 genes by microscopy. iPSC-derived macrophages (KOLF2.1S) or VET cells were inoculated with SARS-CoV-2 at MOI 0.1 for 2 h and stained with RNA probes targeting ORF1a (AF647) and N gene (Cy3), and counterstained with DAPI (Figure 3.2B). Confocal imaging revealed SARS-CoV-2 N and ORF RNA in both VET cells and macrophages following inoculation. Consistent with the low MOI, relatively few cells were RNA-positive. In VET cells, viral RNA displayed a diffuse cytoplasmic distribution, indicative of productive SARS-CoV-2 infection. In contrast, RNA detected in macrophages was localised to discrete puncta, suggesting internalisation and sequestration of viral RNA within vesicular compartments.

Flow cytometry reveals intracellular SARS-CoV-2 nucleoprotein in macrophages

RT-qPCR and smFISH demonstrated the presence of SARS-CoV-2 RNA in macrophages. To determine whether this RNA reflects internalisation of intact virions rather than uptake of free viral RNA, conventional and imaging flow cytometry were used to detect and visualise SARS-

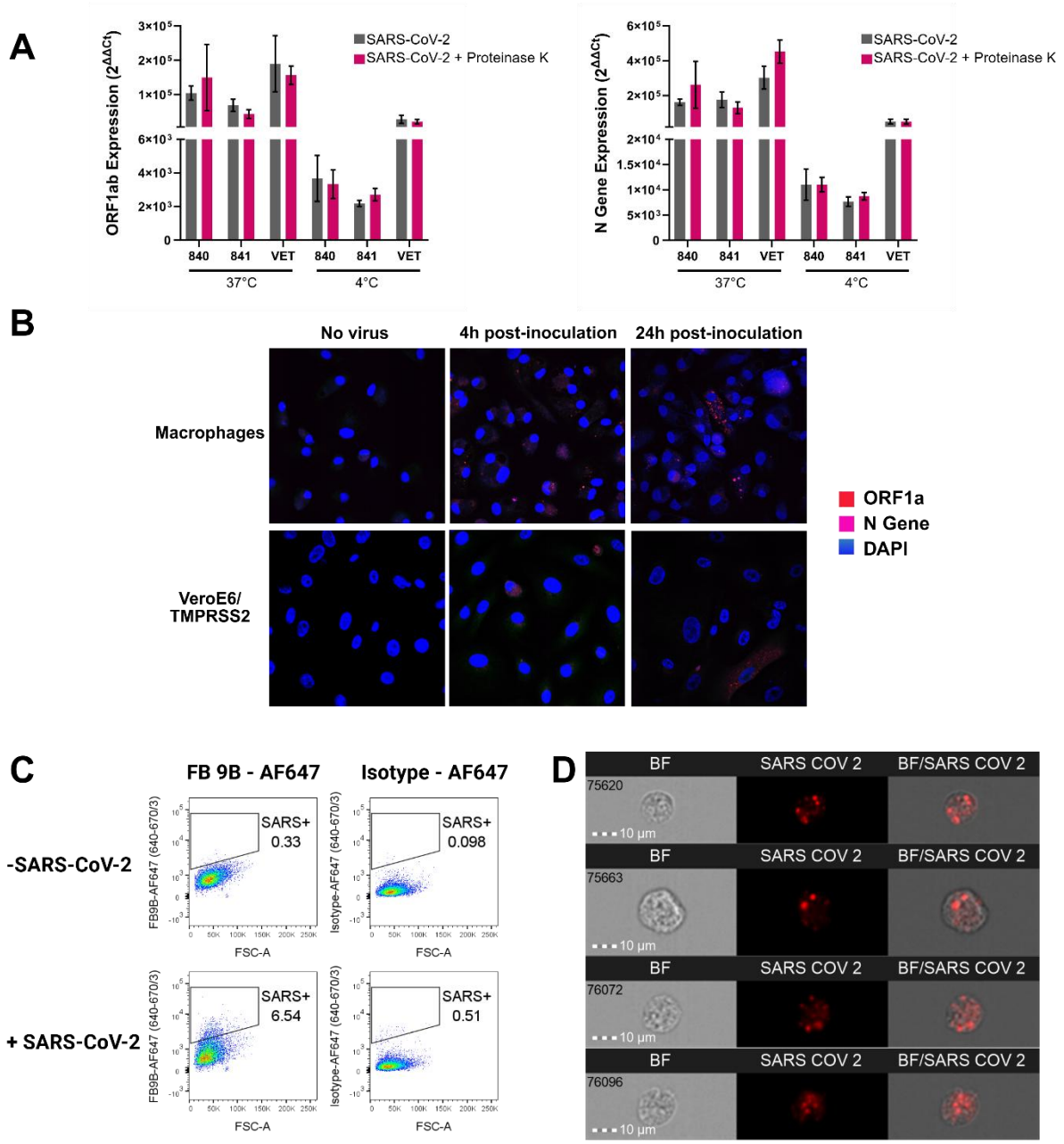

Figure 3.2. SARS-CoV-2 is internalised by macrophages. (A) Quantification of intracellular SARS-CoV-2 genes in macrophages and VET cells 2 h post-inoculation. iPSC-derived macrophages (donors: SFC840-03-03 [840] and SFC841-03-01 [841]) and VET cells were inoculated with SARS-CoV-2 at an MOI of 1 for 2 h at either 37 °C or 4 °C (to inhibit endocytosis). Cells were treated with proteinase K to remove surface-bound virions. SARS-CoV-2 ORF1ab and N gene copy numbers were quantified by TaqMan RT-qPCR and normalised to the RNase P housekeeping gene and expressed relative to no infection control. Data shown are from one representative experiment (three technical replicates; error bars represent SD). **(B)** Single-molecule fluorescence in situ hybridisation (smFISH) detection of SARS-CoV-2 RNA. iPSC-derived macrophages (KOLF 2.1S) were inoculated with Wuhan ORF6-mNeonGreen SARS-CoV-2 at an MOI of 0.1 for 2 h. Cells were treated with proteinase K to remove surface-bound virions. Cells were fixed and permeabilised at 4 h and 24 h post-inoculation, then stained with RNA probes targeting ORF1a (AF647-labelled) or N (Cy3-labelled) genes and counterstained with DAPI. **(C)** Detection of intracellular SARS-CoV-2 by flow cytometry. Macrophages (KOLF 2.1S) were inoculated with SARS-CoV-2 at an MOI of 2 for 2 h and stained with anti-nucleoprotein antibody (FB 9B) or a human IgG1 isotype control. **(D)** Imaging flow cytometry (ImageStream®) images of macrophages containing intracellular SARS-CoV-2. Macrophages were incubated with SARS-CoV-2 at an MOI of 10 for 2 h. Cells were treated with proteinase K to remove surface-bound virions. Nucleoprotein was detected using FB 9B-AF647. Images of four representative macrophages are shown in bright-field, red-channel, and composite views (left to right).

CoV-2 nucleoprotein within macrophages. iPSC-derived macrophages (KOLF2.1S) were inoculated with SARS-CoV-2 at an MOI of 2 for 2 h and stained with anti-nucleoprotein (FB 9B) or isotype control (Figure 3.2C). Flow cytometry showed that SARS-CoV-2 inoculated macrophages were positive for nucleoprotein staining, while the isotype control indicated minimal non-specific binding. Images of SARS-CoV-2–inoculated macrophages stained with FB9B-AF647 were acquired using imaging flow cytometry (ImageStream) (Figure 3.2D). Overlay images of brightfield and fluorescence channels revealed nucleoprotein staining localised to discrete intracellular puncta, consistent with vesicular structures and supporting the smFISH observations of punctate SARS-CoV-2 RNA in macrophages.

Troubleshooting and optimisation of anti-nucleoprotein flow cytometry to detect intracellular SARS-CoV-2

Efficient detection and quantification of intracellular SARS-CoV-2 by flow cytometry required the development and optimisation of an intracellular staining protocol. To maximise sensitivity for detecting low levels of viral antigen, a primary antibody followed by a fluorophore-conjugated secondary antibody strategy was initially selected, with the aim of amplifying the primary signal to detectable levels. Three primary antibodies were evaluated in SARS-CoV-2 infected VET cells: FB 9B (anti-nucleoprotein), FB 9D (anti-spike), and EY 2A (anti-nucleoprotein), each used at 1 µg/mL with an anti-human AF488 secondary antibody (1:1000) (Figure 3.3A). Flow cytometric analysis revealed specific and complete staining of infected VET cells with FB 9B and FB 9D. FB 9B provided the greatest separation between positive and negative populations, likely reflecting the high intracellular abundance of nucleoprotein relative to spike. In contrast, EY2A showed non-specific staining of uninfected VET cells and was excluded from further analysis. FB 9B was therefore selected for subsequent optimisation.

The concentration of FB 9B was titrated in VET cells to identify the concentration for optimal separation between positive and negative samples (Figure 3.3B). A concentration of 0.06 µg/mL produced the greatest separation between nucleoprotein-positive and -negative populations and was selected for downstream experiments. Following optimisation in VET cells, this staining strategy was applied to SARS-CoV-2 inoculated iPSC-derived macrophages using FB 9B (0.06 µg/mL) and the anti-human AF488 secondary antibody (Figure 3.3C). However, no clear separation between uninfected and inoculated macrophages was observed. ImageStream analysis revealed two major factors contributing to this lack of resolution. Macrophages exhibited high autofluorescence in the green fluorescence channels and the secondary antibody

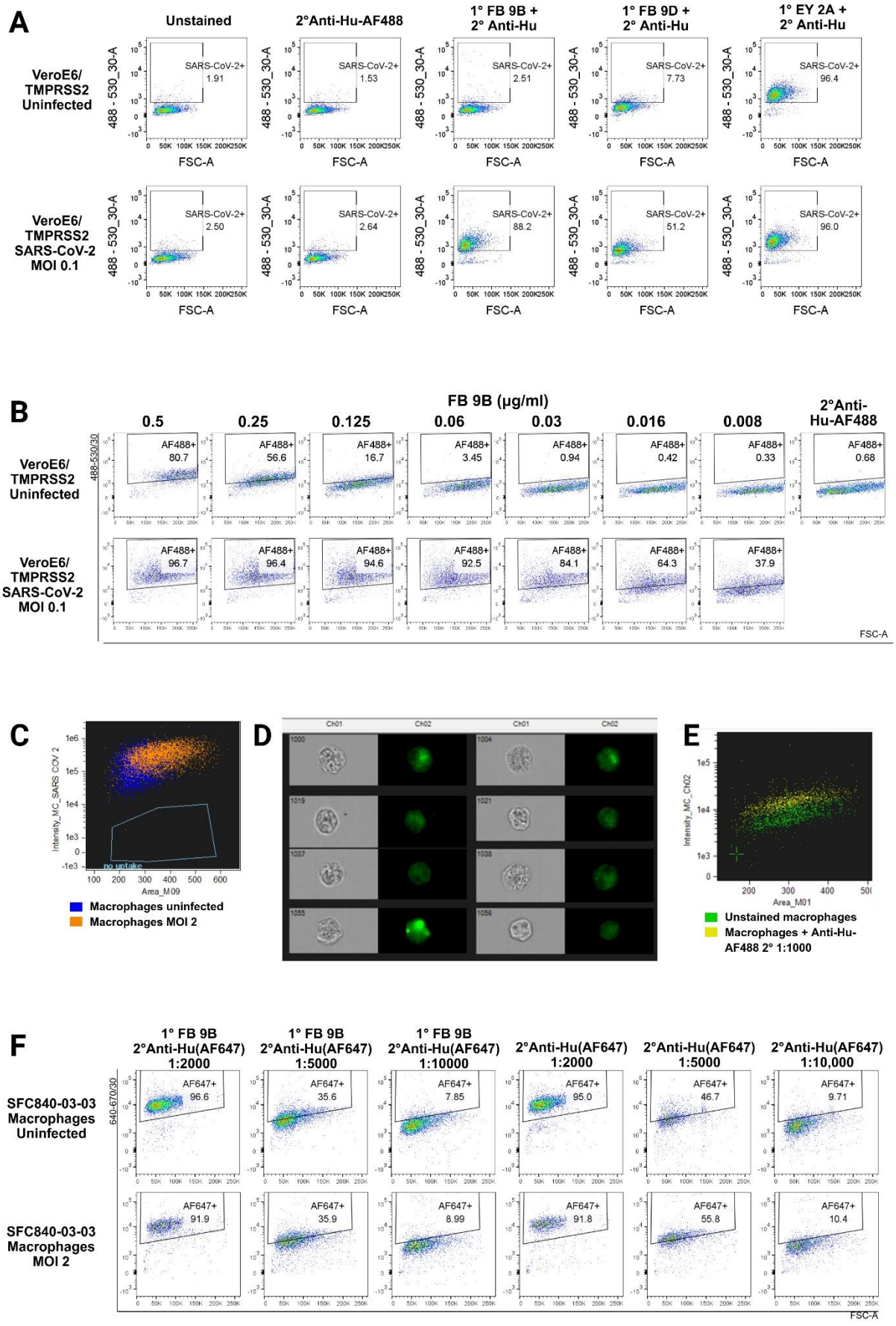
A
Unstained
2°Anti-Hu-AF488
1° FB 9B + 2° Anti-Hu
1° FB 9D + 2° Anti-Hu
1° EY 2A + 2° Anti-Hu
VeroE6/ TMPRSS2 Uninfected
VeroE6/ TMPRSS2 SARS-CoV-2 MOI 0.1
488 - 530_30-A
FSC-A
SARS-CoV-2+
1.91
1.53
2.51
7.73
96.4
2.50
2.64
88.2
51.2
96.0
B
FB 9B (µg/ml)
0.5
0.25
0.125
0.06
0.03
0.016
0.008
2°Anti-Hu-AF488
488-530/30
AF488+
80.7
56.6
16.7
3.45
0.94
0.42
0.33
0.68
96.7
96.4
94.6
92.5
84.1
64.3
37.9
C
Intensity_MC_SARS COV 2
Area_M09
no uptake
Macrophages uninfected
Macrophages MOI 2
D
Ch01
Ch02
E
Intensity_MC_Ch02
Area_M01
Unstained macrophages
Macrophages + Anti-Hu-AF488 2° 1:1000
F
1° FB 9B 2°Anti-Hu(AF647) 1:2000
1° FB 9B 2°Anti-Hu(AF647) 1:5000
1° FB 9B 2°Anti-Hu(AF647) 1:10000
2°Anti-Hu(AF647) 1:2000
2°Anti-Hu(AF647) 1:5000
2°Anti-Hu(AF647) 1:10,000
SFC840-03-03 Macrophages Uninfected
SFC840-03-03 Macrophages MOI 2
640-670/30
AF647+
96.6
35.6
7.85
95.0
46.7
9.71
91.9
35.9
8.99
91.8
55.8
10.4

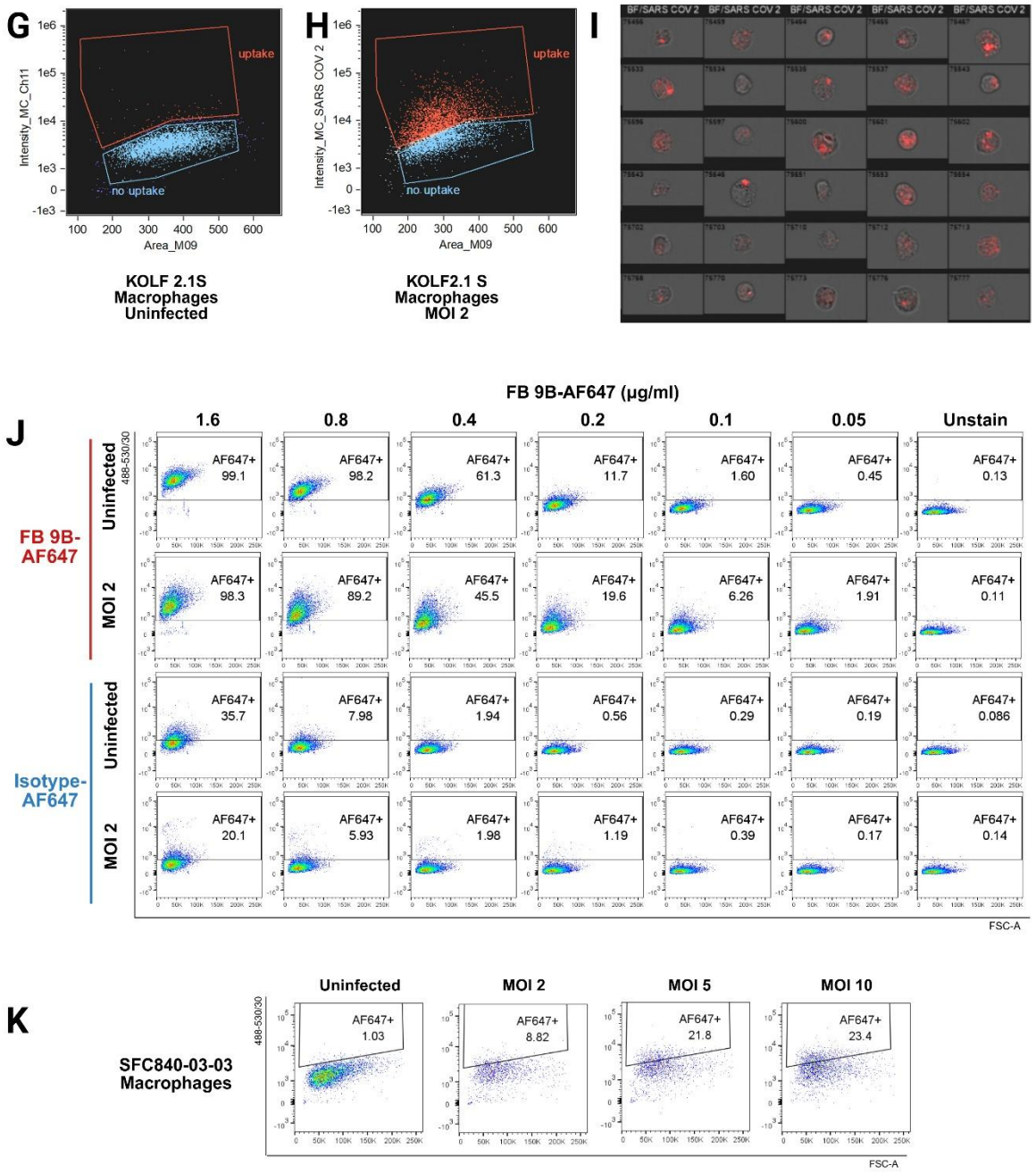

Figure 3.3. Troubleshooting and optimisation of anti-nucleoprotein staining for flow-cytometric detection of SARS-CoV-2. VET cells or iPSC-derived macrophages (KOLF 2.1S) were inoculated with SARS-CoV-2 for 2 h at the indicated MOIs, then fixed, permeabilised, and stained with the specified primary and/or secondary antibodies. **(A)** Comparison of FB 9B, FB 9D (anti-nucleoprotein), and EY 2A (anti-spike) antibodies for intracellular viral detection in VET cells. **(B)** Titration of FB 9B on VET cells, followed by AF488-conjugated anti-human secondary antibody. **(C)** Fluorescence of SARS-CoV-2 positive and negative iPSC-derived macrophages stained with FB 9B and anti-human-AF488. **(D)** Representative ImageStream® images illustrating intrinsic macrophage autofluorescence in the green channel. **(E)** Comparison of unstained macrophages versus those stained with anti-human-AF488 alone. **(F)** Titration of anti-human-AF488 on macrophages, with or without FB 9B. **(G)** Fluorescence of uninfected macrophages stained with FB 9B conjugated to AF647. **(H)** Fluorescence of macrophages infected at MOI 2 and stained with FB 9B-AF647.**(I)** Representative ImageStream® images of macrophages containing intracellular SARS-CoV-2, stained with FB 9B-AF647. **(J)** Titration of FB 9B-AF647 and isotype control on macrophages with or without SARS-CoV-2. (K) Fluorescence of macrophages stained with FB 9B-AF647 following inoculation across a range of MOIs.

bound non-specifically to the macrophages (Figure 3.3D, E). To avoid the auto fluorescent green channel an anti-human AF647 antibody was titrated on uninfected and inoculated macrophages both in the presence and absence of the FB9B primary antibody (Figure 3.3F). This demonstrated persistent non-specific binding even at a 1:10,000 dilution, resulting in approximately 10% apparent positive cells. This high background completely obscured any specific nucleoprotein signal.

To overcome these limitations, a directly conjugated AF647 FB9B antibody was evaluated to eliminate the issues of non-specific secondary antibody binding and detection in the auto fluorescent green channels, but with the potential drawback of reduced signal amplification. Staining with FB 9B-AF647 (1 µg/mL) discriminates between uninfected and SARS-CoV-2 inoculated macrophages (Figure 3.3G, H). While uninfected macrophages remained unstained, there is a small, detectable population of nucleoprotein positive cells in the inoculated condition. Unlike the bimodal distribution observed in infected VET cells, where nucleoprotein staining resolved into discrete positive and negative populations, macrophage staining appeared as a broadened single population. This likely reflects heterogeneity in viral internalisation among macrophages, with variation in the number of internalised virions per cell, as well as less virions internalised compared with the highly permissive VET cells. Imaging flow cytometry further confirmed staining specificity and intracellular localisation. Overlay images of brightfield and AF647 fluorescence revealed nucleoprotein signal localised to discrete intracellular puncta, consistent with vesicular structures (Figure 3.3I).

To further optimise nucleoprotein detection in macrophages, the FB 9B-AF647 antibody was titrated on uninfected and SARS-CoV-2 inoculated macrophages (MOI 2), alongside an AF647-conjugated human IgG1 isotype control (Figure 3.3J). A concentration of 0.4 µg/mL achieved the best separation between positive and negative populations. At this concentration, there was no non-specific staining from the isotype control.

Finally, the effect of MOI on nucleoprotein detection was assessed by inoculating macrophages with SARS-CoV-2 at MOIs of 2, 5, or 10 (Figure 3.3K). At MOI 2, approximately 9% of macrophages were nucleoprotein-positive. This increased to ~22% at MOI 5 and ~23% at MOI 10. Based on these results, an MOI of ≥5 was selected for experiments requiring quantitative flow cytometric detection of SARS-CoV-2 internalisation in macrophages.

In summary, flow cytometric detection of intracellular SARS-CoV-2 nucleoprotein in macrophages is technically challenging due to high autofluorescence and Fc receptor mediated non-specific antibody binding. These limitations were overcome by using a directly conjugated

anti-nucleoprotein antibody (FB9B-AF647) at 0.4 µg/mL and by applying higher viral doses (MOI 5–10) to maximise detectable signal. This optimised approach provided specific and reproducible detection of internalised SARS-CoV-2 antigen in macrophages.

3.2.2 Macrophage internalisation of SARS-CoV-2 is ACE2-independent

The development of ACE2 negative and positive control cell lines

Madin-Darby canine kidney (MDCK) cells are an epithelial cell line and are known historically for their use in propagating influenza viruses. MDCK cells do not express human or canine ACE2 and therefore serve as a negative control cell line in experiments that aim to determine ACE2 levels of cell types with unknown ACE2 expression. To generate a positive human ACE2 expressing cell line, MDCK cells were transduced by lentivirus encoding human ACE2 and puromycin resistance. The cells were selected by puromycin at 2 µg/mL.

Human iPSC-derived macrophages do not express ACE2

Flow cytometry was used to assess ACE2 expression in iPSC-derived macrophages. MDCK control cells and iPSC-derived macrophages from three donors (SFC840-03-03, SFC841-03-01, and KOLF2.1S) were stained with an Fc-silent™ anti-ACE2 antibody (Ab03703-10.3) and detected using streptavidin conjugated to AF647 (Figure 3.4A). Strong staining of MDCK-hACE2 cells, together with the absence of signal in MDCK WT cells, confirmed antibody specificity. No ACE2 expression was detected on iPSC-derived macrophages from any donor, and no non-specific staining was observed with the Fc-silent human IgG1 isotype control. Comparison between the isotype control and anti-ACE2 treated groups was performed using an unpaired two-tailed Mann-Whitney U test. No statistically significant difference was observed ($U = 9$, $p = 0.10$).

Polarised iPSC-derived macrophages do not express ACE2

To determine whether macrophage polarisation induces ACE2 expression, iPSC-derived macrophages (SFC840-03-03 and KOLF2.1S) were polarised to an M1 or M2 phenotype. Flow cytometric analysis revealed no detectable ACE2 expression in either M1- or M2-polarised iPSC-derived macrophages (Figure 3.4B).

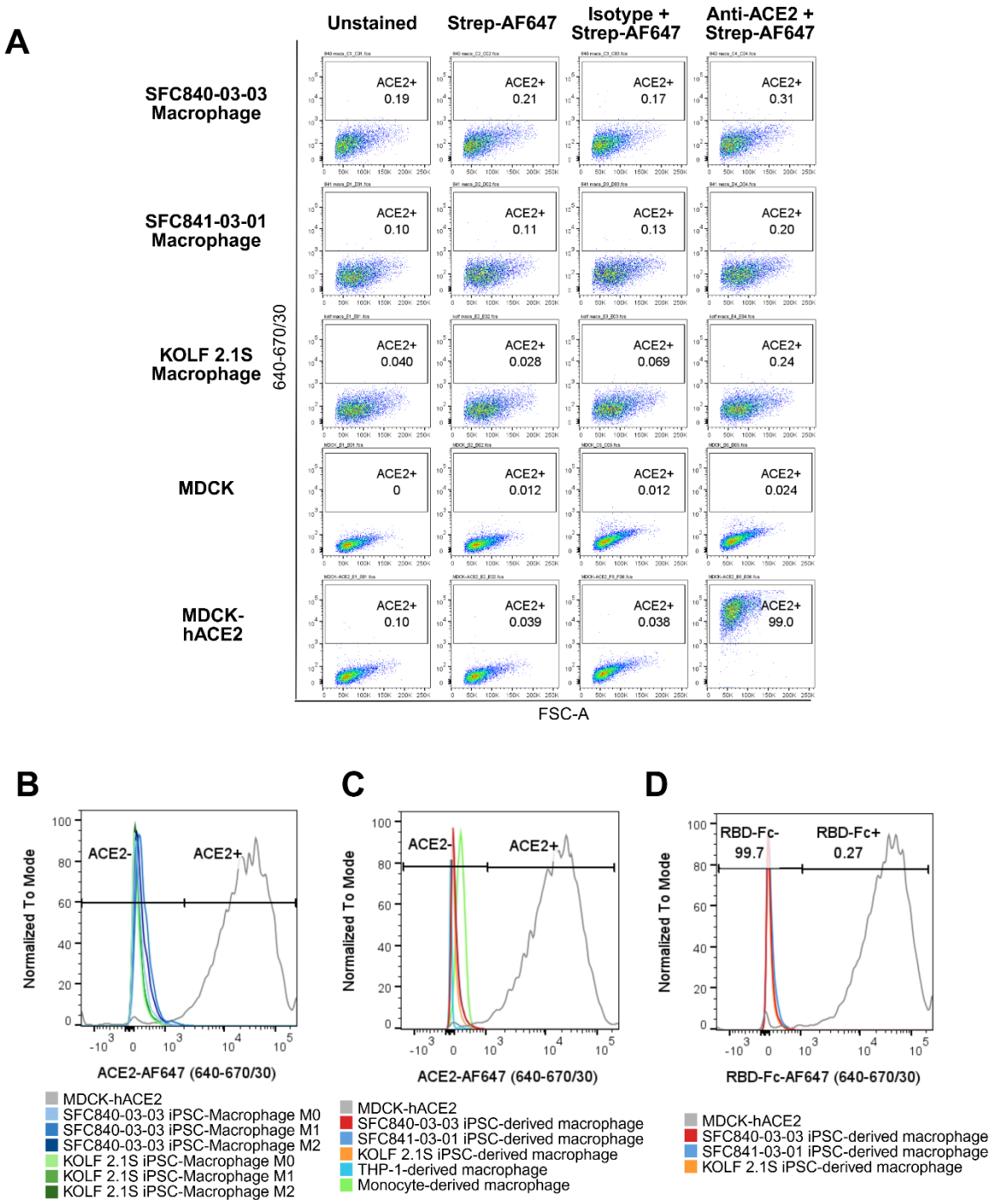

Figure 3.4. Macrophages do not express ACE2. (A) Flow-cytometric analysis of ACE2 staining in iPSC-derived macrophages (donors: SFC840-03-03, SFC841-03-01, and KOLF 2.1). MDCK and MDCK-hACE2 cells were included as negative and positive controls, respectively. Cells were either unstained, stained with streptavidin-AF647 alone, or stained with Fc Silent™ biotinylated anti-fluorescein human IgG1 isotype control (0.3 µg/ml) or Fc Silent™ biotinylated anti-ACE2 antibody (0.3 µg/ml), followed by detection with streptavidin-AF647. ACE2-positive gate was set above the highest background staining in ACE2-negative control cells **(B)** ACE2 staining of iPSC-derived macrophages (KOLF 2.1S and SFC840-03-03) polarised to M0, M1 (20 ng/ml IFNγ and 100 ng/ml LPS), or M2 (50 ng/ml IL-4) phenotypes. **(C)** ACE2 staining of iPSC-derived macrophages (KOLF 2.1S, SFC840-03-03 or SFC841-03-01), THP-1-derived macrophages matured with PMA (5 ng/ml for 3 days), and monocyte-derived macrophages matured with M-CSF (50 ng/ml for 5 days). **(D)** Binding of receptor-binding domain (RBD)-Fc fusion protein to iPSC-derived macrophages and MDCK-hACE2 cells. Cells were incubated with biotinylated, Fc-silenced Wuhan RBD–Fc fusion protein, followed by detection with streptavidin-AF647.

THP-1 and monocyte-derived macrophages do not express ACE2

ACE2 expression was next assessed in two additional in vitro macrophage models: monocyte-derived macrophages (mo-macs) and THP-1–derived macrophages (Figure 3.4C). Human monocytes were isolated from PBMCs by plastic adherence, followed by differentiation with M-CSF. THP-1 monocytes were differentiated to macrophages by PMA. Flow cytometric analysis showed that neither mo-macs nor THP-1–derived macrophages expressed detectable ACE2.

RBD-Fc Fusion molecule confirms lack of ACE2 expression

To independently validate the absence of ACE2, a fusion protein comprising the SARS-CoV-2 receptor-binding domain fused to an Fc region (RBD-Fc) was used as a probe for ACE2 or other RBD-interacting receptors. Flow cytometry demonstrated strong binding of RBD-Fc to MDCK-hACE2 cells, but no detectable binding to iPSC-derived macrophages (Figure 3.4D), further confirming the absence of ACE2 expression in these cells.

Collectively, these results show that human macrophages do not express ACE2 or other detectable RBD-binding receptors under these conditions.

Optimisation of flow cytometric detection of ACE2

A staining protocol was developed for the flow cytometric detection of ACE2. Minimising non-specific background staining was critical, as this could lead to false-positive detection or obscure low-level ACE2 expression.

Three commercially available antibodies were initially evaluated: a rabbit anti-ACE2 monoclonal antibody (SN0754; Invitrogen, MA5-32307), a goat anti-ACE2 polyclonal antibody (Invitrogen, PA5-47488), and a mouse anti-ACE2 monoclonal antibody (2F12A4; PeproTech, 66699). Antibodies were titrated on MDCK control cell lines and detected using species-appropriate secondary antibodies (AF647-conjugated anti-rabbit, AF633-conjugated anti-goat, or AF647-conjugated anti-mouse, respectively).

The rabbit anti-ACE2 monoclonal antibody (SN0754) showed no detectable binding to ACE2-expressing cells (Figure 3.5A). The goat anti-ACE2 polyclonal antibody demonstrated complete staining of MDCK-hACE2 cells and exhibited low-level non-specific binding to MDCK wild-type cells (Figure 3.5B). The mouse anti-ACE2 monoclonal antibody (2F12A4) failed to fully stain MDCK-hACE2 cells, even at the highest concentration tested (20 µg/mL), and showed high levels of non-specific binding to MDCK cells (Figure 3.5C). Based on these results, the goat anti-ACE2

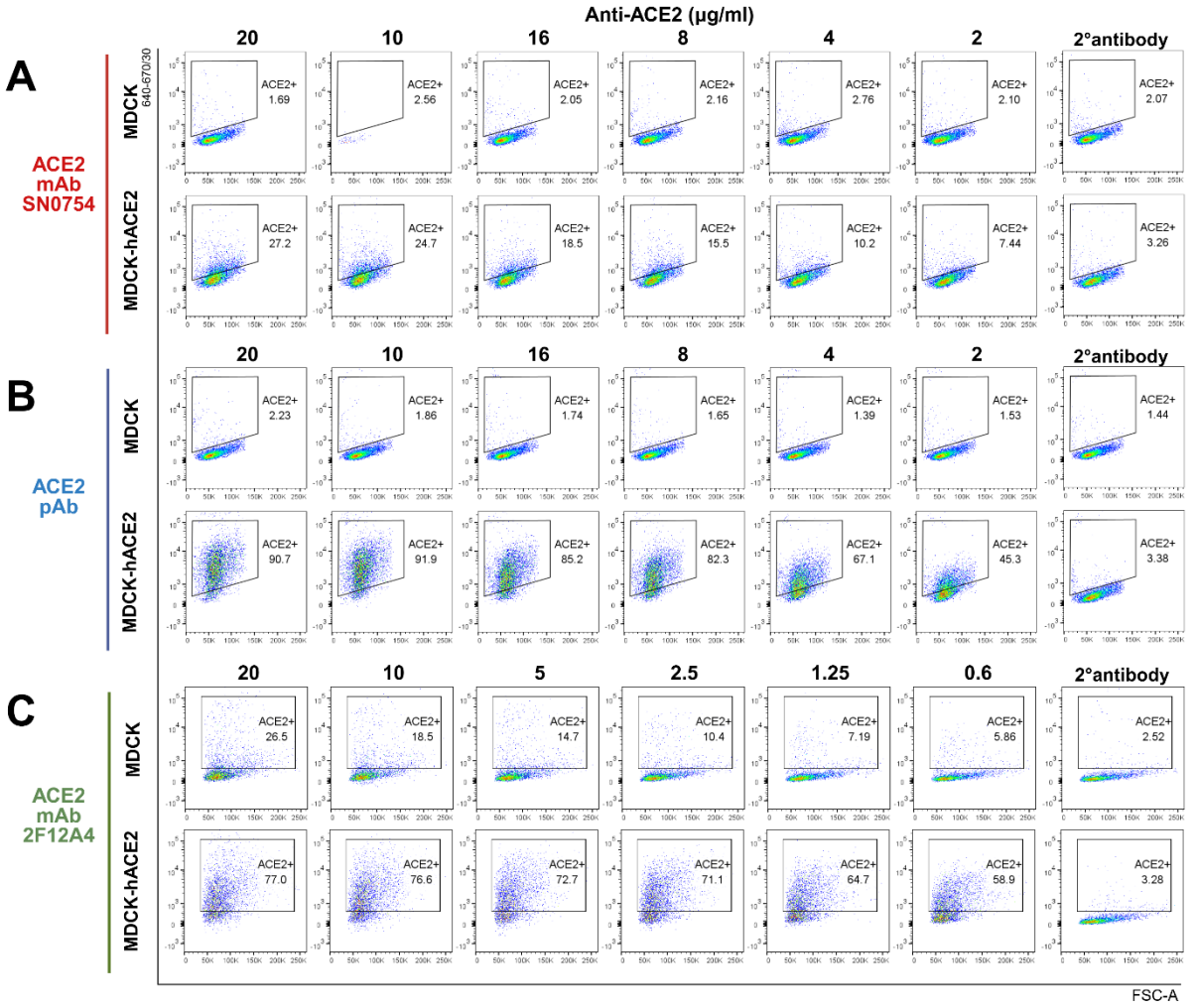
Anti-ACE2 (µg/ml)
A
ACE2 mAb SN0754
MDCK
MDCK-hACE2
640-670/30
20
10
16
8
4
2
2°antibody
ACE2+ 1.69
ACE2+ 2.56
ACE2+ 2.05
ACE2+ 2.16
ACE2+ 2.76
ACE2+ 2.10
ACE2+ 2.07
ACE2+ 27.2
ACE2+ 24.7
ACE2+ 18.5
ACE2+ 15.5
ACE2+ 10.2
ACE2+ 7.44
ACE2+ 3.26
B
ACE2 pAb
ACE2+ 2.23
ACE2+ 1.86
ACE2+ 1.74
ACE2+ 1.65
ACE2+ 1.39
ACE2+ 1.53
ACE2+ 1.44
ACE2+ 90.7
ACE2+ 91.9
ACE2+ 85.2
ACE2+ 82.3
ACE2+ 67.1
ACE2+ 45.3
ACE2+ 3.38
C
ACE2 mAb 2F12A4
5
2.5
1.25
0.6
ACE2+ 26.5
ACE2+ 18.5
ACE2+ 14.7
ACE2+ 10.4
ACE2+ 7.19
ACE2+ 5.86
ACE2+ 2.52
ACE2+ 77.0
ACE2+ 76.6
ACE2+ 72.7
ACE2+ 71.1
ACE2+ 64.7
ACE2+ 58.9
ACE2+ 3.28
FSC-A

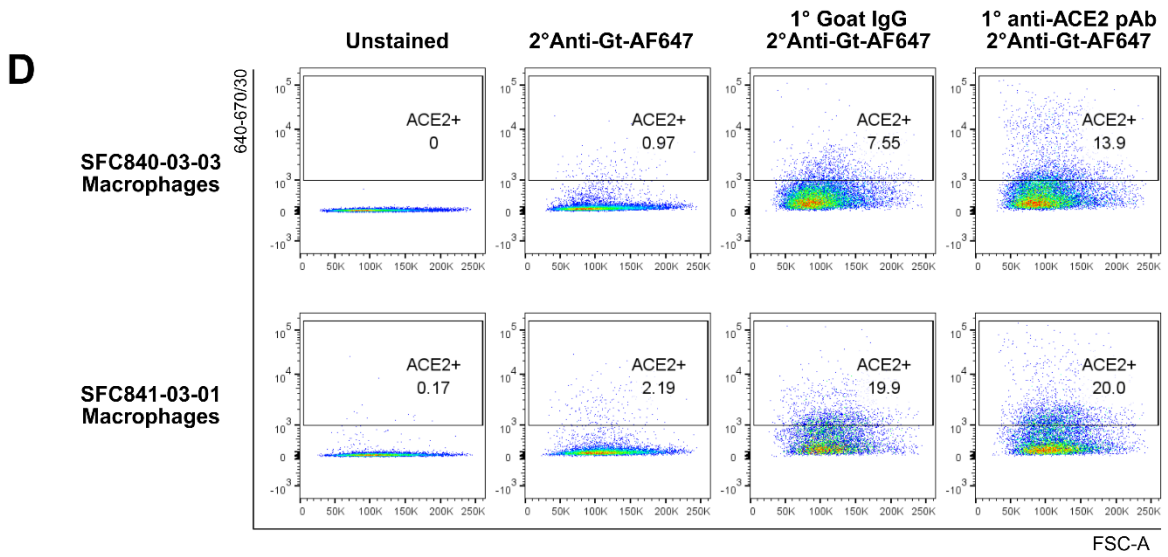
D
Unstained
2°Anti-Gt-AF647
1° Goat IgG 2°Anti-Gt-AF647
1° anti-ACE2 pAb 2°Anti-Gt-AF647
640-670/30
SFC840-03-03 Macrophages
SFC841-03-01 Macrophages
ACE2+ 0
ACE2+ 0.97
ACE2+ 7.55
ACE2+ 13.9
ACE2+ 0.17
ACE2+ 2.19
ACE2+ 19.9
ACE2+ 20.0
FSC-A

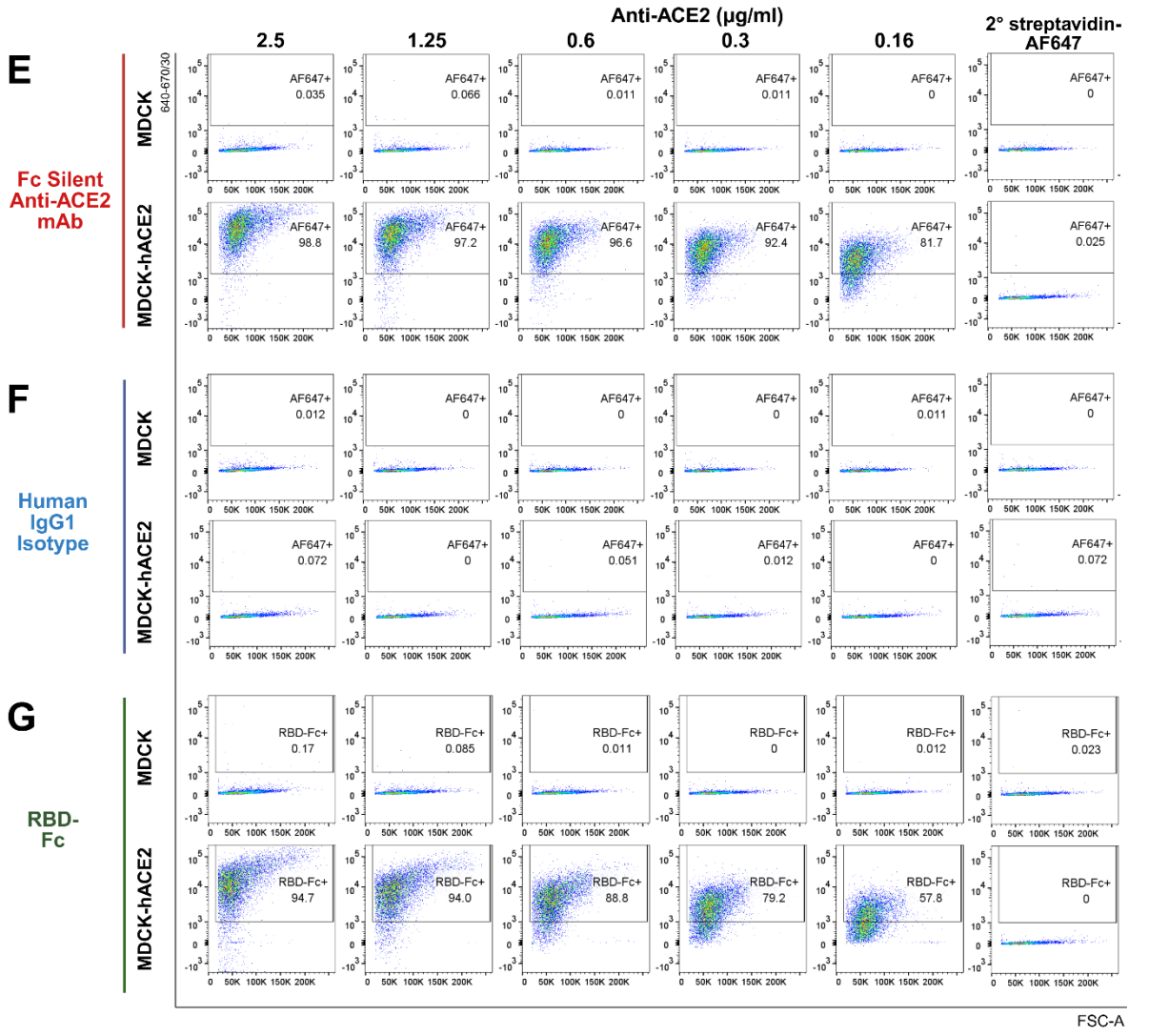

Figure 3.5. Troubleshooting and optimisation of anti-ACE2 staining for flow-cytometric detection of ACE2. iPSC-derived macrophages, MDCK cells, and MDCK-hACE2 cells were stained with the indicated primary and secondary antibodies and analysed by flow cytometry. **(A)** Rabbit anti-ACE2 monoclonal antibody SN0754 (Invitrogen, MA5-32307) was titrated on MDCK and MDCK-hACE2 cells and detected with anti-rabbit-AF647 secondary antibody. **(B)** Goat anti-ACE2 polyclonal antibody (Invitrogen, PA5-47488) was titrated on MDCK and MDCK-hACE2 cells and detected with anti-goat-AF633 secondary antibody. **(C)** Mouse anti-ACE2 monoclonal antibody 2F12A4 (PeproTech, 66699) was titrated on MDCK and MDCK-hACE2 cells and detected with anti-mouse-AF647 secondary antibody. **(D)** iPSC-derived macrophages were blocked with 5% BSA, 5 µg/ml human IgG, and Fc block, then incubated with 10 µg/ml goat anti-ACE2 polyclonal antibody (Invitrogen, PA5-47488) or goat IgG isotype control, followed by detection with anti-goat-AF633 secondary antibody. **(E)** Biotinylated Fc Silent™ anti-ACE2 antibody (Absolute Antibody, Ab03703-10.3) was titrated on MDCK and MDCK-hACE2 cells and detected with AF647-conjugated streptavidin. **(F)** Biotinylated Fc Silent™ anti-fluorescein human IgG1 isotype control (Absolute Antibody, Ab00102-10.3) was titrated on MDCK and MDCK-hACE2 cells and detected with AF647-conjugated streptavidin. **(G)** Biotinylated Fc Silent™ RBD–Fc fusion protein was titrated on MDCK and MDCK-hACE2 cells and detected with AF647-conjugated streptavidin.

polyclonal antibody was selected as the most suitable reagent and used at an optimised concentration of 10 µg/mL.

iPSC-derived macrophages from two donors (SFC840-03-03 and SFC841-03-01) were subsequently stained with the goat anti-ACE2 polyclonal antibody (Figure 3.5D). Prior to staining, cells were blocked with 5% BSA, human IgG (5 µg/mL), and Fc blocking reagent (Miltenyi). Cells were then stained with anti-ACE2 polyclonal antibody or a goat IgG isotype control and detected using an AF633-conjugated anti-goat secondary antibody. Despite Fc receptor blocking, substantial non-specific binding of both primary and secondary antibodies was observed in macrophages from both donors.

To eliminate Fc receptor–mediated non-specific staining, conventional antibodies were abandoned in favour of Fc-silent™ reagents. An Fc-silent™ anti-ACE2 antibody (Absolute Antibody, Ab03703-10.3) and a matched Fc-silent™ human IgG1 isotype control (Absolute Antibody, Ab00102-10.3) were titrated on MDCK control cell lines (Figures 3.5E, F). These antibodies contain proprietary mutations that abrogate Fc receptor binding. To avoid secondary antibody mediated background, both antibodies were biotinylated and detected using AF647-conjugated streptavidin. Titration experiments demonstrated complete staining of MDCK-hACE2 cells with no detectable non-specific binding. The optimal concentration of the Fc-silent™ anti-ACE2 antibody was determined to be 0.3 µg/mL, representing the lowest concentration that achieved full staining of ACE2-positive cells.

In parallel, an Fc-silent receptor-binding domain fusion protein (RBD-Fc) containing LALA mutations in the Fc region was designed and expressed in-house to further minimise Fc receptor interactions. Titration of RBD-Fc on MDCK control cell lines identified an optimal concentration of 2.5 µg/mL to achieve complete staining of ACE2-expressing cells (Figure 3.5G).

In summary, flow cytometric detection of ACE2 in macrophages is technically challenging due to Fc receptor-mediated non-specific antibody binding, which can result in false-positive staining or obscure true signal. These limitations were overcome by the use of biotinylated Fc-silent™ antibodies with streptavidin-based detection, enabling specific and sensitive assessment of ACE2 expression.

3.2.3 SARS-CoV-2 uptake by macrophages is not via an alternative spike binding receptor

Macrophage surface does not bind SARS-CoV-2 spike

The absence of ACE2 expression and the lack of binding of the RBD-Fc fusion protein to macrophages indicate that iPSC-derived macrophages do not express receptors capable of interacting with the RBD of the SARS-CoV-2 spike protein. However, these findings do not exclude the possibility of interactions between macrophages and other regions of spike, mediated by alternative attachment factors, such as pattern-recognition or scavenger receptors.

To investigate this, iPSC-derived macrophages and MDCK control cell lines were incubated with Wuhan HexaPro spike trimer for 1 h at 4 °C to prevent internalisation. Spike binding was assessed by flow cytometry (Figure 3.6A). Spike protein bound strongly to the MDCK-hACE2 cells, even at the lowest concentration tested, confirming assay sensitivity. In contrast, no detectable binding of SARS-CoV-2 spike was observed on the surface of iPSC-derived macrophages. These data indicate that macrophages do not express surface receptors capable of binding the Wuhan SARS-CoV-2 spike protein.

Changes in the spike glycan shield do not affect macrophage binding

The SARS-CoV-2 spike protein is heavily glycosylated across both the S1 and S2 subunits, which are major targets of antibody binding (Figure 3.6C). Macrophages are known to bind and internalise several enveloped viruses through glycan-dependent interactions mediated by lectin or scavenger receptors, often independently of canonical entry receptors[143,144].

The original Wuhan SARS-CoV-2 spike contains 22 N-linked glycosylation sites[145]. However, as shown above, Wuhan spike did not bind to the macrophage surface. Several SARS-CoV-2 variants carry mutations that alter the number of N-linked glycan sites and could therefore alter interactions with macrophage attachment factors or pattern-recognition receptors (Figure 3.6B). Alpha, Beta, BA.5, and XBB1.5 variants retain the same 22 glycosylation sites as Wuhan. In contrast, the Gamma variant contains two additional sites (N20 and N188), Delta lacks one site (N17), and the Omicron KP3.1 variant gains an additional site at N30.

To assess whether these variant-specific changes influence macrophage binding, the binding of recombinant spike proteins from Alpha, Beta, Delta, BA.5, XBB1.5, and KP3.1 variants was assessed (Figure 3.6D). Flow cytometric analysis revealed that all variant spike proteins bound

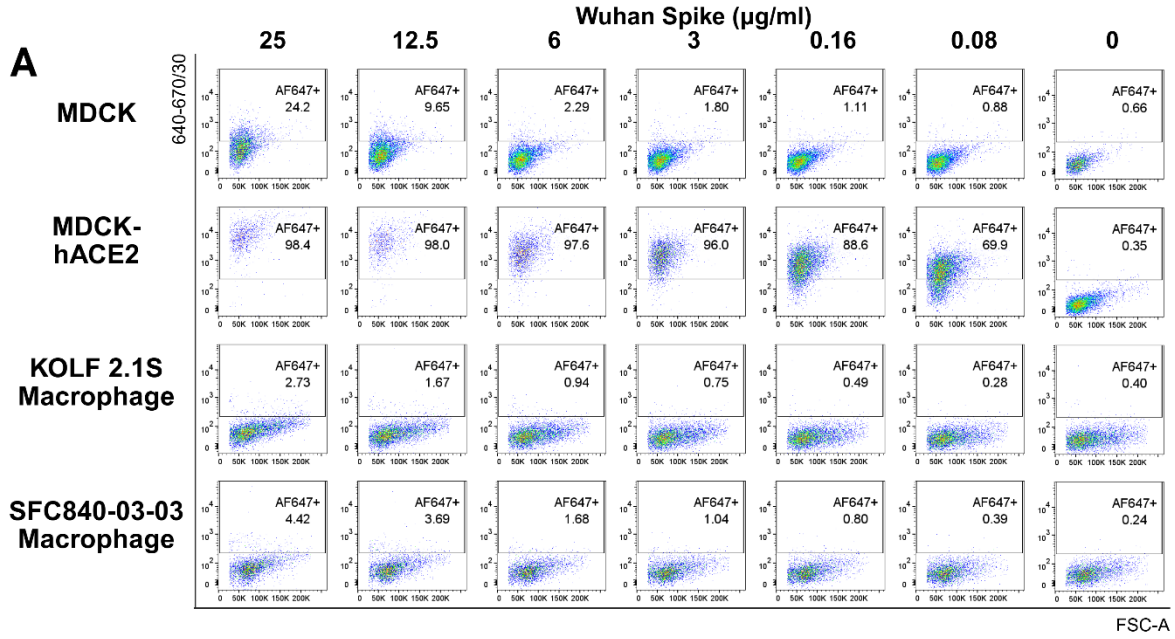

B

	S1 (NTD)											S1 (RBD)		S1 (SD1/SD2)			S2									Glycan Sites
	17	20	30	61	74	122	149	165	188	234	282	331	343	603	616	657	709	717	801	1074	1098	1134	1158	1173	1194	
Wuhan		X	X						X																	22
Alpha		X	X						X																	22
Beta		X	X						X																	22
(Gamma)			X																							24
Delta	X	X	X						X																	21
BA.5		X	X						X																	22
XBB1.5		X	X						X																	22
KP3.1		X							X																	23

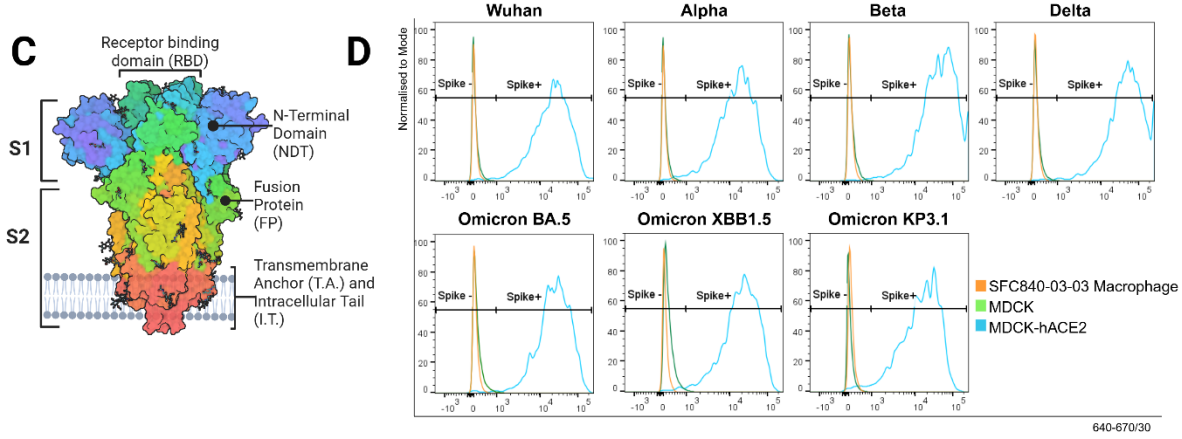

Figure 3.6. Macrophages do not express SARS-CoV-2 spike-binding receptors. (A) Flow-cytometric analysis of Wuhan HexaPro spike trimer binding to iPSC-derived macrophages (SFC840-03-03 and KOLF 2.1S) or to MDCK and MDCK-hACE2 cells. Cells were incubated with a titration of biotinylated, prefusion-stabilised Wuhan HexaPro spike trimer at 4 °C for 1 h, followed by detection with streptavidin–AF647. **(B)** Comparison of SARS-CoV-2 spike N-linked glycosylation sites across variants. The original Wuhan strain contains 22 canonical glycosylation sites; a cross indicates a site that is absent in the indicated variant. **(C)** Cryo-electron microscopy (cryo-EM) structure of the SARS-CoV-2 spike trimer (PDB ID: 6VXX). Schematic adapted from BioRender. **(D)** Flow-cytometric analysis of spike trimers from different SARS-CoV-2 variants binding to iPSC-derived macrophages (SFC840-03-03) or MDCK and MDCK-hACE2 cells. Cells were incubated with 5 µg/ml biotinylated spike trimer at 4 °C for 1 h, followed by detection with streptavidin–AF647.

robustly to MDCK-hACE2 control cells, confirming protein integrity and assay sensitivity. In contrast, none of the variant spike proteins showed detectable binding to macrophage surfaces.

Several alternative SARS-CoV-2 macrophage receptors have been proposed that bind and internalise SARS-CoV-2 via spike protein interactions. This data indicates that SARS-CoV-2 spike protein does not bind to the macrophage surface and therefore rules out the possibility of an alternative macrophage receptor. SARS-CoV-2 internalisation into macrophages must therefore be either non-receptor mediated or mediated by a receptor to other components of the viral envelope.

Challenges in Flow Cytometric Detection of Surface-Bound SARS-CoV-2 Virions

To elucidate the mechanism by which SARS-CoV-2 is internalised into macrophages, it would be informative to determine whether macrophages express surface receptors capable of directly binding the whole virion. To address this, I sought to develop a flow cytometry-based assay to detect virion binding at the cell surface. In principle, detection of surface-bound virus would indicate the presence of a receptor mediating virion attachment. However, despite extensive troubleshooting, this assay proved technically challenging and could not be established, as described below.

The assay was initially established using MDCK-hACE2 cells as a positive control. Cells were incubated with SARS-CoV-2 at an MOI of 3 for 1 h at 4 °C to permit viral binding to ACE2 while preventing internalisation. Cells were then gently washed twice with PBS to remove unbound virions, fixed with paraformaldehyde, and stained with an anti-spike antibody (FB 9D), followed by detection using an anti-human AF488-conjugated secondary antibody (Figure 3.7A). Under these conditions, no positive signal corresponding to surface-bound SARS-CoV-2 was detected on MDCK-hACE2 cells (Figure 3.7B).

Several possible explanations for the lack of signal were considered. First, SARS-CoV-2 may not bind MDCK-hACE2 cells under these conditions; however, this is unlikely, as recombinant spike binds robustly to these cells under identical conditions, and MDCK-hACE2 cells are permissive to SARS-CoV-2 infection. Second, the primary or secondary antibodies may be unsuitable for detecting surface-bound virus; this is also unlikely, as both antibodies have been successfully used previously to detect intracellular SARS-CoV-2. Third, the amount of virus bound to the cell surface may be insufficient to generate a detectable signal by flow cytometry, which was considered the most plausible explanation and therefore investigated further.

To test whether insufficient surface-bound antigen accounted for the lack of signal, a troubleshooting assay was performed using recombinant spike protein in place of intact virions. Both ACE2-positive and ACE2-negative control cells were incubated with titrated amounts of recombinant spike, followed by detection with fluorescent streptavidin (Figure 3.7C). Recombinant spike was used because its binding to ACE2 is well established and because its concentration can be precisely quantified, whereas SARS-CoV-2 stocks are defined only by infectious titre. Cells were incubated with a range of spike concentrations, and estimates of the equivalent MOI were calculated as outlined in Figure 3.7D. The four highest spike concentrations corresponded to estimated MOIs of 21, 7, 2, and 1, spanning the range of the original virion-binding experiment (MOI 3).

Recombinant spike bound robustly to MDCK-hACE2 cells at all concentrations tested, while no binding was detected on MDCK wild-type cells (Figure 3.7E). This indicates that the quantity of virions applied in the original assay was not limiting for signal detection. In VET cells, spike binding was detectable above background at all concentrations but was substantially weaker than in MDCK-hACE2 cells. Signal intensity in MDCK-hACE2 cells was up to 65-fold higher than in VET cells incubated with the same amount of spike protein. This difference is likely attributable to differences in ACE2 surface expression between the cell lines. While there are no published estimates of ACE2 copy number on Vero cells, it is likely to be in the range of hundreds to thousands of molecules per cell. In contrast, MDCK-hACE2 cells overexpress transgenic human ACE2 via lentiviral transduction, and ACE2 expression may plausibly range from 10^4 to 10^6 molecules per cell.

Together, these experiments demonstrate that insufficient antigen availability is unlikely to explain the failure to detect surface-bound SARS-CoV-2 in the original assay. However, they also highlight the technical challenge of detecting virion binding to cells expressing physiological levels of SARS-CoV-2 receptors, compared with cells that overexpress ACE2.

Next, I investigated whether the lack of signal in the initial experiment was due to limitations in antibody detection using the anti-spike antibody FB 9B in combination with the anti-human AF488–conjugated secondary antibody. To test this, MDCK-hACE2 cells were incubated with recombinant spike protein and stained with a panel of anti-spike antibodies, all detected using the same anti-human AF488 secondary antibody (Figure 3.7F). Recombinant spike was detected on the surface of spike-bound cells by all antibodies tested, with the exception of FB 9B, which had been used in the original virion-binding experiment (Figure 3.7G)

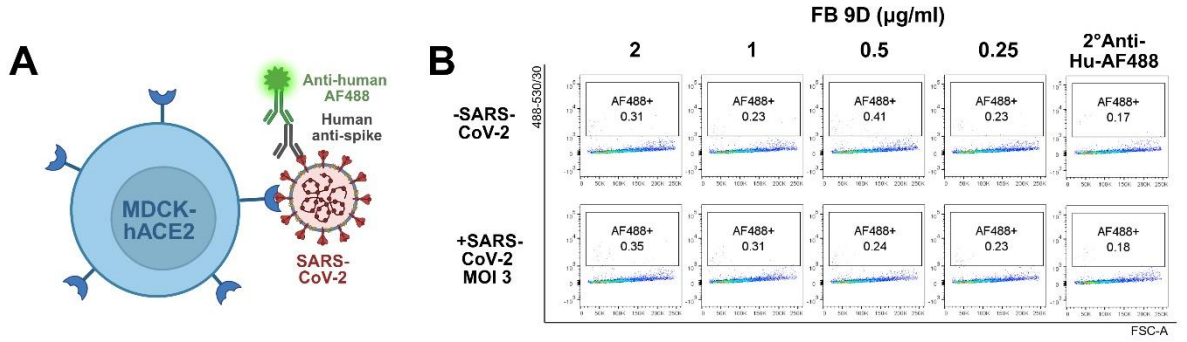

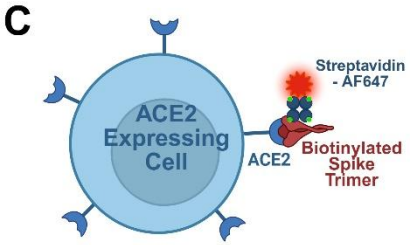

D

Spike (µg)	Spike (g)	Spike (n)	Spike Monomers	Spike Trimers	Virions	Virions/cell	MOI (if P:PFU = 1:1000
0.06	5.56E-08	3.09E-13	1.86E+11	6.2E+10	2.1E+09	20645	21
0.02	1.85E-08	1.03E-13	6.19E+10	2.1E+10	6.9E+08	6882	7
0.01	6.17E-09	3.43E-14	2.06E+10	6.9E+09	2.3E+08	2294	2
0.002	2.06E-09	1.14E-14	6.88E+09	2.3E+09	7.6E+07	765	1
0.001	6.86E-10	3.81E-15	2.29E+09	7.6E+08	2.5E+07	255	0
2.3E-04	2.29E-10	1.27E-15	7.65E+08	2.5E+08	8.5E+06	85	0
7.6E-05	7.62E-11	4.23E-16	2.55E+08	8.5E+07	2.8E+06	28	0
2.5E-05	2.54E-11	1.41E-16	8.50E+07	2.8E+07	9.4E+05	9	0

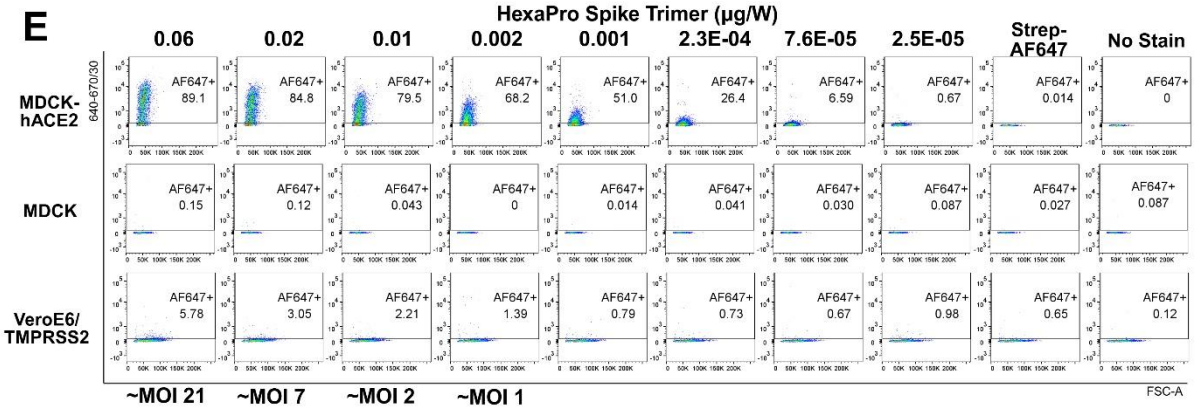

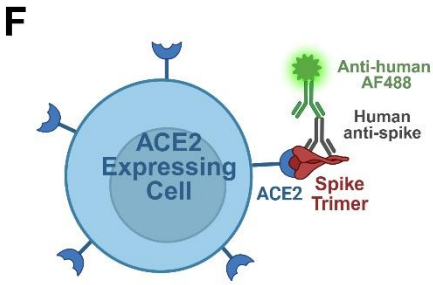

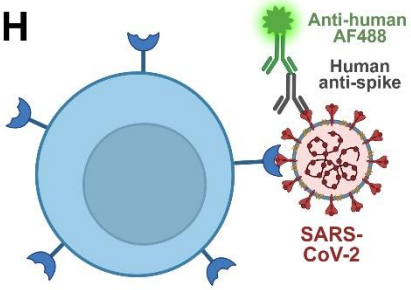

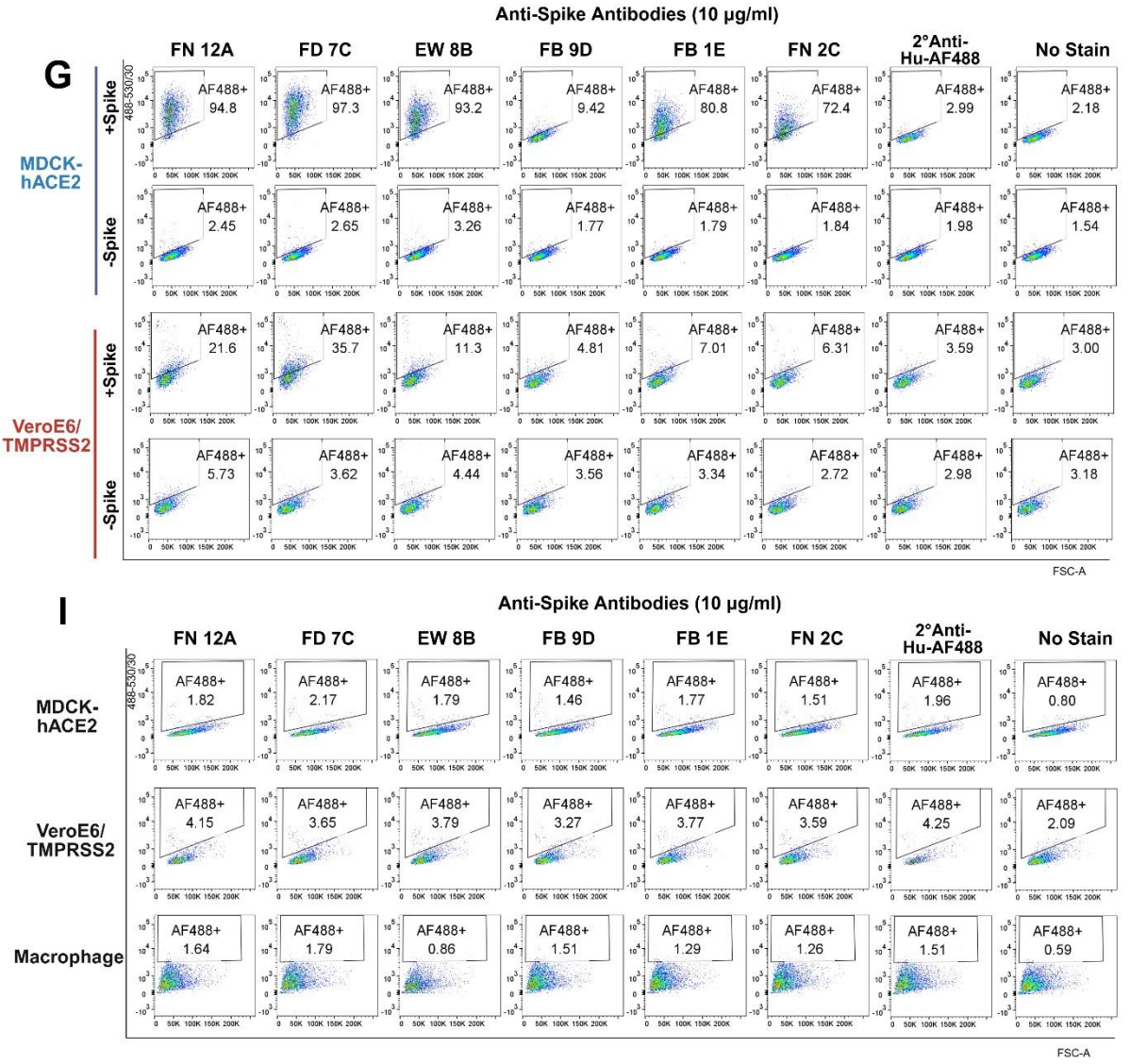

Figure 3.7. Development of a flow cytometric assay to detect extracellular surface-bound SARS-CoV-2 and spike protein (A) Schematic illustrating the flow cytometric detection of extracellular surface-bound SARS-CoV-2 virions on receptor-expressing cells (see panel B). **(B)** Flow cytometric detection of extracellular virions bound to the surface of MDCK-hACE2 cells. Cells were incubated with SARS-CoV-2 at MOI 3, or media alone, at 4 °C for 1 h to allow virion binding to ACE2. Cells were washed twice with ice-cold PBS, fixed with PFA, incubated with a titration of anti-spike antibody (FB 9D), and detected using anti-human AF488. **(C)** Schematic illustrating the flow cytometric detection of surface-bound recombinant Wuhan HexaPro spike protein on receptor-expressing cells (see panel E). Spike protein was biotinylated and detected using streptavidin-AF647. **(D)** Table showing equivalence between recombinant spike protein and viral particles. The number of spike trimers per µg of recombinant protein was calculated assuming a spike monomer molecular weight of 180 kDa. Viral particle equivalents were calculated assuming 30 spike trimers per virion. MOI estimates were derived assuming a particle-to-PFU ratio of 1:1000. **(E)** Flow cytometric detection of surface binding of biotinylated HexaPro spike trimers. MECK-hACE2, MDCK, and VET cells were incubated with a titration of spike trimer at 4 °C for 1 h. Bound spike was detected using streptavidin-AF647. **(F)** Schematic illustrating flow cytometric detection of surface-bound recombinant Wuhan HexaPro spike protein using anti-spike antibodies (see panel G). **(G)** Flow cytometric detection of surface-bound spike protein using a panel of anti-spike antibodies. MECK-hACE2 or VET cells were incubated with spike trimer at 4 °C for 1 h. Following spike coating, anti-spike antibodies (10 µg/ml) were added and detected using anti-human AF488. **(H)** Schematic illustrating flow cytometric detection of extracellular surface-bound SARS-CoV-2 virions on receptor-expressing cells (see panel I). **(I)** Flow cytometric detection of extracellular virions bound to the surface of MDCK-hACE2, VET cells, or iPSC- macrophages (KOLF2.1S). Cells were incubated with SARS-CoV-2 at MOI 20 at 4 °C for 1 h to allow virion binding. Cells were washed twice with ice-cold PBS, fixed with PFA, incubated with anti-spike antibodies (10 µg/ml), and detected using anti-human AF488.

FB 9B has previously been used successfully to detect intracellular SARS-CoV-2, this is significant as this would indicate that this antibody preferentially recognises spike in a post-fusion or intracellularly accessible conformation but does not efficiently bind the prefusion spike conformation present on surface-bound virions. This provides a plausible explanation for why FB 9B was able to detect intracellular, but not extracellular, spike and explains why there was no signal in the initial experiment.

Given that an MOI of 3 should provide sufficient antigen for surface detection, and that surface-bound prefusion spike is detectable by multiple anti-spike antibodies, a final troubleshooting experiment was performed using the original virion-binding conditions. Cells were incubated with SARS-CoV-2 at an MOI of 3 at 4 °C and stained with a panel of six anti-spike antibodies (Figure 3.7H). Under these conditions, there was still no surface-bound SARS-CoV-2 detectable on MDCK-hACE2 cells, Vero E6-TMPRSS2 (VET) cells, or macrophages with any of the antibodies tested (Figure 3.7I).

This series of troubleshooting experiments demonstrate that while recombinant spike protein can bind to the cell surface and be readily detected by antibody staining and flow cytometry, intact SARS-CoV-2 virions cannot be detected under the same conditions. This indicates that the main technical challenge lies in detecting surface-bound virions and explains why this assay could not be successfully established. Reasons why surface-bound recombinant spike, but not surface-bound virions, can be detected could be due to steric hindrance or epitope inaccessibility when virions are bound to the membrane or loss of virion integrity during the experimental process.

3.2.4 Macrophage internalisation of SARS-CoV-2 is not caveolar endocytosis or macropinocytosis

SARS-CoV-2 internalisation into macrophages is not mediated by caveolin-dependent endocytosis

Macrophages do not express high-affinity receptors for the SARS-CoV-2 spike protein. This makes classical receptor-dependent CME unlikely, as this process requires high-affinity receptor-ligand interactions. Consequently, SARS-CoV-2 internalisation into macrophages is more likely to occur via a receptor-independent mechanism or through receptors that recognise other components of the viral particle, such as the lipid envelope.

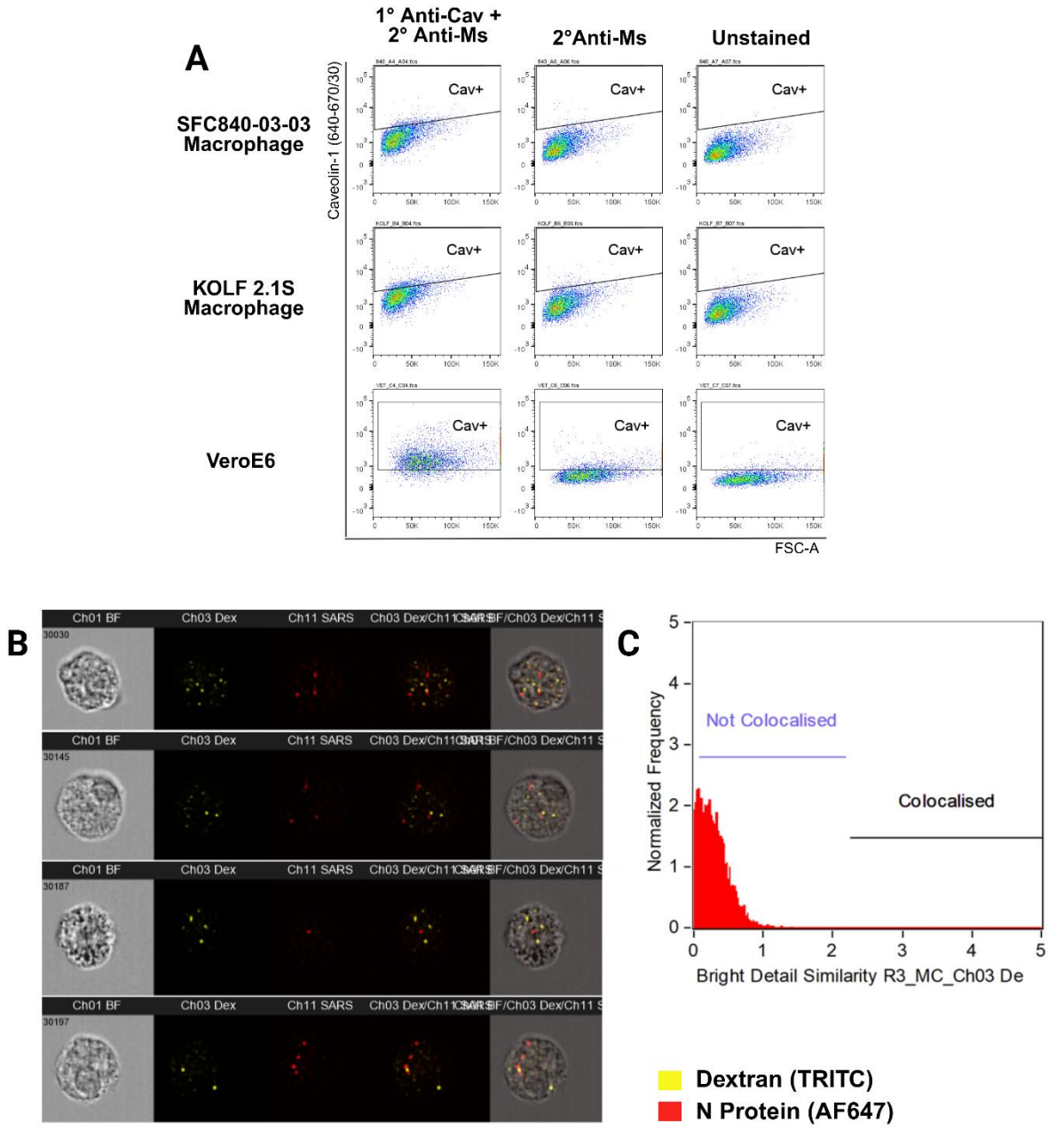

Figure 3.8. SARS-CoV-2 internalisation into macrophages is not caveolar endocytosis or macropinocytosis. (A) Surface and intracellular caveolin-1 expression in iPSC-derived macrophages and Vero cells. iPSC-derived macrophages (SFC840-03-03 and KOLF2.1S) were fixed, permeabilised and blocked. Cells were stained with a mouse anti-caveolin-1 antibody (0.25 µg/mL) and detected with anti-mouse-AF647. Vero cells, which express high caveolin-1 levels, served as a positive control. **(B)** Representative imaging flow cytometry (ImageStream®) images showing iPSC-macrophages (KOLF2.1S) with intracellular SARS-CoV-2 and dextran. Macrophages were co-incubated with SARS-CoV-2 at an MOI = 10 and dextran-TRITC (100 µg/mL) for 2 h, followed by fixation, permeabilisation, and staining with FB 9B-AF647. Bright-field, yellow-channel, red-channel, and composite images were captured using the ImageStream® system and processed in IDEAS software. **(C)** The bright detail similarity R3 feature analysis on SARS-CoV-2 and dextran co-localisation. The bright detail similarity R3 feature is the log transformed pearson's correlation coefficient of foci localised with a radius of 3 pixels of less. Foci with an R3 value less than 3 are not co-localised

Caveolin-mediated endocytosis is a distinct endocytic pathway in which cargo is internalised via caveolae, flask-shaped plasma membrane invaginations enriched in cholesterol, sphingolipids, and the structural protein caveolin-1[146]. This pathway can be either receptor-dependent or receptor-independent and has been implicated in the entry of several viruses, particularly those capable of exploiting lipid–lipid interactions with the host plasma membrane. Given that SARS-CoV-2 is an enveloped virus and that macrophages lack spike-binding receptors, caveolin-mediated endocytosis represented a plausible mechanism for viral internalisation. However, the expression of caveolin-1 in macrophages remains controversial in the literature[147,148].

To determine whether caveolin-mediated endocytosis could operate in macrophages, caveolin-1 surface expression was assessed by flow cytometry (Figure 3.8A). Flow cytometric analysis revealed no detectable caveolin-1 expression in iPSC-derived macrophages, whereas surface caveolin-1 was strongly detected in Vero cells. Together, these data demonstrate that iPSC-derived macrophages lack surface caveolin-1 expression and therefore are unlikely to support caveolin-mediated endocytosis. This indicates that caveolin-dependent pathways do not contribute to SARS-CoV-2 internalisation into macrophages and that alternative entry mechanisms must be responsible.

SARS-CoV-2 internalisation into macrophages does not occur via classical bulk fluid-phase macropinocytosis

Having established that SARS-CoV-2 internalisation into macrophages is unlikely to occur via receptor-mediated CME or caveolar endocytosis, macropinocytosis represented another plausible uptake mechanism. Macropinocytosis is a non-specific form of endocytosis involving the uptake of extracellular fluid and solutes and is exploited by a range of viruses.

To assess co-localisation between SARS-CoV-2 and dextran, macrophages were co-incubated with SARS-CoV-2 and dextran-TRITC. Images of macrophages containing intracellular dextran and SARS-CoV-2 nucleoprotein were acquired using the ImageStream platform (Figure 3.8B). Intracellular co-localisation was quantified using the Bright Detail Similarity (R3) feature, which measures the spatial correlation of bright, punctate signals between two fluorescent channels. R3 values below 3 indicate that the signals occupy distinct intracellular compartments, whereas higher values indicate co-localisation within the same vesicular structures. R3 values for SARS-CoV-2 and dextran ranged between 0 and 1, indicating that viral antigen and dextran occupied distinct intracellular compartments (Figure 3.8C).

As SARS-CoV-2 and dextran were present simultaneously in the extracellular medium yet segregated into separate intracellular compartments following uptake, these data strongly

suggest that SARS-CoV-2 is not internalised into macrophages via classical bulk fluid-phase macropinocytosis.

3.2.5 Macrophage internalisation of SARS-CoV-2 is not mediated by phosphatidylserine receptors TREM2, TIM4 or MERTK

Challenges of using annexin V to block phosphatidylserine - receptor interactions

The lack of SARS-CoV-2 and dextran co-localisation does not exclude the involvement of other macropinocytosis-like uptake pathways, such as apoptotic mimicry. This is the process by which viral phosphatidylserine (PS) binds to phosphatidylserine receptors (PSRs) on the surface of a cell to stimulate macropinocytosis-like internalisation. This represented another plausible mechanism of viral internalisation. Macrophages express multiple PSRs, including TIM4, MerTK, and stabilin, which are among the most prominent[149] (Figure 3.9A).

Annexin V is a calcium-dependent phospholipid-binding protein that is widely used to bind PS and interfere with PS-PSR interactions. To assess whether macrophage PSRs recognise PS on the SARS-CoV-2 envelope, virus was pre-incubated with titrated concentrations of annexin V prior to incubation with macrophages. Viral internalisation was quantified by flow cytometric detection of intracellular nucleoprotein (Figure 3.9B). Unexpectedly, SARS-CoV-2 internalisation increased in a concentration-dependent manner with annexin V treatment, with the highest concentration resulting in a 2.4-fold increase in viral internalisation compared with virus alone (Figure 3.9C).

Although annexin V is commonly used to block PS-mediated interactions, previous studies have reported that annexin V can act as a bridging molecule between PS and PSRs, thereby enhancing uptake rather than inhibiting it. The observed enhancement is therefore consistent with these reports. While increased PS-mediated uptake could suggest involvement of PSRs in SARS-CoV-2 internalisation, the potential for annexin V mediated artefacts precludes definitive conclusions. As annexin V is the only commercially available reagent capable of broadly targeting PS-PSR interactions, subsequent experiments adopted a more targeted approach using receptor-specific knockouts, inhibitors, and blocking antibodies to interrogate the role of individual PSRs.

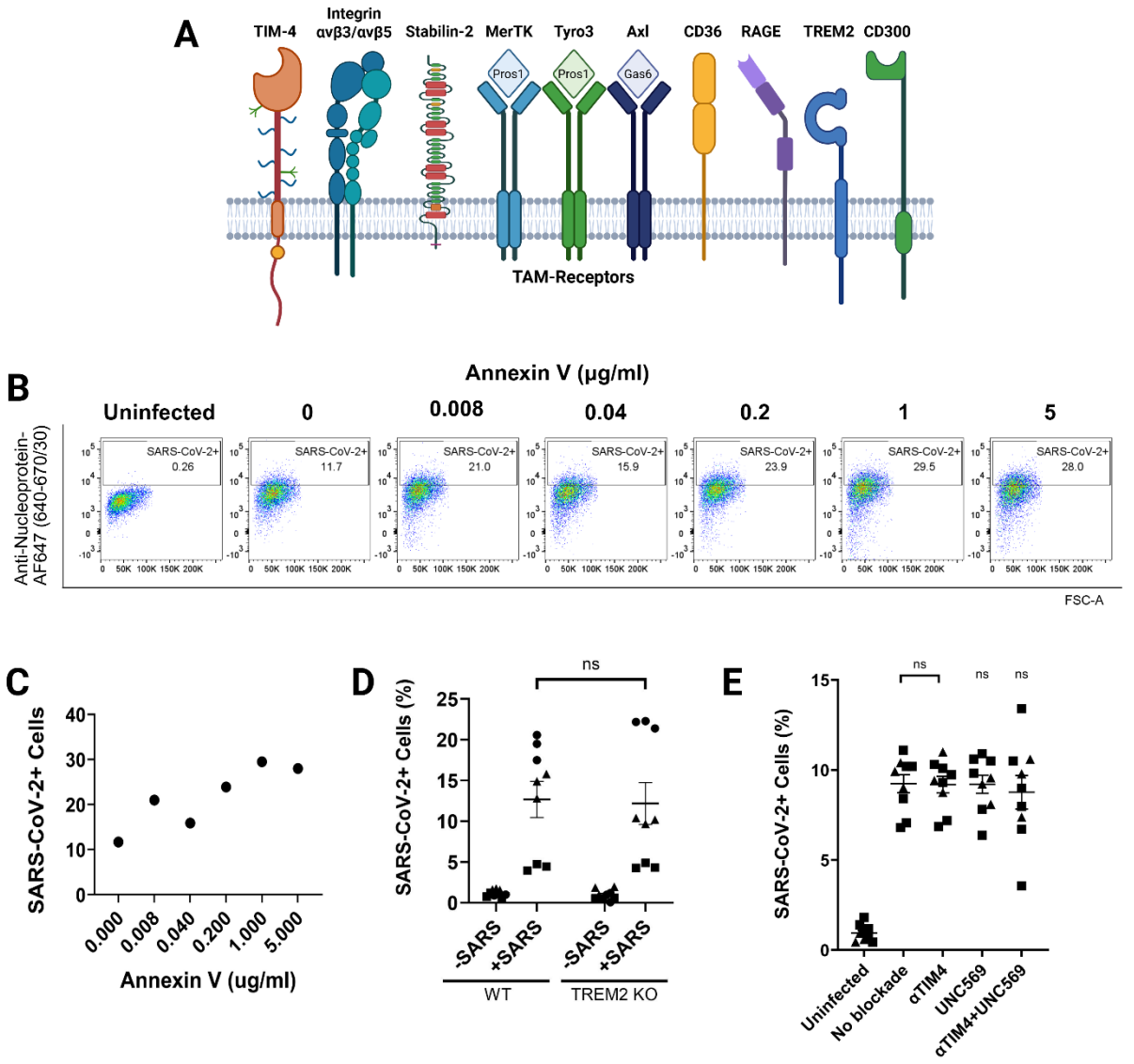

Figure 3.9 SARS-CoV-2 internalisation into macrophages is independent of the phosphatidylserine receptors TREM2, TIM4, and MerTK. (A) Schematic of the most highly expressed phosphatidylserine receptors on macrophages. **(B)** Annexin V coated SARS-CoV-2 internalisation. Virus was incubated with titrated concentrations of annexin V for 1 h and added to iPSC-macrophages (KOLF2.1S) at MOI 2. Virus internalisation was quantified by flow cytometry 2 h post-inoculation. **(C)** Percentage SARS-CoV-2 positive cells plotted against annexin V concentration, From (B). **(D)** SARS-CoV-2 internalisation in wild-type (BIONi010-C) and TREM2 knockout (KO) (BIONi010-C-17) macrophages following infection at MOI 20, measured by flow cytometry 2 h post-inoculation. Mean ± SEM of three independent experiments (n = 3 experiments; three technical replicates per experiment). Statistics: unpaired Student's t-test assuming equal variance (uncorrected) **(E)** SARS-CoV-2 internalisation following TIM4 and/or MerTK blockade. iPSC-macrophages (SFC840-01-01) were pre-treated with anti-TIM4 (2.5 μg/mL) and/or UNC569 (1 μM) and infected at MOI 20 in the continued presence of inhibitors. Internalisation was quantified by flow cytometry 2 h post-inoculation. Mean ± SEM of three independent experiments (n = 3 experiments; three technical replicates per experiment). Statistics: unpaired Student's t-test assuming equal variance (uncorrected)

TREM2 knockout macrophages reveal that TREM2 does not mediate SARS-CoV-2 internalisation

Triggering receptor expressed on myeloid cells 2 (TREM2) is a macrophage and microglial surface receptor that recognises damage-associated lipid patterns [150]. A TREM2 knockout (KO) iPSC line was previously generated from the BIONi010-C donor [65]. To assess the role of TREM2 in SARS-CoV-2 uptake, viral internalisation was compared between wild-type and TREM2 KO iPSC-derived macrophages (Figure 3.9D). Across three independent experiments, no difference in SARS-CoV-2 internalisation was observed between TREM2-deficient macrophages and genotype-matched wild-type controls, indicating that TREM2 does not contribute to viral internalisation.

TIM-4 and MERTK blockade reveals no involvement in SARS-CoV-2 internalisation

TIM4 and Mer receptor tyrosine kinase (MerTK) are major PSRs involved in the recognition and engulfment of apoptotic cells. To investigate their role in SARS-CoV-2 internalisation, macrophages were treated with an anti-TIM4 blocking antibody and UNC569, a potent inhibitor of the TAM family receptor tyrosine kinases, with strongest activity against MerTK but also targeting Axl and Tyro3. Flow cytometric analysis of intracellular nucleoprotein across three independent experiments revealed no significant difference in SARS-CoV-2 internalisation following blockade of TIM4 or MerTK signalling compared with untreated controls (Figure 3.9E). These results indicate that it is unlikely that TIM4 nor MerTK are involved in SARS-CoV-2 internalisation into macrophages.

3.2.6 Investigation of SARS-CoV-2 entry mechanism into macrophages using pharmacological inhibitors

Pharmacological inhibition of major endocytic pathways

To further investigate the route of SARS-CoV-2 internalisation into macrophages, a panel of pharmacological inhibitors targeting major endocytic pathways was screened to assess their effect on viral internalisation. The aim was to establish an assay in which macrophages were pre-incubated with individual inhibitors, followed by exposure to SARS-CoV-2 and quantification of viral internalisation by flow cytometric detection of intracellular nucleoprotein. In principle, inhibition of SARS-CoV-2 internalisation by a given compound would suggest involvement of the targeted pathway or associated intracellular components. Initial optimisation experiments were performed to establish appropriate marker cargo concentrations and inhibitor doses, as outlined below.

Seven pharmacological inhibitors were selected to target components of major endocytic pathways: (1) clathrin-mediated endocytosis (CME), (2) caveolar endocytosis, (3) phagocytosis and macropinocytosis (Figure 3.10A). These inhibitors included dynasore (dynamin inhibitor), chlorpromazine (clathrin assembly inhibitor), 5-(N-ethyl-N-isopropyl) amiloride (EIPA; Na^+/H^+ exchanger inhibitor), cytochalasin D (actin polymerisation inhibitor), wortmannin (PI3K inhibitor), IPA-3 (PAK1 inhibitor), and NSC23766 (Rac1 inhibitor).

Optimisation of marker cargo concentration

To validate pathway inhibition, established marker cargoes were selected as positive controls: transferrin-AF647 (CME), 70 kDa dextran-TRITC (macropinocytosis), and zymosan A-AF488 (phagocytosis). Macrophages were incubated with titrated concentrations of each cargo for 2 h, and uptake was quantified by flow cytometry (Figure 3.10B). Optimal concentrations were defined as those producing fluorescence above background without evidence of saturation.

Determination of inhibitor cytotoxicity

The cytotoxicity of each pharmacological inhibitor in iPSC-derived macrophages was assessed and the 50% cytotoxic concentration (CC_{50}) was determined for each inhibitor (Figure 3.10C).

Determination of inhibitor concentrations for pathway inhibition

Appropriate inhibitor concentrations were then selected using a non-biased approach based on their effects on uptake of the marker cargoes (Figure 3.10D). Each inhibitor was titrated against all three cargoes. In principle, a pathway-specific inhibitor would selectively inhibit uptake of its corresponding marker without substantially affecting uptake via other pathways. At excessive concentrations, off-target effects and non-specific inhibition of multiple pathways would be expected, whereas concentrations that are too low may result in false-negative results.

Dynasore demonstrated the clearest specificity, inhibiting transferrin uptake across all tested concentrations while minimally affecting dextran or zymosan uptake except at the highest concentration. In contrast, the remaining inhibitors exhibited dose-dependent inhibition of their intended marker cargoes but also inhibited uptake of cargoes associated with other endocytic pathways. For example, EIPA, commonly regarded as the most specific inhibitor of macropinocytosis, also caused dose-dependent inhibition of transferrin and zymosan uptake. These findings indicate that the inhibitors are either less pathway-specific than reported or that

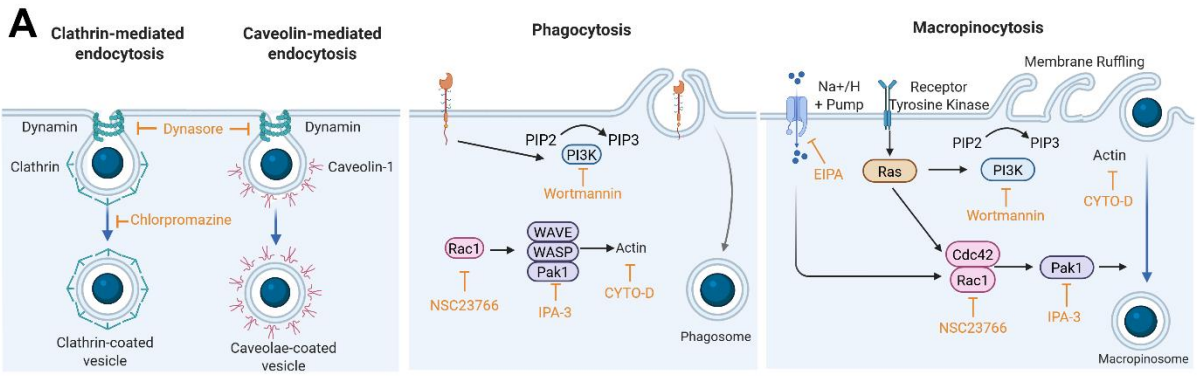

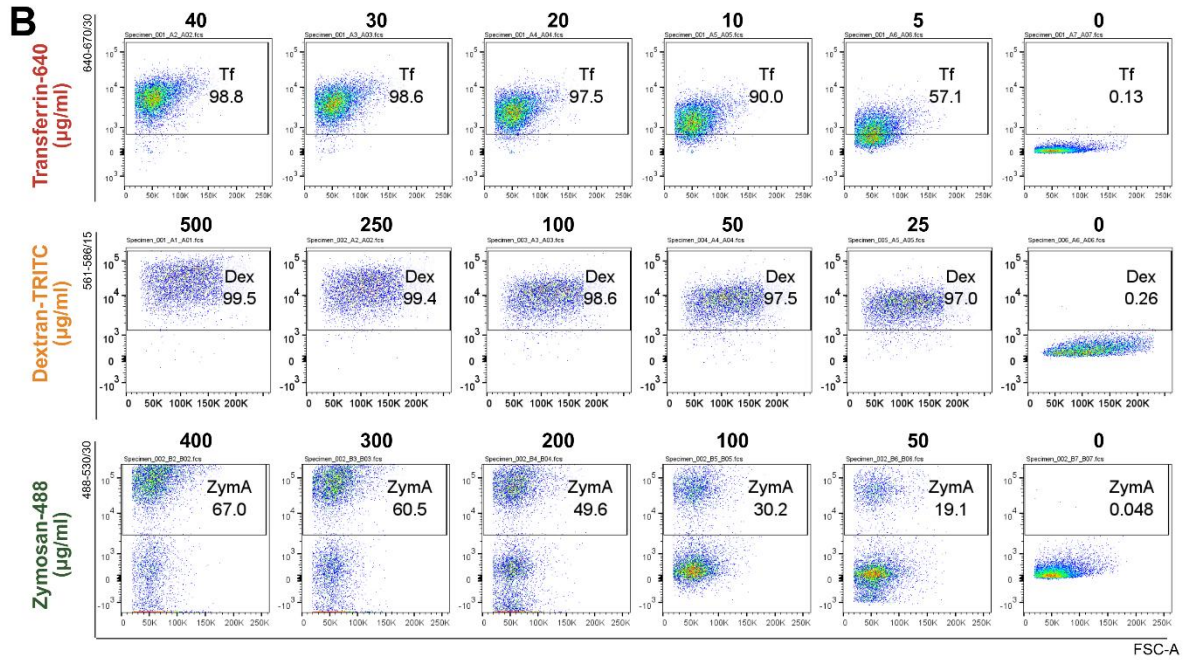

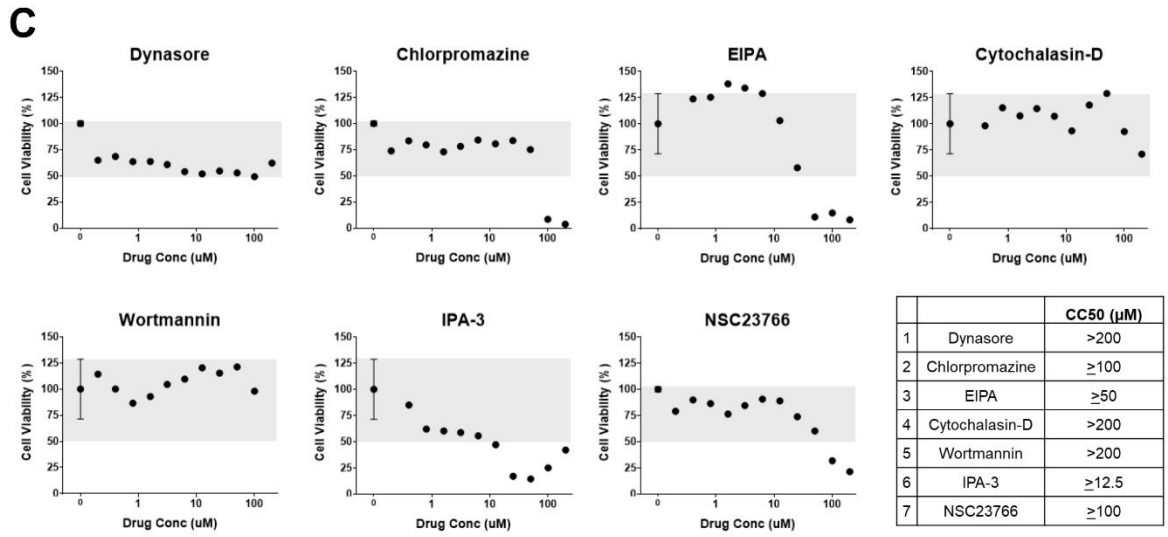

		CC50 (µM)
1	Dynasore	>200
2	Chlorpromazine	≥100
3	EIPA	≥50
4	Cytochalasin-D	>200
5	Wortmannin	>200
6	IPA-3	≥12.5
7	NSC23766	≥100

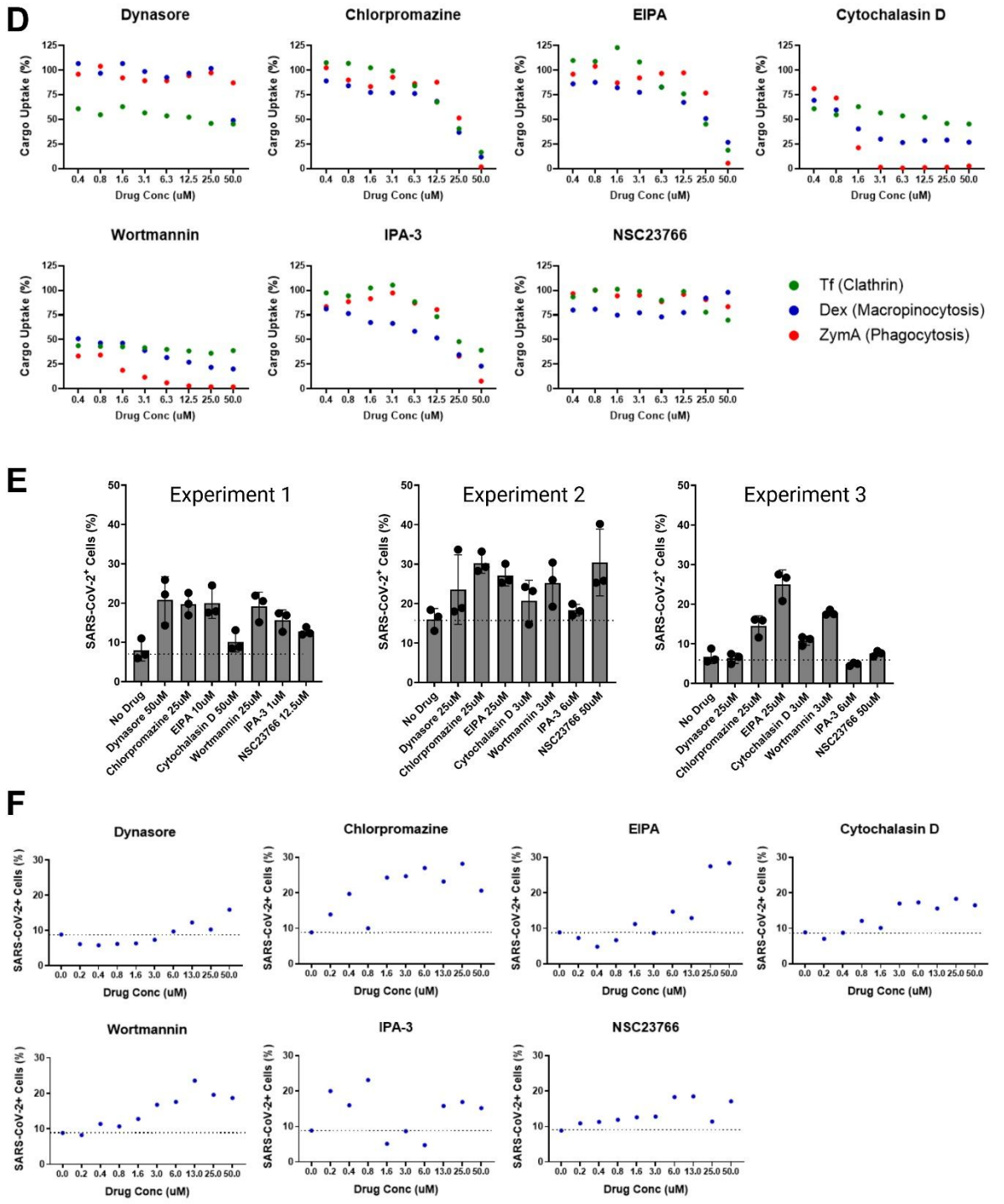

Figure 3.10. Investigation of SARS-CoV-2 entry mechanisms using pharmacological inhibitors. (A) Schematic illustrating caveolar endocytosis, clathrin-mediated endocytosis (CME), macropinocytosis, and phagocytosis, and their pharmacological inhibition. Created with BioRender. **(B)** Titration of marker cargo uptake. Transferrin-AF640 (CME) dextran-TRITC (macropinocytosis), and zymosan A-AF488 (phagocytosis) were titrated on iPSC-macrophages (SFC841-03-01), and uptake was quantified by flow cytometry. **(C)** Cytotoxicity of inhibitors. iPSC-macrophages (SFC841-03-01) were treated with titrated inhibitors and viability was assessed using the CellTiter 96® AQueous One Solution assay (490 nm). CC_{50} values indicate concentrations causing >50% cell death. **(D)** Optimisation of inhibitor concentrations. iPSC-derived macrophages (SFC841-03-01 were pre-treated with inhibitors for 1 h at 37 °C, then incubated with transferrin-AF640 (20 µg/mL), dextran-TRITC (50 µg/mL), or zymosan A-AF488 (300 µg/mL) for 1 h in the continued presence of inhibitors. Uptake was measured by flow cytometry and expressed relative to untreated controls. **(E)** Inhibition of SARS-CoV-2 internalisation. Cells were pre-treated as in (D) and infected with SARS-CoV-2 (MOI 10) for 1 h in the presence of inhibitors. Internalised virus was quantified by flow cytometry. Error bars represent S.D **(F)** Dose-dependent inhibition of SARS-CoV-2 internalisation following pre-treatment with titrated inhibitor concentrations, quantified as in (E).

inhibition of one endocytic route leads to compensatory perturbations in other intracellular trafficking pathways. Final inhibitor concentrations were therefore selected based on the lowest concentration that produced maximal specific inhibition of the intended cargo while remaining below the CC_{50} value.

Effect of pharmacological inhibition on SARS-CoV-2 internalisation

The selected inhibitor concentrations were next applied to assess their effect on SARS-CoV-2 internalisation into macrophages (Figure 3.10E). Unexpectedly, all inhibitors tested, except dynasore at 25 μM, resulted in a reproducible increase in SARS-CoV-2 internalisation into macrophages. To further investigate this effect, each inhibitor was titrated across a range of concentrations and assessed for its effect on viral uptake. These experiments confirmed a dose-dependent enhancement of SARS-CoV-2 internalisation for all inhibitors (Figure 3.10F). The observation that compounds capable of inhibiting marker cargo uptake resulted in enhanced viral internalisation, was unexpected. A likely explanation is that pharmacological disruption of intracellular trafficking pathways induces compensatory upregulation or redirection of alternative uptake mechanisms, resulting in increased viral internalisation. These findings highlight the limitations of relying on pharmacological inhibitors to define viral entry pathways and underscore the importance of comprehensive dose-response analyses rather than conclusions based on single inhibitor concentrations.

3.3 Discussion

Results summary

In this chapter, I investigated the mechanisms by which SARS-CoV-2 is internalised into macrophages, with a particular focus on distinguishing receptor-dependent entry from non-specific uptake pathways. I demonstrate that SARS-CoV-2 is internalised into macrophages despite the absence of detectable expression of the canonical entry receptor ACE2. Furthermore, I found no evidence for high-affinity spike-binding receptors on macrophages. Together, these findings suggest that unopsonised viral uptake is unlikely to be driven by clathrin-mediated endocytosis. The absence of caveolin-1 surface expression on macrophages argues against caveolin-mediated endocytosis. In addition, the lack of co-localisation with dextran indicates that uptake is not consistent with classical bulk fluid-phase macropinocytosis.

Macrophages do not express ACE2

There are several reports in the literature suggesting that, in contrast to this study, report that macrophages express ACE2[78,80,81,151]. Many of these studies have assessed ACE2 expression using bulk approaches such as qPCR, RNA sequencing, or Western blotting. In contrast, I demonstrated lack of surface expression by flow cytometry. I encountered issues with non-specific antibody binding to macrophages mediated by Fc receptors, a well-recognised problem in flow cytometric analysis of myeloid cells. For accurate assessment of receptor expression, even minimal non-specific binding presents a significant limitation, as it can lead to false-positive signals. To overcome this, I adopted alternative strategies designed to minimise Fc-mediated artefacts. The measures required to eliminate non-specific antibody binding highlight how Fc receptor–mediated artefacts may contribute to reports of ACE2 expression on macrophages in other studies that use standard antibodies[78,151]. Establishing the absence of surface ACE2 expression at an early stage in this project was critical, as it ensured that subsequent analyses of SARS-CoV-2 uptake mechanisms were not confounded by assumptions based on potentially misleading literature.

Investigation of clathrin-mediated endocytosis as a SARS-CoV-2 entry mechanism

I explored the hypothesis that macrophages express an alternative spike-binding receptor. It was plausible that a lectin receptor would mediate spike binding through recognition of viral glycans. Recombinant spike protein did not bind detectably to the surface of macrophages by flow cytometry. This suggests that there are no alternative high-affinity receptors for the SARS-CoV-2 spike protein on the surface of macrophages. This was a surprising finding given the body of literature that demonstrate recombinant spike binding to macrophage surface[152], and that propose alternative spike-binding receptors[98,100,104,137,153–155].

However, an important caveat of our experiments is that only spike-receptor interactions of sufficiently high affinity to withstand multiple wash steps would be detected. This work does not therefore exclude the presence of lower-affinity attachment factors that may contribute to viral capture or internalisation by other mechanisms under physiological conditions. In addition, this approach relied on the assumption that recombinant spike protein, expressed in human cells, recapitulates the glycosylation patterns present on native SARS-CoV-2 virions. While this is a reasonable assumption, glycosylation was not directly validated by mass spectrometry and may differ from that of authentic virus.

A further limitation of probing for alternative SARS-CoV-2 receptors using recombinant spike protein is that it precludes identification of receptors that recognise other components of the virion, such as the envelope (E) or membrane (M) proteins, or the lipid constituents of the viral envelope, including phosphatidylserine. To address this, I attempted to develop a flow cytometry-based assay to detect binding of intact virions to the cell surface. However, despite extensive optimisation, virion binding could not be detected even in ACE2-expressing cells. Several factors may account for this, including steric hindrance or epitope inaccessibility when virions are membrane-bound, loss of virion integrity during experimental handling, or the requirement for spike cleavage by host proteases to stabilise binding- processes that may be inefficient at 4 °C. Consistent with this, no published flow cytometry methods reliably quantify surface-bound virions. Although microscopy could provide an alternative approach, similar limitations are likely. Importantly, these findings support that the nucleoprotein signal detected in flow cytometry and ImageStream assays represents intracellular viral material rather than surface-bound virus. To summarise, macrophages lack a high-affinity receptor for SARS-CoV-2 spike, which makes clathrin-mediated endocytosis an unlikely internalisation mechanism.

Investigation of caveolin-mediated endocytosis as a SARS-CoV-2 entry mechanism

I next considered caveolin-mediated endocytosis for completeness, despite it being a less likely pathway, as it is predominantly exploited by non-enveloped viruses. The literature regarding caveolin-1 expression in macrophages is conflicting; however, the prevailing view is that macrophages express low levels of caveolin-1 that are not localised to the cell surface and therefore do not support functional caveolar endocytosis. This interpretation is consistent with my findings, as caveolin-1 surface expression was not detectable on macrophages by flow cytometry. This data suggests that caveolin-mediated endocytosis is unlikely to contribute to SARS-CoV-2 internalisation in macrophages.

Investigation of macropinocytosis as a SARS-CoV-2 entry mechanism

Macropinocytosis initially appeared to be a highly plausible mechanism for SARS-CoV-2 internalisation into macrophages. This pathway is particularly active in macrophages, with reports suggesting that these cells can internalise 25% of their cell volume through fluid-phase uptake each hour[156]. Such capacity could readily account for the efficient accumulation of viral RNA and nucleoprotein observed intracellularly. However, when SARS-CoV-2 was applied to macrophages in the presence of the fluid-phase marker dextran, both were internalised but did not co-localise within the same intracellular compartments. This finding argues against

classical bulk fluid-phase macropinocytosis as the dominant mechanism of SARS-CoV-2 internalisation into macrophages.

Importantly, the absence of dextran co-localisation does not exclude the involvement of other actin-dependent, macropinocytosis-like uptake pathways. One such mechanism is apoptotic mimicry, whereby enveloped viruses exploit PS exposed on their surface to engage PS receptors on host cells. Engagement of these receptors can induce membrane ruffling and internalisation of virus particles into vesicles that share features with macropinosomes, but which do not behave as classical fluid-phase compartments. This model therefore remains compatible with the observed lack of dextran co-localisation.

To explore the potential contribution of PS-mediated uptake, I first attempted to block PS - PS receptor interactions using Annexin V, a PS-binding protein commonly used for this purpose. Unexpectedly, Annexin V treatment did not inhibit SARS-CoV-2 internalisation but instead enhanced uptake in a dose-dependent manner. Although counterintuitive, similar enhancement effects have been reported previously[157]. Rather than excluding PS involvement, this observation may reflect altered PS clustering or membrane organisation that paradoxically promotes uptake. Other than Annexin V, there is no universal blocker of PS that is commercially available. Therefore, I had to take the approach of targeting major PS receptors individually.

I therefore examined the roles of TIM-1 and AXL, two PS receptors commonly implicated in viral apoptotic mimicry, using a TIM-1 blocking antibody and the AXL inhibitor UNC569. In addition, I investigated TREM2, which, although not considered a dominant PS receptor in macrophages, is widely implicated in apoptotic debris clearance in microglia and was readily accessible through an existing iPSC-derived macrophage knockout line in our lab[65,158]. Blockade or loss of these receptors did not reduce SARS-CoV-2 internalisation, suggesting that TIM-1, AXL, and TREM2 are not essential, high-impact mediators of viral uptake in iPSC-derived macrophages under the conditions tested. However, this conclusion must be interpreted cautiously. PS receptor systems are highly redundant, and inhibition of individual receptors may be compensated by others. In addition, receptor expression levels were inferred from the literature rather than directly quantified in this macrophage model, raising the possibility that alternative PS receptors dominate. Furthermore, these experiments did not include functional controls to confirm complete blockade of TIM-1-virus interactions or full inhibition of AXL signalling by UNC569.

Investigation of SARS-CoV-2 entry pathways using pharmacological inhibition

To further investigate whether SARS-CoV-2 uptake involves macropinocytosis-associated signalling, I employed a panel of pharmacological inhibitors targeting key components of the macropinocytic pathway. These inhibitors have previously been used to study HIV-1 entry into macrophages[119]. However, their application in the context of SARS-CoV-2 raised several problems. Firstly, these inhibitors were not specific to macropinocytosis; uptake of transferrin and zymosan, cargo typically internalised via CME and phagocytosis, respectively, was also reduced. This underscores the extensive mechanistic overlap between endocytic pathways in macrophages. Second, and more unexpectedly, despite inhibiting uptake of positive-control cargo, macropinocytosis inhibitors enhanced SARS-CoV-2 internalisation in a dose-dependent manner. Several explanations may account for this phenomenon. Inhibition of one uptake pathway may induce compensatory up-regulation of alternative endocytic routes that SARS-CoV-2 can exploit, but which are not accessible to the control particles used. Alternatively, off-target effects of these inhibitors may indirectly promote viral uptake by altering membrane dynamics, signalling pathways, or intracellular trafficking. At higher concentrations of inhibitor, membrane integrity may be perturbed, which could increase viral internalisation or detection by antibodies. Taken together, these data indicate that blockade of macropinocytosis does not reduce SARS-CoV-2 internalisation into macrophages and may instead alter the routing or processing of virions within the cell. These findings highlight the plasticity of macrophage endocytic pathways and underscore the limitations of relying on single assays or pharmacological approaches to assign viral uptake mechanisms.

Future work

To further define the mechanism of SARS-CoV-2 internalisation into macrophages, future studies should investigate the intracellular localisation of internalised virions. Immunofluorescence microscopy coupled with co-localisation analysis could assess viral localisation relative to markers of early and late endosomes (Rab5/Rab7), lysosomes (LAMP1), and autophagosomes (LC3/p62). Identification of the compartments containing SARS-CoV-2 would provide mechanistic insight into its intracellular trafficking route. Development of a sensitive assay to detect surface-bound SARS-CoV-2 virions would reveal potential interactions between intact virions and the macrophage surface. Although a flow cytometry-based approach was unsuccessful, alternative methods such as quantification of cell-associated viral RNA by RT- qPCR may offer greater sensitivity and enable detection of lower-affinity interactions. Combined with selective wash conditions designed to disrupt lectin or protein-mediated

interactions, such an approach could help identify low-affinity attachment factors that contribute to viral capture by macrophages.

Proposed SARS-CoV-2 mechanism of entry into macrophages

The findings of this chapter argue against a single, receptor-defined pathway for SARS-CoV-2 internalisation into macrophages. The absence of ACE2 and other high-affinity spike-binding receptors, lack of dextran co-localisation, failure of phosphatidylserine receptor blockade to inhibit uptake, and paradoxical enhancement of internalisation following macropinocytosis inhibition collectively indicate a highly plastic uptake process. Rather than engaging a canonical entry mechanism, SARS-CoV-2 appears to exploit the intrinsically high endocytic activity of macrophages, entering through non-targeted processes that are sensitive to global perturbations of membrane trafficking and actin dynamics.

A plausible explanation is non-selective co-uptake during constitutive receptor-mediated endocytosis, whereby extracellular fluid and small particles are internalised alongside specific cargo [159]. Given the small size of SARS-CoV-2 and the high viral concentrations used in vitro, this represents a biologically feasible mechanism. Support for this model was provided by the observation in the next chapter, (Figure 2.3) that an isotype control antibody enhanced viral internalisation, an effect absent with an Fc-silenced variant. This suggests that Fc receptor engagement increases endocytic flux, promoting SARS-CoV-2 uptake independently of direct virus-receptor interactions

Conclusion

In conclusion, this chapter demonstrates that macrophages do not express the canonical SARS-CoV-2 entry receptor ACE2, nor do they express alternative high-affinity spike-binding receptors at the cell surface. Furthermore, the data do not support clathrin- or caveolin-mediated endocytosis as dominant mechanisms of SARS-CoV-2 internalisation into macrophages. Instead, viral uptake occurs independently of a dedicated viral entry receptor and is consistent with non-specific endocytic processes.

Two plausible models for SARS-CoV-2 internalisation into macrophages remain. First, uptake may occur via an actin-dependent, macropinocytosis-like pathway that is distinct from classical bulk fluid-phase macropinocytosis but would be sensitive to disruption of macropinocytic signalling. Second, SARS-CoV-2 may be internalised incidentally during constitutive receptor-mediated endocytosis at the macrophage plasma membrane, whereby small virions are co-internalised with extracellular fluid into forming coated vesicles.

Chapter 4: Macrophage Permissibility to SARS-CoV-2 Infection

4.1 Introduction

Macrophages as targets of viral infection

Macrophages are cellular targets for a wide range of viruses[160]. For a cell to serve as a viral target and support productive infection, two conditions must be met. First, the cell must express an appropriate viral entry receptor, rendering it susceptible to infection. Second, the intracellular environment must support viral replication, thereby conferring permissiveness. Viral infection is defined as the entry of a virus into a host cell followed by expression of the viral genome. Infection may be productive, resulting in viral genome replication and release of progeny virions, or abortive, in which viral replication is restricted and no infectious progeny are produced.

There are several advantages for viruses to target macrophages. As sentinel cells of the innate immune system, macrophages are often among the first cells encountered at sites of infection. They are long-lived, relatively resistant to apoptosis, and capable of migrating between tissues, providing viruses with opportunities for persistence and systemic dissemination. Their broad repertoire of surface receptors and high phagocytic capacity can be exploited for viral entry. Furthermore, macrophages are potent producers of cytokines, which viruses may modulate to promote replication or immune evasion.

However, macrophages also present substantial barriers to infection[161]. They are primed to detect viral pathogens through pattern recognition receptors and rapidly mount antiviral responses, including the production of type I interferons and expression of restriction factors. As non-dividing cells, macrophages possess relatively low intracellular deoxyribonucleotide pools, which can limit replication of certain viruses. Consequently, viral infection of macrophages can result in diverse outcomes, ranging from persistent productive infection to highly restricted or abortive replication.

HIV-1 represents a well-characterised example of a virus that has evolved to exploit macrophages[162,163]. HIV-1 productively infects macrophages via CD4 and CCR5 receptors and encodes factors that counteract intracellular restriction mechanisms and innate immune detection. Infected macrophages can act as long-lived viral reservoirs and contribute to dissemination to susceptible $CD4^+$ T cells.

Macrophages and monocytes are major target cells during dengue infection[164]. Dengue virus productively replicates in macrophages and encodes proteins that antagonise type I interferon signalling. In addition to receptor-mediated entry via C-type lectin receptors and CME, dengue can exploit antibody-dependent enhancement (ADE)[165,166]. During secondary infection with a heterologous serotype, pre-existing subneutralising antibodies form immune complexes with the virus. These complexes engage Fcγ receptors, particularly FcγRIIA, on macrophages, enhancing viral entry, replication, cytokine production and disease severity. Whether SARS-CoV-2 exhibits a classical ADE phenotype similar to dengue remains uncertain.

Other viruses, including human cytomegalovirus, respiratory syncytial virus, hepatitis C virus and Epstein-Barr virus, can also infect macrophages under specific conditions[167–170]. In contrast, many viruses, such as low-pathogenic influenza strains and vesicular stomatitis virus, fail to establish productive infection in macrophages due to the strong intrinsic antiviral environment of these cells[171,172]. Whether SARS-CoV-2 can productively infect macrophages, and under what immunological conditions, remains incompletely defined.

Are macrophages permissive to SARS-CoV-2 infection?

The previous chapter established that, although SARS-CoV-2 is internalised by macrophages, these cells do not express a high-affinity entry receptor such as ACE2 and are therefore not susceptible to canonical receptor-mediated infection. This chapter investigates the fate of SARS-CoV-2 following internalisation and addresses the question of whether macrophages are permissive to productive infection.

The permissiveness of macrophages to SARS-CoV-2 has been widely debated. Several studies have reported increase of viral RNA or protein within macrophages, suggesting infection; however, these studies did not demonstrate release of infectious progeny virus from these cells [82,88,104]. In contrast, Huot et al. and Lv et al. reported infectious virus release from primary murine and macaque alveolar macrophages [51,173]. Grant et al. detected both positive- and negative-sense SARS-CoV-2 RNA in alveolar macrophages from patients with COVID-19, consistent with active replication[50]. Conversely, multiple other studies have concluded that although SARS-CoV-2 can enter macrophages, replication is abortive and does not result in productive infection [72–74,174–179]. Notably, several reports have described enhanced macrophage infection in the presence of antibodies or serum [174,180–183]. On the contrary, another report claims that there is no evidence for macrophage infection in the presence of patient sera[176].

Given this controversy, this chapter investigates the permissiveness of iPSC-derived macrophages to SARS-CoV-2 infection, both in the absence and presence of antibodies

The role of antibodies in viral infection

This chapter examines the internalisation and fate of SARS-CoV-2 virions opsonised by antibodies. Antibodies are soluble glycoproteins that recognise and bind specific antigens. Structurally, they comprise two identical heavy chains and two identical light chains, forming a Y-shaped molecule with two functionally distinct regions: the Fab (fragment antigen-binding) region, which mediates antigen recognition and specificity, and the Fc (fragment crystallisable) region, which determines effector function through engagement of Fc receptors and complement components.

Five major antibody isotypes are present in humans: IgM, IgG, IgA, IgD and IgE, defined by their heavy chain constant regions. IgG is the predominant isotype in serum and is subdivided into four subclasses (IgG1-4), which differ in their ability to engage Fcγ receptors and activate complement.

Antibodies may be classified as neutralising or non-neutralising, based on their capacity to block cell infection or membrane fusion. Beyond neutralisation, antibodies mediate effector functions through their Fc region, including complement activation, antibody-dependent cellular cytotoxicity (ADCC), and antibody-dependent cellular phagocytosis (ADCP).

IgG subclasses vary in effector potency[184]. IgG1 and IgG3 most efficiently engage activating Fcγ receptors and mediate ADCP and complement activation. IgG2 and IgG4 generally exhibit reduced Fcγ receptor binding and effector activity. IgM is a potent activator of complement but does not directly engage Fcγ receptors. IgA can mediate effector functions via Fcα receptors on myeloid cells, whereas IgE functions primarily in allergic and anti-parasitic responses. IgD has a limited and less well-defined role in antiviral immunity.

As macrophages predominantly express Fcγ receptors and IgG is the predominant isotype in serum, this chapter focuses on IgG subclasses and their ability to mediate neutralisation and Fcγ receptor–dependent uptake of SARS-CoV-2. Although IgM-mediated complement activation may enhance macrophage phagocytosis indirectly, non-IgG isotypes were not examined in this study.

Three principal classes of Fcγ receptors are expressed in humans: FcγRI (CD64), FcγRII (CD32), and FcγRIII (CD16)[185]. FcγRI is a high-affinity receptor that binds monomeric IgG1 and IgG3 and mediates phagocytosis and inflammatory signalling. FcγRII exists as activating (FcγRIIA) and

inhibitory (FcγRIIB) isoforms; FcγRIIA promotes phagocytosis, whereas FcγRIIB dampens activation. FcγRIII includes FcγRIIIA, an activating receptor expressed on NK cells and some macrophages, and FcγRIIIB, a GPI-anchored receptor primarily expressed on neutrophils and involved in immune complex clearance. IgG1 and IgG3 bind most efficiently to activating Fcγ receptors, consistent with their strong effector capacity. In this chapter, I examined binding of IgG subclasses to CD32 and CD16.

Antibodies against SARS-CoV-2

In this thesis, I evaluated the ability of COVID-19 patient-derived antibodies to modulate SARS-CoV-2 entry into and infection of macrophages. SARS-CoV-2–specific antibodies have been identified that target multiple regions of the spike protein, including the S1 NTD and RBD and regions within S2 such as the stem helix and fusion peptide. The majority of neutralising antibodies elicited during infection target the RBD [186].

RBD-targeting antibodies have been structurally classified into four groups by Barnes et al [187]. Class 1 and class 2 antibodies bind epitopes that overlap with the receptor-binding motif (RBM) and directly compete with ACE2 binding. Class 1 antibodies preferentially recognise the RBD in the ‘up’ (ACE2-accessible) conformation, whereas class 2 antibodies can bind RBDs in both ‘up’ and ‘down’ conformations. Class 3 and class 4 antibodies bind epitopes outside the RBM. Class 3 antibodies recognise more conserved lateral surfaces of the RBD and can bind independently of RBD conformation. In contrast, class 4 antibodies target cryptic epitopes that are typically exposed only when the RBD adopts the ‘up’ conformation.

Antibodies targeting S2 are often more broadly reactive across coronaviruses due to the higher sequence conservation of S2 compared with S1. However, S2-directed antibodies are generally less potent neutralisers than many RBD-targeting antibodies[188]. Furthermore, the extensive conformational rearrangements that occur in S2 during membrane fusion mean that S2 antibodies are frequently specific to either prefusion or post fusion conformations of spike[189].

Given that RBD-targeting antibodies bind distinct regions of the spike protein and can influence its conformation in different ways, it remains unclear whether epitope specificity affects how SARS-CoV-2 interacts with Fc receptor-expressing cells.

Type I interferon signalling and antiviral restriction in macrophages

Interferons (IFNs) are cytokines that play a central role in antiviral defence[190]. They are classified into three major families. Type I interferons comprise primarily IFN-α and IFN-β, which are

produced by most nucleated cells in response to viral infection following recognition of pathogen-associated molecular patterns (PAMPs). Type I IFNs act in both autocrine and paracrine manners to induce expression of interferon-stimulated genes (ISGs), many of which encode antiviral effector proteins.

Type II interferon consists of a single cytokine, IFN-γ, which is produced mainly by activated T cells and NK cells and signals through the IFN-γ receptor expressed on immune cells, including macrophages. IFN-γ enhances antigen presentation by increasing MHC class I and II expression and promotes macrophage activation. Type III interferons (IFN-λ1, IFN-λ2 and IFN-λ3) exert antiviral functions similar to type I IFNs; however, expression of the IFN-λ receptor is largely restricted to epithelial cells. As macrophages respond predominantly to type I interferons during viral infection, this pathway was examined in this chapter.

Type I IFNs signal through the IFNAR receptor complex, composed of IFNAR1 and IFNAR2 subunits[191]. Ligand binding activates the receptor-associated kinases JAK1 and TYK2, leading to phosphorylation of STAT1 and STAT2. Phosphorylated STAT1 and STAT2 form a complex with IRF9, generating the ISGF3 transcription factor complex. ISGF3 translocates to the nucleus, where it binds interferon-stimulated response elements (ISREs) within promoter regions to induce transcription of ISGs.

In this thesis, type I IFN signalling was investigated using complementary pharmacological and genetic approaches. JAK signalling was inhibited using ruxolitinib, a first-generation JAK1/2 inhibitor with broad kinase activity. To increase specificity, second-generation JAK1-selective inhibitors, abrocitinib and upadacitinib, were also employed. In addition, type I IFN signalling was disrupted using an IFNAR2-blocking antibody and an IFNAR2 knockout iPSC-derived macrophage line described previously[63].

Several ISGs have been shown to restrict RNA virus replication by targeting multiple stages of the viral life cycle[192]. For example, to interfere with RNA virus entry, IFITM2 and IFITM3 inhibit membrane fusion by altering endosomal membrane properties, while cholesterol-25-hydroxylase (CH25H) produces 25-hydroxycholesterol, which disrupts membrane fusion[193,194]. Following entry, viral RNA can be degraded though activation of the 2'–5'-oligoadenylate synthetase (OAS) - RNase L pathway[195]. Viral protein synthesis is restricted by PKR which senses double-stranded RNA and phosphorylates eIF2α, and by IFIT proteins which bind viral RNAs lacking proper 2'-O methylation[196,197]. Additional restriction factors target later stages of replication, for example, MxA (MX1), a dynamin-like GTPase, interferes with viral replication complex formation, while RSAD2 (viperin), an iron-sulphur enzyme, catalyses the production of

the nucleotide analogue ddhCTP which exerts broad antiviral effects[198,199]. Collectively, these pathways establish a potent antiviral state capable of restricting viral replication at multiple levels. Although the specific ISGs responsible for restricting SARS-CoV-2 replication in macrophages remain largely unknown, it is likely that one or more of these antiviral mechanisms are restricting replication.

Chapter hypotheses and aims

The fate of SARS-CoV-2 following internalisation into macrophages remains controversial. This chapter therefore investigates the permissiveness of iPSC-derived macrophages to SARS-CoV-2 infection under different experimental contexts.

The previous chapter established that macrophages do not express ACE2 and that SARS-CoV-2 is internalised via a non-specific uptake mechanism. Based on this, I hypothesised that internalisation through this route would result in degradation of the virus and failure to establish productive replication. However, I considered the possibility that macrophages may be intrinsically capable of supporting SARS-CoV-2 replication if provided with an entry receptor, such as transgenic ACE2 expression. Even in this context, I hypothesised that type I interferon (IFN-I) signalling would likely restrict viral replication. In addition, I hypothesised that antibody-Fc receptor engagement could function as a surrogate attachment mechanism for SARS-CoV-2, potentially altering viral entry and infection outcomes in macrophages.

To address these hypotheses, this chapter addresses the following questions:

- Are iPSC-derived macrophages permissive to productive SARS-CoV-2 infection?
- Does transgenic ACE2 expression render macrophages permissive to productive infection?
- Does antibody opsonisation enhance SARS-CoV-2 internalisation via Fc receptors?
- Can anti–SARS-CoV-2 antibodies mediate productive infection of macrophages?
- Does type I interferon signalling restrict antibody-mediated SARS-CoV-2 infection in macrophages?

4.2 Results

4.2.1 Macrophages are not permissive to SARS-CoV-2 infection

No infectious virus is released from SARS-CoV-2 inoculated macrophages

To determine whether SARS-CoV-2 can productively replicate in macrophages, iPSC-derived macrophages from two donors were inoculated with three SARS-CoV-2 variants at a MOI 1 for 2 h. VET cells were used as a permissive cell control. Supernatants were collected at 24 h PI and infectious viral titres were quantified. No infectious virus was detected in the supernatants of either macrophage donor for any three variants. In contrast, infectious virions of all variants were readily detected in VET cell supernatants (Figure 4.1A). This data indicates that macrophages do not support productive SARS-CoV-2 infection.

SARS-CoV-2 reporter virus indicates absence of viral gene expression in macrophages

Although no infectious virus was released, I next assessed whether viral gene expression occurred in macrophages. A recombinant SARS-CoV-2 reporter virus expressing mNeonGreen (mNG) fused to ORF6 was used, enabling detection of viral gene expression during replication. iPSC-derived macrophages and CCL81 Vero cells were inoculated at MOI 0.1 with ORF6-mNG SARS-CoV-2. At 24 h pi, fluorescence microscopy demonstrated high mNeonGreen expression in Vero cells, confirming active viral replication in this permissive control cell line (Figure 4.1B). In contrast, no mNeonGreen signal was detected in macrophages at any time point examined post-inoculation. These findings indicate that macrophages do not support detectable SARS-CoV-2 gene expression.

smFISH reveals no replication of genomic or subgenomic RNA in macrophages

Despite lack of viral gene expression, I investigated if there was any partial replication of the viral genome, indicated by an increase in viral RNA. I performed single-molecule fluorescence in situ hybridisation (smFISH) using RNA probes targeting the SARS-CoV-2 ORF1ab region (genomic RNA) and the N gene (detecting total RNA, including genomic and subgenomic species) (Figure 4.1C). In Vero cells, strong cytoplasmic signal for both probes was observed by 48 h pi, consistent with high levels of viral RNA accumulation. In contrast, macrophages displayed only sparse, discrete puncta at all time points, suggesting limited amounts of input viral RNA. Quantification of smFISH signals showed that at 4 h pi, both macrophages and Vero cells contained fewer than 100 RNA molecules per cell (Figure 4.1D), consistent with the low MOI 0.1 used to inoculate. By 24 h pi, Vero cells exhibited increased levels of N gene RNA, followed by a

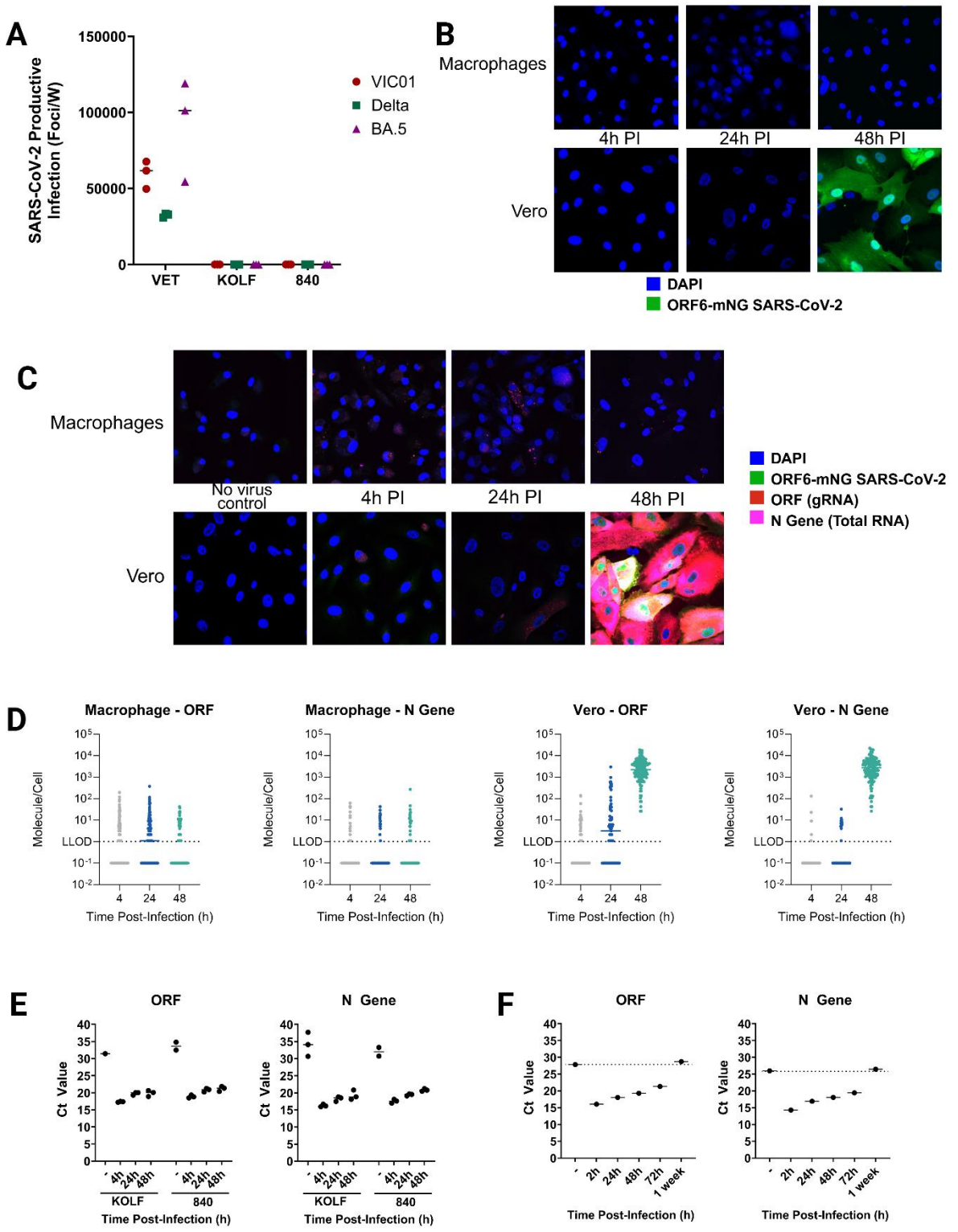

Figure 4.1 Macrophages are not permissive to SARS-CoV-2 infection (A) Infectious virus production by iPSC-derived macrophages from two donors SFC840-03-03 (840), KOLF2.1S(KOLF) and VET cells 24 h post-inoculation with SARS-CoV-2 at MOI 1, quantified by FFA on Vero cells. **(B)** Confocal microscopy images of KOLF2.1S iPSC-derived macrophages and Vero cells following inoculation with Wuhan OF6-mNeonGreen SARS-CoV-2. Cells were inoculated with an MOI 0.1 for 2h. At 4h, 24h and 48h PI, cells were fixed, permeabilised, and nuclei stained with DAPI. **(C)** smFISH confocal microscopy of cells shown in (B) using probes targeting the viral N gene and ORF, conjugated to Alexa Fluor 647 and Cy3, respectively. **(D)** Quantification of smFISH RNA probe signals from (C). **(E)** RT-qPCR quantification of SARS-CoV-2 genomic RNA and N gene transcripts in iPSC-derived macrophages (KOLF2.1S and SFC840-03-03) up to 72 h post-inoculation. **(F)** RT-qPCR quantification of SARS-CoV-2 genomic RNA and N gene transcripts in iPSC-derived macrophages (KOLF2.1S) up to 1 week post-inoculation. Data shown are from one representative experiment (three technical replicates).

marked increase in both genomic and total RNA at 48 h pi, with up to 10,000 RNA molecules per cell. In contrast, macrophages showed no increase in either genomic or total RNA at 24 or 48 h pi. These results demonstrate that macrophages do not support replication of SARS-CoV-2 genomic or subgenomic RNA.

RT-qPCR confirms degradation of viral RNA in macrophages

To confirm the smFISH findings, viral RNA levels were quantified by RT-qPCR using TaqMan probes targeting the ORF1ab and N genes. In macrophages derived from two iPSC donors, Ct values for both ORF and N gene increased over 48 h pi (Figure 4.1E), indicating a decline in viral RNA abundance. Viral RNA continued to decrease over time, and by 7 days pi Ct values were comparable to those of the uninoculated control (Figure 4.1F), suggesting that SARS-CoV-2 RNA had been fully degraded.

Together, these data demonstrate that iPSC-derived macrophages neither support productive infection nor viral RNA replication, and instead progressively degrade internalised SARS-CoV-2 RNA.

4.2.2 Transgenic ACE2-overexpression renders macrophages permissive to SARS-CoV-2 replication

Generation of hACE2-expressing macrophages

Having established that iPSC-derived macrophages do not support SARS-CoV-2 infection, I next sought to determine the underlying reason. Data presented in the previous results chapter demonstrated that macrophages do not express ACE2 or other high-affinity spike-binding receptors. SARS-CoV-2 entry requires binding of the viral spike protein to ACE2, which stabilises the open receptor-binding conformation and permits proteolytic cleavage of spike, enabling membrane fusion and cytosolic entry. To date, ACE2 is the only receptor shown to mediate productive SARS-CoV-2 entry. I therefore hypothesised that the absence of ACE2 expression on macrophages prevents productive infection.

To test this, I generated ACE2-expressing macrophages by lentiviral transduction. To achieve genetic modification of iPSC-derived macrophages, I cloned and produced lentiviral vectors expressing either the human ACE2 (hACE2) or an empty vector (EV) control. Lentiviral transduction of terminally differentiated and non-dividing cells, such as macrophages is difficult to achieve. To overcome this, macrophages were co-transduced with the vpx lentivirus, a lentiviral accessory protein that promotes proteasomal degradation of host restriction factor

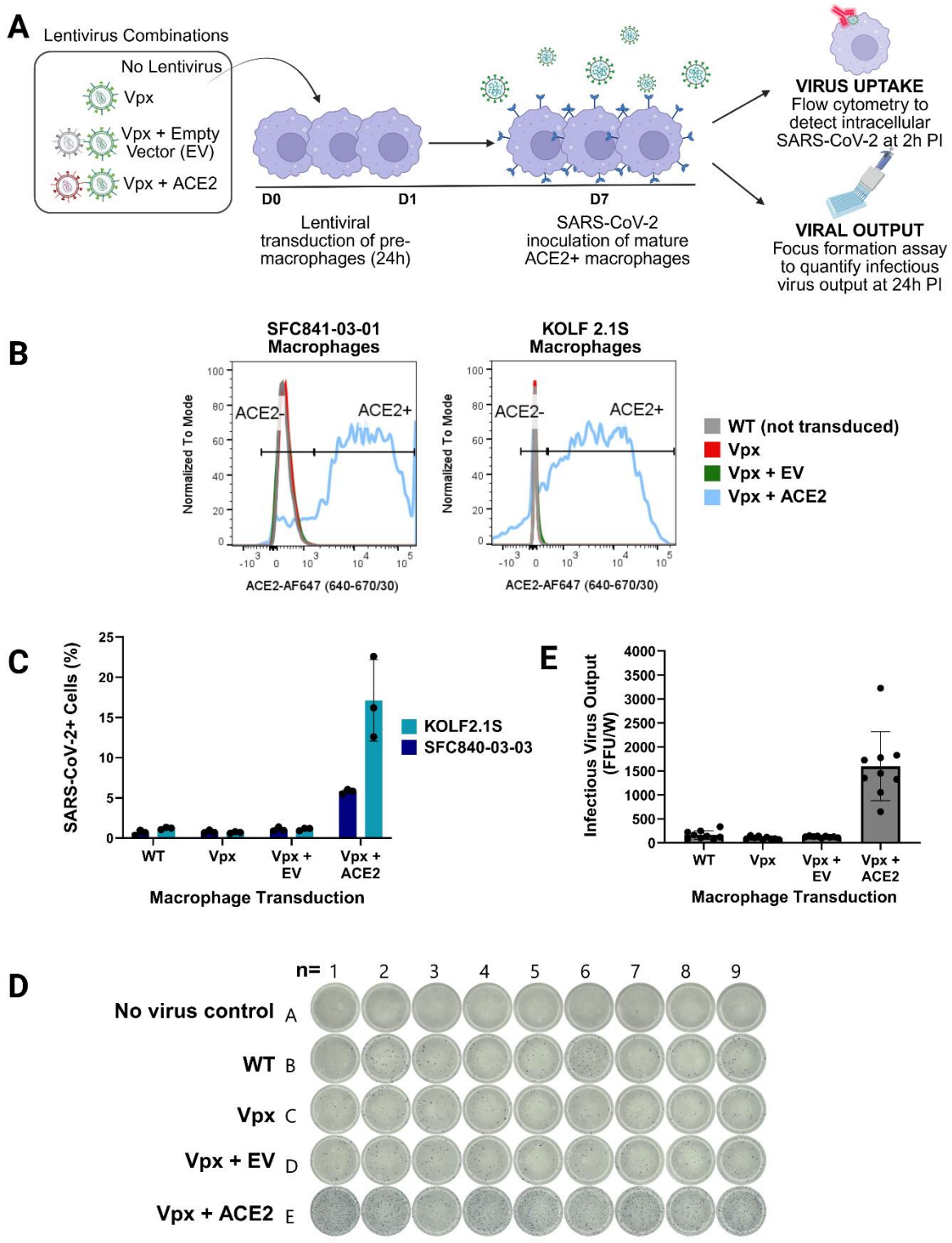

Figure 4.2 Transgenic hACE2-expressing macrophages are permissive to SARS-CoV-2 infection. (A) Schematic of the experimental workflow used to generate transgenic ACE2-expressing macrophages. iPSC-derived pre-macrophages were transduced in suspension for 24 h with either ACE2 or EV lentivirus, in the presence of vpx lentivirus, or with vpx lentivirus alone. Following transduction, lentiviruses were removed and cells were differentiated for 7 days to generate mature macrophages. Internalisation and infection of SARS-CoV-2 was quantified by flow cytometry and FFA respectively. **(B)** Surface ACE2 expression in transduced iPSC-derived macrophages from two donors (SFC841-03-01 and KOLF2.1S), assessed by flow cytometry. **(C)** Internalisation of SARS-CoV-2 by transgenic hACE2+ and WT macrophages. iPSC-derived macrophages from two donors (SFC840-03-03 and KOLF2.1S) were inoculated with SARS-CoV-2 at MOI 5 for 2 h, and intracellular virus was quantified by flow cytometry. **(D)** SARS-CoV-2 infection of transgenic ACE2 and WT macrophages. Infectious virus released from iPSC-derived macrophages (KOLF2.1S) was quantified 24 h PI following infection with SARS-CoV-2 at MOI 10, by titration on Vero cells using a FFA. **(E)** Quantification of the FFA shown in **(D)**. Data shown are from one representative experiment (error bars represent SD).

SAMHD1. SAMHD1 restricts retroviral infection by depleting intracellular dNTP pools. Vpx degradation of this factor therefore leads to increased levels of dNTPs, thereby increasing lentiviral transduction efficiencies.

Pre-macrophages from two independent iPSC donors were transduced in suspension with either ACE2-expressing or EV lentivirus in the presence of Vpx for 24 h, followed by differentiation for 7 days to generate mature macrophages (Figure 4.2A). Flow cytometric analysis confirmed high surface expression of ACE2 in ACE2-transduced macrophages, whereas macrophages transduced with empty vector plus Vpx or Vpx alone lacked detectable ACE2 expression (Figure 4.2B).

hACE2-expressing macrophages are permissive to SARS-CoV-2 infection

Previous data demonstrated that macrophages internalise SARS-CoV-2 via a non-specific uptake mechanism but do not support replication. I therefore investigated whether ACE2 overexpression enhances viral entry and enables productive infection. Macrophages transduced with ACE2 or EV (both in the presence of Vpx), as well as a Vpx-only control, were exposed to SARS-CoV-2. Viral internalisation was quantified at 2 h PI. ACE2-expressing macrophages exhibited increased viral uptake compared with ACE2-negative controls (Figure 4.2C), indicating that ACE2 expression enhances viral entry.

To assess productive infection, supernatants were collected at 24 h pi and infectious virus titres were determined (Figure 4.2D). Infectious SARS-CoV-2 was detected in supernatants from ACE2-expressing macrophages, whereas only low levels of residual inoculum were detected in ACE2-negative controls (Figure 4.2E). These data demonstrate that ACE2 expression enables productive SARS-CoV-2 infection in macrophages. However, viral production remained low. Approximately 100,000 macrophages per well released an average of 1,500 virions, corresponding to ~0.02 VET-infectious virions per cell. Thus, although ACE2 expression renders macrophages permissive to infection, viral replication occurs with low efficiency, suggesting macrophages intrinsically restrict viral replication.

4.2.3 Antibodies enhance SARS-CoV-2 internalisation via Fc-receptors

Antibody-opsonisation enhances SARS-CoV-2 internalisation into macrophages

Up to this point, this thesis has examined the internalisation and infection outcomes of SARS-CoV-2 virions in the absence of antibody. While this may reflect early infection in naïve individuals, virus-specific antibodies are present during later stages of infection or following

prior exposure. Antibodies opsonise virions and promote their uptake by phagocytes via Fc receptor engagement. The following experiments therefore assessed the impact of antibody opsonisation on macrophage internalisation of SARS-CoV-2.

SARS-CoV-2 was pre-incubated with individual IgG1 monoclonal antibodies or control antibodies prior to addition to macrophages. Viral internalisation was quantified by flow cytometry (Figure 4.3A). Opsonisation with RBD and S1 specific antibodies increased viral uptake into macrophages compared with unopsonised virus (Figure 4.3B). The degree of enhanced uptake varied between antibodies. Sera from two individuals with COVID-19 similarly increased viral internalisation. Antibodies against S2 did not enhance the internalisation of SARS-CoV-2. Notably, the E1 isotype antibody also enhanced uptake. The enhancement observed with the E1 isotype antibody likely reflects Fcγ receptor–mediated uptake of antibody–receptor complexes, with concurrent non-specific internalisation of virus present in the extracellular Fluid. No enhancement was observed when Fc receptor engagement was abrogated, either through Fc-silencing mutations or use of a mouse IgG1 control lacking efficient binding to human Fcγ receptors

Assessment of spike binding as a determinant of antibody-mediated viral internalisation

To investigate why different IgG1 monoclonal antibodies mediated varying levels of SARS-CoV-2 internalisation into macrophages, I assessed their binding to recombinant spike protein by ELISA. The antibody concentration corresponding to that used in the macrophage internalisation assays was examined against a recombinant prefusion-stabilised spike trimer.

At the concentration used for opsonisation, all S1 and RBD antibodies and COVID-19 sera (with the exception of FD 1E) demonstrated maximal binding to the immobilised recombinant spike protein, consistent with saturation under these assay conditions (Figure 4.3C). This suggests that, for S1 and RBD antibodies, differences in macrophage internalisation are unlikely to be attributable to insufficient spike binding at the concentrations tested.

In contrast, the anti-S2 antibodies demonstrated low to undetectable binding to the recombinant spike. Many S2-directed antibodies are conformation sensitive and recognise epitopes exposed only in post-fusion S2 or during transient fusion intermediates. As the ELISA antigen consisted of a prefusion-stabilised spike trimer, the relevant S2 epitopes may not be accessible. Notably, the anti-S2 antibody FB 9D did not bind prefusion spike in the ELISA assay, but has previously been used to detect intracellular SARS-CoV-2 in infected Vero cells (data not

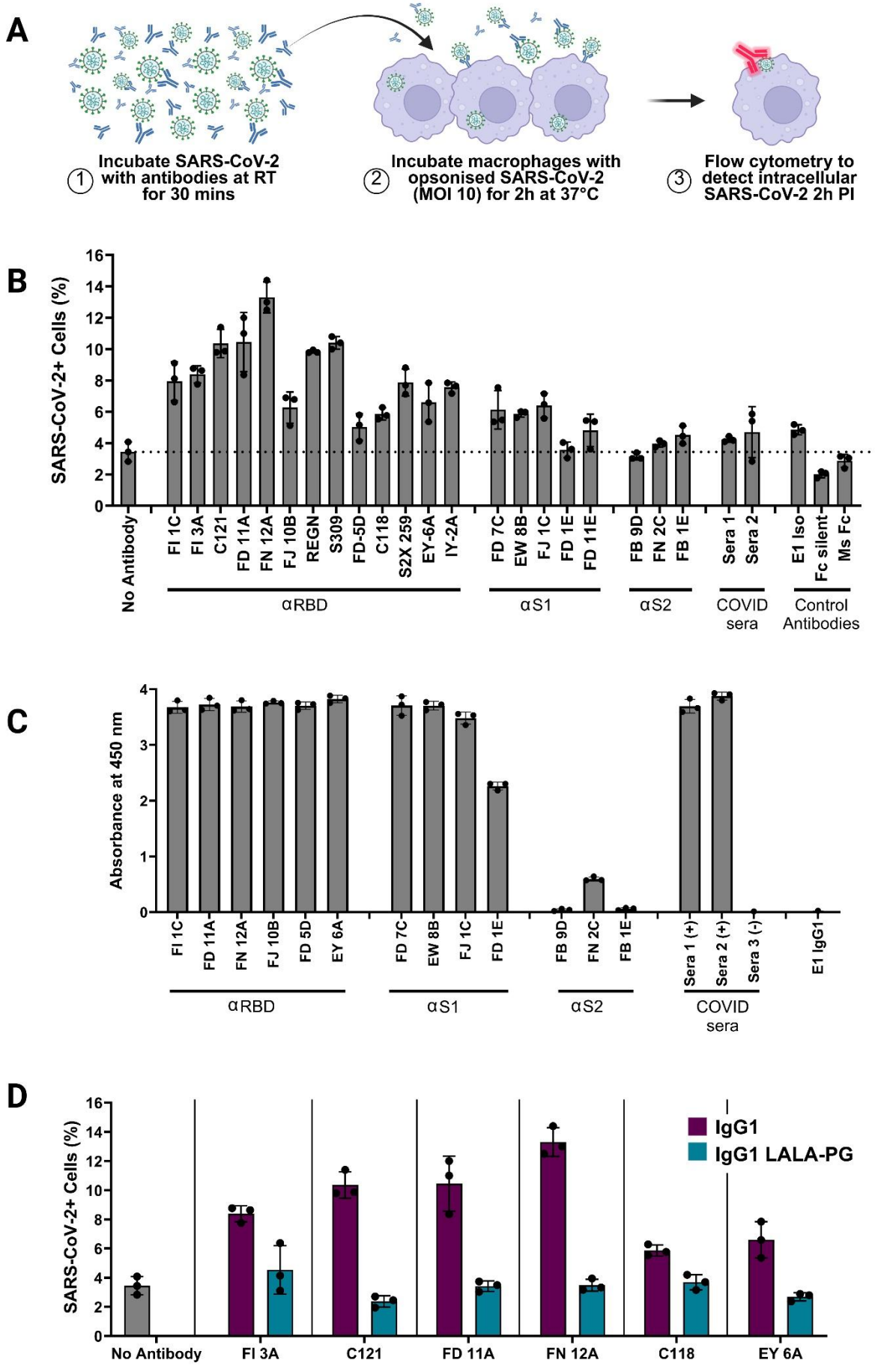
A
Incubate SARS-CoV-2 with antibodies at RT for 30 mins
Incubate macrophages with opsonised SARS-CoV-2 (MOI 10) for 2h at 37°C
Flow cytometry to detect intracellular SARS-CoV-2 2h PI
B
SARS-CoV-2+ Cells (%)
No Antibody
FI 1C
FI 3A
C121
FD 11A
FN 12A
FJ 10B
REGN
S309
FD-5D
C118
S2X 259
EY-6A
IY-2A
FD 7C
EW 8B
FJ 1C
FD 1E
FD 11E
FB 9D
FN 2C
FB 1E
Sera 1
Sera 2
E1 Iso
Fc silent
Ms Fc
αRBD
αS1
αS2
COVID sera
Control Antibodies
C
Absorbance at 450 nm
FI 1C
FD 11A
FN 12A
FJ 10B
FD 5D
EY 6A
FD 7C
EW 8B
FJ 1C
FD 1E
FB 9D
FN 2C
FB 1E
Sera 1 (+)
Sera 2 (+)
Sera 3 (-)
E1 IgG1
αRBD
αS1
αS2
COVID sera
D
SARS-CoV-2+ Cells (%)
IgG1
IgG1 LALA-PG
No Antibody
FI 3A
C121
FD 11A
FN 12A
C118
EY 6A

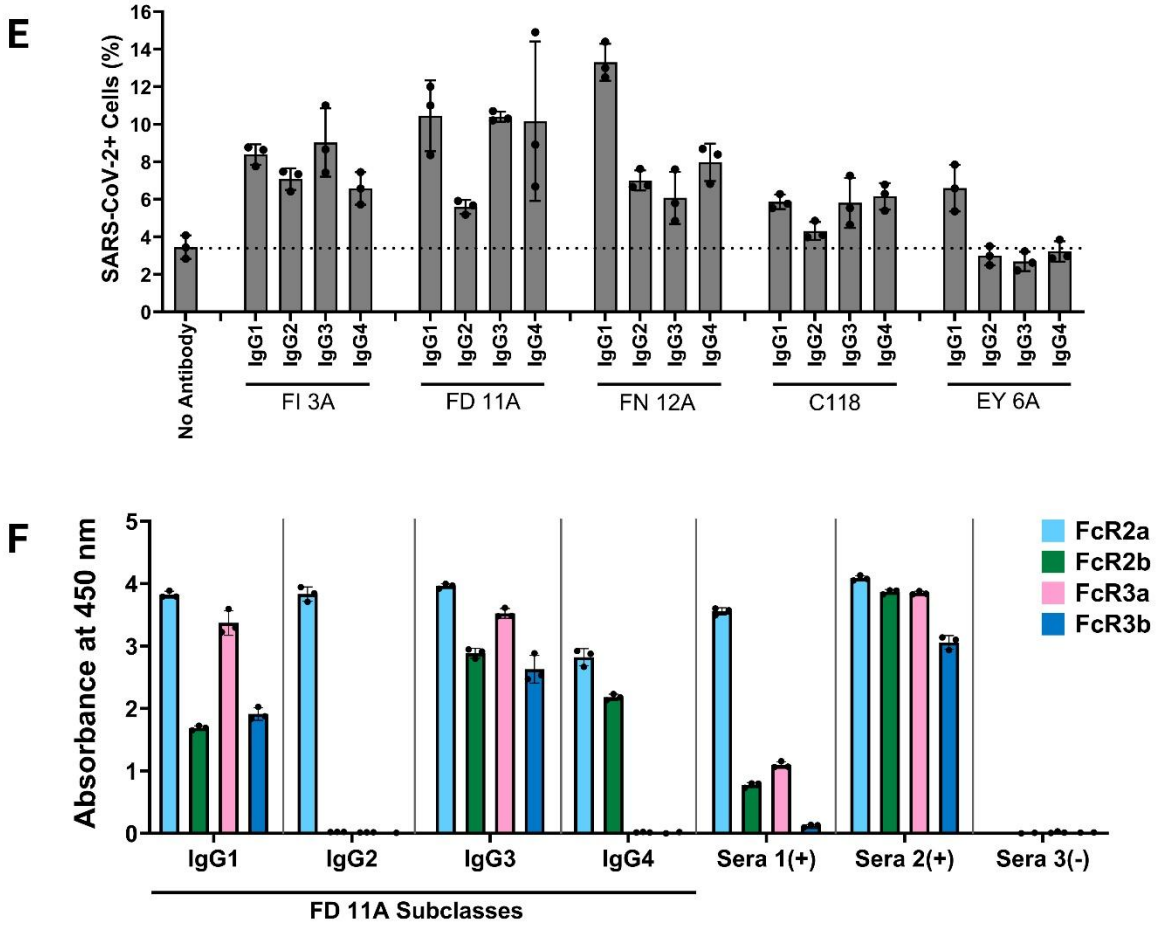

Figure 4.3 Antibodies enhance SARS-CoV-2 internalisation into macrophages via Fcγ receptor-mediated phagocytosis. (A) Schematic of the experimental workflow used to assess antibody-mediated internalisation of SARS-CoV-2 into macrophages. SARS-CoV-2 was incubated with anti-spike antibodies (1 µg/ml) for 30 min at RT prior to addition to iPSC-derived macrophages (MOI 10) for 2 h at 37 °C. Intracellular virus was quantified by anti-nucleoprotein flow cytometry. **(B)** Internalisation of antibody-opsonised SARS-CoV-2 by iPSC-derived macrophages (KOLF2.1S). Macrophages were incubated SARS-CoV-2 (MOI 10) opsonised with the indicated anti-SARS-CoV-2 IgG1 monoclonal antibodies (1 µg/ml), COVID-19 patient serum (NT50 concentration), a human IgG1 isotype control (E1), Fc-silent human IgG1 isotype control (Fc silent), a mouse IgG1 isotype control (Ms Fc) or unopsonised virus (no antibody). The percentage of SARS-CoV-2 positive cells was determined by flow cytometry. **(C)** ELISA assessing binding of antibodies and sera to recombinant pre-fusion stabilised SARS-CoV-2 spike trimer. Antibody concentration was 1 µg/ml. **(D)** iPSC-derived macrophage (KOLF2.1S) internalisation of SARS-CoV-2 opsonised with anti-RBD IgG1 antibodies and corresponding Fc-silenced (LALA-PG) variants. **(E)** Internalisation of SARS-CoV-2 opsonised with anti-RBD antibodies expressed as IgG1-4 subclasses, by iPSC-macrophages (KOLF2.1S). **(F)** Fcγ receptor binding assay. Binding of FN11A IgG1–4 subclasses and positive and negative COVID-19 patient sera to recombinant Fcγ receptors was assessed by ELISA. Data represent one representative experiment (three technical replicates per condition; error bars represent SD).

shown). This supports the interpretation that FB 9D likely recognises an epitope exposed following conformational rearrangement of spike, rather than on prefusion virions.

Taken together, these data indicate that the inability of most anti-S2 antibodies to enhance viral internalisation correlates with a lack of detectable binding to prefusion spike under ELISA conditions. For anti-S1 and anti-RBD antibodies, which achieved comparable levels of spike binding at the concentrations tested, differences in macrophage internalisation are unlikely to reflect differences in binding strength. Instead, these differences may arise from epitope-specific effects on Fc orientation, accessibility, and the efficiency of Fc receptor clustering required for phagocytic uptake.

Fc receptor engagement is required for antibody-mediated enhancement

To determine whether Fc receptor engagement is required for enhanced internalisation of SARS-CoV-2, six anti-RBD IgG1 monoclonal antibodies (FI3A, C121, FD11A, FN12A, C118 and EY6A) were engineered to contain LALA-PG mutations, which abrogate Fcγ receptor binding[200]. SARS-CoV-2 opsonised with LALA-PG mutant antibodies did not exhibit enhanced internalisation into macrophages compared with unopsonised virus (Figure 4.3D). These findings indicate that Fc receptor engagement is necessary for antibody-mediated enhancement of viral uptake.

IgG subclass-dependent differences in Fcγ receptor engagement and macrophage internalisation

Macrophages express multiple Fc receptors that mediate distinct functions, including phagocytosis, cytokine production and regulation of immune activation. Human IgG subclasses engage Fcγ receptors with differing affinities and therefore vary in their capacity to mediate Fc receptor-dependent phagocytosis. To assess the impact of IgG subclass on SARS-CoV-2 uptake, anti-RBD monoclonal antibodies (FI3A, FD11A, FN12A, C118 and EY6A) were expressed as IgG1-4 variants. SARS-CoV-2 was opsonised with each subclass variant, and viral internalisation into macrophages was quantified by flow cytometry (Figure 4.3E).

All IgG subclasses enhanced SARS-CoV-2 internalisation compared with unopsonised virus. Although the level of enhancement varied between antibodies, IgG1 subclasses generally mediated the greatest Fc receptor–dependent internalisation, whereas IgG2 subclasses mediated the least.

To investigate the mechanistic basis for these differences, binding of FD11A IgG1–4 subclasses to Fcγ receptors was assessed using an Fcγ receptor binding assay (Figure 4.3F). Engagement of the activating receptors FcγRIIA (CD32A) and FcγRIIIA (CD16A), as well as the inhibitory receptor

FcγRIIB (CD32B), was measured. FcγRIIIB (CD16B), which is predominantly expressed on neutrophils, was also assessed.

IgG1 and IgG3 subclasses demonstrated strong engagement of activating Fcγ receptors, consistent with their enhanced ability to mediate macrophage internalisation. In contrast, IgG2 and IgG4 exhibited reduced engagement of activating Fcγ receptors, correlating with their comparatively lower internalisation efficiency. FcγRI (CD64), a high-affinity activating receptor expressed on macrophages, was not included in this assay; however, given its preferential binding to IgG1 and IgG3, it may further contribute to the enhanced uptake observed with these subclasses.

Analysis of COVID-19 sera revealed differential Fc receptor engagement profiles. Serum 2 demonstrated strong engagement of multiple Fcγ receptors, whereas Serum 1 primarily engaged FcγRI (CD64). These differences may reflect variation in subclass composition. Both sera engaged FcγRI and enhanced macrophage internalisation of SARS-CoV-2. However, the broader Fcγ receptor engagement observed with Serum 2 suggests the potential for a more diverse Fc-mediated effector response, including enhanced activation through FcγRIIA and FcγRIIIA.

4.2.4 Specific anti-RBD antibodies mediate productive infection of macrophages

Antibodies against RBD permit productive SARS-CoV-2 infection of macrophages

The infectious virus release from macrophages inoculated with antibody-opsonised SARS-CoV-2 was quantified by FFA at 24 h PI (Figure 4.4A). Consistent with previous observations that macrophages are not permissive to SARS-CoV-2 infection, no infectious virus was detected in supernatants from macrophages exposed to unopsonised virus or virus opsonised with isotype control antibody, anti-S1 antibodies, anti-S2 antibodies, or COVID-19 donor serum. Notably, infectious virus was detected in supernatants from macrophages inoculated with SARS-CoV-2 opsonised with specific anti-RBD monoclonal antibodies, FN 12A, C118, S2X-259, EY 6A and IY 2A. These findings indicate that a subset of anti-RBD antibodies enables productive SARS-CoV-2 infection of macrophages.

To confirm that the detected virus resulted from active replication rather than residual input virus, infections were performed in the presence of the SARS-CoV-2 main protease inhibitor nirmatrelvir. Infectious virus production mediated by infection-promoting antibodies was

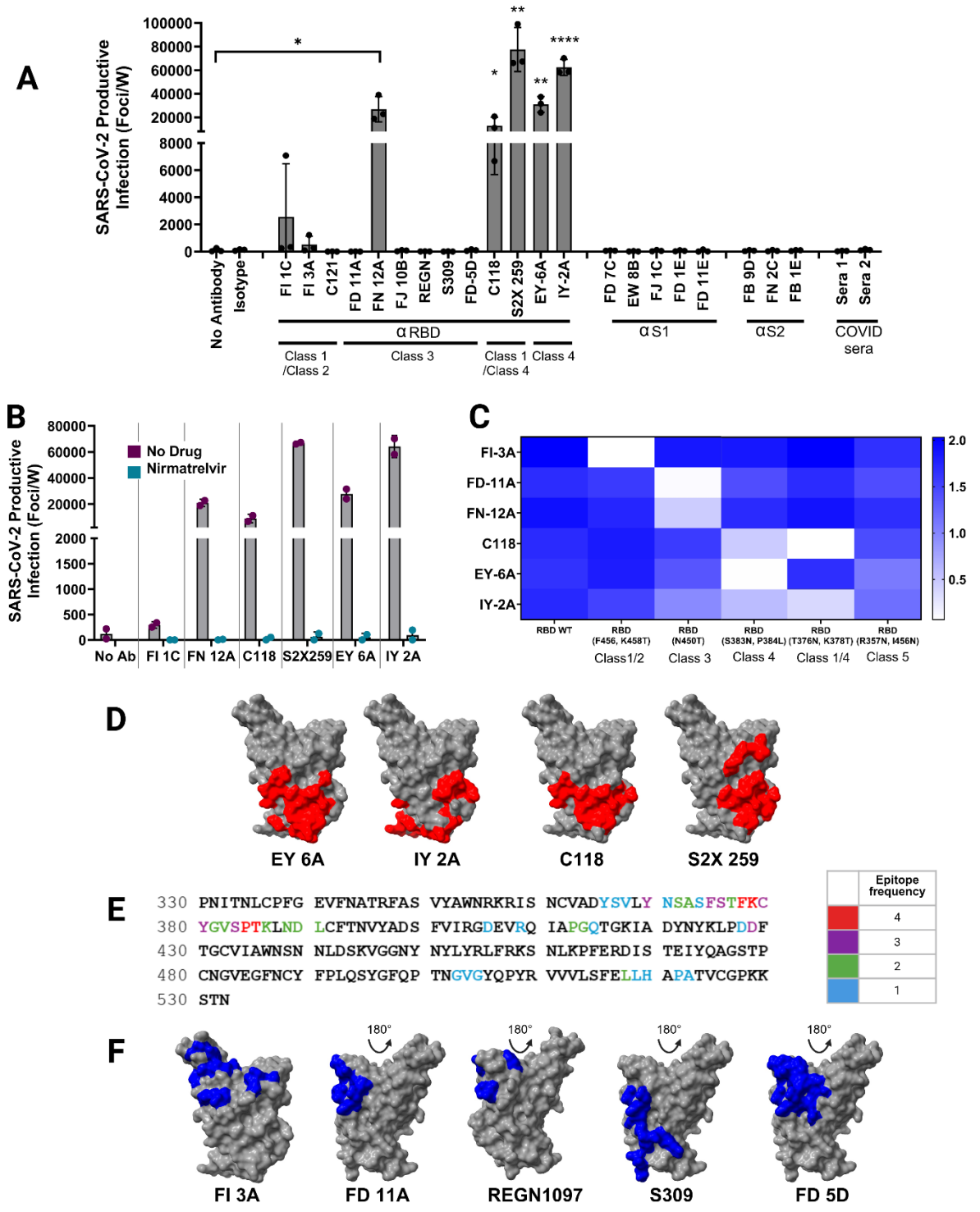

Figure 4.4 Specific anti-RBD antibodies mediate productive infection of macrophages. (A) Infectious virus release from iPSC-derived macrophages inoculated with antibody-opsonised SARS-CoV-2. Macrophages were incubated with the indicated anti-SARS-CoV-2 IgG1 antibodies (1 μg/ml), COVID-19 patient serum (NT_{50} concentration), a human IgG1 isotype control, or unopsonised virus (no antibody). Infectious virus in supernatants was quantified by focus-forming assay on Vero cells. Viral output is expressed as infectious virions released per well (foci) containing 100,000 macrophages. **(B)** Infectious virus release from macrophages inoculated with antibody-opsonised SARS-CoV-2 in the presence of the SARS-CoV-2 protease inhibitor nirmatrelvir. **(C)** RBD glycomutant ELISA used to determine anti-RBD antibody classification. **(D)** Structural mapping of epitopes from infection-promoting antibodies (red) onto the SARS-CoV-2 RBD (PDB: 6M0J), based on published crystal structures. **(E)** Amino acid sequence of the SARS-CoV-2 spike RBD with residues contacted by infection-promoting antibodies highlighted. Residues are coloured according to the number of antibody epitopes in which they occur (0-4). **(F)** Structural mapping of epitopes from non-infection-promoting antibodies (blue) onto the SARS-CoV-2 RBD. Data represent the mean ± SEM of two or three independent experiments (mean of three technical replicates per condition). Statistical significance was determined using an unpaired two-tailed Student's t-test assuming equal variance (uncorrected). *p < 0.05; n.s., not significant.

abolished by nirmatrelvir treatment (Figure 4.4B), confirming that viral release was dependent on productive replication.

Despite detectable replication, viral output remained low. For example, IY 2A mediated infection resulted in approximately 60,000 infectious virions per well containing 100,000 macrophages, corresponding to an average of 0.6 VET-infectious virions per cell. This low replication efficiency is comparable to that observed in transgenic ACE2-expressing macrophages, suggesting that macrophages impose intrinsic restrictions on SARS-CoV-2 replication even when entry is facilitated.

Infection promoting anti-RBD antibodies are predominantly class 4 and share overlapping epitope residues

Four of the five infection-promoting antibodies identified in this thesis are classified as class 4 RBD binders. Class 1, 2 and 3 anti-RBD antibodies did not mediate productive infection in macrophages, with the exception of FN 12A, a class 3. All class 4 antibodies tested promoted infection. Antibody classification was based on published crystal structures.

FN 12A is the only infection-promoting antibody for which a crystal structure has not been resolved; its classification was therefore inferred from competition ELISA data, performed by Dr Jack Tan's lab. Given its infection-promoting activity, it was plausible that FN 12A might actually be a class 4 antibody. To address this, Diana Melnyk generated RBD glycomutants and assessed antibody binding by ELISA (Figure 4.4C). The N450T glycomutant abolished FN 12A binding, whereas other mutations had no effect, consistent with FN 12A recognising a class 3 epitope. The FN 12A exception indicates that although infection-promoting antibodies are enriched within class 4, RBD binding classification alone does not fully predict infection-promoting capacity.

To explore whether infection-promoting antibodies share common structural features, the RBD epitopes of EY 6A, IY 2A, C118 and S2X-259 were examined using published crystal structures of antibody-RBD complexes. Binding residues were mapped onto the SARS-CoV-2 RBD structure (Figure 4.4D). Eleven amino acid residues were shared between at least three of the four infection-promoting antibody epitopes, indicating substantial epitope overlap (Figure 4.4E). Four key residues F377, K378, P384, T385 are common to the epitopes of all four neutralising antibodies. In contrast, structural analysis of five non-infection-promoting class 1–3 antibodies (F1 3A, FD 11A, S309, REGN10987 and FD 5D) revealed no overlap with the shared residues identified among infection-promoting antibodies (Figure 4.4F).

4.2.5 Determinants of antibody-mediated SARS-CoV-2 infection in macrophages

Proposed mechanism of anti-RBD antibody-mediated SARS-CoV-2 entry into macrophage

I hypothesised that specific anti-RBD antibodies may enable productive SARS-CoV-2 infection of macrophages through a cooperative mechanism involving both Fab- and Fc-mediated effects (Figure 4.5A). In the presence of ACE2, ACE2 stabilises the open spike conformation, allowing cleavage by host proteases, and subsequent membrane fusion. In macrophages, binding of specific anti-RBD antibodies stabilises spike in a fusion-permissive conformation, mimicking aspects of ACE2 engagement and promoting exposure of cleavage sites required for membrane fusion. Concurrently, the Fc domains of antibody-virus complexes engage activating Fcγ receptors on macrophages, providing stable virion tethering at the cell surface or within early endosomes. This Fc-dependent attachment may facilitate spike processing by host proteases and subsequent fusion. Antibodies that fail to induce a fusion-permissive conformation are instead likely to promote Fc receptor-mediated uptake followed by degradation. Differences in infection-promoting activity between antibodies may therefore reflect a balance between Fc receptor engagement, spike conformational effects, and, in some cases, competing neutralising activity.

Infection-promoting antibodies exhibit distinct concentration-dependent effects

To explore the mechanism of antibody-mediated SARS-CoV-2 infection, infection-promoting antibodies were titrated and infectious virus output was quantified by FFA (Figure 4.5B). Previous experiments were performed at 1 µg/ml. Antibodies were titrated over a range of 10–0.003 µg/ml.

Three infection-promoting antibodies (IY 2A, C118 and S2X-259) displayed bell-shaped dose-response curves relating antibody concentration to productive infection. At lower concentrations, these antibodies enhanced infection, whereas at concentrations above approximately 1 µg/ml, infectious output declined. This pattern is consistent with a balance between Fc receptor-dependent entry at sub-saturating concentrations and increasing neutralising activity at higher concentrations.

In contrast, EY 6A and FN12A did not exhibit bell-shaped dose-response profiles. Instead, infectious output increased with antibody concentration, plateauing at 10 µg/ml for FN 12A. FN 12A is non-neutralising in ACE2-expressing cells, consistent with the absence of inhibition at higher concentrations. Although EY6A neutralises SARS-CoV-2 in ACE2-expressing cells, increasing concentrations did not reduce infection in macrophages, suggesting that its

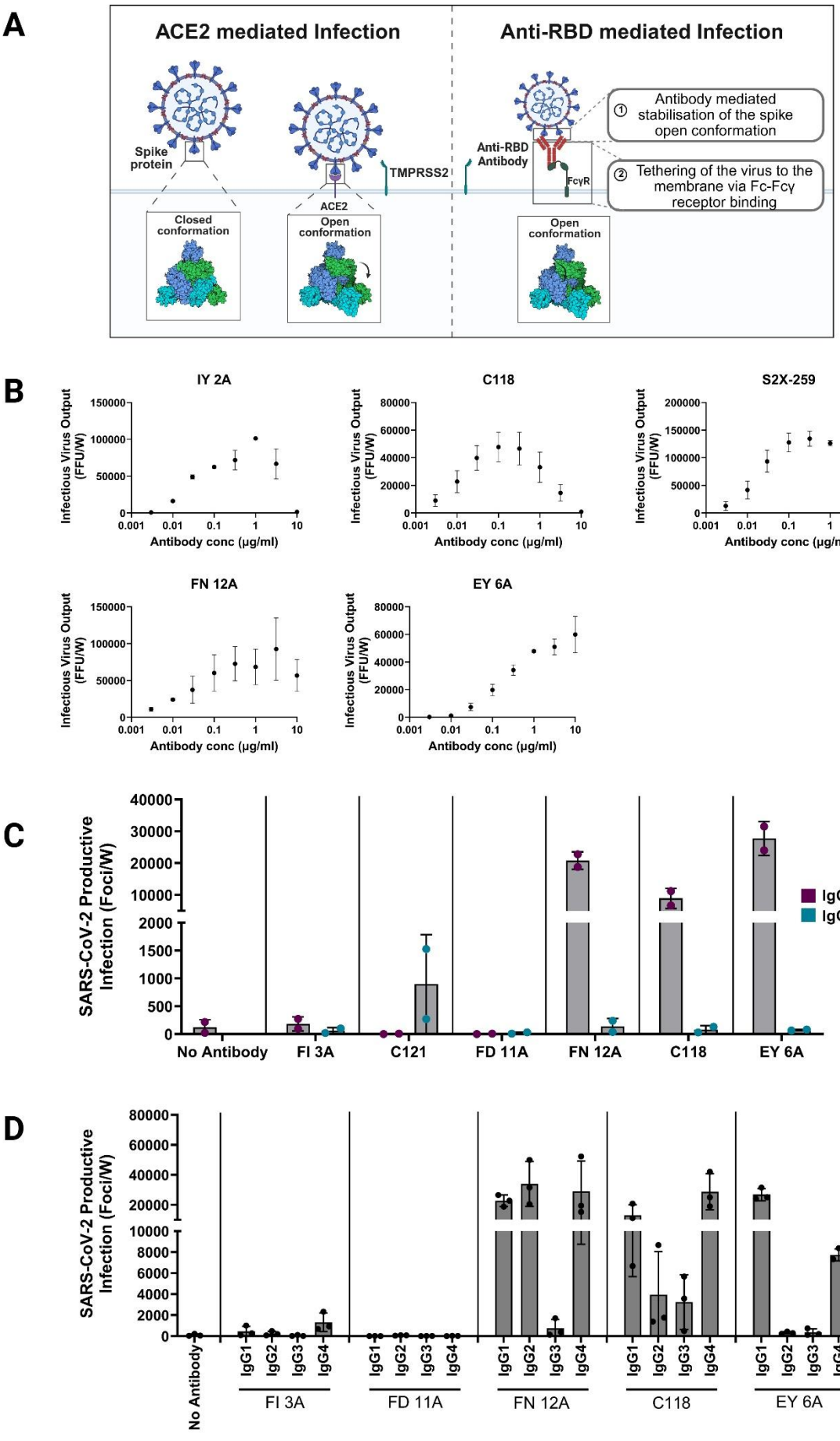
A
ACE2 mediated Infection
Anti-RBD mediated Infection
Spike protein
TMPRSS2
ACE2
Closed conformation
Open conformation
Anti-RBD Antibody
FcγR
Open conformation
① Antibody mediated stabilisation of the spike open conformation
② Tethering of the virus to the membrane via Fc-Fcγ receptor binding
B
IY 2A
C118
S2X-259
FN 12A
EY 6A
Infectious Virus Output (FFU/W)
Antibody conc (µg/ml)
C
SARS-CoV-2 Productive Infection (Foci/W)
IgG1
IgG1 LALA-PG
No Antibody
FI 3A
C121
FD 11A
FN 12A
C118
EY 6A
D
SARS-CoV-2 Productive Infection (Foci/W)
No Antibody
IgG1
IgG2
IgG3
IgG4
FI 3A
FD 11A
FN 12A
C118
EY 6A

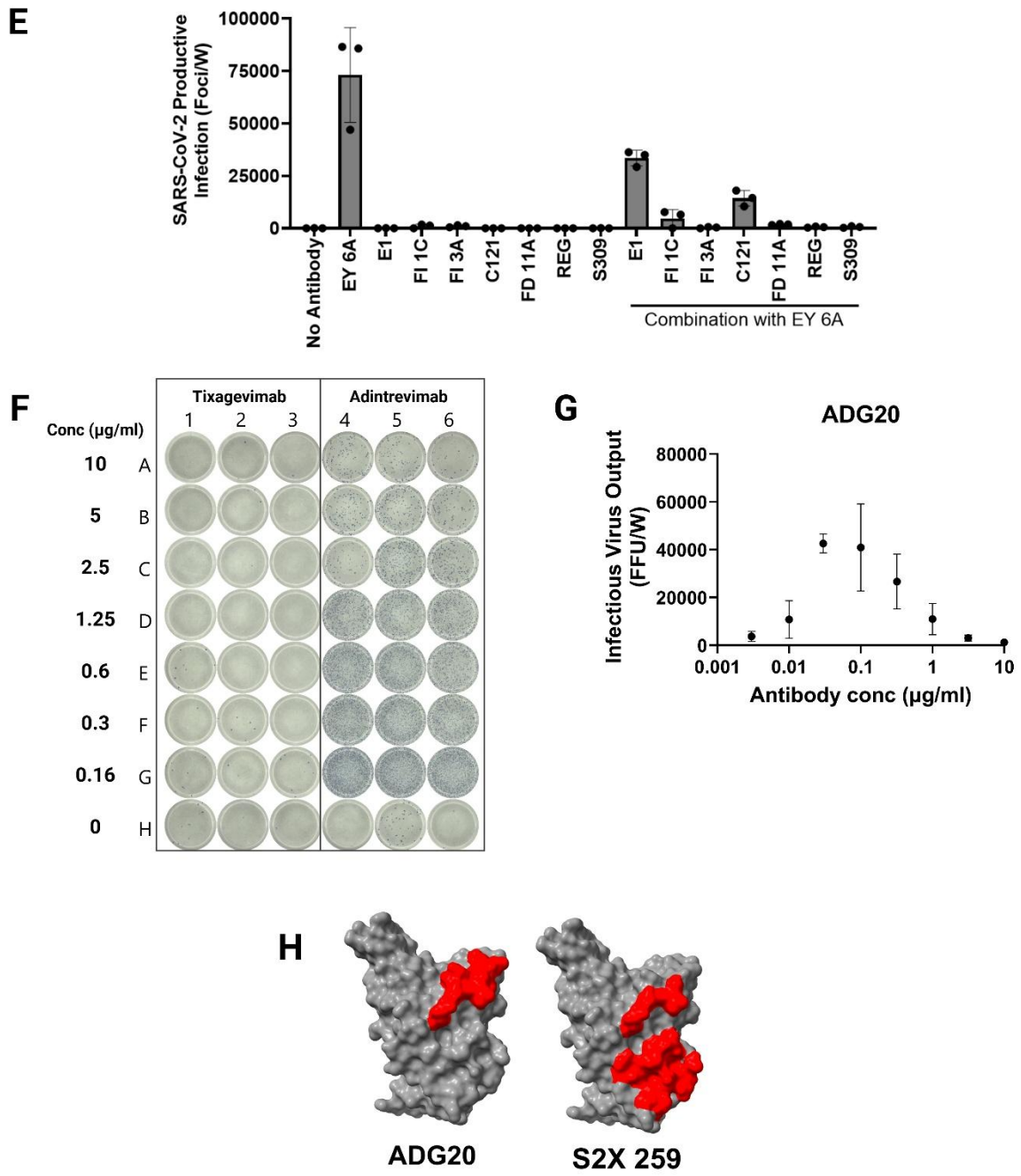

Figure 4.5 Determinants of antibody-facilitated SARS-CoV-2 infection in macrophages. (A) Schematic of the proposed mechanism of antibody-promoted SARS-CoV-2 of macrophages. Productive infection is hypothesised to require Fab-mediated stabilisation of a fusion-permissive spike conformation and Fcγ receptor-mediated virion tethering and entry. **(B)** Dose-response curves showing infectious virus output from macrophages following inoculation with SARS-CoV-2 opsonised with titrated infection-promoting antibodies. Viral output is expressed as infectious virions released (foci) per well containing 100,000 macrophages. **(C)** Infectious virus release from macrophages inoculated with SARS-CoV-2 opsonised anti-RBD IgG1 antibodies and corresponding Fc-silenced (LALA-PG) variants. **(D)** Infectious virus release from macrophages inoculated with SARS-CoV-2 opsonised with anti-RBD antibodies expressed as IgG1-4 subclasses. **(E)** Infectious virus release from macrophages inoculated with SARS-CoV-2 opsonised with the infection-promoting antibody EY 6A and non-infection promoting antibodies, either alone or in combination. Data shown is one representative experiment (three technical replicates; error bars indicate SD). **(F)** FFA plate showing infectious virus output from macrophages following inoculation with SARS-CoV-2 opsonised with titrated therapeutic monoclonal antibodies, tixagevimab (AZD8895) and adintrevimab (ADG20). **(G)** Dose-response curves showing quantification of infectious viral output from panel (F), expressed as infectious virus foci per well containing 100,000 macrophages. **(H)** Structural comparison of ADG20 and S2X-259 epitopes mapped onto the SARS-CoV-2 RBD (PDB: 6M0J), based on published crystal structures. Data in panels B,C,G represent the mean ± SEM of two independent experiments, D = three experiments (mean of three technical replicates per condition). Macrophages in all experiments were derived from KOLF2.1S donor.

neutralising mechanism does not prevent Fc receptor-mediated infection in this context. The proportional increase in infection with increasing antibody concentration is consistent with Fc receptor engagement being limiting within the concentration range tested.

Fc silenced mutants and IgG subclasses reveal antibody-mediated infection mechanism

To directly assess the contribution of Fc receptor engagement to productive infection, Fc-silenced variants of infection-promoting antibodies were generated by introducing LALA-PG mutations, which abrogate Fcγ receptor binding. Macrophages were inoculated with SARS-CoV-2 opsonised with anti-RBD IgG1 antibodies or their corresponding Fc-silenced variants, and infectious virus output was quantified by focus-forming assay (FFA) (Figure 4.5C). Introduction of the LALA-PG mutations completely abolished anti-RBD antibody-mediated productive infection in macrophages. These findings demonstrate that Fcγ receptor engagement is essential for antibody-mediated infection, and that Fab-mediated stabilisation of the RBD alone is insufficient to support productive replication.

To further examine the role of Fcγ receptor interactions, five anti-RBD antibodies (FI3A, FD11A, FN12A, C118 and EY6A) were expressed as IgG1-4 subclasses. For the three infection-promoting antibodies (FN12A, C118 and EY6A), the IgG1 and IgG4 subclasses strongly mediated productive infection (Figure 4.5D). In contrast, expression as the IgG3 subclass nearly abolished antibody-mediated infection. The IgG2 subclass resulted in variable levels of infection across antibodies. These data suggest that antibody-mediated productive infection is influenced by differential engagement of specific Fcγ receptors.

Neutralising polyclonal serum limits antibody-mediated infection of macrophages

Polyclonal serum from two individuals infected with SARS-CoV-2 did not mediate productive infection of macrophages (Figure 4.4A). One possible explanation is the presence of neutralising antibodies within the serum, rather than the absence of class 4 anti-RBD antibodies capable of promoting infection. To test this hypothesis, the infection-promoting antibody EY6A was combined with neutralising monoclonal antibodies. EY 6A alone enabled productive infection of macrophages; however, when neutralising antibodies were added, infectious virus output was significantly reduced (Figure 4.5E). These findings indicate that neutralising antibodies can counteract antibody-mediated infection, likely by preventing spike-mediated fusion prior to Fc receptor-dependent entry. Together, these data suggest that, in the presence of a polyclonal neutralising antibody response, antibody-dependent infection of macrophages is unlikely to occur efficiently in vivo.

Therapeutic monoclonal antibody Adintrevimab mediates productive replication in macrophages

Given that several patient-derived class 4 anti-RBD antibodies mediated productive SARS-CoV-2 infection in macrophages, I investigated whether a therapeutic monoclonal antibody might similarly promote infection. Adintrevimab (ADG20) is an anti-RBD antibody that binds an epitope spanning regions between class 1 and class 4 binding sites. Previously tested class 1/4 antibodies (C118 and S2X-259) both mediated productive infection (Figure 4.4A), leading to the hypothesis that ADG20 may also promote infection in macrophages. To determine whether infection-promoting activity was restricted to class 4-like epitopes, the class 1 therapeutic antibody Tixagevimab (AZD8895) was also evaluated. Both therapeutic antibodies were titrated, and infectious virus output was quantified by FFA (Figure 4.5F). AZD8895 did not mediate productive infection of macrophages. In contrast, ADG20 enabled productive replication. Notably, ADG20 exhibited a bell-shaped dose-response relationship between antibody concentration and productive infection, consistent with other infection-promoting antibodies (Figure 4.5G).

To explore structural correlates of infection-promoting activity, the published crystal structure of the ADG20-RBD complex was examined and binding residues were mapped onto the SARS-CoV-2 RBD structure (Figure 4.5H). ADG20 did not bind the highly conserved residues shared among previously identified infection-promoting antibodies; however, it shared five contact residues (D405, R408, G502, V503 and G504) with the infection-promoting antibody S2X-259. Although ADG20 shares only limited overlap with the residues identified in the four infection-promoting antibodies analysed here, it is possible that broader structural comparison across a larger panel of infection-promoting antibodies would reveal additional shared epitope features.

4.2.6 Type I interferon signalling restricts antibody-mediated SARS-CoV-2 replication in macrophages

JAK inhibition enhances antibody-mediated SARS-CoV-2 replication in macrophages

Despite detectable replication mediated by infection-promoting antibodies, viral output from macrophages remains low compared with titres from susceptible cells. I hypothesised that this reflected restriction of viral replication by type I interferon (IFN-I) signalling. To investigate this, macrophages were treated with the JAK1/2 inhibitor ruxolitinib, which inhibits signalling downstream of the IFNAR1/2 receptor complex (Figure 4.6A).

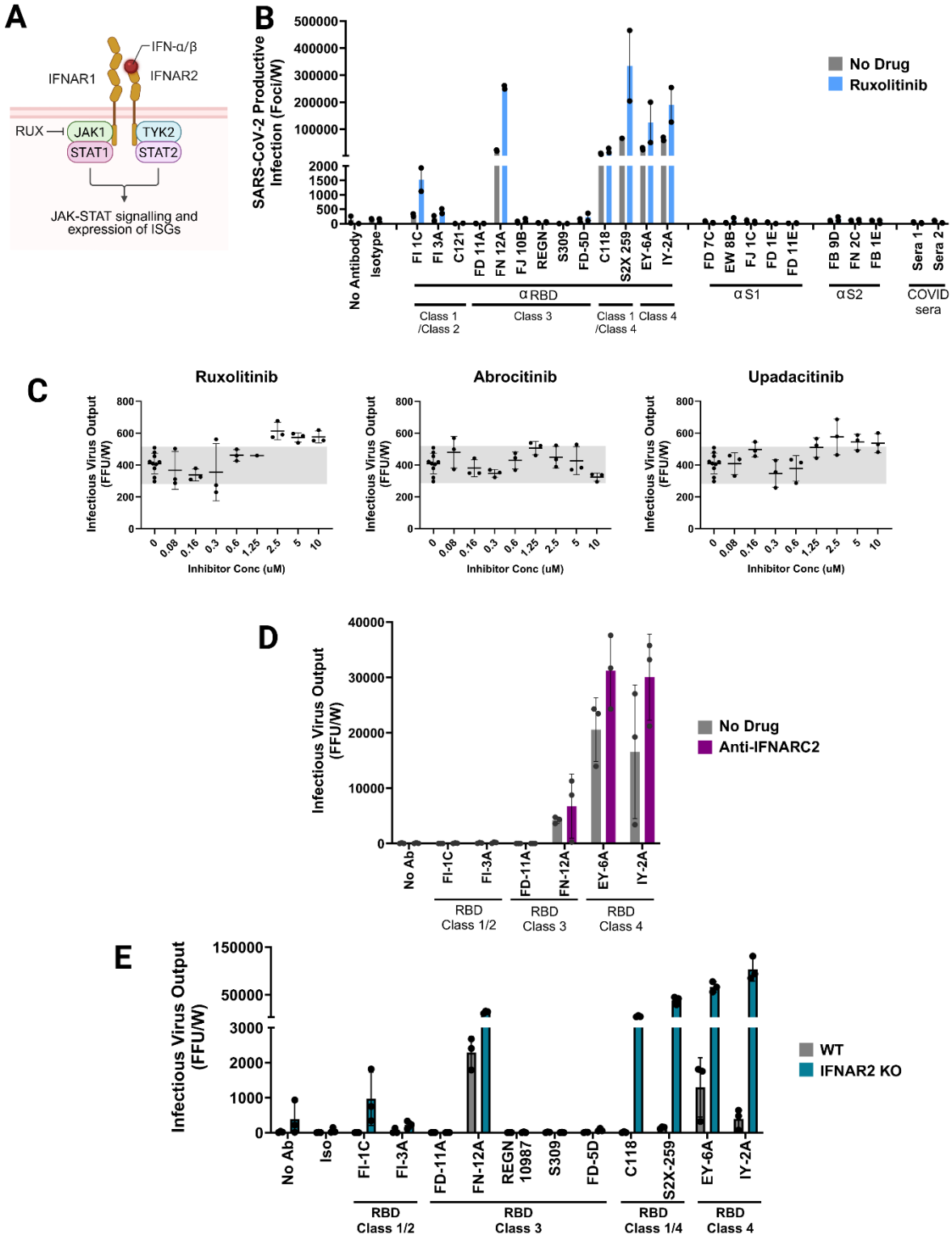

Figure 4.6 Interferon signalling restricts antibody-mediated productive SARS-CoV-2 infection of macrophages. (A) Schematic illustrating type I interferon signalling through the IFNAR receptor and downstream JAK-STAT pathway. **(B)** Infectious virus release from iPSC-derived macrophages (KOLF2.1) inoculated with antibody-opsonised SARS-CoV-2 in the presence or absence of the JAK1 inhibitor ruxolitinib (10 μM; Rux). Infectious virus in supernatants was quantified by FFA on Vero cells. Viral output is expressed as infectious virions (foci) released per well containing 100,000 macrophages. Data represent mean ± SEM of two independent experiments. **(B)** Infectious virus release from iPSC-macrophages (KOLF2.1) inoculated with EY 6A-opsonised SARS-CoV-2 in the presence of JAK1 inhibitors ruxolitinib, abrocitinib, or upadacitinib. **(D)** Infectious virus release from macrophages (KOLF2.1) inoculated with antibody-opsonised SARS-CoV-2 in the presence of an IFNAR2-blocking antibody (1 μg/ml). **(E)** Infectious virus release from wild-type (SFC841-03-01) and IFNAR2 knockout (SFC841-03-01 IFNAR -/-) macrophages inoculated with antibody-opsonised SARS-CoV-2. Data shown from panels C-E are from one representative experiment (three technical replicates; error bars represent SD).

Infectious virus release from macrophages inoculated with antibody-opsonised SARS-CoV-2, in the presence or absence of ruxolitinib, was quantified by FFA at 24 h PI (Figure 4.6B). Ruxolitinib treatment resulted in an approximately two-fold increase in infectious virus output mediated by infection-promoting antibodies. Notably, FI1C and FI3A mediated productive replication in the presence of ruxolitinib but not in untreated macrophages. This data indicates that ruxolitinib is enhancing antibody-mediated SARS-CoV-2 infection of macrophages.

However, ruxolitinib is not specific to JAK1 and has numerous additional kinase targets, including various other kinases that regulate cell cycle progression and transcription, raising the possibility that the observed enhancement could reflect off-target effects [201]. To address this, second-generation JAK1-selective inhibitors, abrocitinib and upadacitinib, were evaluated [202,203]. These inhibitors were titrated in EY6A-mediated infection assays; however, infectious virus output was highly variable under these conditions, precluding definitive conclusions (Figure 4.6C).

IFNAR2 blockade and knock-out enhance antibody-mediated SARS-CoV-2 infection

As an alternative method to inhibiting type I IFN signalling, an anti-IFNAR2 blocking antibody was used. Blockade of the IFNAR receptor resulted in an approximately 1.5-fold increase in antibody-mediated infection (Figure 4.6D). This pharmacological evidence provided a rationale to generate iPSC-derived IFNAR2 knockout (KO) macrophages.

Antibody-mediated SARS-CoV-2 infection was significantly increased in IFNAR2 KO macrophages compared with genetically matched wild-type controls (Figure 4.6E). IFNAR2 deletion resulted in average fold increases of 52-, 420-, 270- and 260-fold for EY6A, C118, S2X-259 and IY2A, respectively. Taken together, the pharmacological and genetic data demonstrate that type I interferon signalling strongly restricts antibody-mediated SARS-CoV-2 replication in macrophages.

4.3 Discussion

Macrophages are not intrinsically susceptible to SARS-CoV-2 infection

This chapter demonstrates that iPSC-derived macrophages are not susceptible to productive SARS-CoV-2 infection. This finding is consistent with the majority of published studies across multiple macrophage models[72–74,174,204]. Reports suggesting productive replication in macrophages are comparatively limited and often rely on detection of viral RNA or protein

without clear demonstration of infectious progeny release [51,82,88,104,173]. Amplification of residual inoculum virus may account for some false positive findings. Importantly, viral internalisation alone does not equate to productive replication.

I hypothesised that the reason macrophages did not support productive infection was because they do not express the ACE2 receptor. Productive SARS-CoV-2 infection requires membrane fusion and release of the viral genome into the cytosol, a process facilitated by ACE2-mediated stabilisation of the spike protein in an open conformation and subsequent proteolytic activation[189,205]. In the absence of ACE2, the non-specific uptake pathway described in the previous chapter is unlikely to support the conformational changes and cleavage events required for fusion, resulting instead in viral degradation.

Consistent with this hypothesis, transgenic expression of hACE2 rendered macrophages permissive to infection. Previous studies have shown that ACE2-expressing THP-1 cells or monocyte-derived macrophages can support replication of SARS-CoV-2 or pseudotyped virus, respectively [72,75,104]. Whereas this thesis demonstrates productive infection using authentic SARS-CoV-2 in human macrophages.

Antibody-mediated entry enables productive infection

This chapter demonstrates that although many IgG antibodies targeting the RBD and spike protein can opsonise SARS-CoV-2 and enhance phagocytic internalisation into macrophages, only a specific subset of antibodies mediate productive infection. I propose that specific anti-RBD antibodies stabilise spike in a fusion-permissive open conformation[206,207]. Concurrently, the Fc domains of antibody-virus complexes engage activating Fcγ receptors on macrophages, providing stable virion tethering at the cell, facilitating spike cleavage and fusion. Antibody-mediated infection appears to reflect a balance between two components: Fab-mediated stabilisation of a fusion-permissive spike conformation and Fcγ receptor-mediated virion tethering and entry.

Epitope specificity determines infection-promoting capacity

Epitope mapping onto SARS-CoV-2 RBD structures revealed substantial overlap among infection-promoting antibodies. Based on the location of these shared residues, infection-promoting antibodies are enriched within class 4; however, the class 3 antibody FN12A demonstrates that it is the precise binding residues, rather than the broader epitope classification, that more accurately predicts infection-promoting capacity. Binding to these

residues on prefusion spike may stabilise the open RBD conformation, suggesting that Fab-mediated conformational effects are a critical component of antibody-mediated infection. A limitation of this study is the limited number of infection-promoting antibodies identified and structurally analysed. Analysis of a larger panel of anti-RBD antibodies would give much more comprehensive insight into which epitope residues will allow an antibody to mediate productive infection. In addition, this study did not directly demonstrate that infection-promoting antibodies stabilise the spike protein in a fusion-permissive open conformation. Addressing this would require structural analyses, such as crystallography or cryo-EM, to compare the conformation of the RBD before and after antibody binding.

Fcγ receptor engagement is required for infection

It was plausible that Fab-mediated stabilisation alone might permit productive infection. However, the complete abrogation of infection observed with Fc-silenced (LALA-PG) antibodies demonstrates that Fcγ receptor engagement is essential. Fc receptor-mediated internalisation may direct virus into a fusion-permissive endocytic pathway, delivering virions to early endosomes where acidification and cathepsin-mediated spike cleavage can occur. Alternatively, Fc-mediated tethering may prolong virion-membrane proximity, allowing sufficient time for spike cleavage by surface proteases or facilitating the close apposition of viral and host membranes required for fusion. This thesis did not investigate whether antibody-mediated infection proceeds via surface proteases or endosomal cathepsins; defining the site of fusion would provide further mechanistic insight.

IgG subclass influences infection efficiency

Opsonisation with all IgG1-4 subclasses enhanced viral uptake into macrophages, with IgG1 and IgG3 mediating the strongest internalisation. Notably, however, IgG1 and IgG4 were the most effective at promoting productive infection, whereas IgG3 mediated minimal infection and IgG2 showed variable effects. This dissociation between uptake and replication suggests that internalisation alone is insufficient to support productive infection.

Two non-mutually exclusive mechanisms may explain these subclass-specific differences. First, IgG3 induces strong Fcγ receptor signalling, which may accelerate trafficking to degradative pathways, including enhanced endosomal–lysosomal fusion, thereby promoting viral degradation and antiviral responses [208,209]. In contrast, IgG1 and IgG4 may provide sufficient Fcγ receptor-dependent tethering to permit entry while avoiding excessive inflammatory signalling that could limit replication.

An additional mechanism may relate to hinge length and flexibility[32]. IgG3 possesses an extended hinge region approximately four-fold longer than that of IgG1, potentially increasing the spatial distance between the virion and the macrophage membrane following Fcγ receptor engagement[210]. Given the geometry-dependent nature of coronavirus fusion, increased virion–membrane spacing could reduce protease accessibility or impair membrane apposition. IgG1 and IgG4 have shorter, flexible hinges that may permit more favourable tethering geometry[211]. In contrast, IgG2 has a short but structurally constrained hinge, which may limit optimal Fc orientation for certain epitopes, potentially explaining the variability observed among IgG2 variants. Together, these findings suggest that both Fcγ receptor signalling and structural properties of IgG subclasses influence the efficiency of antibody-mediated infection.

Future work could test these mechanisms by generating antibody chimeras combining different Fc regions and hinge domains, allowing the relative contributions of signalling and structural features to be determined.

Type I interferon restricts macrophage infection

Whilst specific anti-RBD antibodies can mediate productive SARS-CoV-2 infection of macrophages, replication remains strongly restricted by type I interferon signalling. Macrophages are highly responsive to type I interferon signalling and may exhibit stronger ISG induction than epithelial cell lines. Knockout of IFNAR2 resulted in up to a 420-fold increase in infectious virus output, indicating that intact IFN-I signalling imposes a substantial barrier to replication in these cells. The magnitude of this effect suggests that multiple ISGs act to restrict SARS-CoV-2 in macrophages. A limitation of this study is that it did not evaluate antibody-mediated infection under different macrophage activation states. It is possible that this could influence permissiveness.

Although restriction factors specific to SARS-CoV-2 infection in macrophages have not been demonstrated, several ISGs have been shown to inhibit SARS-CoV-2 replication in susceptible cell types. OAS1 activates RNase L upon sensing viral RNA, leading to RNA degradation [212,213]. LY6E restricts SARS-CoV-2 entry by inhibiting spike-mediated membrane fusion [214,215], and 25-hydroxycholesterol, produced by CH25H, alters membrane cholesterol distribution to impair spike-driven fusion [216]. ZAP (zinc-finger antiviral protein) binds SARS-CoV-2 RNA and promotes its degradation through recruitment of cofactors [217]. IFITM2 and IFITM3 can also restrict SARS-CoV-2 entry by interfering with membrane fusion, particularly in endosomal entry pathways [218]. It is therefore plausible that these restriction factors contribute to limiting antibody-mediated

infection of macrophages. While investigation of individual ISGs was beyond the scope of this study, defining their relative contributions represents an important direction for future work.

Distinction from classical antibody-dependent enhancement

Antibody-mediated infection observed in this study differs mechanistically from classical dengue antibody-dependent enhancement (ADE)[219]. In both systems, antibody-virus complexes engage Fc receptors to facilitate macrophage infection. However, in dengue, enhancement occurs broadly with cross-reactive antibodies during secondary heterologous infection. In contrast, SARS-CoV-2 macrophage infection in this system is mediated only by a specific subset of anti-RBD antibodies, raised against the same viral strain they promote infection of, rather than by broadly cross-reactive antibodies.

The bell-shaped dose-response relationship between antibody concentration and productive infection is a feature shared with classical ADE, reflecting Fc receptor dependent entry at sub-saturating concentrations and increasing neutralisation at higher concentrations. Nevertheless, the underlying mechanisms differ. For SARS-CoV-2, productive infection requires cooperative contributions from both Fcγ receptor engagement and Fab-mediated stabilisation of a fusion-permissive spike conformation. In dengue, by contrast, Fc receptor-mediated entry alone is sufficient to support robust replication.

Importantly, dengue virus is intrinsically adapted to replicate efficiently within macrophages, and ADE substantially increases viral load and contributes to severe systemic disease. In contrast, SARS-CoV-2 is not naturally permissive in macrophages. Even under antibody-facilitated conditions, replication remains low and is strongly restricted by type I interferon signalling. These findings suggest that antibody-mediated macrophage infection in SARS-CoV-2 represents a conditional and limited phenomenon, rather than a classical ADE mechanism associated with widespread viral amplification.

Physiological relevance and in vivo consideration

Antibody-mediated SARS-CoV-2 infection of macrophages could theoretically occur in vivo. The in vitro studies presented here used physiologically relevant human iPSC-derived macrophages and patient-derived antibodies to demonstrate this phenomenon. However, the effect was clearly concentration dependent and was most pronounced at subneutralising antibody concentrations. Such conditions could potentially arise early during infection, or later as antibody levels decline. Importantly, in the presence of neutralising antibodies, the virus is

neutralised, reducing the action of infection-promoting antibodies. Indeed, sera from two SARS-CoV-2-infected individuals did not promote macrophage infection. These findings suggest that antibody-mediated macrophage infection would likely require a scenario in which an infection-promoting antibody is both dominant and present at subneutralising concentrations, a situation that is unlikely during a typical course of infection.

Implications for therapeutic antibodies

A context in which this phenomenon might be more relevant is therapeutic monoclonal antibody administration in immunocompromised individuals. In this thesis, Adintrevimab, a fully human IgG1 anti-RBD monoclonal antibody with class 1/4 epitope features, was identified as infection-promoting in macrophages. Adintrevimab was evaluated in two phase II/III trials[220,221]. The STAMP trial (NCT04805671) was a double-blind, randomised study enrolling 399 high-risk, non-hospitalised adults and adolescents with mild-to-moderate COVID-19[221]. Participants were classified as high risk based on factors including age, obesity, chronic conditions, or immunosuppressive therapy or immunosuppressive condition. Adintrevimab reduced the risk of hospitalisation or all-cause death in infections, and no serious adverse events were reported. The trial was subsequently terminated following the emergence of Omicron variants with reduced neutralisation sensitivity.

Therapeutic monoclonal antibodies are typically selected for strong ACE2-blocking neutralisation (class 1/2) or conserved non-RBM binding (class 3), it is therefore uncommon that Adintrevimab targets the infection-promoting class 1/4 epitope. In addition, therapeutic monoclonals are frequently engineered to modify Fc effector functions. For example, Tixagevimab (a component of Evusheld) contains Fc modifications that reduce Fcγ receptor engagement and did not promote macrophage infection in this study. In contrast, Adintrevimab was engineered to extend serum half-life but retains Fcγ receptor binding capacity[222]. Despite its ability to promote macrophage infection, no evidence of enhanced disease by Adintrevimab was observed in clinical trials. Nevertheless, the trial was not specifically designed to evaluate enhanced disease in profoundly immunocompromised individuals who are often under-represented in randomised controlled trials.

While current clinical data do not support a role for macrophage-mediated enhancement in COVID-19, these findings highlight a theoretical consideration for future antibody design. In viruses more intrinsically adapted to replicate in macrophages, Fcγ receptor–dependent entry mechanisms could have greater pathological relevance. Careful evaluation of Fc receptor

engagement properties should therefore remain an important aspect of therapeutic monoclonal antibody development.

4.4 Conclusions

In summary, this chapter demonstrates that human iPSC-derived macrophages are intrinsically non-permissive to productive SARS-CoV-2 infection yet can be rendered permissive by specific antibody-mediated conditions. A subset of anti-RBD antibodies enables productive infection through a cooperative mechanism requiring both Fab-mediated stabilisation of a fusion-permissive spike conformation and Fcγ receptor-dependent virion tethering. This phenomenon is mechanistically distinct from classical antibody-dependent enhancement, as it is epitope-specific, inefficient, and strongly constrained by type I interferon signalling. While antibody-mediated macrophage infection is theoretically possible in vivo, it likely represents a conditional and tightly regulated event rather than a dominant driver of disease. Together, these findings define a previously uncharacterised, Fc- and epitope-dependent pathway of SARS-CoV-2 entry into macrophages and highlight the importance of considering Fc receptor interactions in future therapeutic antibody design.

Chapter 5: Macrophage Functional Response to SARS-CoV-2

5.1 Introduction and aims

Macrophage responses to SARS-CoV-2 infection

This thesis has so far examined macrophages as a cellular target of SARS-CoV-2 infection. This chapter instead focuses on the role of macrophages as immune effector cells in the progression of COVID-19. Alveolar macrophages (AMs) are key sentinel cells of the lung and are among the first immune cells to encounter respiratory pathogens, including SARS-CoV-2[36]. In response to viral exposure, macrophages contribute to host defence through phagocytosis, antigen presentation, and cytokine secretion[223].

In severe COVID-19, however, macrophage responses become dysregulated and are associated with excessive inflammation, which is thought to contribute to disease pathology[54]. The mechanisms underlying this dysregulation remain incompletely understood. This chapter therefore examines how macrophage functions, including phagocytosis, cytokine production, and antigen presentation, are modulated following exposure to SARS-CoV-2.

Macrophage viability following SARS-CoV-2 exposure

The impact of SARS-CoV-2 on macrophage viability remains incompletely understood. Studies have shown that AMs are depleted in the lungs of patients with severe COVID-19[54]. It remains unclear whether this depletion results from direct infection by SARS-CoV-2 or from alterations in the alveolar microenvironment. In contrast, monocyte-derived macrophages are enriched in the bronchoalveolar lavage fluid of patients with severe disease[224–226]. Together, these observations suggest a shift from tissue-resident AMs, which are associated with homeostasis and resolution of inflammation, to recruited inflammatory monocyte-derived macrophages during severe COVID-19[227]. In vitro studies have demonstrated that SARS-CoV-2 exposure can induce macrophage cell death[178,228–231]. In this chapter, macrophage viability following SARS-CoV-2 exposure was assessed.

Macrophage ROS production following SARS-CoV-2 exposure

Reactive oxygen species (ROS) production is a key feature of macrophage activation and contributes to antimicrobial defence following pathogen recognition[232]. ROS are generated

following receptor-mediated activation and function to damage proteins, lipids, and nucleic acids of internalised pathogens. However, ROS production must be tightly regulated, as excessive or dysregulated ROS generation can lead to oxidative stress and contribute to cellular and tissue damage[233]. There is evidence that SARS-CoV-2 infection may alter macrophage ROS responses, leading to increased oxidative stress [231,234,235]. To investigate this, intracellular ROS production following SARS-CoV-2 exposure was assessed in macrophages.

Macrophage phagocytic capacity following SARS-CoV-2 exposure

Phagocytosis is a key effector function of macrophages that enables the clearance of pathogens and infected cells. This process involves the recognition, internalisation, and degradation of particles through receptor-mediated mechanisms, including pattern recognition, complement, and Fc receptors. Efficient phagocytosis is essential for the resolution of infection and maintenance of tissue homeostasis. Efficient phagocytosis contributes to viral clearance through removal of infected cells and extracellular viral particles. Many viruses have evolved mechanisms to impair macrophage phagocytic function[236–238]. Evidence regarding the impact of SARS-CoV-2 on macrophage phagocytosis remains limited, although some studies suggest that phagocytic function may be impaired following viral exposure [239,240]. Macrophage phagocytic capacity following SARS-CoV-2 exposure was assessed in this chapter.

Macrophage antigen presentation following SARS-CoV-2 exposure

Antigen presentation is a key function of the immune system that enables activation of adaptive immune cells. Antigen presenting cells process endogenous and exogenous antigens and present them on MHC class I and II molecules to activate antigen-specific $CD8^+$ and $CD4^+$ T cells, respectively. While all nucleated cells present endogenous antigens via MHC class I, professional antigen-presenting cells are specialised for presenting exogenous antigens on MHC class II and, in some cases, can cross-present exogenous antigens on MHC class I to activate $CD8^+$ T cells[241].

During respiratory viral infection, dendritic cells are primarily responsible for priming naïve T cells in lymphoid tissues. In contrast, AMs are thought to play a more modulatory role within the lung, presenting antigen to effector T cells to sustain, enhance, or suppress local immune responses[242,243]. Dysregulated T cell responses have been implicated in COVID-19 pathology[244], and altered macrophage antigen presentation may contribute to this process. However, the impact of SARS-CoV-2 exposure on macrophage antigen presentation remains incompletely understood, with limited evidence suggesting reduced MHC expression in macrophages from

patients with severe disease[54]. To investigate this, antigen presentation by SARS-CoV-2-exposed macrophages was examined using a macrophage-T cell co-culture system with patient-derived $CD4^+$ and $CD8^+$ T cells.

Macrophage cytokine production following SARS-CoV-2 exposure

Severe COVID-19 is associated with a hyperinflammatory state often described as a "cytokine storm", characterised by elevated systemic levels of pro-inflammatory cytokines. Macrophages are major contributors to this response and are enriched in the lungs of patients with severe disease, where they exhibit a pro-inflammatory phenotype [54,225,245]. However, the drivers of macrophage activation in COVID-19 remain unclear. Macrophages may be activated through direct sensing of SARS-CoV-2 or through detection of DAMPs or inflammatory mediators released from infected epithelial cells[246,247].

In vitro studies report conflicting findings, with some demonstrating potent cytokine production following SARS-CoV-2 exposure [178,239,240], while others report only modest responses [73,74,248]. In addition, macrophage activation has been reported to occur in the presence of virus-antibody complexes via Fc receptor engagement [181,249–252], and in response to recombinant spike protein[231,253–258].

To address these discrepancies, macrophage cytokine responses to SARS-CoV-2 exposure were characterised in this chapter, including exposure to replication-competent and replication-deficient virus, virus-antibody complexes, and recombinant spike protein.

In addition to cytokine secretion, macrophage inflammatory responses may involve activation of the inflammasome. Unlike many pro-inflammatory cytokines, which are regulated at the transcriptional level, IL-1β secretion requires inflammasome-dependent processing, representing a distinct pathway of macrophage activation[259]. Inflammasome activation has been implicated in SARS-CoV-2-induced inflammation, although the mechanisms and extent of its contribution remain incompletely defined[181,228,252,260]. In this study, IL-1β release was measured as an indicator of inflammasome-associated responses in macrophages following SARS-CoV-2 exposure.

Chapter hypothesises and aims

The role of AMs in COVID-19 remains incompletely understood. This chapter investigates how key macrophage functions, including viability, phagocytosis, antigen presentation, and cytokine production, are modulated following exposure to SARS-CoV-2.

Given that SARS-CoV-2 exhibits limited productive replication in macrophages, it was hypothesised that viral exposure would not impair core macrophage functions such as phagocytosis or antigen presentation. Instead, macrophages were expected to respond primarily through activation pathways, including the production of ROS and inflammatory cytokines. It was further hypothesised that macrophage cytokine responses would vary depending on viral variant and immune context.

To address these hypotheses, the following questions were investigated:

- Does SARS-CoV-2 exposure affect macrophage viability?
- Does SARS-CoV-2 exposure alter macrophage functional responses, including phagocytosis and antigen presentation?
- Does SARS-CoV-2 exposure induce cytokine production by macrophages?
- Are macrophage cytokine responses driven by direct viral sensing or by secondary mediators of infection?

5.2 Results

5.2.1 Macrophage viability and function post-SARS-CoV-2 Infection

Macrophages remain viable post-inoculation with SARS-CoV-2

Macrophage viability following exposure to SARS-CoV-2 was examined. At 24 h PI, macrophages inoculated with unopsonised virus were morphologically indistinguishable from unchallenged macrophages (Figure 5.1A). In contrast, macrophages inoculated with SARS-CoV-2 opsonised with infection-promoting antibodies displayed increased cellular granularity relative to unchallenged cells.

Macrophage viability was assessed using a viability dye and flow cytometry. At 24 h PI, macrophages remained fully viable and comparable to the unchallenged control (Figure 5.1B). Cell viability was also assessed using the CellTiter 96® AQueous One assay, which gave consistent results with the flow cytometry analysis (Figure 5.1C).

Macrophage ROS levels are elevated by antibody-mediated productive SARS-CoV-2 infection

ROS production is a common feature of macrophage activation and reflects intracellular stress or antimicrobial responses. In macrophages inoculated with unopsonised virus, ROS levels were elevated following exposure to VIC01, reaching levels comparable to the TBHP-treated positive control (Figure 5.1D). In contrast, macrophages exposed to the Delta or BA.5 variants exhibited ROS levels comparable to resting macrophages. When macrophages were exposed to the same variants opsonised with infection-promoting antibodies, ROS production increased, relative to unopsonised virus.

Taken together, these findings suggest that unopsonised VIC01 induces oxidative stress in macrophages despite being non-replicating, whereas the Delta and BA.5 variants induce oxidative stress only when replication occurs.

Macrophage phagocytic function is not affected by after inoculation with SARS-CoV-2

A key effector function of macrophages is the phagocytosis of cellular debris and pathogens. Previous reports have suggested that macrophage phagocytic capacity may be impaired following exposure to SARS-CoV-2 [239]. To assess this, the ability of macrophages to internalise Zymosan A-AF488 particles was measured 24 h after inoculation with SARS-CoV-2. Flow cytometric analysis demonstrated that macrophages exposed to SARS-CoV-2 variants exhibited

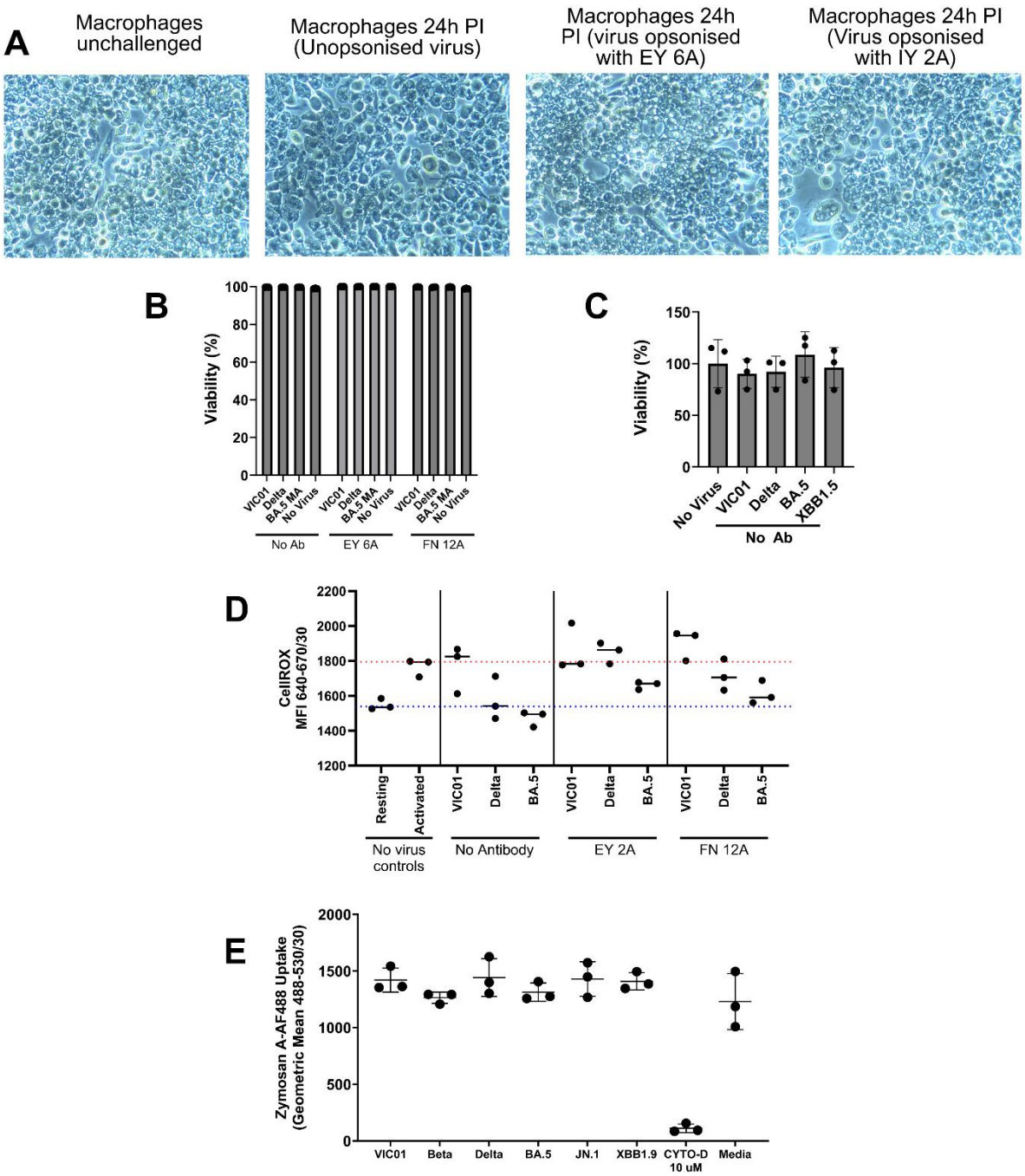

Figure 5.1. Macrophage viability and function following SARS-CoV-2 exposure. (A) Representative microscopy images of macrophages following SARS-CoV-2 infection. iPSC-macrophages (KOLF2.1S) were either unchallenged, inoculated with unopsonised SARS-CoV-2 or SARS-CoV-2 opsonised with infection-promoting antibodies (EY 6A or IY 2A), at an MOI of 3. Images were acquired 24 h PI. **(B)** Viability of macrophages following inoculation with SARS-CoV-2. iPSC-macrophages (KOLF2.1S) were either unchallenged, inoculated with SARS-CoV-2 variants at an MOI of 3, or variants opsonised with infection-promoting antibodies (EY 6A or IY 2A). Cell viability was assessed using a fixable viability dye and measured by flow cytometry. Viability was expressed relative to unchallenged control. **(C)** Viability of macrophages 24h PI, as in (B), measured by CellTiter 96® AQueous One Solution Cell Proliferation Assay reagent. **(D)** Oxidative stress in macrophages following SARS-CoV-2 inoculation. Oxidative stress in cells inoculated as in (B) was measured by CellROX staining and flow cytometry Macrophages were activated with TBHP as a positive control. **(E)** Phagocytic capacity of macrophages following SARS-CoV-2 inoculation. Macrophages (SFC840-03-03) were inoculated with SARS-CoV-2 variants at an MOI of 3 or treated with cytochalasin D (10 μM) to inhibit phagocytosis. Cells were incubated for 24 h before exposure to Zymosan A-AF488 particles for 2 h. Particle uptake was quantified by flow cytometry. Data shown are from one representative experiment (three technical replicates; error bars represent SD).

no significant difference in phagocytic capacity compared with unexposed macrophages (Figure 5.1E).

5.2.2 Development of a Macrophage/ T cell co-culture assay to measure antigen-specific T cell activation

Assay Set up

To measure antigen presentation, I developed a macrophage-T cell co-culture assay combining iPSC-derived macrophages and patient-derived $CD4^+$ and $CD8^+$ T cell clones. Multiple iPSC lines were HLA-typed and the KOLF2.1S line was selected for compatibility with the T cell clones. Macrophages are hereafter referred to as naïve, virus-inoculated, or peptide-loaded depending on stimulation.

Macrophages were inoculated with SARS-CoV-2 for 2 h, incubated overnight to allow for antigen processing, then co-cultured with T cells (1:1 or 1:2 T cell: macrophage) for 5 h in the presence of brefeldin A and monensin, to allow accumulation of intracellular cytokines. Intracellular IFNγ and TNFα in T cells were analysed by flow cytometry (experimental timeline in Figure 5.2A, gating strategy in Figure 5.2B).

Initial tests with NP-specific $CD8^+$ T cells

In an initial experiment (Figure 5.2C) no antigen-specific activation of NP-specific $CD8^+$ T cells by virus-inoculated macrophages (MOI 2) was detected, but artificially stimulated T cells confirmed the intracellular cytokine detection assay was functional. However, this experiment lacked controls to determine whether the absence of activation reflected insufficient antigen availability, ineffective antigen presentation by macrophages, or limited responsiveness of the T cell clone.

Peptide-loaded macrophages confirm antigen presentation competence

A subsequent experiment used a higher MOI (20) and included peptide-loaded macrophages as a positive control (Figure 5.2D). Peptide-loaded macrophages activated a small proportion of $CD8^+$ T cells (10.8%), demonstrating that iPSC-derived macrophages can present NP antigen under these assay conditions. However, since the level of activation was low, it remained a possibility that the iPSC-derived macrophages are poor antigen-presenting cells, the NP-specific CD8+ T cell clone has limited responsiveness, or that the antigen availability in the virus-inoculated macrophages was still too low.

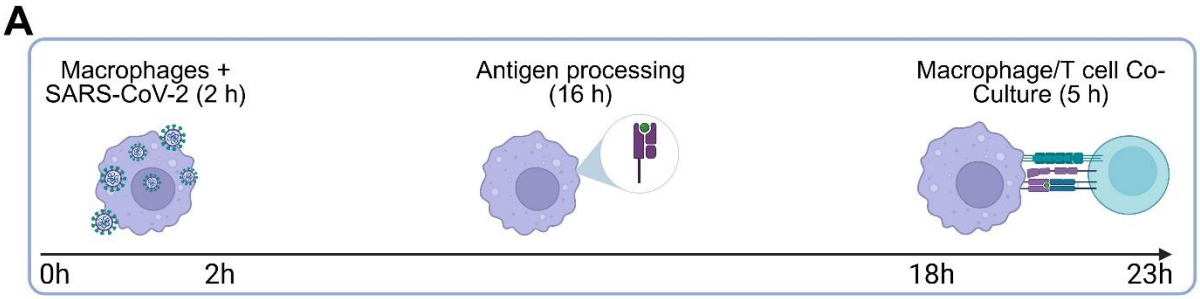
A
Macrophages + SARS-CoV-2 (2 h)
Antigen processing (16 h)
Macrophage/T cell Co-Culture (5 h)
0h
2h
18h
23h

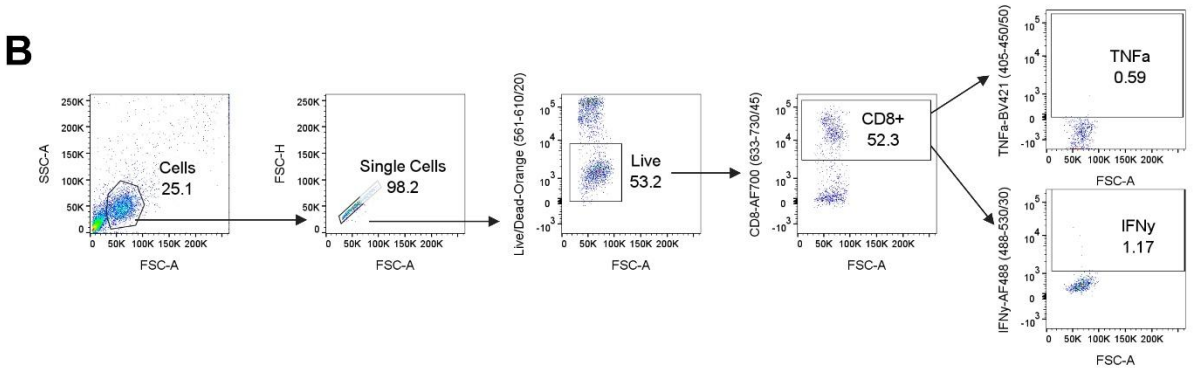
B
SSC-A
Cells
25.1
FSC-A
FSC-H
Single Cells
98.2
Live/Dead-Orange (561-610/20)
Live
53.2
CD8-AF700 (633-730/45)
CD8+
52.3
TNFa-BV421 (405-450/50)
TNFa
0.59
IFNy-AF488 (488-530/30)
IFNy
1.17

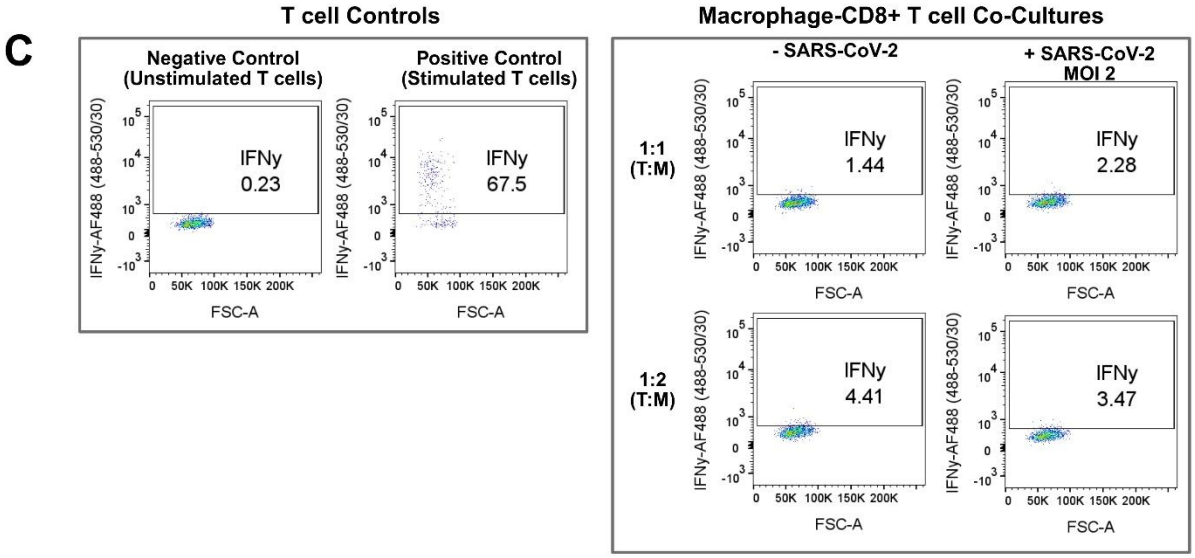
C
T cell Controls
Macrophage-CD8+ T cell Co-Cultures
Negative Control (Unstimulated T cells)
Positive Control (Stimulated T cells)
IFNy-AF488 (488-530/30)
IFNy
0.23
IFNy
67.5
FSC-A
- SARS-CoV-2
+ SARS-CoV-2 MOI 2
1:1 (T:M)
1:2 (T:M)
IFNy
1.44
IFNy
2.28
IFNy
4.41
IFNy
3.47

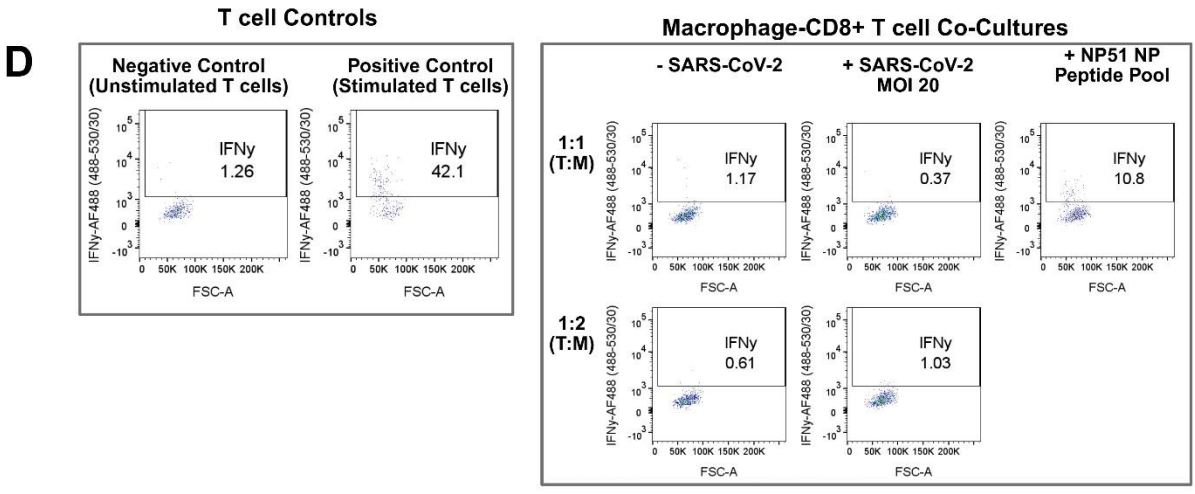
D
T cell Controls
Macrophage-CD8+ T cell Co-Cultures
Negative Control (Unstimulated T cells)
Positive Control (Stimulated T cells)
IFNy-AF488 (488-530/30)
IFNy
1.26
IFNy
42.1
FSC-A
- SARS-CoV-2
+ SARS-CoV-2 MOI 20
+ NP51 NP Peptide Pool
1:1 (T:M)
1:2 (T:M)
IFNy
1.17
IFNy
0.37
IFNy
10.8
IFNy
0.61
IFNy
1.03

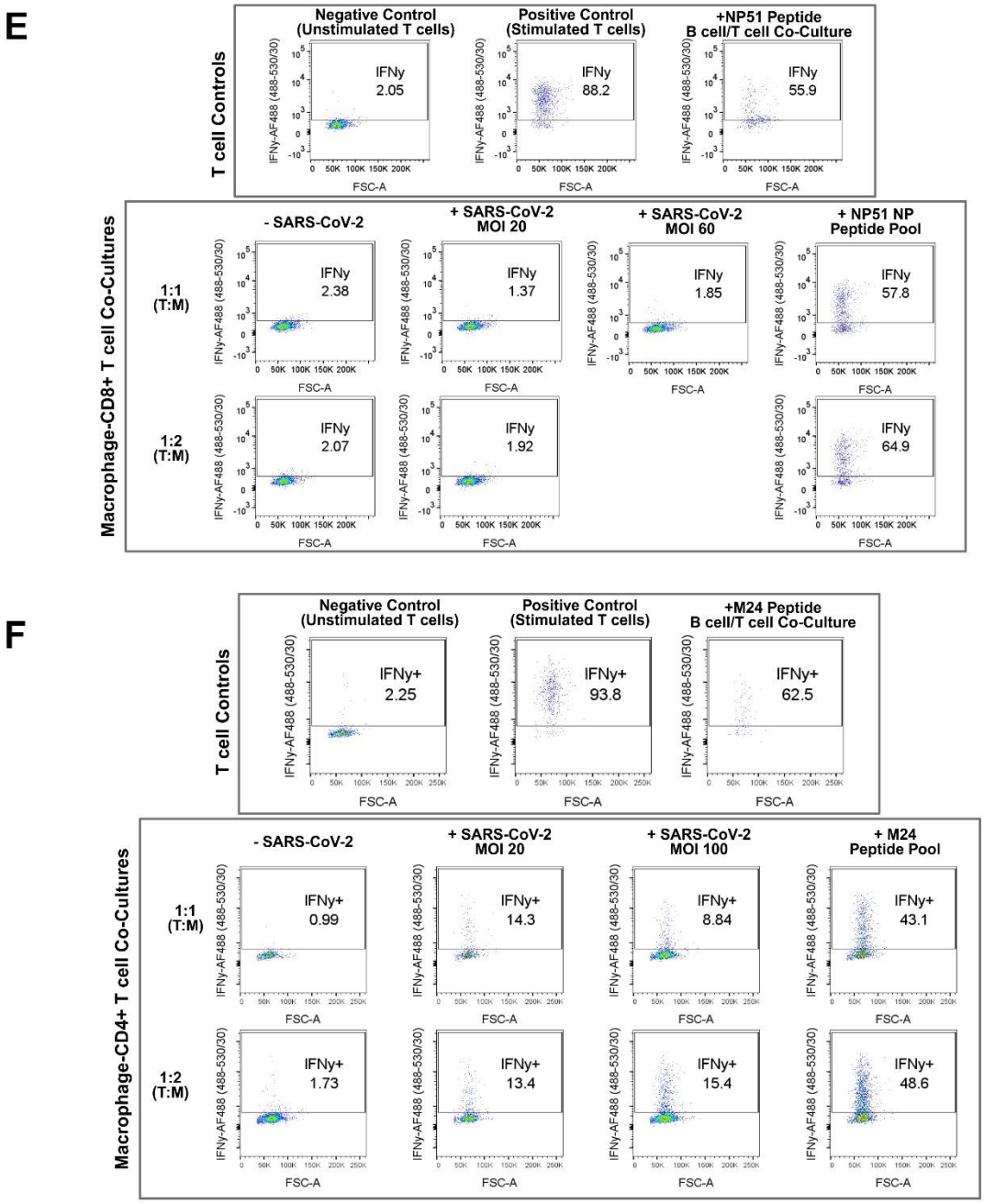

Figure 5.2. Development of a macrophage-T cell co-culture assay to measure antigen-specific T cell activation. (A) Schematic of the macrophage-T cell co-culture assay. iPSC-derived macrophages (KOLF2.1S) were left unchallenged or inoculated with SARS-CoV-2 for 2 h at the indicated MOIs, incubated overnight to allow antigen processing, and then co-cultured with antigen-specific T cells at 1:1 or 1:2 T cell-to-macrophage ratios for 5 h at 37 °C in the presence of brefeldin A and monensin. Positive cytokine controls, MHC-matched peptide controls, and MHC-matched B cell co-cultures were included as indicated. Intracellular IFNγ and TNFα were assessed by flow cytometry; TNFα responses mirrored IFNγ and are not shown. **(B)** Flow cytometry gating strategy for intracellular cytokine staining following macrophage-CD8$^+$ T cell co-culture. **(C)** Intracellular IFNγ production in macrophage-T cell co-culture using HLA-A11:01-restricted nucleoprotein-specific CD8$^+$ T cells (clone 1502-A11-NP51-M6) following macrophage inoculation at an MOI of 2, without peptide or B cell controls. **(D)** As in (C), with macrophage inoculation at an MOI of 20 and inclusion of an NP51 peptide control. **(E)** Intracellular IFNγ production using HLA-A11:01-restricted nucleoprotein-specific CD8$^+$ T cells (clone 1278-A11-NP51-M6), following macrophage inoculation at MOIs of 20 and 60, with MHC-matched B cell (RTH08-1278 BCL) and NP51 peptide controls. **(F)** Intracellular IFNγ production using HLA-DRB101:01-restricted matrix-specific CD4$^+$ T cells (clone 1525-DRB101:01-M24), following macrophage inoculation at MOIs of 20 and 100, with MHC-matched B cell (RTH08-1525 BCL) and M24 peptide controls.

No CD8$^+$ T cell activation by virus-inoculated macrophages despite competent presentation controls

A third experiment used a different NP-specific CD8$^+$ clone and higher MOIs of 20 and 60 (Figure 5.2E). An MHC-matched B cell-T cell co-culture was included as an additional positive control for efficient antigen presentation. This CD8$^+$ T cell clone exhibited substantially greater responsiveness, with IFNγ production reaching 88.2% following artificial stimulation, compared with 42.1% with the previous clone. Peptide-loaded macrophages induced robust CD8$^+$ T cell activation (57.8%), comparable to that observed in peptide-loaded B cell co-cultures (55.9%). However, virus-inoculated macrophages failed to induce antigen-specific CD8$^+$ T cell activation, even at MOI 60. These data indicate a lack of detectable antigen presentation to CD8$^+$ T cells by virus-inoculated macrophages under the tested conditions.

Macrophages activate SARS-CoV-2 specific CD4$^+$ T cells

Subsequent experiments focused on CD4$^+$ T cells. Membrane-specific CD4$^+$ T cells were strongly activated by peptide-loaded macrophages and MHC-matched B cell controls (Figure 5 .2F). Virus-inoculated macrophages also induced antigen-specific CD4$^+$ T cell activation. Increasing the MOI from 20 to 100 did not further enhance CD4$^+$ T cell activation, indicating that antigen availability was sufficient in these experiments.

Together, these data establish a macrophage-T cell co-culture assay using iPSC-derived macrophages, with appropriate controls to enable reliable assessment of antigen-specific T cell activation.

5.2.3 SARS-CoV-2-inoculated macrophages present SARS-CoV-2 antigens to CD4$^+$, but not to CD8$^+$ T cells

SARS-CoV-2 inoculated macrophages activate CD4+, but not CD8+ T cells

The macrophage-T cell co-culture assay was subsequently used to investigate the capacity of SARS-CoV-2-inoculated macrophages to present antigen to CD4$^+$ and CD8$^+$ T cells, with IFNγ and TNFα detection as readouts (Figure 5.3A). Membrane-specific CD4$^+$ T cells and spike-specific CD8$^+$ T cells co-cultured with naïve macrophages did not produce IFNγ or TNFα (Figure 5.3B). In contrast, both CD4$^+$ and CD8$^+$ T cells were robustly activated in co-cultures with peptide-loaded macrophages, CD4$^+$ and CD8$^+$ T cell activation reached 86.1% and 86.6% IFNγ$^+$ cells, respectively. Membrane-specific CD4$^+$ T cells showed antigen-specific IFNγ and TNFα production following co-culture with virus-exposed macrophages (IFNγ$^+$ 41.4%; TNFα$^+$ 62.2%), whereas spike-specific CD8$^+$ T cells did not respond to virus-exposed macrophages (Figure 5.3B). These data indicate preferential presentation on MHC class II over MHC class I.

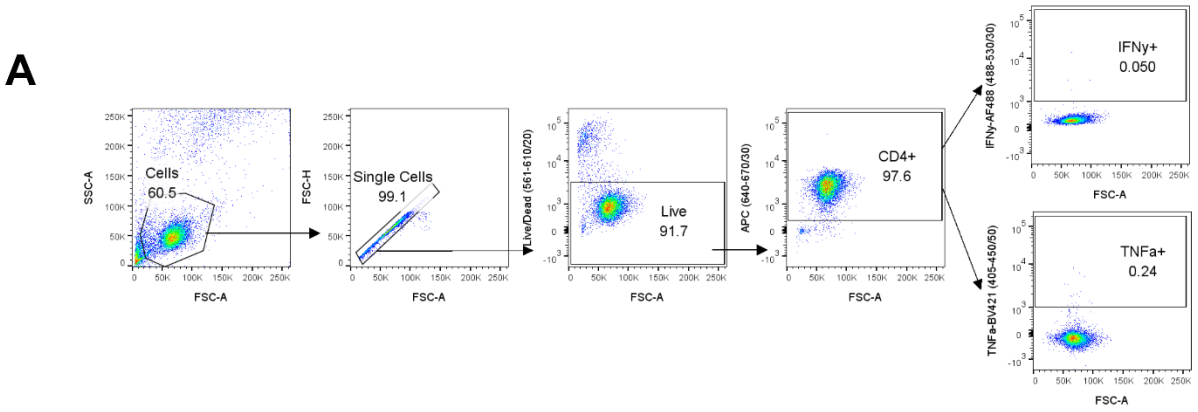
A
Cells
60.5
Single Cells
99.1
Live
91.7
CD4+
97.6
IFNγ+
0.050
TNFa+
0.24
SSC-A
FSC-A
FSC-H
Live/Dead (561-610/20)
APC (640-670/30)
IFNγ-AF488 (488-530/30)
TNFα-BV421 (405-450/50)

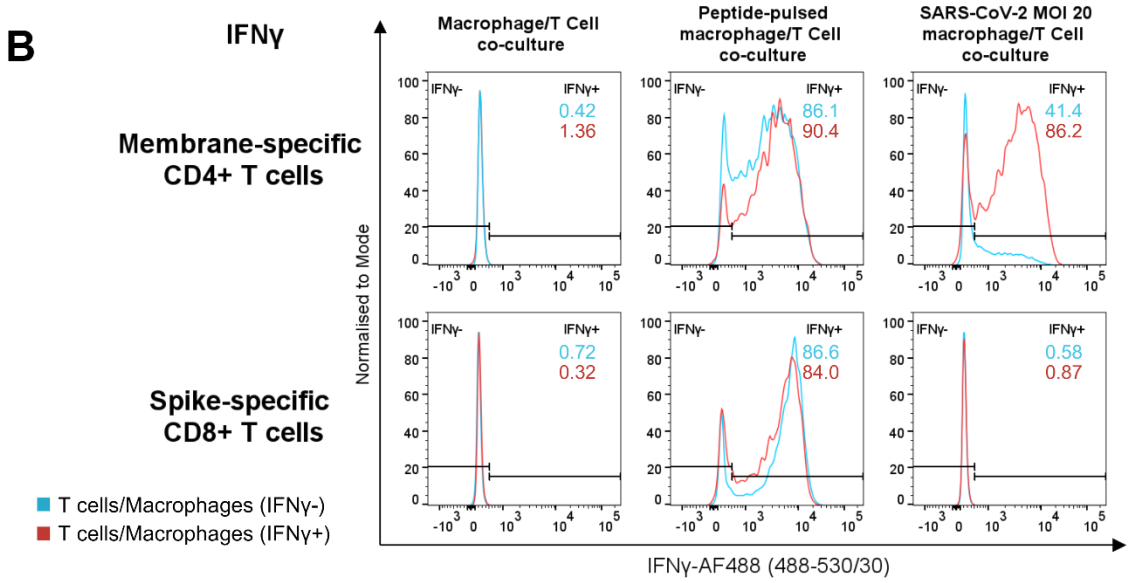
B
IFNγ
Macrophage/T Cell co-culture
Peptide-pulsed macrophage/T Cell co-culture
SARS-CoV-2 MOI 20 macrophage/T Cell co-culture
Membrane-specific CD4+ T cells
Spike-specific CD8+ T cells
IFNγ-
IFNγ+
0.42
1.36
86.1
90.4
41.4
86.2
0.72
0.32
86.6
84.0
0.58
0.87
Normalised to Mode
IFNγ-AF488 (488-530/30)
T cells/Macrophages (IFNγ-)
T cells/Macrophages (IFNγ+)

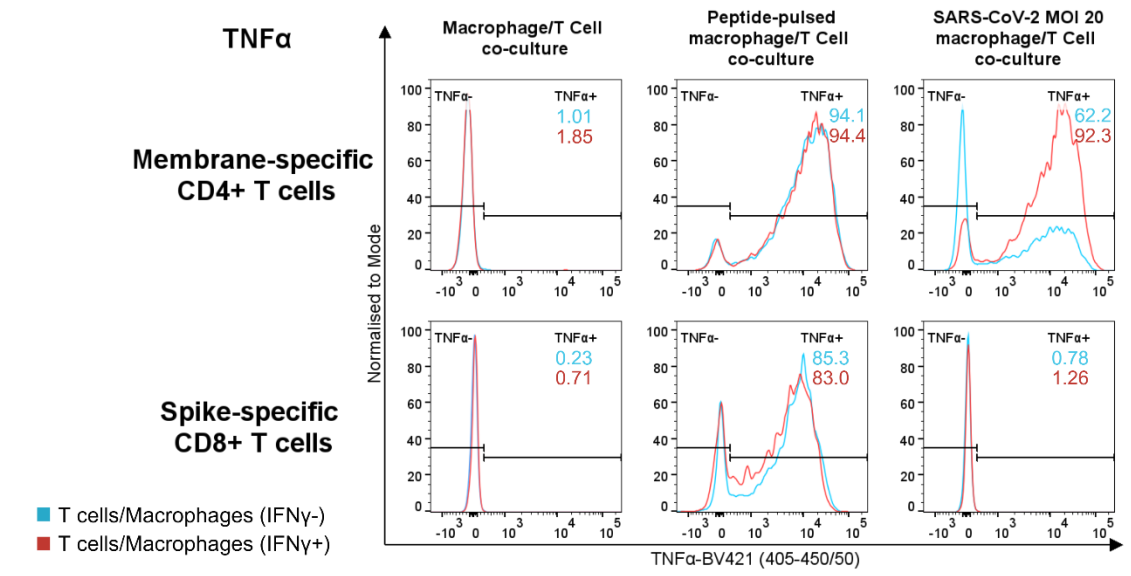
TNFα
Macrophage/T Cell co-culture
Peptide-pulsed macrophage/T Cell co-culture
SARS-CoV-2 MOI 20 macrophage/T Cell co-culture
Membrane-specific CD4+ T cells
Spike-specific CD8+ T cells
TNFα-
TNFα+
1.01
1.85
94.1
94.4
62.2
92.3
0.23
0.71
85.3
83.0
0.78
1.26
Normalised to Mode
TNFα-BV421 (405-450/50)
T cells/Macrophages (IFNγ-)
T cells/Macrophages (IFNγ+)

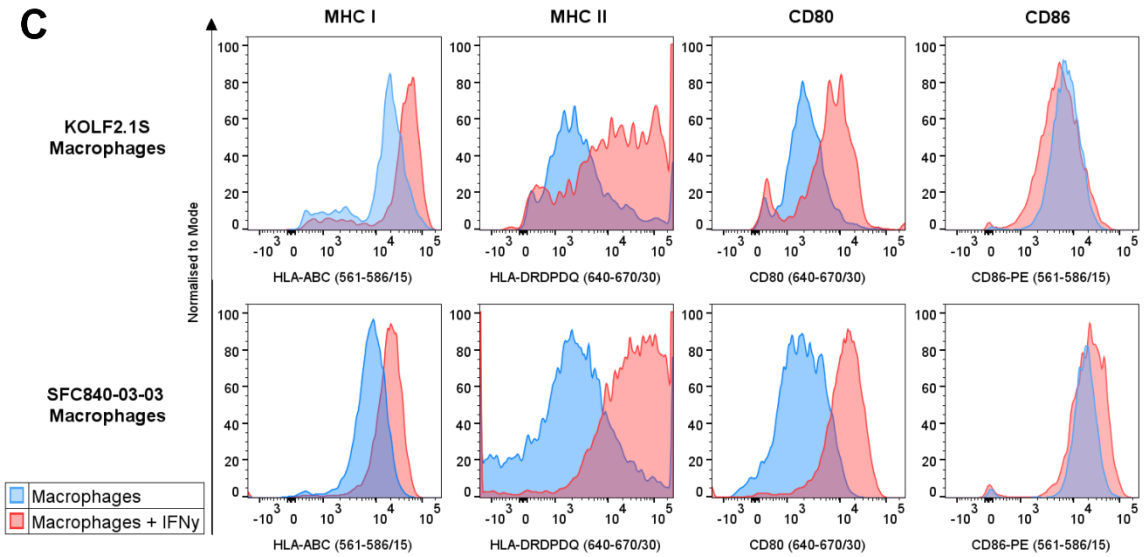

Figure 5.3. Macrophages present SARS-CoV-2 antigens to CD4⁺ but not CD8⁺ T cells, in the absence of viral replication. (A) Flow cytometry gating strategy for intracellular cytokine staining following macrophage–T cell co-culture. **(B)** Intracellular IFNγ and TNFα release from CD4+ T cells co-cultured with SARS-CoV-2 abortively infected macrophages. iPSC-derived macrophages (KOLF2.1) were stimulated with or without IFNγ (20 ng/ml) for 24 h, then either left unchallenged or inoculated with SARS-CoV-2 at an MOI of 20 and incubated overnight to allow antigen processing. Macrophages were co-cultured with membrane-specific CD4⁺ T cells or spike-specific CD8⁺ T cells at a 1:1 ratio for 5 h at 37 °C in the presence of brefeldin A, monensin, and anti-CD107a. Positive peptide control co-cultures were performed using MHC-matched spike (S173 LTD) or membrane (M24) peptides, and positive cytokine control T cells were stimulated with cell stimulation cocktail. Intracellular IFNγ and TNFα production was assessed by flow cytometry following staining with a fixable viability dye and antibodies against CD4, IFNγ, and TNFα. **(C)** MHC and co-receptor expression on macrophages. iPSC-derived macrophages (KOLF2.1) were stimulated with or without IFNγ (20 ng/ml) for 24 h, and surface expression of MHC I (HLA-ABC), MHC II (HLA-DR/DP/DQ), CD80, and CD86 was assessed by flow cytometry.

Macrophage stimulation with IFNγ increases antigen-specific CD4+ T cell activation

During viral infection, macrophages are exposed to IFNγ, which is known to upregulate MHC expression on antigen-presenting cells[261]. To determine whether increased MHC expression could enhance antigen presentation and promote CD8⁺ T cell activation, macrophages were pre-treated with IFNγ prior to co-culture with T cells (Figure 5.3B, denoted by red lines).

IFNγ pre-treatment did not increase T cell activation in peptide-loaded co-cultures, consistent with near-maximal activation under these conditions. In virus-inoculated co-cultures, IFNγ pre-treatment significantly increased CD4⁺ T cell activation, with 1.5-fold and 2-fold increases of IFNγ and TNFα production, respectively. However, IFNγ pre-treatment of macrophages did not enable antigen-specific CD8⁺ activation.

iPSC-derived macrophages express MHC and co-stimulatory molecules

To further assess antigen presentation capacity of iPSC-derived macrophages, surface expression of MHC class I and II and the co-stimulatory molecules CD80 and CD86 was analysed by flow cytometry (Figure 5.3C). iPSC-derived macrophages exhibited high basal expression of MHC class I, which was modestly increased following IFNγ stimulation. In contrast, MHC class II and CD80 were expressed at baseline but were significantly upregulated in response to IFNγ. CD86 was strongly expressed at baseline and was not further enhanced by IFNγ stimulation. Taken together with the macrophage-T cell co-culture data, these expression profiles support the use of iPSC-derived macrophages as a competent antigen-presenting cell model.

5.2.4 Macrophages produce cytokines in response to SARS-CoV-2

Macrophages release IL-6 in response to SARS-CoV-2 infected epithelial cells

I aimed to establish if macrophages release cytokines in response to SARS-CoV-2-infected epithelial cell conditioned media, and whether this response differs between viral variants. IL-6 was selected as a representative cytokine, as it is a major pro-inflammatory mediator released by macrophages in response to infection and tissue damage[16].

Macrophage supernatants were assayed for IL-6 release following exposure to conditioned media from SARS-CoV-2-infected epithelial cells. IL-6 was released by macrophages exposed to conditioned media from infected VET cells but not from uninfected controls (Figure 5.4A). Conditioned media from VIC01-infected cells induced the strongest IL-6 response, comparable to direct Poly(I:C) stimulation. Conditioned media from Delta and BA.5 infections induced weaker IL-6 responses. These findings were reproduced using Calu-3 cells, a human lung epithelial cell line. Although there was some variability in the magnitude of IL-6 release induced by the conditioned media derived from the two cell lines; VIC01 infection consistently elicited a robust macrophage IL-6 response, whereas Delta, BA.5, and XBB1.9 induced weaker responses.

Macrophages release cytokines in response to filtered SARS-CoV-2 virus

I sought to determine whether macrophage cytokine production was driven by detection of soluble mediators released from infected epithelial cells, or by direct sensing of SARS-CoV-2 particles themselves. To exclude these soluble mediators, SARS-CoV-2 stocks were filtered using a 100 kDa molecular weight cut-off ultrafiltration device, thereby removing molecules <100 kDa while retaining intact virions and spike protein (spike monomer ~180 kDa).

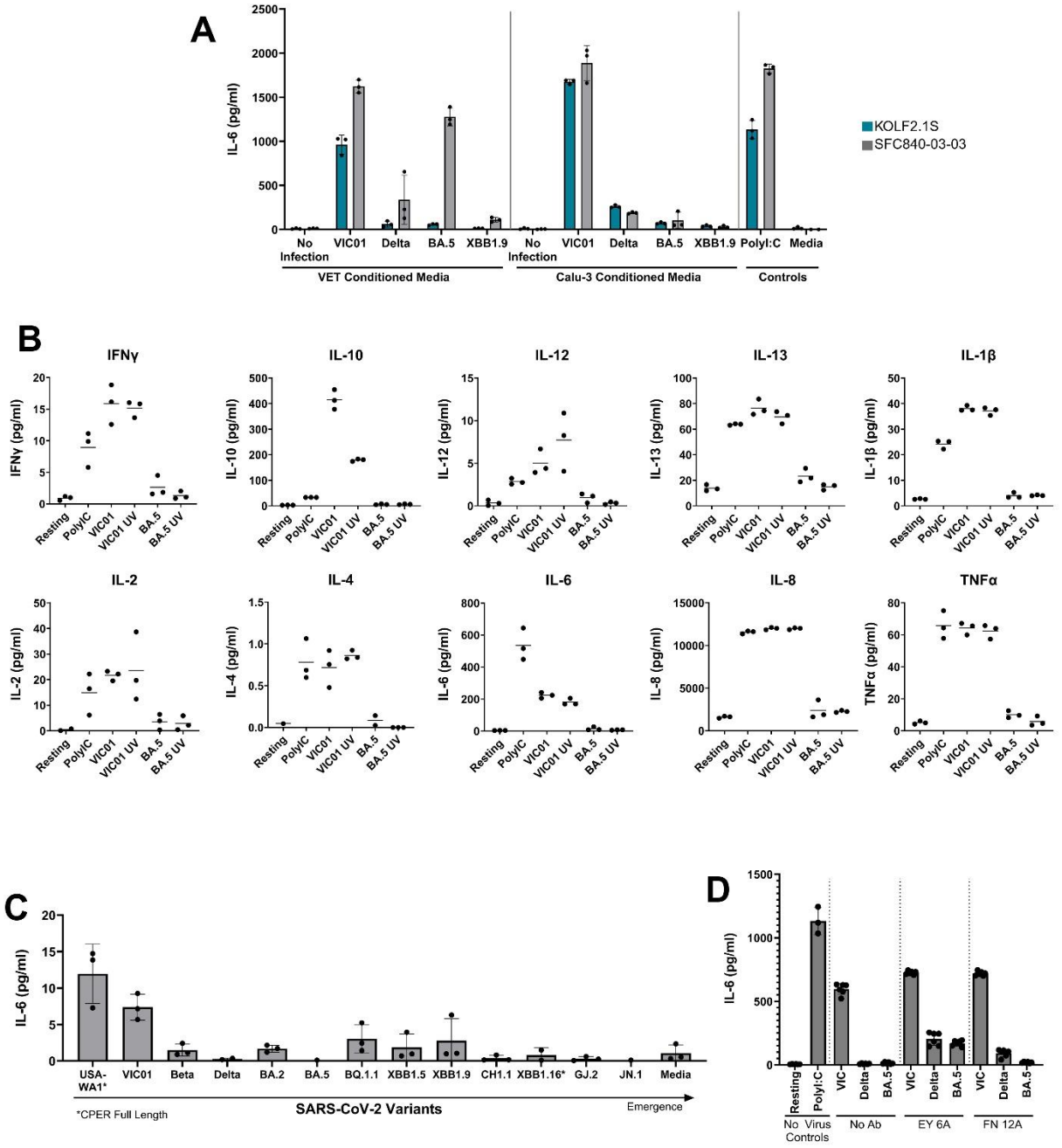

Figure 5.4. Macrophage cytokine responses to SARS-CoV-2 exposure (A) Macrophage IL-6 release in response to conditioned media from SARS-CoV-2-infected Vero E6/TMPRSS2 (VET) cells or Calu-3 cells. VET cells were inoculated with SARS-CoV-2 variants (MOI 1), and conditioned media collected 24 h post-inoculation was applied to iPSC-derived macrophages (donors: SFC840-03-03 and KOLF2.1S). IL-6 levels in macrophage supernatants were quantified by ELISA, 24 h post-exposure. Poly(I:C)-stimulated cells served as a positive control. **(B)** Macrophage cytokine release following exposure to filtered SARS-CoV-2. Macrophages (KOLF2.1S) were inoculated with SARS-CoV-2 VIC01 or BA.5, or stimulated with Poly(I:C) (1 μg/ml). Viral stocks were filtered (100 kDa) and left untreated or UV-C treated to render particles replication deficient. Cytokines in macrophage supernatants were quantified by MSD. **(D)** Macrophage IL-6 release following inoculation with SARS-CoV-2 variants (MOI 3), quantified 24 h PI by ELISA. *Denotes virus generated by CPER reverse genetics. **(D)** Macrophage IL-6 release in response to SARS-CoV-2 exposure or productive infection. Macrophages (SFC840-03-03) were inoculated with SARS-CoV-2 either unopsonised or opsonised by infection-promoting antibodies (EY 6A or FN 12A). IL-6 levels in macrophage supernatants were quantified by ELISA, 24 h post-exposure. Data shown are from one representative experiment (three technical replicates; error bars represent SD).

Macrophages were then inoculated with filtered SARS-CoV-2 VIC01 or BA.5, using either replication-competent virus or UV-C-treated replication-deficient particles. Cytokine release was quantified by multiplex MSD analysis.

Consistent with earlier observations, filtered VIC01 induced robust pro-inflammatory cytokine responses in macrophages, including IL-13, IL-1β, IL-8, and TNFα, comparable to the Poly(I:C) positive control (Figure 5.4B). BA.5 induced minimal cytokine responses, comparable to naïve macrophages. With the exception of IL-10, cytokine production did not differ between macrophages exposed to replication-competent versus UV-inactivated virus.

Early SARS-CoV-2 variants induce a strong cytokine response, whilst later variants do not

The observation that SARS-CoV-2 VIC01 induced robust cytokine responses in macrophages, whereas later variants did not, generated the hypothesis that early SARS-CoV-2 variants were more inflammatory, and that subsequent variants may have adapted to elicit reduced macrophage activation. To investigate this, macrophages were inoculated with a panel of 13 SARS-CoV-2 variants (all virus stocks filtered through 100kDa cut-off). Early isolates, USA-WA1 and VIC01, induced highest IL-6 release (Figure 5.4C). In contrast, variants emerging after VIC01 elicited low or undetectable IL-6 production, comparable to naïve macrophages.

Antibody-mediated infection modestly enhances macrophage cytokine responses

To examine how macrophage inflammatory responses differed between SARS-CoV-2 exposure and antibody-mediated infection, IL-6 release was measured in macrophages inoculated with SARS-CoV-2 variants either unopsonised or opsonised with infection-promoting antibodies (EY6A or FN12A). Opsonisation modestly increased IL-6 production across all three variants. However, the highest cytokine response was consistently observed following exposure to the VIC01 strain, which was only marginally enhanced under conditions of antibody-mediated infection (Figure 5.4D).

5.2.5 Determinants of the macrophage cytokine response to SARS-CoV-2

Variant-specific cytokine responses in macrophages are not driven by spike protein alone

To determine whether the IL-6 responses induced early variants were attributable to the spike protein, macrophages were stimulated with a panel of recombinant HexaPro spike proteins derived from multiple SARS-CoV-2 variants. Initial results contradicted findings obtained using

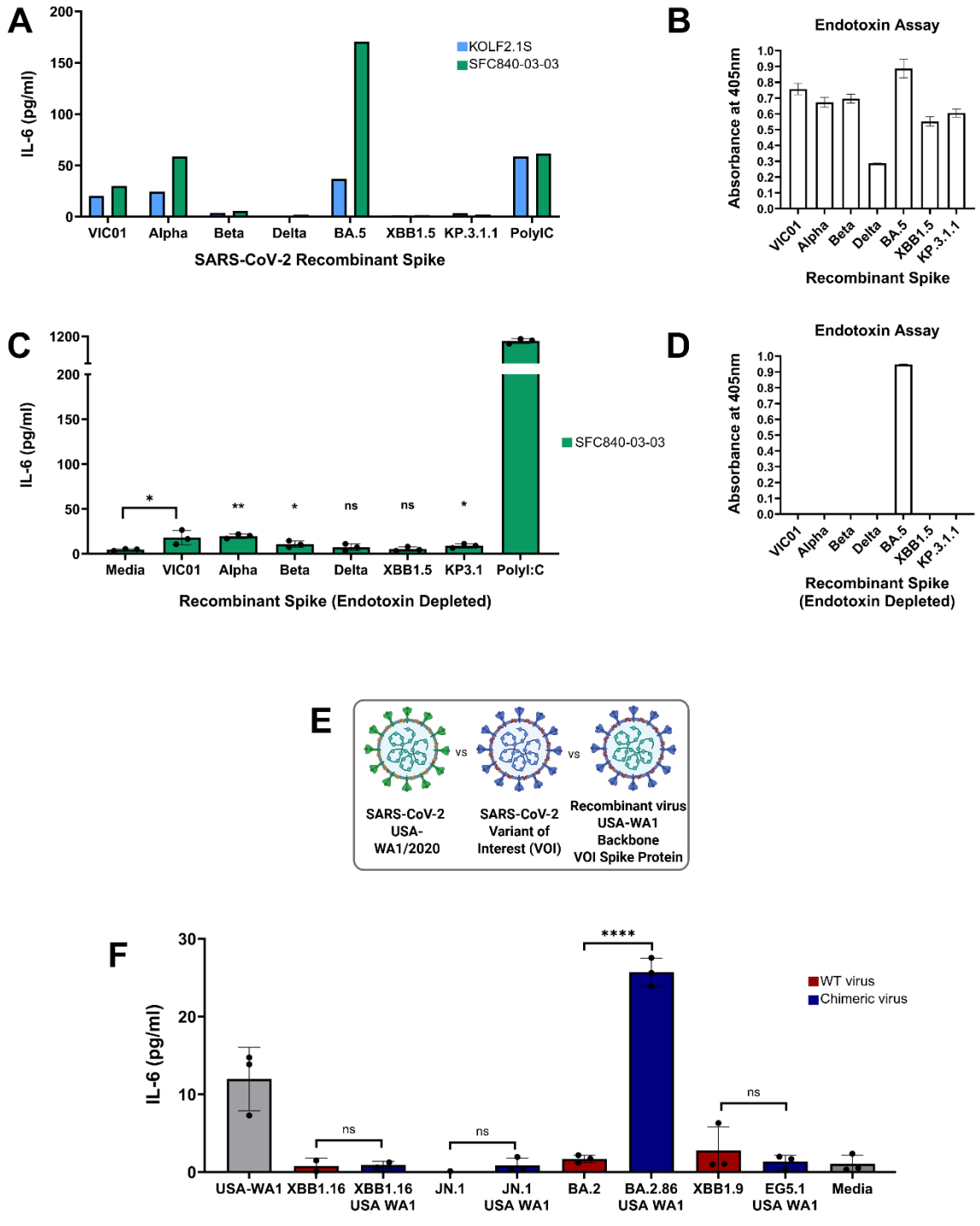

Figure 5.5 Determinants of the macrophage cytokine response to SARS-CoV-2. (A) Macrophage IL-6 release following stimulation with recombinant spike protein. iPSC-derived macrophages (Donors: KOLF2.1S or SFC840-03-03) were stimulated with recombinant spike protein (10 µg/ml) or Poly(I:C). IL-6 release was quantified by ELISA at 24h post-exposure. **(B)** Endotoxin levels in recombinant spike preparations used in (A), measured using a chromogenic endotoxin assay (405 nm). **(C)** Macrophage (SFC840-03-03) IL-6 release following stimulation with endotoxin-depleted recombinant spike protein, quantified as in (A). **(D)** Endotoxin levels in endotoxin-depleted recombinant spike preparations, used in (C) measured as in (B). **(E)** Schematic depicting wild-type and chimeric SARS-CoV-2 viruses used in (F). **(F)** Macrophage IL-6 release following inoculation with wild-type and chimeric SARS-CoV-2 viruses. iPSC-derived macrophages (SFC840-03-03) were inoculated with USA-WA1, chimeric viruses containing a USA-WA1 backbone and variant-of-interest (VOI) spike, or closely matched VOI wild-type viruses (MOI 3). IL-6 levels were quantified 24 h PI by ELISA. Data shown are from one representative experiment (three technical replicates; error bars represent SD).

live virus: recombinant BA.5 spike induced a strong IL-6 response, whereas VIC01 spike induced little or no response (Figure 5.5A).

Macrophage cytokine responses elicited by recombinant proteins have previously been reported to be confounded by endotoxin contamination[262]. I therefore measured endotoxin levels and all recombinant spike proteins exceeded the accepted endotoxin limit for in vitro macrophage assays (0.01 EU/mL; where one endotoxin unit (EU) corresponds to approximately 0.1 ng of endotoxin). Endotoxin concentrations were too high to be interpolated; however the absorbance values closely correlated with induced-IL-6 responses, with BA.5 showing the highest absorbance and strongest cytokine induction, and Delta, XBB1.5, and KP3.1.1 showing the lowest (Figure 5.5B). This strong correlation indicates that endotoxin contamination, rather than spike protein sequence, was responsible for the inflammatory responses observed in this assay. Since the recombinant proteins were expressed in an endotoxin-free system, the endotoxin contamination is likely to have been introduced during the purification process, potentially through the chromatography column.

Recombinant spike proteins were depleted of endotoxin (Figure 5.5D). BA.5 spike remained contaminated and was excluded. Endotoxin-depleted spike induced low-level IL-6 release, comparable to media control (Figure 5.5C). This data indicates that the spike protein alone does not account for the strong IL-6 responses observed following inoculation with SARS-CoV-2 virus, suggesting that other viral components are responsible.

Dissection of Spike and Genomic Contributions to SARS-CoV-2-Induced Macrophage IL-6 Response

To determine whether macrophage IL-6 responses were driven by the SARS-CoV-2 spike protein or by non-spike genomic elements, chimeric viruses were employed. The early SARS-CoV-2 isolate USA-WA1/2020, which was shown to induce a strong inflammatory response in macrophages, was used as a reference strain. This was compared to the cytokine responses induced by omicron variants, shown to induce minimal macrophage inflammation.

To distinguish between spike and backbone-dependent effects, chimeric viruses were generated with the USA-WA1 backbone expressing Omicron spikes (XBB1.16-USA/WA1, JN.1-USA/WA1, BA.2.86-USA/WA1, EG5.1-USA/WA1) and compared to closely-matched Omicron wild-type variants (XBB1.15, JN.1, BA.2, XBB1.9) (Figure 5.5E). Under this experimental design, if the USA-WA1 backbone were responsible for macrophage inflammation, all chimeric viruses would be expected to induce an IL-6 response despite possessing Omicron spike proteins. Conversely, if

the spike protein were the primary determinant, chimeric viruses expressing Omicron spikes would be expected to induce little or no IL-6, similar to Omicron wild-type viruses.

USA-WA1 wild-type induced strong IL-6 release (Figure 5.5F). Three of the four USA-WA1 backbone chimeras induced low to no IL-6, which would suggest that swapping USA-WA1 spike for Omicron spikes largely abrogated the inflammatory response. However, the BA.2.86-USA/WA1 chimera induced a markedly elevated IL-6 response, with 2-fold higher than USA-WA1 wild-type. This unexpected result indicates that factors other than viral genetic composition contribute to macrophage activation. Host-derived contaminants or DAMPs present in viral preparations are possible contributors to the observed differences.

5.3 Discussion

This chapter investigated how macrophage functional responses are modulated following exposure to SARS-CoV-2. Macrophages remained viable and retained core effector functions, including phagocytosis, following viral exposure, indicating that SARS-CoV-2 does not impair fundamental macrophage function under these conditions. However, macrophage activation was evident through the induction of reactive oxygen species and cytokine production by the ancestral strain, but not later variants. Notably, macrophages were able to present antigen to $CD4^+$ but not $CD8^+$ T cells, likely reflecting the processing of SARS-CoV-2 as an exogenous antigen.

Macrophage viability following SARS-CoV-2 exposure

Severe COVID-19 is associated with depletion of AMs, which is likely to limit viral clearance and resolution of inflammation, thereby contributing to disease pathology. The results of this study suggest that macrophage loss is unlikely to be driven by direct sensing of SARS-CoV-2, as macrophages remained fully viable following viral exposure under the conditions tested. However, it is important to note that this study may underestimate macrophage death due to technical limitations, including potential loss of dead cells during flow cytometry analysis. Viability was assessed at 24 h post-inoculation, because pyroptosis is typically a rapid response following inflammasome activation[263]. Nevertheless, delayed effects on macrophage viability cannot be excluded, particularly under conditions of antibody-mediated infection.

These findings suggest that macrophage depletion observed in vivo may instead be driven by factors within the lung microenvironment. One potential mechanism is reduced granulocyte-macrophage colony-stimulating factor (GM-CSF) following loss of GM-CSF-producing alveolar

type II (AT2) cells, a primary target of SARS-CoV-2 infection[54]. This hypothesis could be investigated using co-culture systems combining iPSC-derived AT2 cells and macrophages, with assessment of macrophage viability over extended timepoints.

Alternatively, macrophage loss in severe COVID-19 may result from inflammatory cell death driven by the hyperinflammatory lung environment. Several studies have reported that SARS-CoV-2 exposure induces inflammatory cell death in macrophages [178,228,229]. However, these studies primarily utilised monocyte-derived macrophages, which are more pro-inflammatory and short-lived than tissue-resident AMs and may therefore be more susceptible to pyroptosis. In addition, viral stocks used in these studies were often derived from infected cell supernatants, which will contain inflammatory mediators capable of indirectly driving macrophage activation and cell death.

Taken together, these findings indicate that the mechanisms underlying AM depletion in severe COVID-19 remain incompletely understood. The data presented here suggest that pyroptosis induced by direct viral sensing is unlikely to be the primary driver of macrophage loss. Instead, factors within the inflammatory lung environment represent a more plausible explanation, although further investigation is required to define these mechanisms.

Macrophage ROS production and activation

Reactive oxygen species (ROS) production is a key feature of macrophage activation and contributes to antimicrobial defence but can also drive tissue damage when dysregulated. In this study, ROS production was increased in macrophages following exposure to the ancestral SARS-CoV-2 strain (VIC01), but not Delta or BA.5 variants under unopsonised conditions, indicating that macrophage oxidative responses may vary depending on viral strain.

As macrophages are not productively infected by SARS-CoV-2 under these conditions, these findings support the concept that ROS induction reflects activation in response to viral uptake or associated inflammatory signals, rather than direct viral replication. One possible explanation is that macrophage activation is driven by co-purifying inflammatory mediators or DAMPs present in viral preparations, which may differ between variants. This possibility is explored in more detail in the following section examining macrophage cytokine responses. The observation that ROS production is enhanced in the presence of antibody-mediated infection further suggests that productive infection increases oxidative stress in the macrophage.

Macrophage phagocytic function

Several viruses have been shown to impair macrophage phagocytic capacity as a mechanism to promote viral persistence and reduce clearance. For example, influenza virus, respiratory syncytial virus (RSV), and HIV reduce macrophage phagocytosis through altering phagocytic receptor expression[236–238]. In contrast, the data presented in this thesis indicate that SARS-CoV-2 exposure does not impair macrophage phagocytic capacity under the conditions tested. This is consistent with the observation that macrophages are not a primary site of productive SARS-CoV-2 replication and therefore may not support viral mechanisms that directly interfere with phagocytic function.

Although interactions between SARS-CoV-2 and macrophage phagocytosis have not been extensively characterised, some studies have reported reduced phagocytic capacity following viral exposure [239,240]. However, these effects have been attributed to macrophage polarisation towards a more pro-inflammatory "M1-like" phenotype, rather than direct viral manipulation of phagocytic pathways.

Taken together, these findings indicate that macrophage phagocytic capacity is preserved following SARS-CoV-2 exposure, suggesting that impaired phagocytosis is unlikely to play a major role in disease pathology.

Macrophage antigen presentation and T cell activation

In this study, antigen presentation by iPSC-derived macrophages to SARS-CoV-2-specific, patient-derived T cell clones was investigated. Macrophages presented SARS-CoV-2 antigens via MHC class II and activated $CD4^+$ T cells, but no evidence of antigen presentation via MHC class I or activation of $CD8^+$ T cells was observed. This preferential presentation on MHC class II is consistent with the lack of productive SARS-CoV-2 infection in macrophages. Although the virus is internalised, it does not undergo replication and is therefore processed predominantly as an exogenous antigen for presentation via the MHC class II pathway. In the absence of viral replication, endogenous antigen is not generated for loading onto MHC class I. While macrophages are capable of cross-presentation under certain conditions[241,264], no evidence of cross-presentation of SARS-CoV-2 antigens was observed in this system.

Previous studies have reported reduced MHC expression in macrophages from patients with COVID-19[54], as well as in macrophages exposed to SARS-CoV-2 in vitro [240,265]. In this study, surface expression of MHC and co-stimulatory molecules was confirmed in iPSC-derived macrophages, although expression following viral exposure was not directly assessed. However,

the robust activation of both $CD4^+$ and $CD8^+$ T cells in peptide-loaded controls indicates that antigen presentation pathways were functional and that MHC expression was sufficient to support T cell activation.

SARS-CoV-2 has been reported to downregulate MHC class I expression in infected cells as an immune evasion strategy to limit $CD8^+$ T cell recognition [266–268]. However, this mechanism is unlikely to be relevant in the context of macrophages in this study, as these cells are not productively infected and therefore do not express viral proteins at levels sufficient to drive such evasion pathways. Instead, the absence of $CD8^+$ T cell activation is more likely explained by limited availability of endogenous antigen for MHC class I presentation.

A limitation of this work is that antigen presentation was not evaluated in the context of antibody-mediated replication. It is therefore possible that under these conditions, endogenous antigen could be generated and presented via MHC class I, leading to activation of $CD8^+$ T cells. This suggests that macrophage antigen presentation may be context-dependent, with differential engagement of MHC class I and class II pathways depending on the viral entry pathway and replication status.

Macrophage cytokine responses to SARS-CoV-2

Macrophage cytokines are elevated in severe COVID-19 and contribute to disease pathology[54]. However, it remains unclear whether macrophage activation is driven by direct sensing of SARS-CoV-2 or by secondary inflammatory mediators released from infected epithelial cells.

The findings presented in this thesis suggest that macrophage activation is not triggered by direct viral sensing. In particular, the lack of consistent activation by ancestral virus or spike protein, together with variability across experimental conditions, indicates that additional factors may contribute to macrophage activation. One plausible explanation is the presence of epithelial cell-derived damage-associated molecular patterns (DAMPs) or inflammatory mediators within viral preparations[269]. This is supported by previous studies proposing that macrophage activation in COVID-19 may be driven by factors released from infected epithelial cells [270].

There are several soluble factors released from virally infected cells that could induce macrophage activation[247]. These are generally small molecules and include cytokines (e.g. IFNs, IL-1β, TNFα), alarmins (e.g. HMGB1, S100 proteins), nucleic acids, ATP, histones, and heat shock proteins, all of which are <100 kDa in size. Although filtration using a 100 kDa molecular weight cut-off was used to remove small soluble mediators, this approach does not eliminate larger

inflammatory components. It is highly plausible that one of these larger DAMPS is responsible for the inconsistent macrophage activation observed in these assays. Potential candidates include extracellular vesicles, which are released from SARS-CoV-2-infected epithelial cells and can carry pro-inflammatory cargo capable of activating macrophages [271,272], as well as large nucleic acid complexes such as genomic or mitochondrial DNA, which can activate pattern recognition receptors [269]. While this study did not directly identify the specific mediator responsible, future experiments such as nuclease treatment, extracellular vesicle depletion, or targeted inhibition of pattern recognition receptors could help identify the mediator responsible.

Consistent with this model, conditioned media from epithelial cells infected with the ancestral SARS-CoV-2 strain (VIC01) induced robust macrophage cytokine responses, whereas media from cells infected with Delta or Omicron variants did not. This supports previous observations that earlier SARS-CoV-2 variants may induce stronger macrophage inflammatory responses than later variants [179]. Together, these findings suggest that infection with ancestral strains may promote the release of inflammatory mediators from epithelial cells that strongly activate macrophages, whereas later strains do not. However, it is important to note that Vero cells lack an intact interferon response and may produce exaggerated inflammatory signals compared to more physiologically relevant systems[273]. The use of Calu-3 cells partially addresses this limitation, although co-culture systems incorporating macrophages and epithelial cells would provide a more accurate model of in vivo interactions[274].

A large number of studies have reported that recombinant SARS-CoV-2 spike protein induces macrophage activation[231,253–258,275–277]. However, these findings may be confounded by endotoxin contamination or differences in protein glycosylation[262]. In this study, endotoxin contamination was found to strongly correlate with macrophage activation, and removal of endotoxin abrogated this response. Endotoxin-depleted recombinant spike protein, fully glycosylated by production in mammalian cells, did not induce macrophage activation. These findings, together with previous reports, suggest that spike protein alone is unlikely to be sufficient to induce macrophage activation, although it may contribute to the presence of additional priming signals[278].

Most of this work focused on macrophage cytokine responses to SARS-CoV-2 exposure rather than productive infection. As a result, the findings presented here primarily reflect macrophage activation in response to viral uptake and associated inflammatory signals. Only a single experiment was performed to assess cytokine responses under conditions of antibody-mediated infection, limiting the extent to which replication-dependent effects can be evaluated.

In this experiment, cytokine responses were modestly increased across variants under conditions of productive infection. However, the strongest cytokine responses were observed following exposure to the ancestral VIC01 strain in the absence of replication. This suggests that macrophage activation driven by non-replicating virus or associated inflammatory mediators may represent a major component of the macrophage response to SARS-CoV-2. While productive infection may enhance these responses, it does not appear to be the major initiator of aberrant cytokine production in these cells.

Inflammasome-responses

This study demonstrated that IL-1β was released in response to the ancestral SARS-CoV-2 strain (VIC01), but not the BA.5 variant, suggesting that inflammasome-associated responses may be differentially induced by SARS-CoV-2 variants. However, as IL-1β release alone is not definitive evidence of inflammasome activation, these findings should be interpreted with caution.

Inflammasome activation is a tightly regulated process requiring both a priming signal and a secondary activation signal. The data presented here suggest that macrophage inflammasome-associated responses may be influenced by additional factors present in the viral preparation, such as epithelial-derived DAMPs, which could provide a priming stimulus. This is consistent with previous studies proposing that macrophage inflammasome activation in the context of SARS-CoV-2 infection may depend on secondary signals derived from infected cells [269,278].

Several studies have reported inflammasome activation in macrophages and monocytes following SARS-CoV-2 exposure [181,228,252,260,279], including reports that viral proteins such as the S1 subunit and viroporins (ORF3a, E and M) can induce inflammasome-associated responses [229,230]. However, these findings are variable and may depend on experimental system, cell type, and the presence of additional inflammatory signals, highlighting the complexity of inflammasome activation in this context.

In this study, assessment of inflammasome activation was limited to measurement of IL-1β release, which is commonly used as a proxy for inflammasome activity. However, definitive evidence of inflammasome activation would require additional readouts, including caspase-1 activation, gasdermin D cleavage, ASC speck formation, and pyroptosis assays, ideally in combination with IL-1β and IL-18 quantification. As these analyses were beyond the scope of this study, the findings presented here should be interpreted as indicative of inflammasome-associated responses rather than direct evidence of inflammasome activation.

Limitations

A limitation of this study is that it primarily examined macrophage responses to non-specific viral uptake rather than antibody-mediated productive infection. This reflects the timing of the work, which preceded the identification of antibody-mediated infection of macrophages. As a result, the findings presented here primarily focus on macrophage activation in response to viral exposure rather than replication.

It remains possible that productive infection could alter macrophage cytokine responses beyond those observed in this study. However, as discussed in the previous results chapter, antibody-mediated infection of macrophages is unlikely to occur at significant levels in vivo due to the presence of polyclonal neutralising antibodies, which are expected to dominate over infection-promoting antibodies. Consequently, while replication-dependent effects cannot be excluded, they are unlikely to represent the primary driver of macrophage activation in physiological settings.

Instead, non-specific uptake of SARS-CoV-2 is likely to represent the predominant mode of interaction between macrophages and the virus in vivo. This supports the focus of this chapter on macrophage responses to viral exposure and associated inflammatory signals.

5.4 Conclusions

This chapter demonstrates that non-specific uptake of SARS-CoV-2 does not result in substantial dysregulation of key macrophage functions, including phagocytosis, antigen presentation, and cytokine production, under the conditions tested. These mechanisms are therefore unlikely to contribute to severe COVID-19 pathology. While exposure to the ancestral SARS-CoV-2 strain induced a modest cytokine response in macrophages, later variants such as Delta and Omicron elicited minimal or no cytokine production. These variant-specific differences are likely driven by inflammatory mediators released from infected epithelial cells, which differentially activate macrophages. Together, these findings suggest that macrophage activation in response to SARS-CoV-2 is not primarily driven by direct viral detection, but rather by secondary signals derived from the infected tissue environment. As these mediators are likely to be key drivers of macrophage inflammation, further investigation of epithelial-macrophage interactions will be important to define how this crosstalk contributes to COVID-19 pathology.

Chapter 6: General Discussion

Results summary

This thesis demonstrates that macrophages are not a target of SARS-CoV-2 productive infection. Instead, SARS-CoV-2 is internalised via non-specific uptake pathways that do not support viral replication. Provision of a surrogate receptor, such as transgenic ACE2, renders macrophages permissive to infection, consistent with the requirement for receptor-mediated spike activation to enable membrane fusion. In addition, a subset of anti-RBD antibodies was shown to mediate productive infection of macrophages through a cooperative mechanism involving both Fab-mediated stabilisation of a fusion-permissive spike conformation and Fcγ receptor-dependent virion tethering. Despite efficient internalisation, SARS-CoV-2 exposure did not result in substantial dysregulation of macrophage function, with only modest cytokine responses observed for ancestral variants and minimal responses for later variants. These findings suggest that direct interactions between SARS-CoV-2 and macrophages are unlikely to be a primary driver of disease pathology, although macrophages may still contribute to inflammation through indirect mechanisms within the infected lung environment.

SARS-CoV-2 is internalised into macrophages by a non-specific mechanism

In the first results chapter, I investigated the mechanisms underlying SARS-CoV-2 internalisation into macrophages. While several potential entry pathways were examined, a definitive mechanism could not be identified. The absence of caveolin-1 expression, lack of co-localisation with dextran, and exclusion of canonical endocytic pathways suggest that entry does not occur via clathrin-mediated endocytosis, caveolin-dependent uptake, or classical macropinocytosis. Instead, the data support a model in which SARS-CoV-2 is internalised through non-specific uptake pathways associated with the inherently high endocytic activity of macrophages. This may involve a macropinocytosis-like process or co-uptake of virions within fluid compartments during receptor-mediated endocytosis of unrelated cargo.

To date, there have been limited detailed mechanistic studies of SARS-CoV-2 internalisation into macrophages. These findings therefore provide new insight into how SARS-CoV-2 interacts with macrophages and suggest that viral uptake is not driven by a specific entry programme but rather reflects incidental internalisation. This supports the view that SARS-CoV-2 does not actively target macrophages for productive infection, but instead is passively taken up, providing important context for subsequent analyses of macrophage infection and function.

Macrophages are not susceptible to SARS-CoV-2 infection

In the second results chapter, I demonstrated that internalisation of SARS-CoV-2 via non-specific uptake does not result in productive infection. This is consistent with the absence of receptor-mediated stabilisation of the spike protein in a fusion-permissive conformation, limiting membrane fusion and promoting trafficking to degradative compartments. These findings help reconcile conflicting reports in the literature. Detection of viral RNA or protein within macrophages likely reflects viral uptake rather than productive infection.

In contrast, expression of hACE2 rendered macrophages permissive to infection, highlighting the importance of receptor-mediated spike activation for productive entry. While previous studies have reported SARS-CoV-2 infection in ACE2-expressing macrophage-like cells, these were largely conducted using THP-1 cells or pseudotyped virus[72,75,104]. This study therefore provides evidence of ACE2-mediated infection using authentic SARS-CoV-2 in human macrophages.

Antibody-mediated entry renders macrophages permissive to infection

These findings support the conclusion that macrophages possess an intracellular environment permissive to viral replication when appropriate entry conditions are met. This is consistent with the observation that a subset of anti-RBD antibodies can mediate productive infection. These findings are consistent with recent work by Pickering et al. (2024), who demonstrated that antibody-mediated mechanisms can facilitate SARS-CoV-2 infection of macrophages[174]. The present study builds upon these observations by further characterising the antibody features associated with this phenomenon. While Pickering et al. identified both class 1 and class 4 antibodies as capable of mediating infection, the findings presented here suggest that productive infection is most strongly associated with class 4 and class 1/4 overlapping antibodies. In addition, I performed structural mapping of antibody epitopes onto the RBD enabled identification of specific residues that may contribute to infection-promoting activity.

In addition, Pickering et al. reported evidence of infection in primary and iPSC-derived human macrophages based on nucleoprotein staining, with infectious virus release demonstrated in THP-1 monocytes only. In this work, I demonstrate infectious virus release from human iPSC-derived macrophages from multiple donors, providing further support for productive infection of human macrophages.

Consistent with Pickering et al., ruxolitinib enhanced antibody-mediated infection; however, given its broad off-target effects, interpretation of this result alone is limited. This was addressed

in my thesis by demonstrating enhanced infection using IFNAR2 antibody blockade and IFNAR2 knockout macrophages, confirming a central role for interferon signalling in restricting infection.

Based on these findings, I propose a cooperative mechanism of antibody-mediated infection involving Fab-mediated stabilisation of a fusion-permissive spike conformation and Fcγ receptor-dependent tethering of virions to the cell surface. I built on the work by Pickering et al. by examining the requirement for Fc receptor engagement. I demonstrated using Fc-silenced mutants and IgG subclass variants, that Fab-mediated effects alone are insufficient for antibody-mediate infection, and that infection also requires virion tethering by Fc-Fcγ receptor binding. Subclass-dependent differences on infection efficiency suggest that the proximity of virion tethering to the surface is critical.

Relevance of antibody-mediated infection in vivo

These findings raise the question of whether antibody-mediated macrophage infection occurs in vivo. Although the use of patient-derived antibodies and human macrophages in this study supports physiological relevance, the concentration-dependent nature of this mechanism suggests that it is most likely to occur within a narrow window of subneutralising antibody concentrations. In the presence of polyclonal serum, neutralising antibodies may dominate, as observed in this study. However, the composition of an individual's antibody response varies depending on factors such as prior infection. Conditions in which infection-promoting antibodies are relatively enriched may arise following exposure to antigenically distinct viral variants, particularly given that class 4 anti-RBD antibodies target more conserved epitopes. Consistent with this, studies by Pickering et al. and Junqueira et al. have reported that a subset of serum samples can promote infection in myeloid cells, suggesting that this phenomenon may occur under specific immunological conditions[174,181].

If antibody-mediated infection does occur in vivo, its contribution to disease pathology remains uncertain. Limited experiments from this thesis indicate only a modest increase in macrophage cytokine induction following productive infection. It is therefore possible that antibody-mediated infection, in combination with an inflammatory environment, could contribute to macrophage activation and disease progression, although further investigation is required.

While the role of antibody-mediated macrophage infection in disease remains unclear, these findings have important implications for the design of therapeutics. Adintrevimab, a clinically developed anti-RBD monoclonal antibody, was identified here as infection-promoting in macrophages. Although this antibody did not demonstrate adverse effects in clinical trials, its

ability to mediate Fc-dependent entry highlights a potential consideration for future therapeutics[221]. Adintrevimab has subsequently been developed into Pemivibart, a class 1/4 anti-RBD antibody that received FDA emergency authorisation in March 2024[280]. Given its epitope similarity to Adintrevimab and lack of Fc silencing, it is highly plausible that this antibody will also promote infection. These findings underscore the importance of evaluating Fc receptor interactions and, where appropriate, engineering Fc regions to modulate effector functions in the development of antiviral monoclonal antibodies.

In addition, Fc receptor-dependent viral entry provides a potential mechanism by which antibody-mediated effects could influence disease outcomes. Although there is currently no evidence of vaccine-enhanced disease in COVID-19, these results emphasise the importance of inducing robust neutralising antibody responses and carefully characterising antibody profiles during vaccine development[281].

Macrophage contributions to COVID-19 pathology

The primary focus of this DPhil has been on the examination of direct interaction between the virus and macrophages. However, many questions remain regarding how these cells contribute to disease pathogenesis. Chapter 5 examined how macrophage function is affected by SARS-CoV-2 exposure. These findings suggest that direct exposure to virus does not induce marked hyperinflammation or dysregulation in macrophages and is therefore unlikely to be a primary driver of disease. Nevertheless, there is substantial evidence that macrophages adopt a hyperinflammatory phenotype in severe COVID-19[15]. Based on the findings presented here, it is likely that macrophage activation is driven indirectly by the inflammatory lung environment, rather than by direct viral infection. This may result from inflammatory mediators released by infected epithelial cells, as well as cytokines produced by recruited immune cells.

Investigating the interactions between physiologically relevant models of SARS-CoV-2-infected epithelium and macrophages therefore represents an important area for future study. In addition, these experiments suggest that there may be variant-specific differences in inflammatory mediator release from infected epithelial cells. Identifying these differences could reveal novel targets for therapeutic intervention in COVID-19.

It was beyond the scope of this study to investigate the contribution of monocyte-derived macrophages in the lung; despite the fact that there is substantial evidence that large numbers of monocyte-derived macrophages infiltrate the lung in severe COVID-19 and are major contributors to the cytokine response[54]. Instead, the primary focus of this thesis was on alveolar

macrophages, which remain comparatively less well studied, in part due to the limited availability of physiologically relevant model systems. In addition to increased cytokine secretion that the monocyte-derive macrophage also release, the loss or dysfunction of alveolar macrophages may uniquely contribute to disease severity, through impaired regulation of inflammation and tissue repair. Further investigation into the factors that influence alveolar macrophage viability and function within the SARS-CoV-2-infected lung is therefore warranted.

The finding that macrophages are susceptible to antibody-mediated viral entry may not be restricted to this cell type. In principle, any cell that lacks ACE2 expression but expresses Fcγ receptors and is capable of supporting viral fusion and limited replication could be susceptible to Fc-dependent, antibody-mediated entry. This raises the possibility that other Fcγ receptor-expressing cells, including dendritic cells, B cells, endothelial cells, and microglia, may also internalise antibody-opsonised SARS-CoV-2 under certain conditions. However, whether such uptake results in productive infection is likely to depend on the intrinsic permissiveness of each cell type and the balance of antiviral restriction mechanisms. These possibilities call for further investigation.

Conclusions

In conclusion, this thesis demonstrates that human macrophages are intrinsically non-permissive to productive SARS-CoV-2 infection but can be rendered permissive through antibody-mediated mechanisms that depend on both Fcγ receptor engagement and epitope-specific effects. These findings show that viral entry into macrophages does not necessarily result in productive infection, and that outcomes are determined by a combination of entry mechanism, antibody properties, and innate antiviral responses.

This work helps clarify conflicting reports in the literature and suggests that macrophages are unlikely to act as major sites of viral replication in COVID-19 but may still play important roles in shaping immune responses. The identification of Fc-dependent antibody-mediated entry also highlights a consideration for the design of therapeutic antibodies. Further work will be required to determine the relevance of these mechanisms in vivo and to define how they may operate in other immune cell types and viral infections.

References

1. Zhou, P. *et al.* A pneumonia outbreak associated with a new coronavirus of probable bat origin. *Nature* **579**, 270–273 (2020).

2. Wu, F. *et al.* A new coronavirus associated with human respiratory disease in China. *Nature* **579**, 265 (2020).

3. Hoffmann, M. *et al.* SARS-CoV-2 Cell Entry Depends on ACE2 and TMPRSS2 and Is Blocked by a Clinically Proven Protease Inhibitor. *Cell* **181**, 271-280.e8 (2020).

4. Jackson, C. B., Farzan, M., Chen, B. & Choe, H. Mechanisms of SARS-CoV-2 entry into cells. *Nature Reviews Molecular Cell Biology 2021 23:1* **23**, 3–20 (2021).

5. Walls, A. C. *et al.* Structure, Function, and Antigenicity of the SARS-CoV-2 Spike Glycoprotein. *Cell* **181**, 281 (2020).

6. Wrapp, D. *et al.* Cryo-EM structure of the 2019-nCoV spike in the prefusion conformation. *Science* **367**, 1260 (2020).

7. Donoghue, M. *et al.* A novel angiotensin-converting enzyme-related carboxypeptidase (ACE2) converts angiotensin I to angiotensin 1-9. *Circ. Res.* **87**, (2000).

8. Starr, T. N. *et al.* Deep mutational scans for ACE2 binding, RBD expression, and antibody escape in the SARS-CoV-2 Omicron BA.1 and BA.2 receptor-binding domains. *PLoS Pathog.* **18**, e1010951 (2022).

9. Sungnak, W. *et al.* SARS-CoV-2 entry factors are highly expressed in nasal epithelial cells together with innate immune genes. *Nature Medicine 2020 26:5* **26**, 681–687 (2020).

10. V'kovski, P., Kratzel, A., Steiner, S., Stalder, H. & Thiel, V. Coronavirus biology and replication: implications for SARS-CoV-2. *Nat. Rev. Microbiol.* **19**, 155 (2020).

11. Snijder, E. J. *et al.* A unifying structural and functional model of the coronavirus replication organelle: Tracking down RNA synthesis. *PLoS Biol.* **18**, e3000715 (2020).

12. Sola, I., Almazán, F., Zúñiga, S. & Enjuanes, L. Continuous and Discontinuous RNA Synthesis in Coronaviruses. *Annu. Rev. Virol.* **2**, 265–288 (2015).

13. Guan, W. *et al.* Clinical Characteristics of Coronavirus Disease 2019 in China. *N. Engl. J. Med.* **382**, 1708–1720 (2020).

14. Lucas, C. *et al.* Longitudinal analyses reveal immunological misfiring in severe COVID-19. *Nature 2020 584:7821* **584**, 463–469 (2020).

15. Merad, M. & Martin, J. C. Pathological inflammation in patients with COVID-19: a key role for monocytes and macrophages. *Nat. Rev. Immunol.* **20**, 355–362 (2020).

16. Blanco-Melo, D. *et al.* Imbalanced Host Response to SARS-CoV-2 Drives Development of COVID-19. *Cell* **181**, 1036 (2020).

17. Del Valle, D. M. *et al.* An inflammatory cytokine signature predicts COVID-19 severity and survival. *Nature Medicine 2020 26:10* **26**, 1636–1643 (2020).

18. Hadjadj, J. *et al.* Impaired type I interferon activity and inflammatory responses in severe COVID-19 patients. *Science* **369**, 718–724 (2020).

19. P, H. *et al.* Dexamethasone in Hospitalized Patients with Covid-19. *N. Engl. J. Med.* **384**, 693–704 (2021).

20. Williamson, E. J. *et al.* Factors associated with COVID-19-related death using OpenSAFELY. *Nature 2020 584:7821* **584**, 430–436 (2020).

21. Bortolotti, D. *et al.* Tlr3 and tlr7 rna sensor activation during sars-cov-2 infection. *Microorganisms* **9**, 1820 (2021).

22. Moreno-Eutimio, M. A., López-Macías, C. & Pastelin-Palacios, R. Bioinformatic analysis and identification of single-stranded RNA sequences recognized by TLR7/8 in the SARS-CoV-2, SARS-CoV, and MERS-CoV genomes. *Microbes Infect.* **22**, 226–229 (2020).

23. Park, S. H. An Impaired Inflammatory and Innate Immune Response in COVID-19. *Mol. Cells* **44**, 384 (2021).

24. Su, W. *et al.* SARS-CoV-2 viral proteins trigger pain via TLR2/4-MyD88 pathway. *Front. Mol. Neurosci.* **18**, 1163636 (2025).

25. Planès, R., Bert, J. B., Tairi, S., Benmohamed, L. & Bahraoui, E. SARS-CoV-2 Envelope (E) Protein Binds and Activates TLR2 Pathway: A Novel Molecular Target for COVID-19 Interventions. *Viruses* **14**, (2022).

26. Zheng, M. *et al.* TLR2 senses the SARS-CoV-2 envelope protein to produce inflammatory cytokines. *Nat. Immunol.* **22**, 829–838 (2021).

27. Robbiani, D. F. *et al.* Convergent antibody responses to SARS-CoV-2 in convalescent individuals. *Nature 2020 584:7821* **584**, 437–442 (2020).

28. Brouwer, P. J. M. *et al.* Potent neutralizing antibodies from COVID-19 patients define multiple targets of vulnerability. *Science (1979).* **369**, 643–650 (2020).

29. Barnes, C. O. *et al.* SARS-CoV-2 neutralizing antibody structures inform therapeutic strategies. *Nature* **588**, 682 (2020).

30. Amanat, F. *et al.* SARS-CoV-2 mRNA vaccination induces functionally diverse antibodies to NTD, RBD, and S2 ll SARS-CoV-2 mRNA vaccination induces functionally diverse antibodies to NTD, RBD, and S2. *Cell* **184**, 3936-3948.e10 (2021).

31. Nimmerjahn, F. & Ravetch, J. V. Divergent immunoglobulin g subclass activity through selective Fc receptor binding. *Science* **310**, 1510–1512 (2005).

32. Vidarsson, G., Dekkers, G. & Rispens, T. IgG Subclasses and Allotypes: From Structure to Effector Functions. *Front. Immunol.* **5**, 520 (2014).

33. Mills, C. D., Kincaid, K., Alt, J. M., Heilman, M. J. & Hill, A. M. M-1/M-2 macrophages and the Th1/Th2 paradigm. *J. Immunol.* **164**, 6166–6173 (2000).

34. Murray, P. J. *et al.* Macrophage activation and polarization: nomenclature and experimental guidelines. *Immunity* **41**, 14 (2014).

35. Guilliams, M. & Scott, C. L. Does niche competition determine the origin of tissue-resident macrophages? *Nat. Rev. Immunol.* **17**, 451–460 (2017).

36. Hussell, T. & Bell, T. J. Alveolar macrophages: plasticity in a tissue-specific context. *Nat. Rev. Immunol.* **14**, 81–93 (2014).

37. Trapnell, B. C., Carey, B. C., Uchida, K. & Suzuki, T. Pulmonary alveolar proteinosis, a primary immunodeficiency of impaired GM-CSF stimulation of macrophages. *Curr. Opin. Immunol.* **21**, 514 (2009).

38. Prussin, A. J., Garcia, E. B. & Marr, L. C. Total Virus and Bacteria Concentrations in Indoor and Outdoor Air. *Environ. Sci. Technol. Lett.* **2**, 84 (2015).

39. van Wilgenburg, B., Browne, C., Vowles, J. & Cowley, S. A. Efficient, long term production of monocyte-derived macrophages from human pluripotent stem cells under partly-defined and fully-defined conditions. *PLoS One* **8**, (2013).

40. Vaughan-Jackson, A. *et al.* Differentiation of human induced pluripotent stem cells to authentic macrophages using a defined, serum-free, open-source medium. *Stem Cell Reports* **16**, 1735–1748 (2021).

41. Ding, T. *et al.* Comprehensive review of macrophage models: primary cells and immortalized lines across species. *Front. Immunol.* **16**, 1640935 (2025).

42. Shiratori, H. *et al.* THP-1 and human peripheral blood mononuclear cell-derived macrophages differ in their capacity to polarize in vitro. *Mol. Immunol.* **88**, 58–68 (2017).

43. Daigneault, M., Preston, J. A., Marriott, H. M., Whyte, M. K. B. & Dockrell, D. H. The identification of markers of macrophage differentiation in PMA-stimulated THP-1 cells and monocyte-derived macrophages. *PLoS One* **5**, (2010).

44. Kohro, T. *et al.* A comparison of differences in the gene expression profiles of phorbol 12-myristate 13-acetate differentiated THP-1 cells and human monocyte-derived macrophage. *J. Atheroscler. Thromb.* **11**, 88–97 (2004).

45. Tedesco, S. *et al.* Convenience versus biological significance: Are PMA-differentiated THP-1 cells a reliable substitute for blood-derived macrophages when studying in vitro polarization? *Front. Pharmacol.* **9**, 318678 (2018).

46. Knoll, R., Schultze, J. L. & Schulte-Schrepping, J. Monocytes and Macrophages in COVID-19. *Front. Immunol.* **12**, 2952 (2021).

47. Wang, C. *et al.* Alveolar macrophage dysfunction and cytokine storm in the pathogenesis of two severe COVID-19 patients. *EBioMedicine* **57**, (2020).

48. Hönzke, K. *et al.* Human lungs show limited permissiveness for SARS-CoV-2 due to scarce ACE2 levels but virus-induced expansion of inflammatory macrophages. *European Respiratory Journal* **60**, 2102725 (2022).

49. Vu Manh, T. P. *et al.* SARS-CoV2 infection in whole lung primarily targets macrophages that display subset-specific responses. *Cell. Mol. Life Sci.* **81**, 351 (2024).

50. Grant, R. A. *et al.* Circuits between infected macrophages and T cells in SARS-CoV-2 pneumonia. *Nature 2021 590:7847* **590**, 635–641 (2021).

51. Huot, N. *et al.* SARS-CoV-2 viral persistence in lung alveolar macrophages is controlled by IFN-γ and NK cells. *Nature Immunology 2023 24:12* **24**, 2068–2079 (2023).

52. Merad, M. & Martin, J. C. Pathological inflammation in patients with COVID-19: a key role for monocytes and macrophages. *Nat. Rev. Immunol.* **20**, 355–362 (2020).

53. Liao, M. *et al.* Single-cell landscape of bronchoalveolar immune cells in patients with COVID-19. *Nature Medicine 2020 26:6* **26**, 842–844 (2020).

54. Chen, S. T. *et al.* A shift in lung macrophage composition is associated with COVID-19 severity and recovery. *Sci. Transl. Med.* **14**, 5168 (2022).

55. Mehta, P. *et al.* COVID-19: consider cytokine storm syndromes and immunosuppression. *The Lancet* **395**, 1033–1034 (2020).

56. Zhou, Z. *et al.* Heightened Innate Immune Responses in the Respiratory Tract of COVID-19 Patients. *Cell Host Microbe* **27**, 883-890.e2 (2020).

57. Diao, B. *et al.* Reduction and Functional Exhaustion of T Cells in Patients With Coronavirus Disease 2019 (COVID-19). *Front. Immunol.* **11**, 827 (2020).

58. Giamarellos-Bourboulis, E. J. *et al.* Complex Immune Dysregulation in COVID-19 Patients with Severe Respiratory Failure. *Cell Host Microbe* **27**, 992-1000.e3 (2020).

59. Merad, M., Subramanian, A. & Wang, T. T. An aberrant inflammatory response in severe COVID-19. *Cell Host Microbe* **29**, 1043–1047 (2021).

60. Afzal, M. *et al.* Determination of resilience of a panel of broadly neutralizing mAbs to emerging variants of SARS-CoV-2 generated using reverse genetics. *iScience* **28**, 112451 (2025).

61. Fernandes, H. J. R. *et al.* ER Stress and Autophagic Perturbations Lead to Elevated Extracellular α-Synuclein in GBA-N370S Parkinson's iPSC-Derived Dopamine Neurons. *Stem Cell Reports* **6**, 342–356 (2016).

62. Dafinca, R. *et al.* C9orf72 Hexanucleotide Expansions Are Associated with Altered Endoplasmic Reticulum Calcium Homeostasis and Stress Granule Formation in Induced Pluripotent Stem Cell-Derived Neurons from Patients with Amyotrophic Lateral Sclerosis and Frontotemporal Deme…. *Stem Cells* **34**, 2063 (2016).

63. Hanrath, A. T. *et al.* Type I interferon receptor (IFNAR2) deficiency reveals Zika virus cytopathicity in human macrophages and microglia. *Front. Immunol.* **13**, 1035532 (2022).

64. Rasmussen, M. A. *et al.* Transient p53 suppression increases reprogramming of human fibroblasts without affecting apoptosis and DNA damage. *Stem Cell Reports* **3**, 404–413 (2014).

65. Hall-Roberts, H. *et al.* TREM2 Alzheimer's variant R47H causes similar transcriptional dysregulation to knockout, yet only subtle functional phenotypes in human iPSC-derived macrophages. *Alzheimers Res. Ther.* **12**, (2020).

66. Huang, K. Y. A. *et al.* Breadth and function of antibody response to acute SARS-CoV-2 infection in humans. *PLoS Pathog.* **17**, e1009352 (2021).

67. Hansen, J. *et al.* Studies in humanized mice and convalescent humans yield a SARS-CoV-2 antibody cocktail. *Science* **369**, 1010 (2020).

68. Pinto, D. *et al.* Cross-neutralization of SARS-CoV-2 by a human monoclonal SARS-CoV antibody. *Nature 2020 583:7815* **583**, 290–295 (2020).

69. Jette, C. A. *et al.* Broad cross-reactivity across sarbecoviruses exhibited by a subset of COVID-19 donor-derived neutralizing antibodies. *Cell Rep.* **36**, (2021).

70. Tortorici, M. A. *et al.* Broad sarbecovirus neutralization by a human monoclonal antibody. *Nature 2021 597:7874* **597**, 103–108 (2021).

71. Lee, J. Y. *et al.* Absolute quantitation of individual SARS-CoV-2 RNA molecules provides a new paradigm for infection dynamics and variant differences. *Elife* **11**, (2022).

72. Labzin, L. I. *et al.* Macrophage ACE2 is necessary for SARS-CoV-2 replication and subsequent cytokine responses that restrict continued virion release. *Sci. Signal.* **16**, eabq1366 (2023).

73. Zhang, Z., Penn, R., Barclay, W. S. & Giotis, E. S. Naïve Human Macrophages Are Refractory to SARS-CoV-2 Infection and Exhibit a Modest Inflammatory Response Early in Infection. *Viruses* **14**, (2022).

74. Niles, M. A. *et al.* Macrophages and Dendritic Cells Are Not the Major Source of Pro-Inflammatory Cytokines Upon SARS-CoV-2 Infection. *Front. Immunol.* **12**, 647824 (2021).

75. Duan, T. *et al.* ACE2-dependent and -independent SARS-CoV-2 entries dictate viral replication and inflammatory response during infection. *Nature Cell Biology 2024 26:4* **26**, 628–644 (2024).

76. Bayati, A., Kumar, R., Francis, V. & McPherson, P. S. SARS-CoV-2 infects cells after viral entry via clathrin-mediated endocytosis. *J. Biol. Chem.* **296**, 100306 (2021).

77. Song, X. *et al.* Little to no expression of angiotensin-converting enzyme-2 on most human peripheral blood immune cells but highly expressed on tissue macrophages. *Cytometry Part A* **103**, 136–145 (2023).

78. Nogami, M. *et al.* Peripheral alveolar macrophages express more ACE2 immunoreactivity than in hilar area in human autopsied lung. *BMC Res. Notes* **18**, 336 (2025).

79. Keidar, S. *et al.* Mineralocorticoid receptor blocker increases angiotensin-converting enzyme 2 activity in congestive heart failure patients. *Circ. Res.* **97**, 946–953 (2005).

80. Muus, C. *et al.* Single-cell meta-analysis of SARS-CoV-2 entry genes across tissues and demographics. *Nat. Med.* **27**, 546 (2021).

81. Zhao, Y. *et al.* Single-Cell RNA Expression Profiling of ACE2, the Receptor of SARS-CoV-2. *Am. J. Respir. Crit. Care Med.* **202**, 756 (2020).

82. Yao, Y. *et al.* Surface translocation of ACE2 and TMPRSS2 upon TLR4/7/8 activation is required for SARS-CoV-2 infection in circulating monocytes. *Cell Discovery 2022 8:1* **8**, 1–17 (2022).

83. Han, B. *et al.* ACE2-independent SARS-CoV-2 virus entry through cell surface GRP78 on monocytes – evidence from a translational clinical and experimental approach. *EBioMedicine* **98**, (2023).

84. Lian, Q. *et al.* Differential effects of macrophage subtypes on SARS-CoV-2 infection in a human pluripotent stem cell-derived model. *Nature Communications 2022 13:1* **13**, 1–14 (2022).

85. Hamming, I. *et al.* Tissue distribution of ACE2 protein, the functional receptor for SARS coronavirus. A first step in understanding SARS pathogenesis. *J. Pathol.* **203**, 631 (2004).

86. Jalloh, S. *et al.* CD169-mediated restrictive SARS-CoV-2 infection of macrophages induces pro-inflammatory responses. *PLoS Pathog.* **18**, e1010479 (2022).

87. Ziegler, C. G. K. *et al.* SARS-CoV-2 Receptor ACE2 Is an Interferon-Stimulated Gene in Human Airway Epithelial Cells and Is Detected in Specific Cell Subsets across Tissues. *Cell* **181**, 1016-1035.e19 (2020).

88. Mitsui, Y. *et al.* Expression of the readthrough transcript CiDRE in alveolar macrophages boosts SARS-CoV-2 susceptibility and promotes COVID-19 severity. *Immunity* **56**, 1939-1954.e12 (2023).

89. Watanabe, Y., Bowden, T. A., Wilson, I. A. & Crispin, M. Exploitation of glycosylation in enveloped virus pathobiology. *Biochimica et Biophysica Acta (BBA) - General Subjects* **1863**, 1480–1497 (2019).

90. Geijtenbeek, T. B. H. & Van Kooyk, Y. DC-SIGN: a novel HIV receptor on DCs that mediates HIV-1 transmission. *Curr. Top. Microbiol. Immunol.* **276**, 31–54 (2003).

91. Tassaneetrithep, B. *et al.* DC-SIGN (CD209) Mediates Dengue Virus Infection of Human Dendritic Cells. *J. Exp. Med.* **197**, 823 (2003).

92. Gong, Y., Qin, S., Dai, L. & Tian, Z. The glycosylation in SARS-CoV-2 and its receptor ACE2. *Signal Transduction and Targeted Therapy 2021 6:1* **6**, 396- (2021).

93. Feng, Z. *et al.* Structural and functional insights into the evolution of SARS-CoV-2 KP.3.1.1 spike protein. *Cell Rep.* **44**, (2025).

94. Newby, M. L. *et al.* Variations within the Glycan Shield of SARS-CoV-2 Impact Viral Spike Dynamics. *J. Mol. Biol.* **435**, 167928 (2022).

95. Watanabe, Y., Allen, J. D., Wrapp, D., McLellan, J. S. & Crispin, M. Site-specific glycan analysis of the SARS-CoV-2 spike. *Science* **369**, 330–333 (2020).

96. Hoffmann, D. *et al.* Identification of lectin receptors for conserved SARS-CoV-2 glycosylation sites. *The EMBO Journal 2021 40:19* **40**, EMBJ2021108375- (2021).

97. Neetu *et al.* Identification of SARS-CoV-2-binding lectins on a commercial lectin array. *Scientific Reports 2025 15:1* **15**, 21687- (2025).

98. Thépaut, M. *et al.* DC/L-SIGN recognition of spike glycoprotein promotes SARS-CoV-2 trans-infection and can be inhibited by a glycomimetic antagonist. *PLoS Pathog.* **17**, e1009576 (2021).

99. Amraei, R. *et al.* CD209L/L-SIGN and CD209/DC-SIGN Act as Receptors for SARS-CoV-2. *ACS Cent. Sci.* **7**, 1156–1165 (2021).

100. Gao, C. *et al.* SARS-CoV-2 Spike Protein Interacts with Multiple Innate Immune Receptors. *bioRxiv* 2020.07.29.227462 (2020) doi:10.1101/2020.07.29.227462.

101. Guo, L. *et al.* Epigenetic glycosylation of SARS-CoV-2 impact viral infection through DC&L-SIGN receptors. *iScience* **24**, 103426 (2021).

102. Gupta, J. *et al.* SARS CoV-2 spike protein variants exploit DC-SIGN/DC-SIGNR receptor for evolution and severity: an in-silico insight. *VirusDisease 2023 34:2* **34**, 278–296 (2023).

103. Lempp, F. A. *et al.* Lectins enhance SARS-CoV-2 infection and influence neutralizing antibodies. *Nature 2021 598:7880* **598**, 342–347 (2021).

104. Jalloh, S. *et al.* CD169-mediated restrictive SARS-CoV-2 infection of macrophages induces pro-inflammatory responses. *PLoS Pathog.* **18**, e1010479 (2022).

105. Pelkmans, L. & Helenius, A. Endocytosis via caveolae. *Traffic* **3**, 311–320 (2002).

106. Kiss, A. L. & Botos, E. Endocytosis via caveolae: alternative pathway with distinct cellular compartments to avoid lysosomal degradation? *J. Cell. Mol. Med.* **13**, 1228 (2009).

107. Marjomäki, V. *et al.* Internalization of Echovirus 1 in Caveolae. *J. Virol.* **76**, 1856–1865 (2002).

108. Wang, H. *et al.* SARS coronavirus entry into host cells through a novel clathrin- and caveolae-independent endocytic pathway. *Cell Res.* **18**, 290–301 (2008).

109. Fielding, C. J., Bist, A. & Fielding, P. E. Intracellular cholesterol transport. *Biochemistry* **38**, 2506–2513 (1999).

110. Arakawa, R., Abe-Dohmae, S., Asai, M., Ito, J. I. & Yokoyama, S. Involvement of caveolin-1 in cholesterol enrichment of high density lipoprotein during its assembly by apolipoprotein and THP-1 cells. *J. Lipid Res.* **41**, 1952–1962 (2000).

111. Matveev, S., Van Der Westhuyzen, D. R. & Smart, E. J. Co-expression of scavenger receptor-BI and caveolin-1 is associated with enhanced selective cholesteryl ester uptake in THP-1 macrophages. *J. Lipid Res.* **40**, 1647–1654 (1999).

112. Wu, C. C. *et al.* OxLDL upregulates caveolin-1 expression in macrophages: Role for caveolin-1 in the adhesion of oxLDL-treated macrophages to endothelium. *J. Cell. Biochem.* **107**, 460–472 (2009).

113. Fu, Y. *et al.* Caveolin-1 plays a critical role in the differentiation of monocytes into macrophages. *Arterioscler. Thromb. Vasc. Biol.* **32**, (2012).

114. Gargalovic, P. & Dory, L. Caveolin-1 and Caveolin-2 Expression in Mouse Macrophages. *Journal of Biological Chemistry* **276**, 26164–26170 (2001).

115. Kiss, A. L., Túri, A., Müllner, N. & Tímár, J. Caveolin isoforms in resident and elicited rat peritoneal macrophages. *Eur. J. Cell Biol.* **79**, 343–349 (2000).

116. Lei, M. G. & Morrison, D. C. Differential expression of caveolin-1 in lipopolysaccharide-activated murine macrophages. *Infect. Immun.* **68**, 5084–5089 (2000).

117. Lee, M. K. S. *et al.* High-density lipoprotein inhibits human M1 macrophage polarization through redistribution of caveolin-1. *Br. J. Pharmacol.* **173**, 741–751 (2016).

118. Xu, Y. *et al.* Proinflammatory Phenotype and Increased Caveolin-1 in Alveolar Macrophages with Silenced CFTR mRNA. *PLoS One* **5**, e11004 (2010).

119. Carter, G. C., Bernstone, L., Baskaran, D. & James, W. HIV-1 infects macrophages by exploiting an endocytic route dependent on dynamin, Rac1 and Pak1. *Virology* **409**, 234–250 (2011).

120. Gargalovic, P. & Dory, L. Caveolins and macrophage lipid metabolism. *J. Lipid Res.* **44**, 11–21 (2003).

121. Hiromura, M. *et al.* Caveolin-1, a binding protein of CD26, is essential for the anti-inflammatory effects of dipeptidyl peptidase-4 inhibitors on human and mouse macrophages. *Biochem. Biophys. Res. Commun.* **495**, 223–229 (2018).

122. Salata, C. *et al.* Ebola Virus Entry: From Molecular Characterization to Drug Discovery. *Viruses* **11**, 274 (2019).

123. Mercer, J. & Helenius, A. Virus entry by macropinocytosis. *Nat. Cell Biol.* **11**, 510–520 (2009).

124. Zhang, Y. Y. *et al.* SARS-CoV-2 hijacks macropinocytosis to facilitate its entry and promote viral spike–mediated cell-to-cell fusion. *J. Biol. Chem.* **298**, 102511 (2022).

125. Porebski, B. *et al.* Discovery of a novel inhibitor of macropinocytosis with antiviral activity. *Molecular Therapy* **32**, 3012–3024 (2024).

126. Ahn, W. M. *et al.* SARS-CoV-2 Spike Protein Stimulates Macropinocytosis in Murine and Human Macrophages via PKC-NADPH Oxidase Signaling. *Antioxidants* **13**, 175 (2024).

127. Mercer, J. & Helenius, A. Gulping rather than sipping: macropinocytosis as a way of virus entry. *Curr. Opin. Microbiol.* **15**, 490–499 (2012).

128. Masereel, B., Pochet, L. & Laeckmann, D. An overview of inhibitors of Na+/H+ exchanger. *Eur. J. Med. Chem.* **38**, 547–554 (2003).

129. Vanlandschoot, P. & Leroux-Roels, G. Viral apoptotic mimicry: An immune evasion strategy developed by the hepatitis B virus? *Trends Immunol.* **24**, 144–147 (2003).

130. Brindley, M. A. & Pisciotta, M. A. Viral apoptotic mimicry and the role of phosphatidylserine receptors. *mSphere* https://doi.org/10.1128/MSPHERE.00089-25 (2025) doi:10.1128/MSPHERE.00089-25.

131. Amara, A. & Mercer, J. Viral apoptotic mimicry. *Nature Reviews Microbiology 2015 13:8* **13**, 461–469 (2015).

132. Mercer, J. & Helenius, A. Vaccinia virus uses macropinocytosis and apoptotic mimicry to enter host cells. *Science (1979).* **320**, 531–535 (2008).

133. Meertens, L. *et al.* The TIM and TAM families of phosphatidylserine receptors mediate dengue virus entry. *Cell Host Microbe* **12**, 544–557 (2012).

134. Jemielity, S. *et al.* TIM-family proteins promote infection of multiple enveloped viruses through virion-associated phosphatidylserine. *PLoS Pathog.* **9**, (2013).

135. Bhattacharyya, S. *et al.* Enveloped viruses disable innate immune responses in dendritic cells by direct activation of TAM receptors. *Cell Host Microbe* **14**, 136–147 (2013).

136. Bohan, D. *et al.* Phosphatidylserine receptors enhance SARS-CoV-2 infection. *PLoS Pathog.* **17**, (2021).

137. Wang, S. *et al.* AXL is a candidate receptor for SARS-CoV-2 that promotes infection of pulmonary and bronchial epithelial cells. *Cell Res.* **31**, 126 (2021).

138. Sim, J. R. *et al.* Amelioration of SARS-CoV-2 infection by ANO6 phospholipid scramblase inhibition. *Cell Rep.* **40**, 111117 (2022).

139. Singh, P. *et al.* SARS-CoV-2 spike fusion peptide trans interaction with phosphatidylserine lipid triggers membrane fusion for viral entry. *mBio* **15**, (2024).

140. Haas, A. The phagosome: Compartment with a license to kill. *Traffic* **8**, 311–330 (2007).

141. Flannagan, R. S., Jaumouillé, V. & Grinstein, S. The cell biology of phagocytosis. *Annual Review of Pathology: Mechanisms of Disease* **7**, 61–98 (2012).

142. Kim, Y. *et al.* Trypsin enhances SARS-CoV-2 infection by facilitating viral entry. *Archives of Virology 2021 167:2* **167**, 441–458 (2022).

143. Londrigan, S. L., Tate, M. D., Brooks, A. G. & Reading, P. C. Cell-surface receptors on macrophages and dendritic cells for attachment and entry of influenza virus. *J. Leukoc. Biol.* **92**, 97 (2012).

144. Li, Y. *et al.* The Importance of Glycans of Viral and Host Proteins in Enveloped Virus Infection. *Front. Immunol.* **12**, 638573 (2021).

145. Watanabe, Y., Allen, J. D., Wrapp, D., McLellan, J. S. & Crispin, M. Site-specific glycan analysis of the SARS-CoV-2 spike. *Science (1979).* **369**, 330–333 (2020).

146. Pelkmans, L., Bürli, T., Zerial, M. & Helenius, A. Caveolin-Stabilized Membrane Domains as Multifunctional Transport and Sorting Devices in Endocytic Membrane Traffic. *Cell* **118**, 767–780 (2004).

147. Carter, G. C., Bernstone, L., Baskaran, D. & James, W. HIV-1 infects macrophages by exploiting an endocytic route dependent on dynamin, Rac1 and Pak1. *Virology* **409**, 234–250 (2011).

148. Harris, J., Werling, D., Hope, J. C., Taylor, G. & Howard, C. J. Caveolae and caveolin in immune cells: Distribution and functions. *Trends Immunol.* **23**, 158–164 (2002).

149. Naeini, M. B., Bianconi, V., Pirro, M. & Sahebkar, A. The role of phosphatidylserine recognition receptors in multiple biological functions. *Cellular & Molecular Biology Letters 2020 25:1* **25**, 23- (2020).

150. Wang, Y. *et al.* TREM2 lipid sensing sustains the microglial response in an Alzheimer's disease model. *Cell* **160**, 1061–1071 (2015).

151. Song, X. *et al.* Little to no expression of angiotensin-converting enzyme-2 on most human peripheral blood immune cells but highly expressed on tissue macrophages. *Cytometry Part A* **103**, 136–145 (2023).

152. Park, C. *et al.* Murine Alveolar Macrophages Rapidly Accumulate Intranasally Administered SARS-CoV-2 Spike Protein leading to Neutrophil Recruitment and Damage. *Elife* **12**, (2024).

153. Amraei, R. *et al.* CD209L/L-SIGN and CD209/DC-SIGN Act as Receptors for SARS-CoV-2. *ACS Cent. Sci.* **7**, 1156 (2021).

154. Mori, Y. *et al.* KIM-1/TIM-1 is a Receptor for SARS-CoV-2 in Lung and Kidney. *medRxiv* 2020.09.16.20190694 (2022) doi:10.1101/2020.09.16.20190694.

155. Wei, C. *et al.* HDL-scavenger receptor B type 1 facilitates SARS-CoV-2 entry. *Nature Metabolism 2020 2:12* **2**, 1391–1400 (2020).

156. Steinman, R. M., Brodie, S. E. & Cohn, Z. A. Membrane flow during pinocytosis. A stereologic analysis. *J. Cell Biol.* **68**, 665 (1976).

157. Tontanahal, A., Arvidsson, I. & Karpman, D. Annexin Induces Cellular Uptake of Extracellular Vesicles and Delays Disease in Escherichia coli O157:H7 Infection. *Microorganisms* **9**, (2021).

158. Wang, X., Wang, Y., Yang, L., Zhang, Y. & Yang, L. TREM2+ macrophages: a key role in disease development. *Front. Immunol.* **16**, 1550893 (2025).

159. Alberts, B. *et al.* Transport into the Cell from the Plasma Membrane: Endocytosis. https://www.ncbi.nlm.nih.gov/books/NBK26870/ (2002).

160. Nikitina, E., Larionova, I., Choinzonov, E. & Kzhyshkowska, J. Monocytes and Macrophages as Viral Targets and Reservoirs. https://doi.org/10.3390/ijms19092821 (2018) doi:10.3390/ijms19092821.

161. Banete, A., Barilo, J., Whittaker, R. & Basta, S. The Activated Macrophage – A Tough Fortress for Virus Invasion: How Viruses Strike Back. *Front. Microbiol.* **12**, 803427 (2022).

162. Gorry, P. R. *et al.* Macrophage tropism of human immunodeficiency virus type 1 isolates from brain and lymphoid tissues predicts neurotropism independent of coreceptor specificity. *J. Virol.* **75**, 10073–10089 (2001).

163. Woottum, M. *et al.* Macrophages: Key Cellular Players in HIV Infection and Pathogenesis. *Viruses 2024, Vol. 16, Page 288* **16**, 288 (2024).

164. Flipse, J. *et al.* Antibody-Dependent Enhancement of Dengue Virus Infection in Primary Human Macrophages; Balancing Higher Fusion against Antiviral Responses. *Scientific Reports 2016 6:1* **6**, 29201- (2016).

165. Teo, A., Tan, H. D., Loy, T., Chia, P. Y. & Chua, C. L. L. Understanding antibody-dependent enhancement in dengue: Are afucosylated IgG1s a concern? *PLoS Pathog.* **19**, e1011223 (2023).

166. Wells, T. J., Esposito, T., Henderson, I. R. & Labzin, L. I. Mechanisms of antibody-dependent enhancement of infectious disease. *Nat. Rev. Immunol.* **25**, 6–21 (2025).

167. Sinzger, C., Plachter, B., Grefte, A., The, T. H. & Jahn, G. Tissue Macrophages Are Infected by Human Cytomegalovirus In Vivo. *J. Infect. Dis.* **173**, 240–245 (1996).

168. Panuska, J. R. *et al.* Productive infection of isolated human alveolar macrophages by respiratory syncytial virus. *J. Clin. Invest.* **86**, 113–119 (1990).

169. Fletcher, N. F. *et al.* Activated Macrophages Promote Hepatitis C Virus Entry in a Tumor Necrosis Factor-Dependent Manner. *Hepatology* **59**, 1320 (2014).

170. Tugizov, S. *et al.* Epstein-Barr Virus (EBV)-Infected Monocytes Facilitate Dissemination of EBV within the Oral Mucosal Epithelium. *J. Virol.* **81**, 5484–5496 (2007).

171. Cline, T. D., Beck, D. & Bianchini, E. Influenza virus replication in macrophages: balancing protection and pathogenesis. *J. Gen. Virol.* **98**, 2401 (2017).

172. Solmaz, G. *et al.* TLR7 controls VSV replication in CD169+ SCS macrophages and associated viral neuroinvasion. *Front. Immunol.* **10**, 431955 (2019).

173. Lv, J. *et al.* Distinct uptake, amplification, and release of SARS-CoV-2 by M1 and M2 alveolar macrophages. *Cell Discov.* **7**, 24 (2021).

174. Pickering, S. *et al.* Antibodies to the RBD of SARS-CoV-2 spike mediate productive infection of primary human macrophages. *Nature Communications 2024 15:1* **15**, 1–17 (2024).

175. Zheng, J. *et al.* Severe Acute Respiratory Syndrome Coronavirus 2–Induced Immune Activation and Death of Monocyte-Derived Human Macrophages and Dendritic Cells. *J. Infect. Dis.* **223**, 785 (2020).

176. García-Nicolás, O., Godel, A., Zimmer, G. & Summerfield, A. Macrophage phagocytosis of SARS-CoV-2-infected cells mediates potent plasmacytoid dendritic cell activation. *Cellular & Molecular Immunology 2023 20:7* **20**, 835–849 (2023).

177. Martínez-Colón, G. J. *et al.* SARS-CoV-2 infection drives an inflammatory response in human adipose tissue through infection of adipocytes and macrophages. *Sci. Transl. Med.* **14**, (2022).

178. Zheng, J. *et al.* Severe Acute Respiratory Syndrome Coronavirus 2–Induced Immune Activation and Death of Monocyte-Derived Human Macrophages and Dendritic Cells. *J. Infect. Dis.* **223**, 785–795 (2021).

179. Gallo, A. *et al.* Transcriptomic profiles of monocyte-derived macrophages exposed to SARS-CoV-2 VOCs reveal immune-evasion escape driven by delta. *J. Transl. Med.* **23**, 151 (2025).

180. Mese, K. *et al.* FcγRIIa-mediated antibody-dependent uptake of SARS-CoV-2 enhances IL-6 expression of monocytes. *Eur. J. Microbiol. Immunol. (Bp).* **14**, 380–391 (2024).

181. Junqueira, C. *et al.* FcγR-mediated SARS-CoV-2 infection of monocytes activates inflammation. *Nature 2022 606:7914* **606**, 576–584 (2022).

182. Kuzmina, N. A. *et al.* SARS-CoV-2 antibody–dependent enhancement of infection depends on antibody binding to both ACE2 and Fc receptors. *JCI Insight* **11**, (2026).

183. Yang, Y. *et al.* Antibody-Dependent Heterotypic Syncytia Drive COVID-19 Inflammation and Disease Progression. *bioRxiv* 2026.02.11.705426 (2026) doi:10.64898/2026.02.11.705426.

184. Nimmerjahn, F. & Ravetch, J. V. Divergent immunoglobulin g subclass activity through selective Fc receptor binding. *Science* **310**, 1510–1512 (2005).

185. Mancardi, D. & Daëron, M. Fc Receptors in Immune Responses. *Reference Module in Biomedical Sciences* B978-0-12-801238-3.00119-7 (2014) doi:10.1016/b978-0-12-801238-3.00119-7.

186. Chen, Y. *et al.* Broadly neutralizing antibodies to SARS-CoV-2 and other human coronaviruses. *Nature Reviews Immunology 2022 23:3* **23**, 189–199 (2022).

187. Barnes, C. O. *et al.* SARS-CoV-2 neutralizing antibody structures inform therapeutic strategies. *Nature 2020 588:7839* **588**, 682–687 (2020).

188. Ng, K. W. *et al.* SARS-CoV-2 S2–targeted vaccination elicits broadly neutralizing antibodies. *Sci. Transl. Med.* **14**, 3715 (2022).

189. Hoffmann, M., Kleine-Weber, H. & Pöhlmann, S. A Multibasic Cleavage Site in the Spike Protein of SARS-CoV-2 Is Essential for Infection of Human Lung Cells. *Mol. Cell* **78**, 779-784.e5 (2020).

190. Hoffmann, H. H., Schneider, W. M. & Rice, C. M. Interferons and viruses: an evolutionary arms race of molecular interactions. *Trends Immunol.* **36**, 124 (2015).

191. McNab, F., Mayer-Barber, K., Sher, A. & Wack, A. Type I interferons in infectious disease. *Nat. Rev. Immunol.* **15**, 87–103 (2015).

192. Husain, M. Influenza Virus Host Restriction Factors: The ISGs and Non-ISGs. *Pathogens* **13**, 127 (2024).

193. Zu, S. *et al.* 25-Hydroxycholesterol is a potent SARS-CoV-2 inhibitor. *Cell Research 2020 30:11* **30**, 1043–1045 (2020).

194. Shi, G. *et al.* Opposing activities of IFITM proteins in SARS-CoV-2 infection. *The EMBO Journal 2020 40:3* **40**, EMBJ2020106501- (2020).

195. Harioudh, M. K. *et al.* Oligoadenylate synthetase 1 displays dual antiviral mechanisms in driving translational shutdown and protecting interferon production. *Immunity* **57**, 446-461.e7 (2024).

196. Cesaro, T. & Michiels, T. Inhibition of PKR by Viruses. *Front. Microbiol.* **12**, 757238 (2021).

197. Pichlmair, A. *et al.* IFIT1 is an antiviral protein that recognizes 5'-triphosphate RNA. *Nat. Immunol.* **12**, 624–630 (2011).

198. Gizzi, A. S. *et al.* A naturally occurring antiviral ribonucleotide encoded by the human genome. *Nature* **558**, 610–614 (2018).

199. Haller, O., Staeheli, P. & Kochs, G. Interferon-induced Mx proteins in antiviral host defense. *Biochimie* **89**, 812–818 (2007).

200. Lo, M. *et al.* Effector-attenuating Substitutions That Maintain Antibody Stability and Reduce Toxicity in Mice. *J. Biol. Chem.* **292**, 3900–3908 (2017).

201. Sivadas, A., Byram, K. W., Valdebran, M. & Beck, T. Understanding JAK inhibitor toxicity. *J. Am. Acad. Dermatol.* **93**, e199–e200 (2025).

202. Virtanen, A. *et al.* JAK inhibitor selectivity: new opportunities, better drugs? *Nature Reviews Rheumatology 2024 20:10* **20**, 649–665 (2024).

203. Shawky, A. M., Almalki, F. A., Abdalla, A. N., Abdelazeem, A. H. & Gouda, A. M. A Comprehensive Overview of Globally Approved JAK Inhibitors. *Pharmaceutics* **14**, 1001 (2022).

204. García-Nicolás, O. *et al.* No Evidence for Human Monocyte-Derived Macrophage Infection and Antibody-Mediated Enhancement of SARS-CoV-2 Infection. *Front. Cell. Infect. Microbiol.* **11**, 644574 (2021).

205. Xu, C. *et al.* Conformational dynamics of SARS-CoV-2 trimeric spike glycoprotein in complex with receptor ACE2 revealed by cryo-EM. *Sci. Adv.* **7**, (2021).

206. Rencilin, C. F. *et al.* Cryo-EM reveals conformational variability in the SARS-CoV-2 spike protein RBD induced by two broadly neutralizing monoclonal antibodies. *RSC Adv.* **15**, 14385 (2025).

207. Zhao, Z. *et al.* Omicron SARS-CoV-2 mutations stabilize spike up-RBD conformation and lead to a non-RBM-binding monoclonal antibody escape. *Nat. Commun.* **13**, 4958 (2022).

208. Damelang, T., Rogerson, S. J., Kent, S. J. & Chung, A. W. Role of IgG3 in Infectious Diseases. *Trends Immunol.* **40**, 197–211 (2019).

209. Castro-Dopico, T. & Clatworthy, M. R. IgG and Fcγ receptors in intestinal immunity and inflammation. *Front. Immunol.* **10**, 453927 (2019).

210. Cleary, K. L. S., Chan, H. T. C., James, S., Glennie, M. J. & Cragg, M. S. Antibody distance from the cell membrane regulates antibody effector mechanisms. *J. Immunol.* **198**, 3999 (2017).

211. Miteu, G. D. Structure–function relationships of human IgG subclasses: implications for therapeutic antibody engineering and clinical application. *Discover Applied Sciences 2025 7:10* **7**, 1148- (2025).

212. Lytras, S. *et al.* Resurrection of 2'-5'-oligoadenylate synthetase 1 (OAS1) from the ancestor of modern horseshoe bats blocks SARS-CoV-2 replication. *PLoS Biol.* **21**, e3002398 (2023).

213. Danziger, O., Patel, R. S., DeGrace, E. J., Rosen, M. R. & Rosenberg, B. R. Inducible CRISPR activation screen for interferon-stimulated genes identifies OAS1 as a SARS-CoV-2 restriction factor. *PLoS Pathog.* **18**, (2022).

214. Mar, K. B. *et al.* LY6E is a pan-coronavirus restriction factor in the respiratory tract. *Nat. Microbiol.* **8**, 1587–1599 (2023).

215. Ma, Y. *et al.* Glycosylphosphatidylinositol biosynthesis functions as a conserved host defense pathway against coronaviruses via regulation of LY6E. *PLoS Pathog.* **21**, e1013441 (2025).

216. Zang, R. *et al.* Cholesterol 25-hydroxylase suppresses SARS-CoV-2 replication by blocking membrane fusion. https://doi.org/10.1073/pnas.2012197117/-/DCSupplemental doi:10.1073/pnas.2012197117/-/DCSupplemental.

217. Nchioua, R. *et al.* SARS-CoV-2 Is Restricted by Zinc Finger Antiviral Protein despite Preadaptation to the Low-CpG Environment in Humans. https://coronavirus.jhu.edu/map.html (2020).

218. Xu, F. *et al.* IFITM3 Inhibits SARS-CoV-2 Infection and Is Associated with COVID-19 Susceptibility. *Viruses* **14**, 2553 (2022).

219. Sawant, J., Patil, A. & Kurle, S. A Review: Understanding Molecular Mechanisms of Antibody-Dependent Enhancement in Viral Infections. *Vaccines (Basel).* **11**, 1240 (2023).

220. Ison, M. G. *et al.* Prevention of COVID-19 Following a Single Intramuscular Administration of Adintrevimab: Results From a Phase 2/3 Randomized, Double-Blind, Placebo-Controlled Trial (EVADE). *Open Forum Infect. Dis.* **10**, (2023).

221. Ison, M. G. *et al.* Efficacy and Safety of Adintrevimab (ADG20) for the Treatment of High-Risk Ambulatory Patients With Mild or Moderate Coronavirus Disease 2019: Results From a Phase 2/3, Randomized, Placebo-Controlled Trial (STAMP) Conducted During Delta Predominance and …. *Open Forum Infect. Dis.* **10**, (2023).

222. Popejoy, M. *et al.* asm.org/microbe | 1 Results from the Phase 2/3 Randomized, Double-Blind, Placebo-Controlled Trial to Evaluate the Efficacy and Safety of Adintrevimab (ADG20) in the Treatment of Ambulatory Participants with Mild or Moderate COVID-19 (STAMP).

223. Guan, F. *et al.* Tissue macrophages: origin, heterogenity, biological functions, diseases and therapeutic targets. *Signal Transduction and Targeted Therapy 2025 10:1* **10**, 93- (2025).

224. Desterke, C., Turhan, A. G., Bennaceur-Griscelli, A. & Griscelli, F. PPARγ Cistrome Repression during Activation of Lung Monocyte-Macrophages in Severe COVID-19. *iScience* **23**, 101611 (2020).

225. Liao, M. *et al.* Single-cell landscape of bronchoalveolar immune cells in patients with COVID-19. *Nat. Med.* **26**, 842–844 (2020).

226. Grant, R. A. *et al.* Circuits between infected macrophages and T cells in SARS-CoV-2 pneumonia. *Nature* **590**, 635 (2021).

227. Battaglia, D. M. *et al.* SARS-CoV-2 infection induces pro-fibrotic and pro-thrombotic foam cell formation. *Nature Microbiology 2025 10:10* **10**, 2616–2630 (2025).

228. Ferreira, A. C. *et al.* SARS-CoV-2 engages inflammasome and pyroptosis in human primary monocytes. *Cell Death Discovery 2021 7:1* **7**, 43- (2021).

229. Ambrożek-Latecka, M. *et al.* SARS-CoV-2 and its ORF3a, E and M viroporins activate inflammasome in human macrophages and induce of IL-1α in pulmonary epithelial and endothelial cells. *Cell Death Discov.* **10**, 1–11 (2024).

230. Lu, M. *et al.* Recombinant SARS-Cov-2 spike protein S1 subunit upregulates P2 × 7-NLRP3 leading to macrophage pyroptosis promoting acute lung injury. *Respir. Res.* **27**, 76 (2026).

231. Barhoumi, T. *et al.* SARS-CoV-2 Coronavirus Spike Protein-Induced Apoptosis, Inflammatory, and Oxidative Stress Responses in THP-1-Like-Macrophages: Potential Role of Angiotensin-Converting Enzyme Inhibitor (Perindopril). *Front. Immunol.* **12**, 728896 (2021).

232. Canton, M. *et al.* Reactive Oxygen Species in Macrophages: Sources and Targets. *Front. Immunol.* **12**, 734229 (2021).

233. Xie, J. *et al.* The role of reactive oxygen species in severe acute respiratory syndrome coronavirus 2 (SARS-COV-2) infection-induced cell death. *Cell. Mol. Biol. Lett.* **29**, 138 (2024).

234. Zhu, S., Li, W., Hao, Y., Zhang, L. & Gao, P. TIPE2 suppresses ferroptosis and pro-inflammatory polarization in macrophages triggered by SARS-CoV-2 spike protein. *Scientific Reports 2025 15:1* **15**, 30246- (2025).

235. Wei, X. *et al.* Macrophage peroxisomes guide alveolar regeneration and limit SARS-CoV-2 tissue sequelae. *Science* **387**, eadq2509 (2025).

236. Cooper, G. E. *et al.* Viral Inhibition of Bacterial Phagocytosis by Human Macrophages: Redundant Role of CD36. *PLoS One* **11**, e0163889 (2016).

237. Wenzek, C. *et al.* CD47 restricts antiviral function of alveolar macrophages during influenza virus infection. *iScience* **25**, 105540 (2022).

238. Kedzierska, K. *et al.* Defective phagocytosis by human monocyte/macrophages following HIV-1 infection: underlying mechanisms and modulation by adjunctive cytokine therapy. *Journal of Clinical Virology* **26**, 247–263 (2003).

239. Salina, A. C. G. *et al.* Efferocytosis of SARS-CoV-2-infected dying cells impairs macrophage anti-inflammatory functions and clearance of apoptotic cells. *Elife* **11**, (2022).

240. Munnur, D. *et al.* Altered ISGylation drives aberrant macrophage-dependent immune responses during SARS-CoV-2 infection. *Nat. Immunol.* **22**, 1416–1427 (2021).

241. Muntjewerff, E. M., Meesters, L. D. & van den Bogaart, G. Antigen Cross-Presentation by Macrophages. *Front. Immunol.* **11**, (2020).

242. Blumenthal, R. L. *et al.* Human alveolar macrophages induce functional inactivation in antigen-specific CD4 T cells. *Journal of Allergy and Clinical Immunology* **107**, 258–264 (2001).

243. Upham, J. W., Strickland, D. H., Bilyk, N., Robinson, B. W. & Holt, P. G. Alveolar macrophages from humans and rodents selectively inhibit T-cell proliferation but permit T-cell activation and cytokine secretion. *Immunology* **84**, 142 (1995).

244. Chen-Camaño, R., DeAntonio, R. & López-Vergès, S. T-cell exhaustion in COVID-19: what do we know? *Front. Immunol.* **16**, 1678149 (2025).

245. Shaath, H., Vishnubalaji, R., Elkord, E. & Alajez, N. M. Single-Cell Transcriptome Analysis Highlights a Role for Neutrophils and Inflammatory Macrophages in the Pathogenesis of Severe COVID-19. *Cells* **9**, (2020).

246. Li, M. *et al.* Signaling pathways in macrophages: molecular mechanisms and therapeutic targets. *MedComm (Beijing).* **4**, e349 (2023).

247. Land, W. G. Role of DAMPs in respiratory virus-induced acute respiratory distress syndrome—with a preliminary reference to SARS-CoV-2 pneumonia. *Genes & Immunity 2021 22:3* **22**, 141–160 (2021).

248. Maemura, T. *et al.* Antibody-Dependent Enhancement of SARS-CoV-2 Infection Is Mediated by the IgG Receptors FcγRIIA and FcγRIIIA but Does Not Contribute to Aberrant Cytokine Production by Macrophages. *mBio* **12**, e01987-21 (2021).

249. Park, Y. J. *et al.* Pyrogenic and inflammatory mediators are produced by polarized M1 and M2 macrophages activated with D-dimer and SARS-CoV-2 spike immune complexes. *Cytokine* **173**, 156447 (2024).

250. Geyer, C. E. *et al.* Hyperinflammation by Human Macrophages Induced by SARS-CoV-2 Anti-Spike IgG Is Dependent on Glucose and Fatty Acid Metabolism. *Eur. J. Immunol.* **55**, e70087 (2025).

251. Mes, L. *et al.* Anti-SARS-CoV-2 Spike IgA2 Induces Inflammation by Human Macrophages. *Eur. J. Immunol.* **55**, e70068 (2025).

252. Sefik, E. *et al.* Inflammasome activation in infected macrophages drives COVID-19 pathology. *Nature 2022 606:7914* **606**, 585–593 (2022).

253. Marrone, L. *et al.* Tirofiban prevents the effects of SARS-CoV-2 spike protein on macrophage activation and endothelial cell death. *Heliyon* **10**, (2024).

254. Khan, S. *et al.* SARS-CoV-2 spike protein induces inflammation via TLR2-dependent activation of the NF-κB pathway. *Elife* **10**, (2021).

255. Dosch, S. F., Mahajan, S. D. & Collins, A. R. SARS coronavirus spike protein-induced innate immune response occurs via activation of the NF-κB pathway in human monocyte macrophages in vitro. *Virus Res.* **142**, 19–27 (2009).

256. Palestra, F. *et al.* SARS-CoV-2 Spike Protein Activates Human Lung Macrophages. *Int. J. Mol. Sci.* **24**, 3036 (2023).

257. Pantazi, I. *et al.* SARS-CoV-2/ACE2 Interaction Suppresses IRAK-M Expression and Promotes Pro-Inflammatory Cytokine Production in Macrophages. *Front. Immunol.* **12**, 683800 (2021).

258. Zhu, S., Li, W., Hao, Y., Zhang, L. & Gao, P. TIPE2 suppresses ferroptosis and pro-inflammatory polarization in macrophages triggered by SARS-CoV-2 spike protein. *Scientific Reports 2025 15:1* **15**, 30246- (2025).

259. Dai, Y., Zhou, J. & Shi, C. Inflammasome: structure, biological functions, and therapeutic targets. *MedComm (Beijing).* **4**, e391 (2023).

260. Rodrigues, T. S. *et al.* Inflammasomes are activated in response to SARS-cov-2 infection and are associated with COVID-19 severity in patients. *Journal of Experimental Medicine* **218**, (2020).

261. Bhanpattanakul, S. *et al.* Modulation of MHC expression by interferon-gamma and its influence on PBMC-mediated cytotoxicity in canine mast cell tumour cells. *Scientific Reports 2024 14:1* **14**, 17837- (2024).

262. Cinquegrani, G. *et al.* SARS-CoV-2 Spike protein is not pro-inflammatory in human primary macrophages: endotoxin contamination and lack of protein glycosylation as possible confounders. *Cell Biology and Toxicology 2021 38:4* **38**, 667–678 (2022).

263. Yu, P. *et al.* Pyroptosis: mechanisms and diseases. *Signal Transduction and Targeted Therapy 2021 6:1* **6**, 128- (2021).

264. Kawasaki, T. *et al.* Alveolar macrophages instruct CD8+ T cell expansion by antigen cross-presentation in lung. *Cell Rep.* **41**, 111828 (2022).

265. Taefehshokr, N. *et al.* SARS-CoV-2 NSP5 antagonizes MHC II expression by subverting histone deacetylase 2. *J. Cell Sci.* **137**, (2024).

266. Moriyama, M., Lucas, C., Monteiro, V. S. & Iwasaki, A. Enhanced inhibition of MHC-I expression by SARS-CoV-2 Omicron subvariants. *Proc. Natl. Acad. Sci. U. S. A.* **120**, e2221652120 (2023).

267. Yoo, J. S. *et al.* SARS-CoV-2 inhibits induction of the MHC class I pathway by targeting the STAT1-IRF1-NLRC5 axis. *Nature Communications 2021 12:1* **12**, 6602- (2021).

268. Moriyama, M., Lucas, C., Monteiro, V. S. & Iwasaki, A. Enhanced inhibition of MHC-I expression by SARS-CoV-2 Omicron subvariants. *Proc. Natl. Acad. Sci. U. S. A.* **120**, e2221652120 (2023).

269. Barnett, K. C. *et al.* An epithelial-immune circuit amplifies inflammasome and IL-6 responses to SARS-CoV-2. *Cell Host Microbe* **31**, 243-259.e6 (2023).

270. Thorne, L. G. *et al.* SARS-CoV-2 sensing by RIG-I and MDA5 links epithelial infection to macrophage inflammation. *EMBO J.* **40**, 107826 (2021).

271. Sbarigia, C., Vardanyan, D., Buccini, L., Tacconi, S. & Dini, L. SARS-CoV-2 and extracellular vesicles: An intricate interplay in pathogenesis, diagnosis and treatment. *Frontiers in Nanotechnology* **4**, 987034 (2022).

272. Bachiller, S. *et al.* SARS-CoV-2 post-acute sequelae linked to inflammation via extracellular vesicles. *Front. Immunol.* **16**, (2025).

273. Desmyter, J., Melnick, J. L. & Rawls, W. E. Defectiveness of interferon production and of rubella virus interference in a line of African green monkey kidney cells (Vero). *J. Virol.* **2**, 955–961 (1968).

274. Barreto-Duran, E. *et al.* The interplay between the airway epithelium and tissue macrophages during the SARS-CoV-2 infection. *Front. Immunol.* **13**, 6017 (2022).

275. Khan, S. *et al.* SARS-CoV-2 spike protein induces inflammation via TLR2-dependent activation of the NF-κB pathway. *Elife* **10**, (2021).

276. Chiok, K., Hutchison, K., Miller, L. G., Bose, S. & Miura, T. A. Proinflammatory Responses in SARS-CoV-2 and Soluble Spike Glycoprotein S1 Subunit Activated Human Macrophages. *Viruses* **15**, 754 (2023).

277. Shirato, K. & Kizaki, T. SARS-CoV-2 spike protein S1 subunit induces pro-inflammatory responses via toll-like receptor 4 signaling in murine and human macrophages. *Heliyon* **7**, e06187 (2021).

278. Theobald, S. J. *et al.* Long-lived macrophage reprogramming drives spike protein-mediated inflammasome activation in COVID-19. *EMBO Molecular Medicine 2021 13:8* **13**, EMMM202114150- (2021).

279. Hsieh, L. L. *et al.* Bystander monocytic cells drive infection-independent NLRP3 inflammasome response to SARS-CoV-2. *mBio* https://doi.org/10.1128/MBIO.00810-24 (2024) doi:10.1128/MBIO.00810-24.

280. Wolfe, C. R. *et al.* Safety and Efficacy of Pemivibart, a Long-Acting Monoclonal Antibody, for Prevention of Symptomatic COVID-19: Interim Results From a Phase 3 Randomized Clinical Trial (CANOPY). *Clin. Infect. Dis.* **81**, 439 (2025).

281. Gartlan, C. *et al.* Vaccine-Associated Enhanced Disease and Pathogenic Human Coronaviruses. *Front. Immunol.* **13**, 882972 (2022).